RECOGNITION OF MYCOBACTERIAL ANTIGENS BY CONVENTIONAL AND UNCONVENTIONAL HUMAN T-CELLS

Johanne M. Pentier

A thesis submitted to Cardiff University in fulfilment of

the requirement for the Degree of Doctor of Philosophy

Institute of Infection and Immunity

School of Medicine

Cardiff University

2014

ACKNOWLEDGEMENTS

My sincere thanks go to my supervisors Prof. Andy Sewell, Dr. Pierre Rizkallah and Dr John Miles for their help throughout my thesis. I would first like to thank Andy for his support, advice, firmness and meticulous attention to detail, and for his extraordinary sense of humour which considerably eased the whole process! I would like to thank Pierre for his guidance and encouragement. I would also like to thank John for his support, his faith in my abilities, and his constant optimism.

I would particularly like to thank Dr. Garry Dolton for his knowledge, time, and friendship throughout my PhD. His passion for science, appetite for knowledge, enthusiasm, and his conscientious approach to work were inspiring. My thanks go also to Dr Dave Cole, who was always available when I needed support.

I would like to express my appreciation to my dear friends, Andrea and Rosaria, for their friendship, love and encouragement, and to Mat Clement and James McLaren for the laughter that we shared. Thanks also to all the members of Cardiff T-cell modulation group, and to my colleagues and friends from the Henry Wellcome Building.

I thank all of you for making my time in Cardiff so memorable.

I dedicate this thesis and my work to my inspirational dad, Olivier, my courageous mum, Anne, and my best friend and sister, Gaëlle.

DECLARATION

This work has not previously been accepted in substance for any other degree or award and is not concurrently submitted in candidature for any degree.

Signed.....(candidate) Date.....

STATEMENT 1

This thesis is being submitted in partial fulfilment of the requirement for the degree of PhD.

Signed.....(candidate) Date.....

STATEMENT 2

This thesis is the result of my own independent work/investigation, except where otherwise stated. Other sources are acknowledged by explicit references.

Signed.....(candidate) Date.....

STATEMENT 3

I hereby give consent for my thesis, if accepted, to be available for photocopying and for inter-library loan, and for the title and summary to be made available to outside organizations.

Signed.....(candidate) Date.....

ABSTRACT

Human T-cells play a major role in controlling and clearing Mycobacterial infections. The adaptive immune system deploys a complex network of specialised T-cell subsets in order to tailor an optimum immune response. Two categories of T-cells have been described that are characterised by the ligands they recognise: "conventional" T-cells (polymorphic, HLA-restricted, peptide-specific) and "unconventional" T-cells (non-polymorphic, restricted by HLA-like molecules, non-peptide-specific). Both T-cell categories were shown to be important for the elimination of cells infected with *Mycobacterium tuberculosis* (*M. tuberculosis*) and their role, specificities and functionalities are under active investigation in order to develop optimum vaccination strategies. A large interest in unconventional T-cells, such as MR1-restricted MAITs or CD1-specific T-cells, and their role in mycobacterial infections has recently arisen. I initiated my studies by dissecting T-cell responses generated during direct *ex vivo* boosting of PBMCs with antigen presenting cells that had phagocytosed *Mycobacterium smegmatis* (*M. smegmatis*). *M. smegmatis* is a non-pathogenic bacterium and is mainly eliminated by the innate immune system. However, T-cells might respond to *M. smegmatis* antigens and therefore play a role in clearing the pathogen. Using polychromatic flow cytometry, I successfully identified major $CD3^+$ conventional and unconventional *M. smegmatis*-specific T-cell populations and evaluated their respective frequencies and distribution. The identification of a significant frequency of *M. smegmatis*-specific unconventional MAITs pushed me to further analyse the specificity of this interesting T-cell subset. At the time of my studies, the ligand(s) presented by MR1 to MAITs were still undiscovered. However, structural models of MR1 groove moiety provided evidences that MR1 could potentially present peptides to MAITs. Therefore, I attempted to identify the molecular and cellular mechanisms by which an *M. tuberculosis*-specific MAIT clone recognises peptide loaded on MR1 and to refold this MHC-like protein. Vaccination strategies have been mainly focusing on targeting CD8 T-cells, known to be essential for the host defence against mycobacterial infections. Therefore a huge effort is made to discover new immunodominant mycobacterial epitopes. Collaborators isolated the HLA-A*0201-restricted D454 T-cell clone specific to the LLDAHIPQL epitope derived from the highly immunogenic Esx-G protein. The LLDAHIPQL sequence is conserved across mycobacterial species thus offering potential for pan-mycobacterial vaccination. I aimed at proving that D454 TCR binds to HLA-A*0201-LLDAHIPQL. I successfully obtained an HLA-A*0201-LLDAHIPQL crystal structure, the first bacterially-derived HLA-peptide complex, and identified the key mechanisms involved in the molecular recognition of HLA-A*0201-LLDAHIPQL by a conventional TCR.

PUBLICATIONS

Comparison of peptide-major histocompatibility complex tetramers and dextramers for the identification of antigen-specific T cells.

Dolton G, Lissina A, Skowera A, Ladell K, Tungatt K, Jones E, Kronenberg-Versteeg D, Akpovwa H, **Pentier JM**, Holland CJ, Godkin AJ, Cole DK, Neller MA, Miles JJ, Price DA, Peakman M, Sewell AK. *Clinical and Experimental Immunology*. July, 2014.

Advances in T-cell epitope engineering.

Pentier JM, Sewell AK, Miles JJ. *Frontiers in Immunology*. June, 2013.

Peptide length determines the outcome of TCR/peptide-MHCI engagement.

Ekeruche-Makinde J, Miles JJ, van den Berg HA, Skowera A, Cole DK, Dolton G, Schauenburg AJ, Tan MP, **Pentier JM**, Llewellyn-Lacey S, Miles KM, Bulek AM, Clement M, Williams T, Trimby A, Bailey M, Rizkallah P, Rossjohn J, Peakman M, Price DA, Burrows SR, Sewell AK, Wooldridge L. *Blood.* February, 2013.

T-cell receptor-optimized peptide skewing of the T-cell repertoire can enhance antigen targeting.

Ekeruche-Makinde J, Clement M, Cole DK, Edwards ES, Ladell K, Miles JJ, Matthews KK, Fuller A, Lloyd KA, Madura F, Dolton GM, **Pentier J**, Lissina A, Gostick E, Baxter TK, Baker BM, Rizkallah PJ, Price DA, Wooldridge L, Sewell AK. *Journal of Biological Chemistry*. October, 2012.

Manuscript submitted to the *Journal of Immunology* in September 2014:

Naïve CD8+ T cell precursors specific for viral and self-derived targets display structured TCR repertoires and composite antigen-driven selection dynamics.

Co-authorship between Miles JJ and **Pentier JM**

TABLE OF CONTENT

LIST OF FIGURES

ABBREVIATIONS

GENERAL

7-AAD	7-aminoactinomycin D
APC	Antigen presenting cell
APC Flurochrome	Allophycoyanin
APC-Cy7 Flurochrome	Allophycoyanin-cychrome 7
APLs	Altered peptide ligands
ATP	Adenosine triphosphate
BCR	B cell receptor
C	Constant TCR gene fragment
CBS	Central Biotechnology Services
CD (number)	Cluster of differentiation (number)
cDNA	complementary Deoxyribonucleic acid
CDR	Complementarity determining regions
CLIP	Class II-associated invariant-chain peptide
CPL	combinatorial peptide libraries
CTLs	Cytotoxic T lymphocytes
D	Diversity TCR gene fragment
DN	Double negative thymocytes (CD4- CD8-)
DNA	Deoxyribonucleic acid
DP	Double positive thymocyte to (CD4+ CD8+)
DTT	Dithiothreitol
E.coli	Escherichia coli
EBV	Epstein-Barr virus
ELISA	Enzyme linked immunosorbent assay
ELISpot	Enzyme linked immunospot
ER	Endoplasmic reticulum
F	Structure factor
F0	Observed structure factor
fAB	Antigen binding fragment
FACS	Fluorescence activated cell sorting
FC	Calculated structure factor
FCS	Foetal calf serum
FITC	Fluorescein isothiocyanate
FMO	Fluorescence minus one
FPLC	Fast protein liquid chromatography
HIV	Human Immunodeficiency Virus
HLA	Human leukocyte antigen
IBs	Inclusion bodies
IFN-γ	Interferon-γ
IgE	Immunoglobulin E
IgG	Immunoglobulin G
Ii	Invariant chain
IL	Interleukin
IPTG	Isopropyl-1-thio-β-D-galactopyranoside

ITAM	Immunoglobulin receptor family tyrosine based activation motif
J	Joining TCR gene fragment
K	Kelvin
KD	Equilibrium dissociation constant
kD	Kilodalton
Koff	Rate of dissociation
Kon	Rate of association
LAT	Linker for activation of T cells
Lck	Lymphocyte-specific protein tyrosine kinase
MAIT	Mucosal associated invariant T cells
mAU	milli absorbance units
MFI	Mean/Median fluorescence intensity
mg	Milligram
MHC I	Major Histocompatibility Class I
MHC II	Major Histocompatibility Class II
MIIC	MHC II compartment
MIP-1α	Macrophage Inflammatory Protein-1α (CCL3)
MIP-1β	Macrophage Inflammatory Protein-1β (CCL4)
ng	Nanogram
NK	Natural Killer cells
OD	Optical Density
PAMPs	Pathogen associated molecular patterns
PB	Pacific blue
PBMC	Peripheral blood mononuclear cells
PBS	Phosphate buffer solution
PDB	Protein data bank
PE	Phycoerythrin
PE-Cy7	Phycoerythrin cychrome-7
PerCP	Peridinin Chlorophyll Protein
PHA	Phytohaemagglutinin
PKC	Protein kinase C
pMHC	peptide- major histocompatibility complex
PRRs	Pattern recognition receptors
PTK	Protein tyrosine kinase
pTα	pre-T-cell α chain
RAG	Recombination activation genes
RANTES	Regulated on activation, Normal T expressed and secreted
R-factor	Residual factor
RU	Response units
SDS-PAGE	Sodium dodecyl sulfate – polyacrylamide gel electrophoresis
SH	Src homology
SMACs	supramolecular activation clusters
SP	Single positive thymocyte (CD4+ or CD8+)
SPR	Surface plasmon resonance
TAP	Transporter associated with antigen processing

TCM	Central memory T-cells
TCR	T-cell receptor
TEM	Effector memory T-cells
T_H	T helper cells
TNF-α	Tumour necrosis factor
TRAJ	T-cell receptor alpha joining gene
TRAV	T-cell receptor alpha variable gene
TRBJ	T-cell receptor beta joining gene
TRBV	T-cell receptor beta variable gene
Tregs	Regulatory T-cells
V	Variable TCR gene fragment
vdW	Van der Waals
Zap-70	Zeta associated protein of 70kD
β2m	β2 microglobulin
ΔCp	Heat capacity xvi
ΔG	Binding free energy
ΔH	Change in enthalpy
ΔS	Change in entropy
µg	Microgram

AMINO ACIDS

A	Ala	Alanine
C	Cys	Cysteine
D	Asp	Aspartic acid
E	Glu	Glutamic acid
F	Phe	Phenylalanine
G	Gly	Glycine
H	His	Histidine
I	Ile	Isoleucine
K	Lys	Lysine
L	Leu	Leucine
M	Met	Methionine
N	Asn	Asparagine
P	Pro	Proline
Q	Gln	Glutamine
R	Arg	Arginine
S	Ser	Serine
T	Thr	Threonine
V	Val	Valine
W	Trp	Tryptophan
Y	Tyr	Tyrosine

CHAPTER 1. INTRODUCTION

1.1 Overview of the immune system

Environmental pressures drive evolution of the human immune system to guarantee the protection and homeostasis of the host. Like an army, the immune system is composed of different regiments of cell subsets with intrinsic missions and functions. Each regiment encodes a specific arsenal of probes and weapons to seek and destroy pathogenic microorganisms and abnormal cellular activity.

The first-line regiment – termed the innate immune system – is composed of phagocytic cells and the blood proteins that make up the complement system. The cell types of the innate immune system include monocytes, macrophages, dendritic cells and natural killer (NK) cells. These cells interact directly with pathogenic microorganisms at the portal of entry. The recognition receptors used by innate immune cells are germline encoded and exhibit limited diversity. Recognition by innate immune cells is confined to compounds and structures that are shared between groups of microorganisms (e.g. membrane, cell wall or nucleic acid components). These 'universal' antigens are called pathogen associated molecular patterns (PAMPs) (Janeway and Medzhitov, 2002). PAMPs are recognised by the pattern recognition receptors (PRRs) found at the surface of innate immune cells. PRRs are designed to quickly scan for the presence of microbes. Considered the sentinels of the body, innate immune cells intimately communicate with the second line of immune defence: the adaptive immune system. In contrast to the innate immune system, the adaptive immune system is able to adapt to hypervariable antigens, memorise their structure and regulate the magnitude of response at each successive exposure to the same antigen. The key to adaptive immunity is held by the vast array of different antigen receptors that the body makes and expresses on the surface of cells called lymphocytes. The adaptive immune system is divided into two main sub-regiments; humoral immunity and cellular immunity. Humoral immunity is mediated by B-cells (or B-lymphocytes) that secrete antibodies, promote inflammation and neutralise antigens. Cellular immunity is mediated by T-cells (or T-lymphocytes) that recognise small parts of pathogens presented at the cell surface by molecules called major histocompatibility complex (MHC) molecules. Some T-cells act to orchestrate the entire immune response using soluble messenger molecules called lymphokines while others act to seek and destroy infected or neoplastic cells directly.

1.2 Adaptive immune system

The adaptive immune system is composed of lymphocytes. The lymphoid lineage accounts for up to 30% of the total leukocytes found in the human body. Lymphocytes are split into two main subsets: B-cells and T-cells.

1.2.1 B-cell lineage

B-cells express somatically encoded soluble or membrane bound immunoglobulin receptors termed antibodies and B-cell receptors (BCRs) respectively. BCRs and antibodies are highly specific for an antigenic epitope and bind with high affinity. BCRs serve as cell receptors and deliver intracellular activating and survival signals upon interaction with a pathogenic antigen. BCRs mediate B-cell activation, division, survival, promote the secretion of inflammatory cytokines and control antibody secretion. Antibody is a soluble form of the BCR. Antibodies are able to coat viruses and bacteria by binding strongly to surface epitopes and contribute to their clearance in three ways. First, antibodies bind to pathogens and prevent anchorage to target cells preventing the invasion of virus, bacteria and associated toxins. Second, antibodies facilitate the uptake of pathogens by binding via the fragment crystallisable (Fc) receptors to phagocytic cells promoting phagocytosis of invaders. Third, proteins of the complement system interact with antibodies bound to pathogens and mediate their lysis.

My work was oriented towards T-cells hence B-cells will not be considered further here. The rest of this thesis will focus on the T-cell lineage of lymphocytes.

1.2.2 T-cell lineage

T-cells express a somatically encoded, cell surface, heterodimeric protein: the T-cell receptor (TCR). The TCR comes in either of two forms: One is made by the combination of a γ- and a δ-chain (γδTCR) and the other by the combination of a α- and β-chain (αβTCR). These receptors define the lymphocytes that express them as either γδ or αβ T-cells.

1.3 T-cell biology

1.3.1 γδ T-cells

The frequency of γδ T-cells in human is low at around 0.5-10% of circulating T-cells (Kalyan and Kabelitz, 2013) however it is much higher in certain tissues such as mucosa and the gut where they can reach 25-60% (Groh et al., 1989, Kalyan and Kabelitz, 2013). At the current time, rather little is known about the exact nature of human γδ T-cell antigens. Studies have mainly focused interest on two members of the CD1 MHC-like molecule – the CD1c and CD1d platforms – which presents lipids such as phosphatidylethanolamine (Hayday and Vantourout, 2013), phospholipids including cardiolipin (Dieude et al., 2011) and α-galactosyl-ceramide compounds (Uldrich et al., 2013) to γδ T-cells. However, other molecules have been described to bind to human γδ T-cells such as the non-polymorphic butyrophilin 3A1 (Harly et al., 2012) and the endothelial protein receptor C (EPCR) (Willcox et al., 2012). Although the field of γδ T-cell ligands is in its infancy, recent molecular findings have stimulated a renaissance in γδ T-cell research and it is expected that the molecular mechanisms behind how these interesting lymphocytes contribute to human immunity will be revealed soon.

My work concentrated on the far better characterised αβ T-cell subset that constitutes the vast majority of human T-cells.

1.3.2 αβ T-cells

αβ T-cells are the most common of T-cells in humans (Kalyan and Kabelitz, 2013). Most αβ T-cells recognise short peptides presented at the cell surface by MHC class I (MHC I) or class II (MHC II) molecules (describe in section 1.4). Peptide-MHC (pMHC) molecules represent the conventional ligands of αβ T-cells and T-cells that recognise pMHC are said to be 'conventional'. Recent discoveries have described how some αβ T-cells can recognise lipids and bacterial metabolites presented by MHC class I-like molecules. These newly discovered T-cell subtypes are broadly described as being 'unconventional' T-cells and will be reviewed in section 1.7.

Most αβ T-cells express either the CD4 or CD8 co-receptors on their surface. These surface glycoproteins define the two major αβ T-cell subsets. CD4 T-cells recognise pMHC II ligands and are termed 'helper' T-cells while CD8 T-cells recognise pMHC I ligands and are called 'cytotoxic' or 'killer' T-cells. I will describe these two populations in turn.

1.3.2.1 CD4 helper T-cells

T helper cells (T_H) mainly orchestrate and maintain the homeostasis of immune responses. T_H subsets express the CD4 co-receptor at the cell surface and are activated upon interaction of the TCR with pMHC II molecules (Konig et al., 1995, Konig et al., 2002). T_H cells are characterised by the production of cytokines that drive innate and adaptive effector functions and lead to an efficient immune response. Six T_H cell subsets have been described so far T_H1, T_H2, T_H9, T_H17, T_H22 and follicular helper cells each defined by a cytokine "signature".

T_H1 cells are characterised by release of IFNγ and generally drive cell-mediated cytotoxicity against intracellular bacteria. IFNγ promotes macrophage and cytotoxic T-lymphocyte (CTL) activation (Swain et al., 2012). T_H2 cells characteristically express interleukin-4 (IL-4) and are specialised in driving the immune system towards the elimination of extracellular pathogens by recruiting basophils and activating eosinophils (Okoye and Wilson, 2011). Similar roles have been reported for the T_H9 cell subset. However, the latter cells mainly play a role in immunity against intestinal parasites (Kara et al., 2014).

T_H17 and T_H22, secrete IL-17 and IL-22 respectively. T_H17 and T_H22 cells mediate anti-microbial activity against extracellular pathogens by promoting phagocytosis by monocytes and macrophages (Yu and Gaffen, 2008, Liang et al., 2006). In addition, T_H22 cells are involved in tissues regeneration by promoting epithelial cell growth (Witte et al., 2010). T follicular helper cells promote the humoral response against extracellular pathogens by triggering B-cell survival, maturation and proliferation (Kara et al., 2014) (see **Table 1.1**). Interestingly, T_H cells can acquire different effector roles under certain cytokine environments (Wan, 2010). The T_H effector function plasticity permits precise tailoring of the response to different pathogens.

Effector T-cell	Type	Function	antigen	MHC restriction	Phenotype/chemokine receptor and ligand	Major effector molecules release
CD4 helper T-cells (Th)	**Th 1**	-Promote macrophage activation -mediate cytotoxic response against intracellular infection	Peptides	MHC-II	• **CD3, αβTCR, CD4** • CXCR3, CXCL9/10/11	**IFNγ**, TNFα/β, IL-21
	Th2	-Promote humoral response and macrophage activation -mediate host response against extracellular pathogens	Peptides	MHC-II	• **CD3, αβTCR, CD4**, • CCR3/4/8, CCL1/11/13/17	**IL-4**, IL-5, IL-13
	Th9	-mediate host response against intestinal microbial infection	Peptides	MHC-II	• **CD3, αβTCR, CD4** • CCR3/6. CXCR3, CCL11/13/20, CXCL9/10/11	**IL-9**, IL-10
	Th17	-promote immune response against microbial infection -enhance neutrophils and macrophages recruitment and activation	Peptides	MHC-II	• **CD3, αβTCR, CD4** • CCR2/6/4, CCL2/20/17	**IL-17A, IL-17F,** IFNγ, IL-4, IL-13
	Th22	-mediate immune response against bacterial infection at epithelial barriers - Induce epithelial cell proliferation (tissue regeneration)	Peptides	MHC-II	•**CD3, αβTCR, CD4** • CCR4/10, CCL17/28	**IL-22**, IL-13, TNF-α
	Follicular helper (T_{FH})	-Promote B-cell antibody production and memory phenotype acquiring	Peptides	MHC-II	• **CD3, αβTCR, CD4** • CXCR5, CXCL13	**IL-21**

Table 1.1 CD4 helper T-cell subsets.

1.3.2.2 CD8 "killer" T-cells

Upon interaction with pathogenic antigens, naive CD8 T-cells mature and expand into cytotoxic CD8 'killer' T-cells or cytotoxic T lymphocytes (CTLs). CTLs are specialised for the detection and elimination of intracellular pathogens and tumours. CTLs secrete perforin that perforates the target cell membrane. These killer cells also secret granzymes that gain entry through the perforin pores and induce apoptosis in the target cell. Moreover, CTLs express high levels of the cell surface molecule CD95 ligand that interacts with the CD95 receptor on target cell driving apoptosis. Studies have highlighted the critical role of the co-receptor during activation of most CD8 T-cells (Purbhoo et al., 2001). Indeed, the CD8 co-receptor enhances the engagement of low affinity antigens loaded on MHC I by the TCR (Holler and Kranz, 2003, Cole et al., 2012).

1.4 αβ T-cell ligands

As described above, conventional αβ T-cell recognition occurs when αβ TCRs bind to a foreign peptide displayed by the cellular presentation platforms called MHCs. MHCs are divided into two major classes: MHC I and MHC II. MHC II molecules are expressed by leukocytes and present peptides of 10 to 34 amino acids in length (Rudolph et al., 2006) to CD4 T-cells. MHC II are encoded by HLA-DP, -DQ and -DR genes. In contrast, MHC I molecules are expressed at the surface of almost all nucleated cells and present shorter peptides ranging from 8 to 13 amino acids in length to CD8 T-cells. In humans, MHC I are encoded by the highly polymorphic HLA-A, -B and -C genes.

1.4.1 Peptide-MHC class II

1.4.1.1 Structure

MHC class II molecules consist of an α chain (comprised of α_1 and α_2 domains) associated with a β chain (comprised of β_1 and β_2 domains). α_1 and β_1 are respectively folded into a β sheet and an α-helix and form a peptide-binding platform. The α and β chains of MHC II are linked by a disulphide bond (Brown et al., 1993) (**Figure 1.1**). I detail in the next section the manufacturing and presentation processes of exogenous peptide onto MHC II.

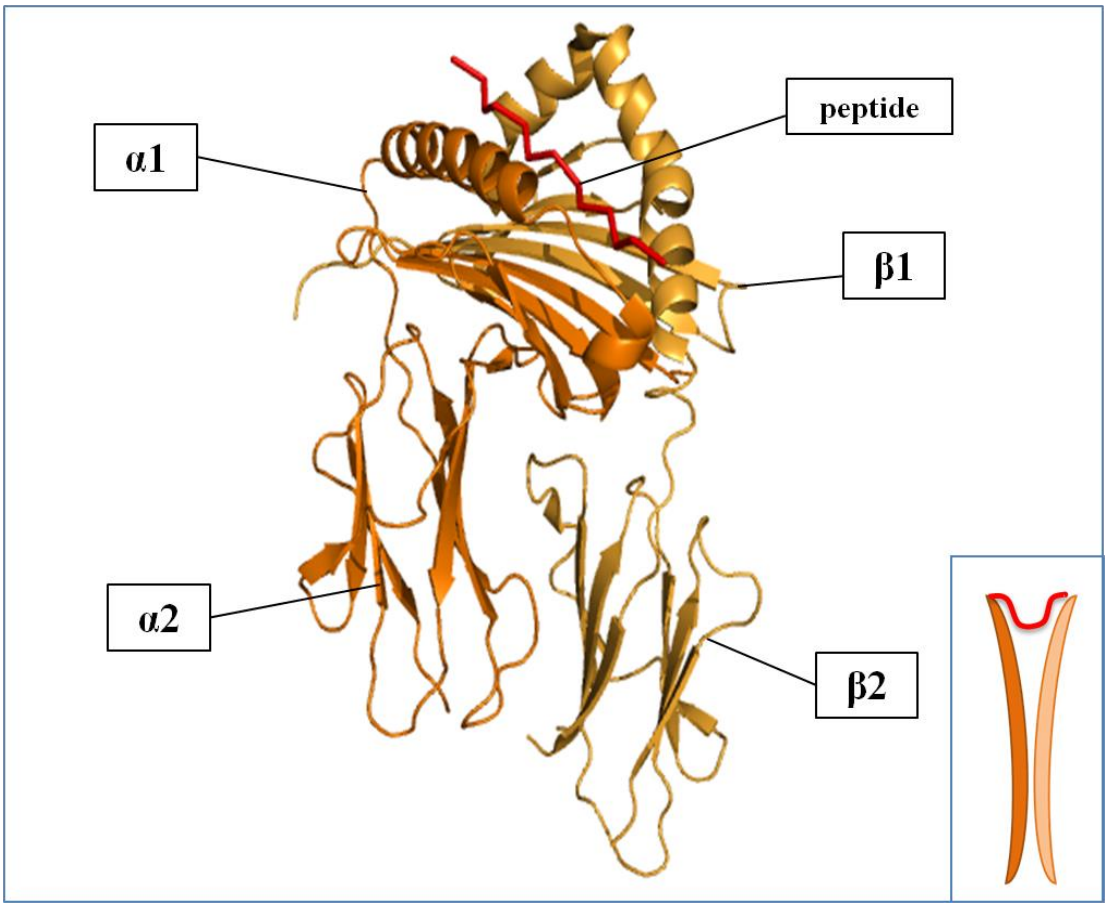

Figure 1.1 The structure of MHC II molecules.
MHC II is composed of an α chain and a β chain both divided into two subunits, α1 and α2 are shown in orange and β1 and β2 chains coloured in yellow. The peptides loaded into the two MHC II groove is shown in red. A schematic cartoon of the structure that will be used in subsequent diagrams is inset.

1.4.1.2 Peptide processing onto MHC II

MHC II presents peptides from exogenous proteins to CD4 T-cells. Exogenous proteins or microorganisms are internalised by leukocytes and transported within the cell by membrane bound vesicles where they are digested by hydrolyse proteases. These vesicles fuse with endosomes providing further proteolytic enzymes that complement the digestion process producing small peptides fragments.

MHC II α and β chains are co-expressed with a third protein called the invariant chain (Ii) (Bakke and Dobberstein, 1990). The Ii chain is composed of an endocytic targeting domain that retains the αβ heterodimer inside the endoplasmic reticulum (ER). The class II associated invariant chain peptide (CLIP) domain or CLIP peptide of the Ii is nestled inside the MHC II groove thereby maintaining the assembly of the MHC II α and β chains together and preventing the binding of endogenous peptides. The complex exits the ER and travels first through the Golgi and endolysosome to endosomal compartments. The high acidity inside endolysosome releases the CLIP peptide allowing the binding of peptides with higher affinity for the MHC II groove (Roche and Cresswell, 1991). The Cathepsin enzyme and HLA-DM molecule facilitates peptide loading onto MHC II (Stebbins et al., 1995). The newly formed αβ MHC II heterodimer loaded with an exogenous peptide is transported to the cell surface and ultimately fuses with the cell membrane where it is available for interrogation by CD4 T-cells (Wolf and Ploegh, 1995) (**Figure 1.2**). The MHC II processing pathway is leaky as it has been shown that exogenous peptide can be presented by MHC I particularly in dendritic cells and monocytes. This phenomenon is called cross presentation (Albert et al., 1998, Goodridge et al., 2013, Qu et al., 2009).

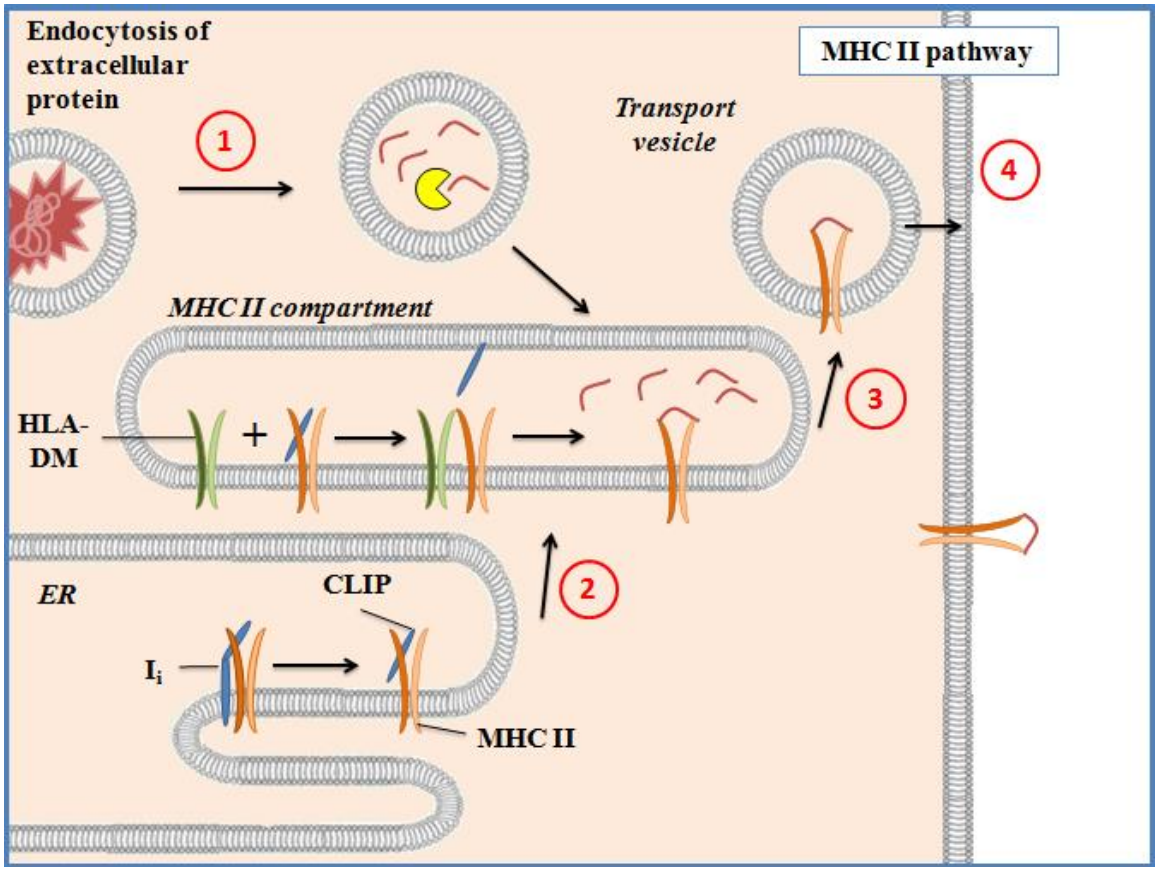

Figure 1.2 Processing and presentation of exogenous T-cell antigens onto MHC II molecules.

Phagocytised proteins are degraded by enzymes inside lysosomes into small peptides (1) and transported into a special MHC II compartment where they are loaded onto MHC II. In the meantime, MHC II molecules are assembled in the ER to be transported in the MHC II compartment (2). Peptide-MHC II then leaves then the compartment (3) to be directed to the cell surface to be presented to $CD4^+$ T-cells (4).

1.4.2 Peptide-MHC class I

1.4.2.1 Structure

MHC I molecules are composed of an α chain (or heavy chain) comprised of three domains (α_1, α_2 and α_3). The α_1/α_2 domain consists of a β sheet supporting two α helixes that cradle the bound peptide cargo. The α_3 domain is associated non-covalently with β2-microglobulin (β2m) (**Figure 1.3**). Each α chain is internally linked by a disulfide bond (Bjorkman et al., 1987). MHC I molecules look very similar to MHC II, reflecting their common role of presenting peptides to the TCR.

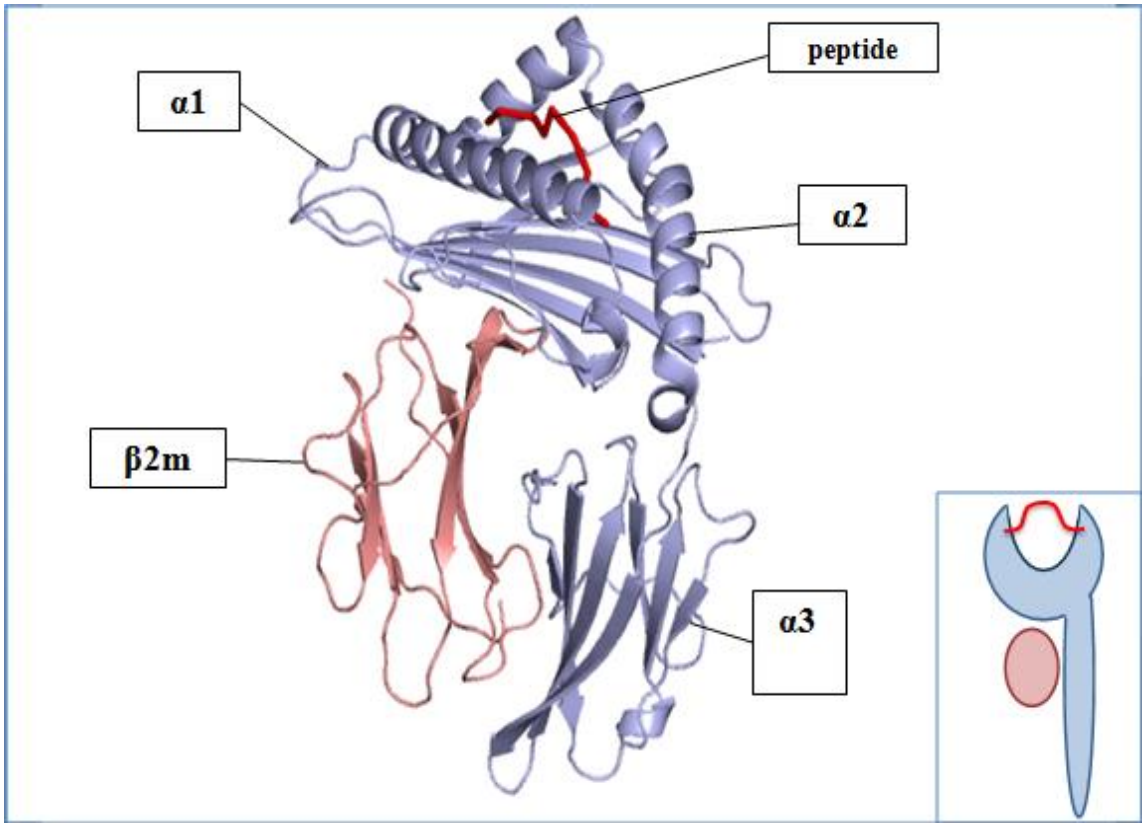

Figure 1.3 The structure of MHC I molecules.
MHC I α heavy chain (shown in blue) is comprised of three α chain subunits (α1, α2 and α3) and is associated to the β2 microglobulin (β2m) shown in salmon. The peptide loaded into the MHC I groove is shown in red. A schematic cartoon of the structure that will be used in subsequent diagrams is inset.

I detail in the next section the manufacturing and presentation processes of endogenous peptides onto MHC I.

1.4.2.2 Peptide processing onto MHC I

The majority of MHC I-associated peptides are produced in the cytoplasm by a large multi-subunit protease complex called the proteasome. The proteasome is composed of multiple ATP-dependant proteases that cleave nuclear/cytosolic proteins into small peptide fragments (Rivett et al., 1992). After cleavage by the proteasome, peptides are chaperoned by several heat shock proteins (HSP) and shuttled toward the ER. The heterodimeric transporter associated with antigen processing (TAP) protein translocates peptides into the lumen of the ER (Lauvau et al., 1999). The protein cluster formed by TAP, ERp75 and tapasin proteins is called the peptide loading complex and catalyses the loading of the peptide onto the MHC I groove (Cresswell, 2000) (**Figure 1.4**). The folding of MHC I α-chains and β2m begins in the ER. The association of the α-chains and β2m chains is mediated by two ER bound proteins: calnexin and calreticulin.

Calreticulin retains the newly formed MHC I heterodimer inside the ER until an endogenous peptide is transferred into the groove of the MHC I (Degen and Williams, 1991, David et al., 1993) .The peptide-MHC class I complex then dissociates from the peptide loading complex and is transported by chaperones towards the surface of the cell.

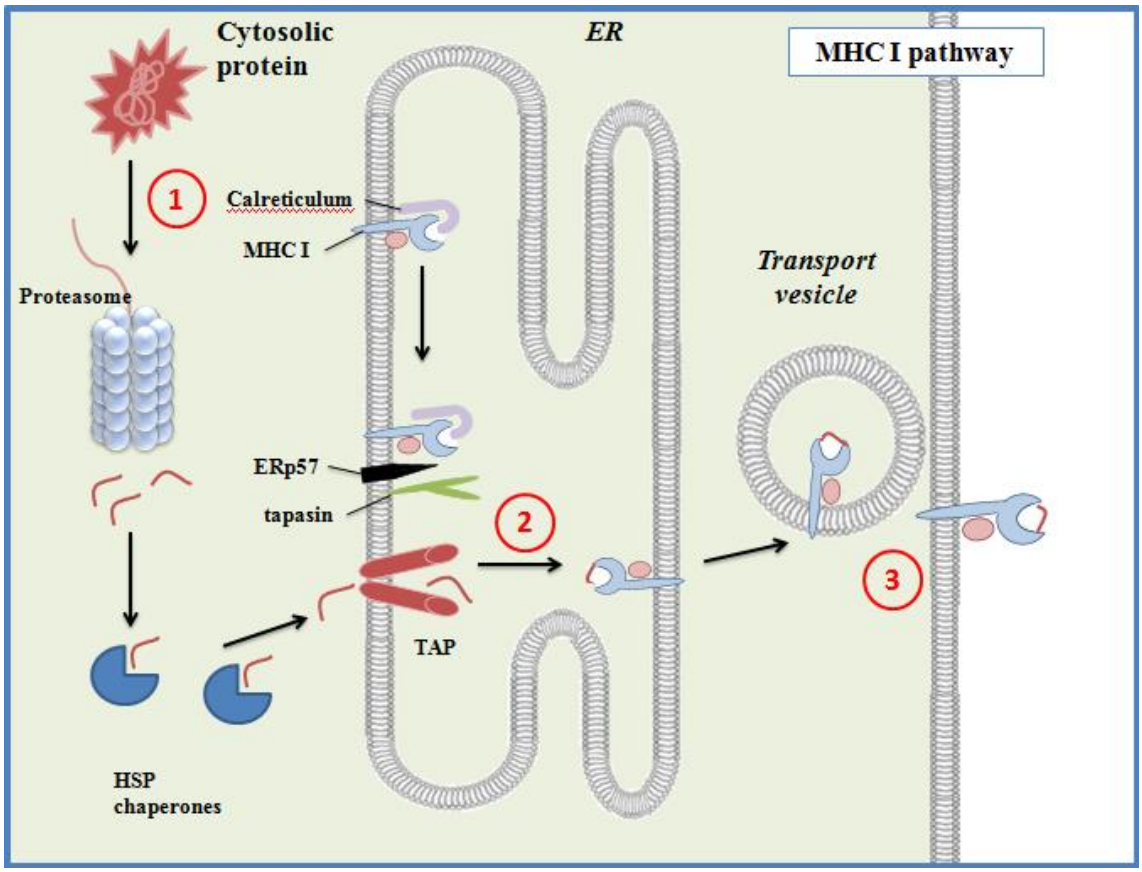

Figure 1.4 Processing and presentation of endogenous T-cell antigens onto MHC I molecules.

Intracellular proteins are degraded by the proteasome into small peptides (1) and transported by the TAP complex into the ER to be loaded onto the MHC I molecule (2). The peptide-MHC complex is then conveyed toward the cell surface to be presented to CD8 T-cells (3).

1.5 Structure of the αβ T-cell receptor

A clonotypic αβ T-cell expresses multiple copies of a single αβ TCR that is able to recognise peptides presented by MHC I or MHC II. The TCR is a glycosylated heterodimeric membrane-bound protein that is composed of an α-chain (TCRα) and a β-chain (TCRβ). The TCR is highly architecturally similar to the fragment antigen binding (Fab) of an immunoglobulin molecule. Each TCR chain is composed of a constant domain (Cα and Cβ) and a variable domain (Vα and Vβ). The variable domains possess three flexible hypervariable regions called complementarity-determining region (CDR) loops and named CDR1, CDR2 and CDR3. CDR1 and CDR2 loops have been shown to engage principally with solvent exposed residues of the MHC while the CDR3 loops engage with residues of both the MHC and the bound peptide (Rudolph et al., 2006) (**Figure 1.5**). Hyper variability of CDR3 loops is conferred by the recombination of the 3 genes from the V, D and J loci during T-cell development. This mechanism is called V(D)J recombination (described in section 1.5.3) and allows many different CDR3 loop shapes which in turn can engage many different peptide-MHC combinations.

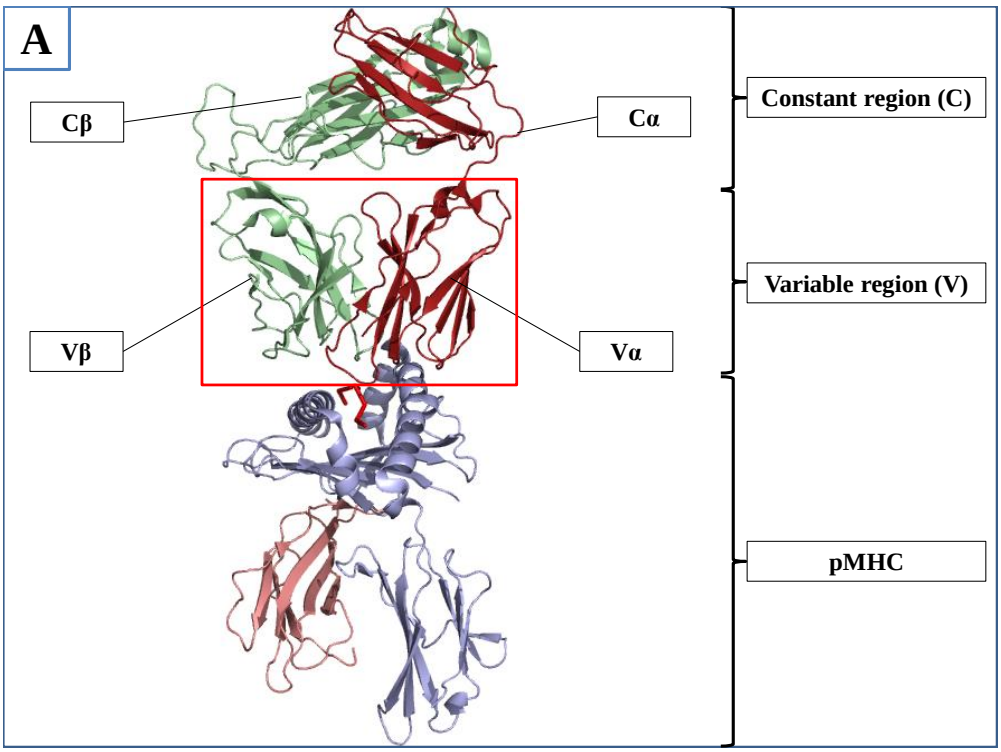

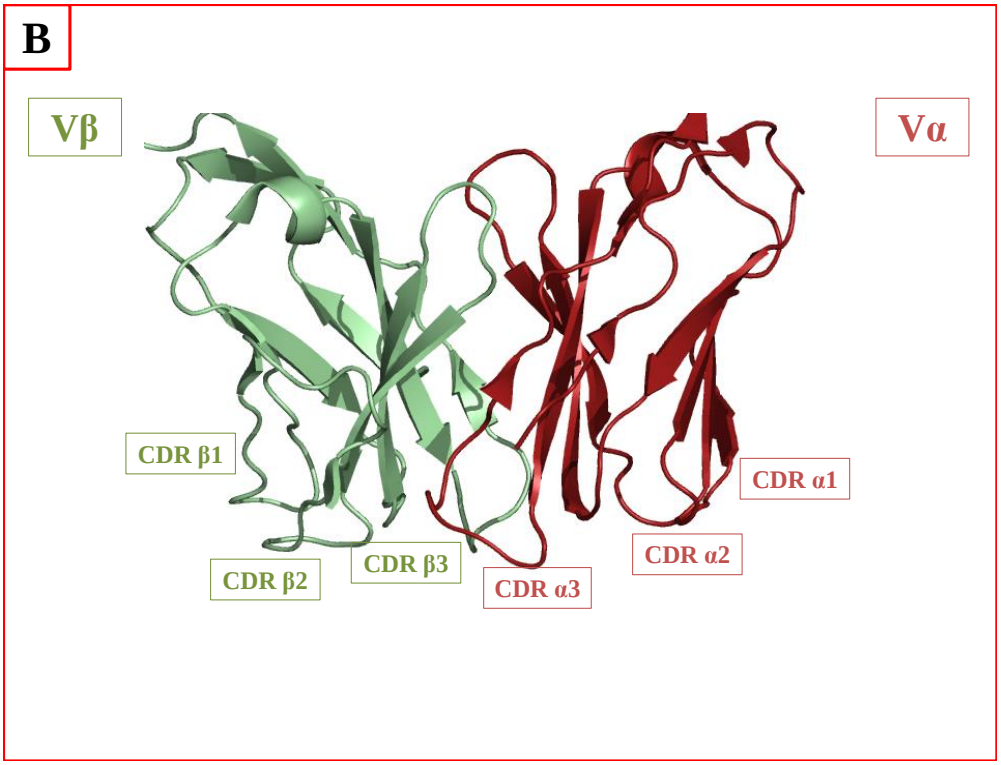

Figure 1.5 Co-crystal structure of an αβ TCR in complex with HLA-A2 presenting an epitope from the telomerase reverse transcriptase (ILAKFLHWL).
A. The αβ TCR is composed of an α chain shown in red and β chain shown in green. Each chain is composed of a constant domain (C) and a variable domain (V). **B.** An expanded view to show that each variable domain makes contact with the pMHC I molecule via 3 CDR loops (CDR1-3) (pdb: 4MNQ).

1.6 Manufacture of TCR genes

1.6.1 T-cell development and TCR education

T-cell development begins with the differentiation of pluripotent hematopoietic stem cells into lymphoid precursors in the bone marrow. These then migrate to the thymus and differentiate into thymocytes. Thymic development entails genetic and phenotypic maturation steps leading to the generation of a quality controlled TCR and the designation to the CD4 or CD8 T-cell subsets. Expression of the co-receptors CD4 and CD8 defines steps of T-cell development.

Lymphoid precursors are known to express neither CD4 or CD8 co-receptor nor TCR and are called triple negative thymocytes (TN) (Blom and Spits, 2006). TN thymocytes first undergo recombination of the TCRβ chain gene locus by VDJ recombination (described in 1.6.2) and are then defined as CD4/CD8 double negative thymocytes (DN). The newly formed TCRβ chain associates with a pre-TCRα chain (pTα) (Fehling et al., 1995) and the CD3 complex (CD3εδ, CD3εγ and CD3εζ) implicated in TCR signal transduction. This immature TCR is called the pre-TCR. Following the expression of the pre-TCR/CD3 complex, DN thymocytes express both CD4 and CD8 co-receptors (Spits, 2002). Thymocytes are thenceforth called double positive (DP) thymocytes. Signalling through the pre-TCR/CD3 complex triggers the gradual downregulation of the pTα and initiates the VJ rearrangement of TCRα gene locus. Following successful rearrangement of the TCRα chain a fully functional αβTCR/CD3 complex is expressed at the surface of the cell.

Newly formed αβ thymocytes undergo selection in the thymic environment. This quality control process ensures that thymocytes are likely to be useful but unlikely to be self-reactive. This auditioning procedure consists of both positive and negative selection. Thymocytes bearing TCRs with a high affinity for self pMHC are culled while those with a low affinity for pMHC survive and proceed to the next step of maturation. This process ensures that only T-cells expressing TCRs that exhibit weak affinity for self pMHC populate the periphery. Thymocytes that bear TCRs that fail to recognise self pMHC do not receive a survival signal and are said to ‘die by neglect’. T-cells that successfully negotiate thymic auditioning have the capacity to react strongly to non-self peptides in the context of autologous MHCs. This requirement for an autologous MHC is termed ‘MHC-restriction’.

Overall, it is estimated that only about 3% of all the thymocytes generated from the lymphoid progenitor survive thymic selection to become naive T-cells (Shortman et al., 1991). DP thymocytes that pass through thymic editing express either CD4 or CD8 co-receptor (**Figure 1.6**). The mechanisms involved in the development of these single positive (SP) thymocytes are not yet fully understood.

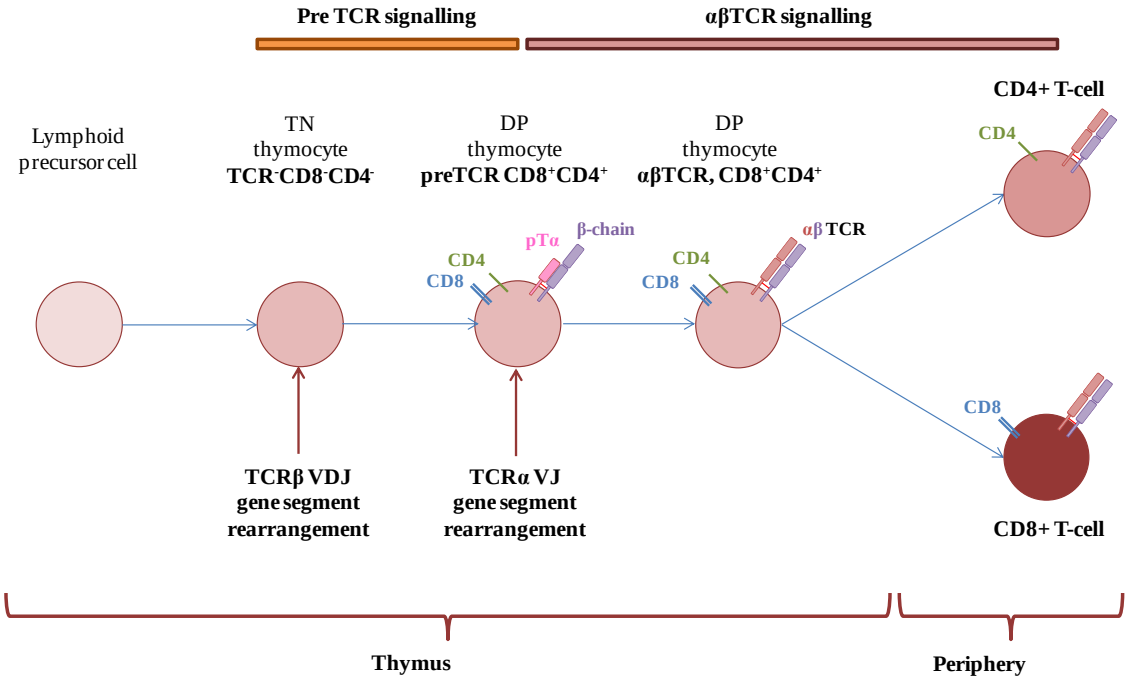

Figure 1.6 Steps of cell surface marker expression during T-cell development. After migrating from the bone marrow, the lymphoid precursor cell differentiates into a TCR/CD4/CD8 triple negative (TN) thymocyte. During this phase, TN thymocytes rearrange the TCRβ VDJ gene segments to produce a functional TCRβ chain and express a pre TCRα chain (pTα) forming a pre-TCR. Subsequently, TN thymocytes upregulate expression of both CD4 and CD8 co-receptors to become double positive (DP) thymocytes. Signalling through the pre-TCR triggers the rearrangement of the TCRα V and J gene segments to produce a functional TCRα chain. DP thymocytes now express a fully functional αβ TCRs on cell surface which is quality controlled during a process called thymic positive/ negative selection. The DP thymocyte downregulates one of the co-receptor to become single positive (SP) thymocytes. SP thymocytes exit the thymus to colonise the periphery.

1.6.2 V(D)J recombination

The diversity of the TCR repertoire is acquired during the thymic selection of thymocytes when the gene segments V, (D) and J from the TCRβ and TCRα chain gene loci are recombined. This step of TCR gene rearrangement is called somatic recombination or V(D)J recombination. As mentioned in section 1.6.1, the germline TCRβ chain gene locus in thymocytes is the first to be rearranged. The TCRβ locus is located on chromosome 7 and is composed of 54 variable (Vβ), 2 constant (Cβ), 2 diversity (Dβ) and 13 junction (Jβ) gene segments (Rowen et al., 1996). The somatic rearrangement of the TCRβ involves the 'shuffling' of the V, D and J gene segments by juxtaposition and rejoining of their sequences. This mechanism is assisted by recombination activation genes (RAGs) encoding for two enzymes RAG-1 and RAG-2. The somatic recombination starts with the joining of the Dβ with the Jβ segment forming the segment DβJβ which is then recombined with the Vβ segment. The VβDβJβ segment produced constitutes the variable region of the future TCRβ chain. The VβDβJβ is then joined to the Cβ gene segment and, if the rearrangement is productive, this gene is transcribed and translated to produce a fully functional TCRβ chain containing all four segments. The TCRβ chain assembles with the pTα chain to produce the first TCR expressed by the DN immature thymocytes (called the pre-TCR). If the pre-TCR provides a complete activation signal to thymocytes, the TCRα gene loci rearrangement is initiated in order to produce a TCRα chain.

The TCRα gene locus is found on chromosome 14 and contains 47 variable (Vα), 57 junction (Jα) and 1 constant (Cα) gene segments. The rearrangement of the TCRα locus is similar to the TCRβ however there is no D gene segment. The process starts first with the joining of the Jα and the Vα segment. If rearrangement of the TCRα gene on the first chromosome does not produce a functional TCR in terms of producing a positive selection signal then rearrangement can take place on the second chromosome. This results in the possible expression of two different TCRαβ with an identical TCRβ chain in the periphery (Padovan et al., 1993, Petrie et al., 1993). Unsuccessful rearrangement of a functional TCRα gene from either chromosome leads to apoptosis. Overall, V(D)J rearrangement of human αβ TCR genes can theoretically produce over 10^{18} TCR combinations (Sewell, 2012). In reality, the number of αβ TCRs *in vivo* is much smaller than this theoretical possibility and the human TCRαβ repertoire is estimated to be $2.5x10^{7}$ (Arstila et al., 1999).

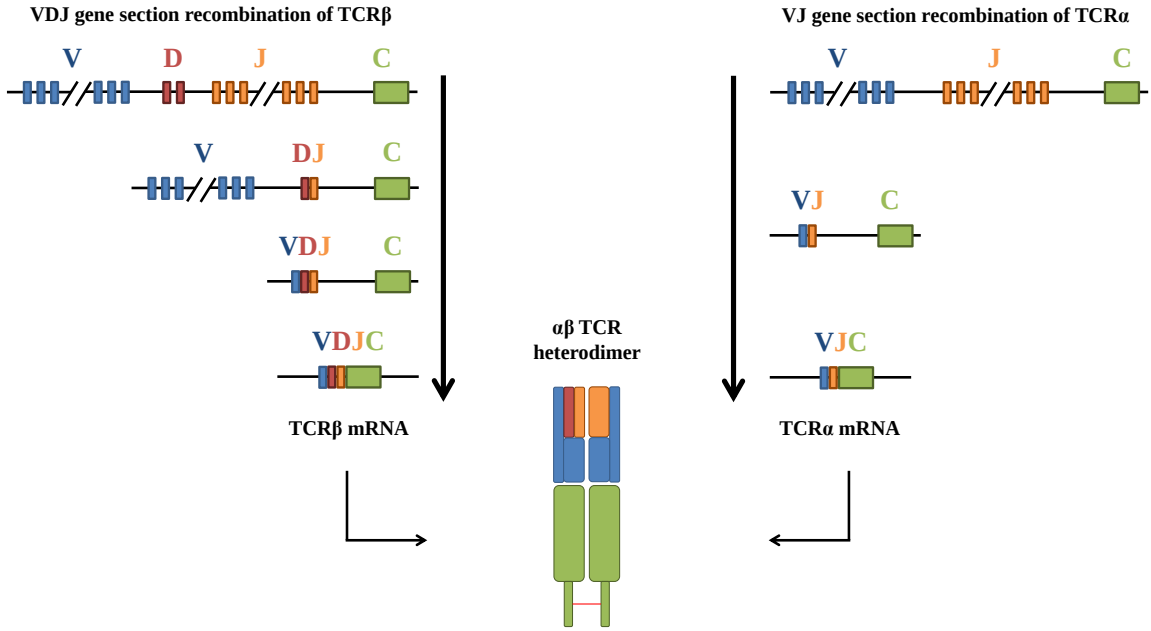

Figure 1.7 Steps of the V(D)J gene section recombination to produce a functional αβ TCR heterodimer.

The somatic TCR gene arrangement starts with the recombination of the V and D gene segments. This step occurs only in the TCRβ locus as the D gene segment is inexistent in the TCRα locus. Newly formed VD segment rearranges with the J segment to form the VβDβJβ in the TCRβ locus and VαJα in the TCRα locus and are incorporated in the respective C segment. Newly rearrange TCRβ and TCRα genes formed are expressed at different stage of the T-cell development to form a fully functional αβ TCR heterodimer.

1.7 Unconventional T-cells

Recent studies have described T-cells that do not recognise conventional pMHC ligands; these T-cells are described as being 'unconventional'. In some cases, there is compelling structural evidence for the recognition of unconventional T-cell ligands (Uldrich et al., 2013, Kjer-Nielsen et al., 2012). Some unconventional T-cells recognise lipids presented by the CD1 family proteins. This family is composed of two groups. Group 1 CD1 comprise CD1a, CD1b and CD1c while CD1d is in group 2. Recent structural studies have documented how some αβ TCRs can recognise lipids presented by the non-classical MHC (MHC1b) molecule CD1d (Uldrich et al., 2013). Other αβ TCRs are restricted by another MHC1b molecule called MR1 (Kjer-Nielsen et al., 2012). MR1-restricted T-cells are called mucosal associated invariant T-cells (MAITs). It is not yet clear how many types of different unconventional T-cell types there are. Some key, recently discovered, unconventional T-cells are described below.

1.7.1 CD1d-resricted T-cells (NK T cells)

Classical type I NK T-cells are restricted by the group 2 CD1 molecule CD1d and express an invariant TCRα chain Vα24 Jα18 paired with Vβ11 chain in human (Bendelac et al., 2007). The first antigen discovered for type I NK T-cells was the glycosphingolipid α-galactosylceramide (α-GalCer) loaded on CD1d (Bendelac et al., 1995, Borg et al., 2007). However, other ligands have been identified such as bacterial glycolipids also presented by the CD1d platform (Godfrey et al., 2010b).

Another NK T-cell class has been identified in the last decade. Type II NK T-cells are also known to be restricted by CD1d. Type II NK T-cells recognise hydrophobic compounds including sulfatides (Jahng et al., 2004) and non lipid molecules (Godfrey et al., 2010a). Type II NK T cells also express an invariant αβ TCR (Vα3.2 Jα9 or Vα8Jα9 associated with Vβ8).

NK T-cells are mainly specialised in cytokine production. Interestingly, the nature of the cytokine released depends on the tissues and microenvironment (Godfrey et al., 2000). Recent studies have highlighted that some NK T-cell are involved in suppression of tumour rejection (Berzofsky and Terabe, 2008) and the inhibition of autoimmunity (Jahng et al., 2004).

1.7.2 Group 1 CD1-restricted T-cells

While, numerous studies have been aimed at unravelling the mysteries of NK T-cells, relatively few have explored the T-cell subsets restricted by group 1 CD1 family molecules (CD1a, CD1b and CD1c). Interestingly, this population is surprisingly important in peripheral blood. Indeed, they can represent from 1/300 to 1/10 of peripheral T-cells and are known to be present in the CD4 and $CD4^-/CD8^-$ double negative (DN) population (Bendelac et al., 2007, de Lalla et al., 2011). Their role has only been assessed recently and was shown to share features with T_H1 cells.

1.7.3 MR1-restricted T-cells MAITs

This recently discovered group of unconventional T-cells possess an invariant TCR designed for the detection of bacterially-infected cells through the monomorphic MHC Ib molecule MR1 (Gold et al., 2010). Mucosal associated invariant T-cells (MAITs) are classified as innate cells due to their restricted TCR repertoire but share characteristics of adaptive immunity such as acquirement of memory phenotype (Martin et al., 2009), cytolytic activity (Bendelac et al., 2007) and undergo thymic selection (Gold et al., 2013). MAITs are also found in high frequencies in the liver (~45%) and low frequencies in peripheral blood (1-4% of the total lymphocytes) (Martin et al., 2009). Like NK T-cells, they express an invariant TCRα chain Vα7.2 Jα33 that associates chiefly with Vβ2 and Vβ13 chains. MAIT biology is discussed in detail in chapter 4.

1.8 Mycobacteria

My work aimed at examining T-cell responses to intracellular bacteria with special emphasis on mycobacteria. I will describe these bacterial species including their phylogenetic nomenclature, the diseases they cause and how the immune is system intimately involved in their transmission.

1.9 Mycobacteria classification

Mycobacteria are gram-positive, aerobic bacteria that belong to the family of *Mycobacteriaceae* and to the genus *Mycobacterium*. The *Mycobacterium* genus contains more than 120 species. The vast majority of these species are non-pathogenic such as the well-studied *Mycobacterium smegmatis* (*M. smegmatis*).

However, certain species such as *Mycobacterium tuberculosis* (*M. tuberculosis*), *Mycobacterium bovis* (*M. bovis*) and *Mycobacterium leprae* (*M. leprae*) are virulent human and animal pathogens. *Mycobacterium* species can be classified into two major groups – slow growing and fast growing species. There are also several different *Mycobacterium* subclasses (Grange and Yates, 1986). (see **Table 1.2**). I will describe details of the three pathogenic *Mycobacterium* species below as these important species have been studied extensively.

Slow growing species			**Fast growing species**		
***Mycobacterium Tuberculosis* complex**	***Mycobacterium Avium* complex**	**Ungrouped**	***Mycobacterium fortuitum* clade**	***Mycobacterium parafortuitum* clade**	**Ungrouped**
-M. Tuberculosis *-M. bovis* *- M. affricanum*	*- M. avium* *- M. avium paratuberculosis*	*-M leprae* *- M. marinum*	*-M. fortuitum* *-M. senegalense* *- M. brisbanense*	*- M. parafortuitum* *- M. fortuitum*	*- M. smegmatis* *- M. elephantis*

Table 1.2 Categorisation of important *Mycobacterium* species.

1.10 *Mycobacterium tuberculosis*

1.10.1 *M. tuberculosis* infection

M. tuberculosis is an important human pathogen that is transmitted between individuals via air droplets. Once inhaled, *M. tuberculosis* targets phagocytic cells found in the lung alveoli. *M. tuberculosis* infection is mainly characterised by an intense cough, fever and, in advance stages of the disease, severe diarrhoea. The disease associated with *M. tuberculosis* infection is called Tuberculosis (TB). TB severity varies with the dose of infection and the efficiency of an individual's immune system. 10 to 25 % of TB infections are extra-pulmonary and affect mainly people with weakened immune systems particularly HIV-infected individuals. This form of TB infection is characterised by the dissemination of *M. tuberculosis* toward other organs such as lymph node, pleura and osteoarticular sites (Golden and Vikram, 2005).

Even though TB mortality has steadily decreased since 1990, it still represents a major global disease burden. In 2012, the World Health Organisation estimated that 1.3 million people died and more than 8.7 million fell ill as a result of *M. tuberculosis* infection. Moreover, co-infection with HIV has dramatically escalated in the developing countries. Pockets of TB infection can be found in the United States, Europe, some areas of former Soviet Union and the UK (WHO Global tuberculosis report 2014-Executive summary). *M. tuberculosis* infection is characterised by different steps that I will briefly described in the following sections.

1.10.2 *M. tuberculosis* transmission

The human immune system plays a key role in *M. tuberculosis* transmission. As previously mentioned, *M. tuberculosis* is transmitted via the airways and infects mainly phagocytic cells such as monocytes, neutrophils, dendritic cells and macrophages located in the lungs (Kang et al., Wolf et al., 2007). As such, the recruitment of neutrophils during the first stage of the infection is beneficial to the expansion of *M. tuberculosis*. Progressive accumulation of dead neutrophils and live bacteria forms structures called granulomas in the lungs (Davis and Ramakrishnan, 2009). The bacilli remain in the granulomas and are excreted via the airways for transmission. After entry in the lung, *M. tuberculosis* and macrophages compete against each other for survival. In about 15% of *M. tuberculosis* infected patients, the bacilli can traffic to other organs leading to the development of an acute disease called extra-pulmonary TB (Peto et al., 2009). *M. tuberculosis* infection is often divided in different stages as described below.

1.10.2.1 Phagocytosis of M. tuberculosis by monocytes/ macrophages

Recognition of *M. tuberculosis* by innate immune cells is initiated by the binding of *M. tuberculosis* PAMPs to cell surface Toll-Like Receptors (TLRs) (Banaiee et al., 2006, Bafica et al., 2005). Upon *M. tuberculosis* recognition, these cells release cytokines and chemokines to produce a pro-inflammatory environment that promotes recruitment of monocytes and macrophages at the site of infection (Cooper et al., 2011). Once recruited, macrophages phagocytose the bacteria through interactions between *M. tuberculosis* cell surface glycoproteins and cell surface complement receptors or mannose receptors (Schlesinger et al., 1994) or via Fc receptor binding to antibody opsonised bacteria (Cosma et al., 2003). This interaction results in the phagocytosis of the bacillus by specialised vesicles called endosomes (Cohn, 1963).

The survival of *M. tuberculosis* requires the inhibition of certain macrophage intracellular pathways specialised in the maturation of phagolysosomes. These pathways include disruption of endosome trafficking towards lysosomes (Hart et al., 1972); the fusion of phagosomes with lysosomes (Hart et al., 1972); and inhibition of macrophage apoptosis which is beneficial for *M. tuberculosis* persistence in host (Blomgran et al., 2012). Once these pathways are inhibited, *M. tuberculosis* resides and multiplies in early endosomal compartments until macrophages enter apoptosis and are targeted by innate immune cells that are in turn infected; thereby spreading the infection. *M. tuberculosis* is propagated via a vicious circle that transmits infection from macrophage to macrophage by manipulating their life cycle.

1.10.2.2 Equilibrium between M. tuberculosis and the adaptive immune system

A delayed onset of the adaptive immune response is observed during TB infection. Lymphocytes can take up to 40 days before being recruited and activated by *M. tuberculosis* epitopes (Poulsen, 1950). This delay could be partially explained by the inhibition of *M. tuberculosis*-infected DC migration toward lymph nodes delaying the presentation of *M. tuberculosis* epitopes to CD4 T-cells (Blomgran and Ernst, 2011). Moreover, a large population of *M. tuberculosis* specific regulatory T-cells (T_{reg}) can be detected during *M. tuberculosis* infection and could delay CD4 and CD8 T-cell migration toward the lungs (Shafiani et al., 2010). Boosting of adaptive immune cells with *M. tuberculosis* decreases bacterial load and TB symptoms in most individuals. This phase is called TB latency and is characterised by the control of the bacillus growth by the immune system but a failure to clear it.

Studies have highlighted various mechanisms involved in the persistence of *M. tuberculosis* in the host. It is thought that inhibition of MHC II expression by *M. tuberculosis* infected macrophages could delay the presentation of *M. tuberculosis* epitopes to CD4 T-cells (Egen et al., 2011, Noss et al., 2001). Individuals with latent TB are not thought to transmit infection. However, ~10% of individuals with latent TB infection will go on to develop active TB later in life (Schwartzman, 2002) and can then spread infection.

1.10.2.3 Reactivation of M. tuberculosis

M. tuberculosis-infected individuals can develop an active disease after an asymptomatic period due to disruption of *M. tuberculosis* latency. *M. tuberculosis* reactivation produces an active, transmissible disease state and occurs in around 5-10% of latently infected individuals (Schwartzman, 2002). Various conditions are known to increase the risk of reactivation. The main risks of *M. tuberculosis* reactivation are associated with immuno-suppression due to HIV virus (Kwan and Ernst, 2011), chemotherapy or immunotherapy (Nadkarni et al., 2007). There is also an enhanced risk of reactivation in elderly patients thought to be due to the ageing of the immune system.

1.10.3 Clearance of *M. tuberculosis*

Most patients infected with *M. tuberculosis* do not exhibit symptoms of TB and either live with a latent asymptomatic TB disease or clear the bacterium. Efficiency of the immune system in the clearance and containment of the bacterium is mediated by the inflammatory environment that drives anti-microbial innate and adaptive immunity. Studies have described the role of IFNγ, TNFα and vitamin D as crucial for *M. tuberculosis* containment. Indeed, an IFNγ-mediated immune response promotes the activation of macrophages and CTLs. In macrophages, IFNγ promotes maturation of phagolysosomes and favours antigen presentation to T-cells (MacMicking et al., 2003) and the production of nitric oxide (NO) (Chan et al., 1992) essential for degradation of bacteria. Furthermore, vitamin D induces expression of a protein called LL-37 by macrophages. LL-37 contributes to the lysis of the bacterium (Martineau et al., 2007). Interestingly, vitamin D deficiency has been shown to be associated with active TB. Thus a combination of cytokines and vitamins is thought to aid the clearance of *M. tuberculosis* by the innate immune system. Unfortunately 5-10 % of infected patients still develop active TB disease.

1.10.4 Treatment of *M. tuberculosis* infection

The introduction of antibiotic treatments has decreased *M. tuberculosis* prevalence worldwide. *M. tuberculosis* infection is mainly treated with combinations of antibiotics such as isoniazid/rifampicin/pyrazinamide/ethambutol cocktails. However, the extensive use of these antibiotics has triggered multidrug resistance *M. tuberculosis* strains (MDR-*M. tuberculosis*).

A prophylactic *M. tuberculosis* vaccine was developed in the beginning of the 20th century by a French research group using an attenuated strain of *Mycobacterium bovis* (*M. bovis*) called Bacille Calmette-Guerin (BCG) vaccine. The vaccine, its efficacy and limitations will be discussed in section 1.10.6.

1.10.5 *Mycobacterium bovis*

M. bovis is a slow growing Mycobacterium closely related to *M. tuberculosis*. *M. bovis* mainly infects animals including cattle, badgers and cats where it induces a TB disease. Transmission of *M. bovis* from animal to human was a major problem prior milk pasteurisation and still represents one of the biggest challenges facing the cattle farming industry. Indeed, *M. bovis* can contaminate humans via aerosols, meat and faeces. *M. bovis* related-TB symptoms in animals are very similar to those triggered by *M. tuberculosis* in human. An attenuated form of *M. bovis* called BCG has been used as a human TB vaccine for almost 100 years.

1.10.6 BCG vaccine

The Bacillus Calmette Guerin (BCG) vaccine is an attenuated strain of *M. bovis* developed in the early 1920's by Calmette and Guerin at the Pasteur institute in France to prevent TB infection. The vaccine was obtained after subculturing *M. bovis* for 39 passages in potato media. BCG vaccine effectively reduces transmission of *M. bovis* between animals (Calmette, 1931, Wedlock et al., 2007, Hope et al., 2011). During attenuation the bacillus has been shown to have lost several immunogenic virulence factors necessary for survival inside macrophages.

BCG vaccine efficacy has been mixed and disappointing in preventing TB in adult populations (varies between 0% in south India and 80% in the UK) (Rodrigues and Smith, 1990, Colditz et al., 1994)). Nevertheless, the vaccine is believed to have contributed to the eradication of tuberculosis in Europe and has shown good protection in infants (Zodpey et al., 1998, Colditz et al., 1995). BCG vaccine is protective against *Mycobacterium leprae* (Merle et al., 2010). Different hypotheses have been suggested to explain the low efficacy of BCG vaccination in TB. It has been suggested that exposure to environmental *Mycobacterium* species could confer protection against *M. tuberculosis*.

Thus, the benefits of BCG vaccination could be masked by the natural exposure to TB antigens (the *masking hypothesis*) (Palmer and Long, 1966, Andersen and Doherty, 2005).

Another hypothesis postulates that a previous natural immunisation to *M. tuberculosis*-like antigens could prevent the replication of BCG bacilli after injection. Thus, the load and duration of BCG antigen presentation to the immune system is decreased resulting in reduced potency (the *blocking hypothesis*) (Brandt et al., 2002). Studies have also shown that the efficacy of the BCG vaccine is dramatically reduced in *M. tuberculosis*-HIV co-infected individuals where immune integrity is compromised (Arbelaez et al., 2000).

1.11 *Mycobacterium leprae*

Mycobacterium leprae is the causative agent of Leprosy and currently affects 1 in 10,000 of the global population (W.H.O.-leprosy). Leprosy has highly variable clinical manifestations that oscillate between two polar forms. Interestingly, the adaptive immune system signature varies within this spectrum of leprosy forms. The first form is known as tuberculoid leprosy and is characterised by the generation of granulomas in the lungs and nerve damage due to the immune-mediated destruction of *M. leprae* infected Schwann cells in peripheral nerves. This forms triggers a high cell-mediated T_H1 immune response that maintain minimum symptoms and possibly clear the bacilli. However, at the other end of the spectrum, the more pathogenic clinical form is called lepromatous leprosy. Lepromatous leprosy induces mainly a T_H2 response and fails to activate a T_H1 response resulting in severe symptoms such as numerous skin lesions and nerve destruction (Britton and Lockwood, 2004, Cosma et al., 2003). Dissection of the T-cell subsets patients with leprosy showed the presence of many unconventional T-cells such as CD1 restricted and γδ T-cells (Layre et al., 2009, Willcox et al., 2007).

Due to its slow growth and host dependency, *M. leprae* is difficult to expand *ex vivo*. However, *M. leprae* can be cultivated in the footpads of mice and armadillos providing good source of bacilli (Shepard, 1960, Kirchheimer and Storrs, 1971). The development of multidrug therapies such as antibiotic cocktails has dramatically decreased leprosy prevalence worldwide. However, leprosy is still a health problem in developed countries where more than 200,000 new cases emerge every year (W.H.O.-leprosy).

1.12 Aims

T-cells orchestrate immunity and are pivotal to the removal of cells infected with intracellular pathogens. When I initiated my thesis studies there was renewed interest in the study of T-cell responses to *Mycobacterium tuberculosis* (*M. tuberculosis*). In particular, new 'innate-like', 'unconventional' T-cell populations such as MAITs were being strongly implicated as key immune cells during *M. tuberculosis* infection. My work was aimed at studying T-cell responses to mycobacteria. I used *Mycobacterium smegmatis* (*M. smegmatis*) as a model of *M. tuberculosis* infection as I was able to openly work with this non-pathogenic mycobacterium in the laboratory. I was particularly interested in documenting the breadth of T-cell responses raised against *M. smegmatis* and the division of these responses between conventional (HLA-restricted, peptide-recognising) and unconventional (non-HLA restricted, non peptide-recognising) T-cell populations. I believe that unconventional T-cells are particularly interesting because they do not rely on the HLA molecules that are known to vary widely throughout the population as described above. Unconventional T-cells recognise bacteria via non-polymorphic MHC-like molecules such as CD1a, CD1b, CD1c, CD1d and MR1. These molecules are invariant in the human population and therefore offer opportunities for pan population vaccination. The specific aims of this thesis are:

1. To define the frequency of conventional and unconventional T-cells generated during direct *ex vivo* exposure to intracellular mycobacteria.

2. To investigate the molecular and cellular mechanism by which unconventional MAIT cells recognise cells infected with Mycobacterium.

3. To undertake the first dissection of the molecular recognition of *M. tuberculosis* by a conventional TCR.

CHAPTER 2. MATERIALS AND METHODS

2.1 Cell culture

2.1.1 Mammalian culture media

R0 medium: RPMI (Invitrogen) supplemented with 100 international units (iu) of Penicillin and 100 µg of streptomycin (Invitrogen), 2mM L-glutamine (Invitrogen).

R2 medium: R0 medium supplemented with 2% Foetal Calf Serum FCS (Inactivated FCS; Life technology).

R10 medium: R0 medium supplemented with 10% FCS (Inactivated FCS; Life technology).

T-cell culture medium: R10 supplemented with 100 iu/mL of interleukin-2 (Novartis) and 25 µg/mL of interleukin-15 (Peprotech).

T-cell expansion medium: R10 supplemented with 20 iu/mL of interleukin-2 (IL-2; Novartis), 25 µg/mL of interleukin-15 (IL-15; Peprotech) and 1 µg/mL of purified phytohemagglutinin (PHA; Alere).

Red blood cell lysis buffer (pH 7.2-7.4): 155 mM NH_4Cl, 10 mM $KHCO_3$, 0,1 mM EDTA.

MACS buffer: D-PBS no $MgCl_2$, no $CaCl_2$ (Life Technology), 5 g/L BSA, 0.74 g/L EDTA.

Freezing buffer: 90% of FCS (Life Technology) and 10% of Dimethyl sulfoxide (DMSO; Sigma).

2.1.2 Preparation of human peripheral blood mononuclear cells (PBMCs) from blood

Peripheral blood was collected from healthy donors by venepuncture into a sterile falcon tube (Corning Life Science) containing heparin (LEO Laboratories Ltd) at a final concentration of 100 iu/mL of blood. Blood was layered onto an equal volume of a LymphoPrep (Sigma) solution (density 1.077 +/- 0.001 g/mL; Progen) and centrifuged for 20 minutes at 537 x g (Hareaus megafuge, 1.0 R) with the centrifuge brake turned off. PBMCs were layered above the LymphoPrep and collected with a 3 mL Pasteur pipette. PBMCs were washed with R10 medium (section 2.1.1) and centrifuged at 435 x g for 10 minutes. Red blood cells were lysed using the red blood lysis buffer (section 2.1.1) and incubated at 37 °C for 10 minutes then washed with R10 medium and centrifuged 5 minutes at 300 x g.

2.1.3 Origin of T-cells used in this thesis

CD8 T-cell clones used throughout this thesis are listed below in **Table 2.1**. D426 B1 and D454 CD8 T-cell clones were provided by Prof. David Lewinsohn, Oregon Health and Science University, Portland. Morpheus was extracted from D426 B1.

Name clone	**HLA Restriction**	**Natural Epitope**	**TCR (Arden)**	**Origin :Organism/Protein (owner)**
D426 B1	MR1	unknown	Defined in chapter 4	*M. tuberculosis* (Lewinsohn, D. et al.)
D454	A*0201	LLDAHIPQL	Vα 2.1 Vβ 16.1	*M. tuberculosis*/Esx-G (Lewinsohn, D. et al.)
Morpheus	-	-	Vα 1.4 Vβ 24.1	Originate from the D426 B1 line/*M. tuberculosis*/Esx-G (Lewinsohn, D. et al)
NLV4-10	A*0201	NLVPMVATV	V β 13.1	Cytomegalovirus pp65 protein (Garry Dolton et al.)

Table 2.1 List of human CD8 T-cells used throughout this thesis.

2.1.4 Expansion and maintenance of CD8 T-cell clones

CD8 T-cell clones were expanded from existing culture or cryopreserved stocks in a T-25 tissue culture flask (Greiner bio-one) at a concentration of 1 x 10^6 CD8 T-cell clones into 15 mL of an expansion mixture. The expansion mixture was prepared as follows: 15 x 10^6 allogeneic PBMCs (obtained from a minimum of three healthy donors) were γ-ray irradiated at 3000 centi-gray (Caesium source) and washed with 50 mL of R10 medium at 300 x g for 10 minutes. The allogeneic PBMCs were then resuspended in 15 mL of T-cell expansion media (section 2.1.1) and added to 1 x 10^6 CD8 T-cells. The cells were incubated at 37°C and 5% CO_2. After 5 days, half of the media was exchanged with T-cell culture media (section 2.1.1). CD8 T-cell clones were used in assays after a minimum of 8 days following the expansion protocol to allow TCRs to be up-regulated to the T-cell membrane.

2.1.5 Extraction of IRAPVLYDL specific T-cells from D426 B1 by IFNγ secretion assay and limiting dilution

2.1.5.1 IFNγ secretion assay

IRAPVLYDL specific T-cells were extracted from D426 B1 clone using IFNγ secretion assay, Cell enrichment and detection kit (PE) from Miltenyi Biotec. Before proceeding to the IFNγ secretion assay, D426 B1 cells were washed once in R0 medium (section 2.1.1) and centrifuged at 300 x g for 5 minutes, resuspended into R2 medium and rested overnight at 37 °C and 5% CO_2. 1 x 10^6 cells were plated in a single well 96 round bottom well plate (Greiner bio-one) in R2 medium, pulsed with 50 μM of IRAPVLYDL and incubated 4 hours at 37˚C and 5% CO2. The cells were washed with 10 mL of cold MACS Buffer and centrifuged at 300 x g for 10 minutes. The supernatant was removed and the pellet was resuspended in 80 μl of cold R2 medium and 20 μl of IFNγ Catch Reagent (anti-IFNγ monoclonal antibody; (mouse IgG1) conjugated to cell surface specific monoclonal antibody (mouse IgG2a); Miltenyi Biotec). The cells were mixed thoroughly and placed on ice for 5 minutes. 10 mL of 37°C warm R2 medium were added and the cells were incubated 45 minutes at 37˚C and 5% CO2, whilst rotating. Antibody treated cells were washed with cold MACS buffer and centrifuged at 300 x g for 10 minutes.

The pellet was treated with 80 µl of cold MACS buffer and 20 µl of IFNγ Detection antibody (PE) (anti-IFNγ monoclonal antibody (mouse IgG1) conjugated to R-phycoerythrin (PE); Miltenyi Biotec) and were placed on ice for 10 minutes. Another wash with MACS buffer followed by a centrifugation step at 300 x g for 10 minutes was performed. The cell pellet was re-suspended in 80 µl of cold MACS buffer and 20 µl of anti-PE micro-beads (Miltenyi Biotec). Cells were incubated at 4°C whilst rotating for 15 minutes. Cells were washed with 10 mL of cold MACS buffer and centrifuged at 300 x g for 10 minutes. The supernatant was removed. Cells were then resuspended in 500 µl of cold MACS buffer and run through an MS column (Miltenyi Biotec). IFNγ specific labelled cells were extracted through the MS column using a magnetic field (Miltenyi Biotec). IFNγ specific labelled and unlabelled cells were rested separately in T-cell culture medium overnight.

2.1.5.2 T-cell limiting dilution

Post sorting as described above, both IFNγ specific and unspecific T-cells were cloned at a concentration of 0.5 cells per single well of a round bottom-well plate (Greiner bio-one) and expended in T-cell expansion media as detailed in section 2.1.1. Cells were incubated at 37 °C and 5% CO_2 for 5 days before the medium was changed for the T-cell culture media.

2.1.6 Boosting of PBMCs with *M. smegmatis*

2.1.6.1 Phagocytosis of M. smegmatis by antigen presenting cells

Chosen antigen presenting cells (APCs) were incubated with R10 medium lacking penicillin/streptomycin. APCs were incubated with *M. smegmatis* for 2 hours at a concentration of 3.5 x 10^6 APC to 35 x 10^6 cfu *M. smegmatis* (MOI 10 x *M. smegmatis* cell for 1 x APC (10:1)) in 10 mL of R10 medium lacking penicillin/streptomycin in a T-75 (Greiner bio-one) to allow phagocytosis. Following the phagocytosis, the cells were incubated for 2 hours with 100 units/mL of penicillin and 100 µg/mL of streptomycin (Life technology). APCs were washed 3 times with R10 medium and treated with PBS supplemented with 2 mM EDTA prior to removal from the tissue culture plastic. Cells were than washed twice with R10 medium and centrifuged at 300 x g for 5 minutes and resuspended in R10 medium to be used in assays.

2.1.6.2 Boosting of PBMCs with M. smegmatis infected autologous dendritic cells

PBMCs from a healthy donor were extracted from peripheral blood. Half were cryopreserved into 1 mL of freezing buffer. Monocytes were extracted from the other half and used to generate dendritic cells (DCs).

Monocyte differentiation into dendritic cells

Monocytes were extracted from healthy PBMCs obtained from peripheral blood using anti-CD14 antibody magnetic beads (Milteny biotec). CD14 positive cells were cultured at 2 x 10^6 per well in a 6 well plate in 5 mL of R10 medium supplemented with 100 ng/mL of recombinant human GM-CSF (Peprotech), 50 ng/mL recombinant human IL-4 (Peprotech). After 3 days, half of the medium was renewed. After 6 days of incubation, the differentiation status of monocytes into DCs was assessed by flow cytometry by measuring the expression of the following cell surface markers: CD209, CD1a and CD14. Cells were stained with 2µL of anti-CD209 (eBioscience), 2µL of anti- CD1a (eBioscience) and 2µL of anti-CD14 (eBioscience) antibodies and analysed by flow cytometry (**Figure 2.1**). DCs were then co-cultured with *M. smegmatis* using the protocol detailed in section 2.1.6.1.

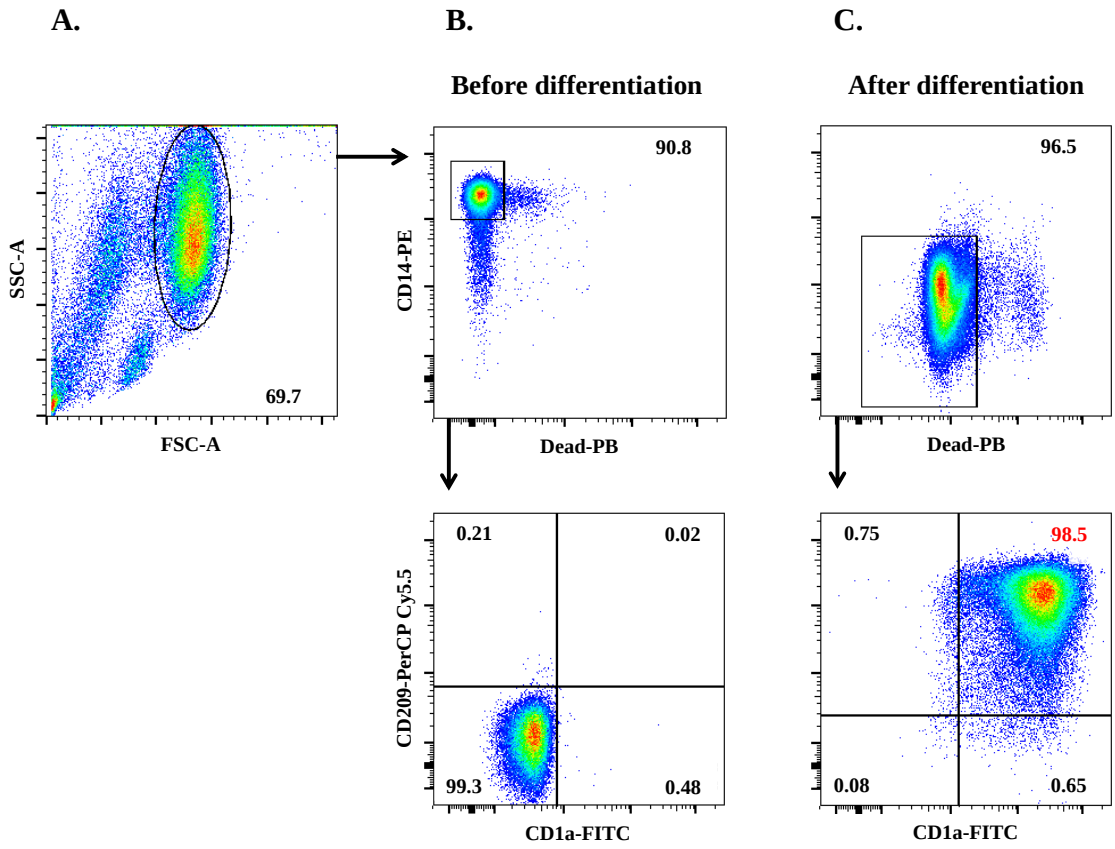

Figure 2.1. Differentiation "status" of monocytes into dendritic cells.
Monocytes (**A.**) extracted from PBMCs as explained above were tested for their expression of CD14 marker before differentiation (**B. top quadrant**) and after differentiation (**C. top quadrant**) protocol was applied. The expression of CD209 and CD1a marker was tested for $CD14^+$ monocytes before differentiation (**B. bottom quadrant**) and $CD14^-$ monocytes after differentiation (dendritic cells **C. Bottom quadrant**). The red percentage on **C. Bottom quadrant** correspond the percentage of dendritic cells.

Boosting of PBMCs with autologous DCs

Cryopreserved PBMCs were thawed out and were plated into 24 well plate at a concentration of 3.5 x 10^6 cells per 2 mL of T-cell culture media, one day before boosting. Cells were then counted and plated at 5 x 10^6 cells per well in a 24 well plate and co-cultured with 2 x 10^5 *M. smegmatis* infected DCs in R10 medium supplemented with 20 iu/mL IL-2. Half the media was replaced every 3 days for 13 days.

2.1.6.3 Boosting of PBMCs with M. smegmatis infected A549 cells

PBMCs were extracted from blood and plated in R10 medium at a concentration of 5 x10^6 PBMCs for 2 x10^5 *M. smegmatis* infected A549 cells per well of a 24 well plate in R10 supplemented with 20 iu/mL IL-2. Half the media was replaced every 3 days.

2.1.7 Origin and culture of lymphoblastoid cell lines

The Hmy.2.C1R cell line, called C1R in this thesis, is a class I negative EBV transformed B cell line. A HLA-A*0201 expressing C1R (C1R-A2) cell line was generated in-house by colleagues (Wooldridge et al., 2005). C1R-A2 were cultured in R10 medium (section 2.1.1).

A549 is lung adenocarcinoma epithelial adherent cell line and can be cultured in R10 medium in flask (Greiner bio-one). Cells were scraped off the flask using EDTA 2 mM for 10 minutes at 37 °C. Cells were then washed with R10 medium and resuspended in a new flask at a concentration of 1 x 10^4 cells/cm^2. This step was repeated when the cell reached 90 % confluent.

Cell name	**HLA expression**	**Source**
C1R-A2	A*0201 C*4 (small amount expressed)	(Wooldridge et al., 2005)
A549	A*2501/3001 B*18/4403 C*1203/1601	More information:(Adams et al., 2005)

Table 2.2 Lymphoblastoid cell lines used in this thesis.

2.1.8 Confocal Microscopy

Coverslips (Warner Instruments) were added to the wells of a 24 flat bottom-well plate and treated with 500 µL of poly-L-lysin (Sigma Aldrich) for 5 minutes at RT. The solution was then removed from the well and the coverslips were washed twice with sterile water and dried at 37°C for 2 hours. 5 x 10^4 ± *M. smegmatis* A549 cells were added to each well and incubated for 3 hours in 500 µL of R10 to allow adherence of A549 cells to the coverslips. After incubation, cells were treated with 500 µL of a 2%-formaldehyde-PBS solution for 20 minutes followed by a wash with water. The coverslips were then removed from the plate and cells were put in a drop of Mowiol (Sigma Aldrich) between coverslip and a glass slide (Thermo Scientific). The slide was stored at 4°C in the dark and analysed for the GFP protein fluorescence emission at a wavelength of 495 nm using a Leica TCS SP5 confocal microscope (Leica Microsystems).

2.2 T-cell activation assays

2.2.1 Single peptide activation assay

CD8 T-cells were washed with R0 medium and rested in R2 medium overnight before being used in an activation assay. In single well of an 96 round bottom-well plate, 3 x 10^4 T-cells were primed with 6 x 10^4 APCs per 100 µL of R2 medium and a titration of peptide from 10^{-4} to 10^{-15} M for 13 hours at 37˚C and 5% CO_2. The 96 well plate was centrifuged at 35 x g to sediment cells to the bottom of the wells. 60 µl per well of supernatant was harvested and diluted with 60 µl of R2 medium. Supernatants were analyzed by MIP-1β enzyme-linked immunosorbent assay (ELISA) (described in section 2.2.4).

2.2.2 Combinatorial peptide library screening assays

2.2.2.1 Description of a nonamer combinatorial peptide library (CPL)

The nonamer CPL (Pepscan Presto) contains 180 nonamer peptide mixtures. Each mixture contains nonamer peptides with one amino acid fixed at one position and an equimolar mix of the 20 proteinogenic amino acids in all other positions. The cysteine residue was omitted from the random positions to avoid formation of disulphide bonds between peptides within the mixture and peptide aggregation.

Each mixture is composed of 1.7 x 10^{10} peptides and the whole library contains 5 x 10^{11} peptides and encompasses almost all possible nonamer peptides. T-cells were challenged with a nonamer library and their activation towards each mixture was evaluated by the release of MIP-1β chemokine or the IFNγ cytokine and measured by ELISA.

2.2.2.2 Screening T-cell clones using a nonamer peptide library

CD8 T-cells were washed with R0 medium and rested in R2 medium overnight. APCs were plated in single well of a 96 round bottom-well plate at a concentration of 6 x 10^4 APCs per 45 µl and pulsed with 5 µl of peptide mixture from a nonamer peptide library at a final concentration of 100 µM for 1 hour at 37°C and 5% CO_2. 3 x 10^4 CD8 T-cells per 50 µl were added to pulsed APCs. Plates were incubated overnight at 37 °C and 5% CO_2 and centrifuged at 35 x g for 5 minutes. 60 µl of supernatant were harvested and diluted in 60 µl of R2 medium and analysed by MIP-1β or IFNγ ELISA.

2.2.3 Chromium release assay

For a chromium (Cr^{51}) release assay, 2 x 10^6 APCs were washed with R10 medium. The dry pellet was incubated with 60 µCi of Cr^{51} for 1 hour at 37 °C and 5% CO_2, washed with 10 mL of R10 medium and centrifuged at 300 x g for 5 minutes. Cells were re-suspended into 5 mL of R10 medium and rested for an hour to release the excess of Cr^{51}. APCs were then washed with R10 medium and plated at a concentration of 2,000 APCs per 45 µl of R10 medium in single well of a 96 round bottom-well plate. Cells were pulsed with a titration of peptide from 10^{-4} to 10^{-15} M for 30 minutes at 37˚C. 1 x 10^4 T-cells were added to the pulsed APCs and incubated for 4 hours at 37˚C and 5% CO_2. 20 µl per well of supernatant were collected and added to 150 µl of Optiphase supermix scintillation cocktail (Perkin Elmer). The Cr^{51} radiation from the wells was measured using a Micro-$Beta^2$ counter (Perkin Elmer). Percentage cytotoxicity was then calculated using the following equation: Specific lysis= [(experimental lysis-spontaneous lysis)/(maximum lysis-spontaneous lysis)] x 100%.

2.2.4 Enzyme-linked immunosorbent assay (ELISA)

All antibodies used during the development of MIP-1β ELISA came from the DuoSet ELISA/ human CCL4/MIP-1β development system kit (R&D Systems). All washes were performed by an AquaMax 2000 microplate washer (MFS analytical technologies).

A half well flat bottom ELISA microplate (Corning Costar) was coated with 50 µl of a 1.5 µg/ml of mouse anti-human MIP-1β antibody (capture antibody) and incubated overnight at room temperature (RT). The plate was washed 3 times with 190 µl of 0.05% Tween 20-PBS (wash buffer) and 150 µl of a 1% BSA-PBS (diluent buffer) solution was added to each well. The plate was incubated for 1 hour at RT and washed 3 times with 190 µl of wash buffer and 50 µl of cell supernatant collected from an activation assay was added to wells. Furthermore, a recombinant human MIP-1β standard (R&D Systems) was titrated from 1,000 to 62.5 pg/ml. The plate was incubated 1 hour and 15 minutes at RT and washed 3 times with 190µl of wash buffer. The plate was then coated with 50 µl of a 50 ng/ml of a biotinylated goat anti-human MIP-1β antibody (detection antibody) and incubated 1 hour and 15 minutes at RT. The plate was washed 3 times with 190 µl of wash buffer and 100 µl of a streptavidin conjugated to horseradish-peroxidase was added to the wells. The plate was incubated 20 minutes followed by 3 washes with wash buffer. 100 µl of a 1:1 ratio colour reagents A and B (R&D Systems) were added to the wells and incubated for a maximum of 20 minutes. The reaction was blocked by adding 50 µl of a H_2SO_4 solution. The OD_{450} of each well was read using a Bio-rad iMark microplate reader with correction set to 570 nm.

2.2.5 Enzyme linked immunospot (ELISpot) assay for IFNγ

All antibodies and reagents used during the development of IFNγ ELISpot came from the ELISpot assay kit (ALP) for human IFNγ from Mabtech. All antibodies were diluted in D-PBS (Life Technologies). Development buffers (alkaline phosphatase development buffers) came from Bio-rad. The plate was washed with 150 µl of sterile D-PBS (Life Technologies).

A PVDF-backed plate (Millipore) was coated with 50 µl of a 10 µg/ml coating antibody (1-D1K) and incubated 4 hours at 37˚C or overnight at 4 °C. ELISpot plates were washed 5 times, blocked with 100 µl of 10% FCS (Inactivated FCS; Invitrogen) and incubated at RT for 1 hour in foil. After the media was decanted, T-cells were added to each well and incubated with either *M. smegmatis* infected APCs or peptide overnight at 37˚C in foil with appropriate controls. After 5 washes, 50 µl of a 1 µg/ml biotinylated monoclonal antibody 7-B6-1-biotin was added to each well and incubated 2 hours at RT in the dark. The plate was washed 5 times and incubated with 50 µl of a 1 µg/ml per well of a streptavidin-alkaline phosphatase and incubated 2 hours at RT in the dark. After 5 washes, 50 µl of substrate solution was added to the wells and the plate was incubated 30 to 45 minutes in the dark at RT followed by 3 washes. A mixture of alkaline phosphatase buffers (Bio-rad) were added to the wells to reveal the spots left by IFNγ secreting cells. Spots were counted using an automated ELISpot Reader System ELR02 (Autoimmune Diagnostika).

2.2.6 Intracellular staining (ICS)

Cells were washed with R0 medium and plated overnight in R2 medium. Cells were treated with Golgi Plug (Brefeldin A; BD) (0.5 µL per mL of cell culture), Golgi Stop (Monensin; BD) (0.7 µL per mL of cell culture) and CD107a-FITC antibody (5 µL per mL of cell culture) and plated into single well of a 96 well round bottom plate at a concentration of 3 x 10^5 cells per 100 µL of R2 medium per well. Cells were stimulated with either 50 µM of peptide or 3 x 10^5 *M. smegmatis* infected APCs and incubated for 5 hours at 37°C and 5% CO_2. After 3 washes with PBS, cells were then stained with dead cell marker Vivid-Pacific Blue (see concentration and brand in table 2.2) and incubated for 5 minutes in the dark and then stained with cell surface markers antibodies using adequate concentration (table 2.2) and incubated for 20 minutes at 4 °C.

Marker	Color	Brand	Clone	concentration per 300 000 cells/50µL PBS
CD8	APCCy7	Miltenyi Biotec	BW135/80 (mouse IgG2a)	2 µL
	APC	Miltenyi Biotec	BW135/80 (mouse IgG2a)	2 µL
	PE	Miltenyi Biotec	BW135/80 (mouse IgG2a)	2 µL
	Vioblue (PB)	Miltenyi Biotec	BW135/80 (mouse IgG2a)	2 µL
	Brill Vio 421	Biolegend	RPA-T8 (Mouse IgG1)	1 µL
CD4	FITC	Miltenyi Biotec	VIT4 (mouse IgG2a)	2 µL
	APC	Miltenyi Biotec	VIT4 (mouse IgG2a)	2 µL
	PECy7	Miltenyi Biotec	VIT4 (mouse IgG2a)	1 µL
	Brill Vio 421	Biolegend	RPA-T4 (Mouse IgG1)	1 µL
CD3	PerCP	Miltenyi Biotec	BW264/56 (mouse IgG2a)	2 µL
	PerCP	Biolegend	UCHT1	1 µL
CD19	PB	Biolegend	HIB19 (Mouse IgG1)	2 µL
CD14	PB	Biolegend	M5E2 (Mouse IgG2a)	2 µL
CD56	FITC	Miltenyi Biotec	REA196	2 µL
MR1	-	Hansen, T. et al.	26.5 (Mouse IgG2)	50 µg/mL
Goat α-mouse Ig	FITC	BD Bioscience	Polyclonal	2 µL
	APC	BD Bioscience	Polyclonal	2 µL
	PE	BD Bioscience	Polyclonal	2 µL
Vivid green	PB	Life Technologies	x	2 µL (from 1/40 dilution in PBS)
Aqua	Am-cyan	Life Technologies	x	2 µL (from 1/40 dilution in PBS)

Table 2.3 Cell surface marker antibodies.

The staining was followed by 3 washes with a solution of PBS supplemented with 2% FCS. Cells were treated with Cytofix/Cytoperm for 20 minutes on ice and washed with Perm/Wash solution (1X; BD). Cells were then stained for intracellular markers including cytokine (MIP-1β, IFNγ and TNFα) and other cell markers (see table 2.3 for concentrations). Stained cells were then washes 3 times with Perm/Wash buffer (BD) and then resuspended in 1% formaldehyde in PBS. Analysis of the results was carried out using the FACS Canto II (BD) and Flowjo software (Treestar Inc Ashland Oregon).

Marker	Color	Brand	Clone	Concentration for 300 000 cells/50µL PBS
αβTCR	PE	Biolegend	IP26	2 µL
	FITC	Biolegend	IP26	2 µL
	APC	Biolegend	IP26	2 µL
γδTCR	PE	Miltenyi Biotec	11F2 (mouse IgG1)	2 µL
	FITC	Miltenyi Biotec	11F2 (mouse IgG1)	2 µL
	APC	Miltenyi Biotec	11F2 (mouse IgG1)	2 µL
W6/32	-	Abcam	W6/32	50 µg/mL
Vα 7.2	APC	Lewinsohn, D. et al	3C6	2 µL
CD107a	FITC	BD Biosciences	H4A3	1 µL
TNFα	PECy7	BD Bioscience	MAb11	0.5 µL
MIP-1β	PE	BD Bioscience	D21-1351	0.5 µL
IFNγ	APC	Miltenyi Biotec	45-15 (mouse IgG1)	0.5 µL

Table 2.4 Intracellular marker specific antibodies.

2.2.7 Carboxyfluorescein diacetate Succinimydyl Ester (CFSE)

CFSE powder (Invitrogen) was resuspended in ddH2O to give a 10 mM stock solution that was filtered and aliquoted. 1 x 10^6 cells were re-suspended into PBS and CFSE was added to a final concentration of 1 µM. Cells were incubated at 37 °C in a water bath for 7 minutes and washed 3 times with PBS supplemented with 10% of FCS.

2.3 Flow cytometry

Cell surface markers and T-cell receptor expression on T-cells and cell lines were monitored by antibody and pMHC tetramer staining. The analysis was carried out by flow cytometry using a FACSCanto II (BD) and Flowjo software (Treestar Inc).

2.3.1 Fluorescent conjugated anti-human antibodies for detection of cell surface and intracellular protein expression.

The antibody concentration used to stain 3 x 10^5 cells is described in tables 2.2 and 2.3. Cells were washed with PBS in FACS tubes and resuspended in 50 μL of PBS to be stained first with a dead stain dye Vivid green or Aqua for 5 minutes at RT in the dark. Then cell surface markers were added to cells at concentration listed in tables 2.2 and 2.3 and incubated for 20 minutes on ice. Cells were then washed with PBS supplemented with 2% FCS and resuspended in 150 μL of PBS/2% FCS prior to flow cytometry.

2.3.2 pMHC tetramer staining of T-cell clones and PBMCs

3 x 10^5 cells were washed, re-suspended into 50 μL of PBS in a FACS tube. Cells were treated with 50 nM of the protein kinase inhibitor PKI dasatinib (Axon Medchem) for 30 minutes at 37 °C and 5% CO_2. Cells were then stained with 0.5-1 μg of PE - conjugated pMHC I tetramer for 30 minutes on ice followed by a wash with PBS supplemented with 2% FCS. After washing, cells were resuspended in 150 μL of PBS/2% formaldehyde and analysed by flow cytometry.

2.4 Bacterial culture and assays

2.4.1 Bacterial culture media and reagents

Luria-Bertani (LB) medium: 10 g/L tryptone (Fisher Scientific), 5 g/L yeast extract (Fisher Scientific), 5 g/L NaCl (Fisher Scientific) and supplemented with 50 mg/L carbenicillin (Sigma-Aldrich).

LB agar plate medium: 15 g/L agar bacteriological (Oxoid), 10 g/L tryptone (Fisher Scientific), 5 g/L yeast extract (Fisher Scientific), 5 g/L NaCl (Fisher Scientific) and supplemented with 50 mg/L carbenicillin (Sigma-Aldrich).

TYP media: 16 g/L tryptone (Fisher Scientific), 16 g/L yeast extract (Fisher Scientific), 5 g/L potassium phosphate dibasic (Acros organics).

Lemco culture media: 5 g/L Lemco powder (Oxoid), 10 g/L tryptone (BD), 5 g/L NaCl (Fisher Scientific), 0.5 mL/L Tween 80 (Sigma-Aldrich).

Lemco agar plate: 5 g/L Lemco powder (Oxoid), 10 g/L tryptone (BD), 5 g/L NaCl, 15 g/L agar bacteriological (Oxoid).

TFB1 solution: 30 mM KOAc, 50 mM MnCl2, 100 mM KCl pH 5.8, 10 mM CaCl2 and 15% v/v glycerol.

TFB2 solution: 10 mM Na-MOPS pH7, 10 mM KCl, 75 mM CaCl2 and 15% v/v glycerol.

2.4.2 Bacterial strains

2.4.2.1 Escherichia coli strains

Rosetta 2 (DE3) pLysS *Escherichia coli* (*E.coli*) (Novagen) competent cells were used for protein expression and were grown in TYP medium.

One Shot (TOP10) *E.coli* (Invitrogen) competent cells were used as host for DNA amplification and were grown in TYP medium.

2.4.2.2 Mycobacterium smegmatis strains

***Mycobacterium smegmatis* (*M. smegmatis*)** (mc^2155 strain) was offered by Prof Tim Walsh and Dr Matthias Eberl.

***M. smegmatis-gfp*$^+$** (mc^2155 strain expressing GFP (pFLAME7)) was offered by Prof Tim Walsh and Dr Matthias Eberl.

2.4.3 Mycobacterium smegmatis culture

10 mL of Lemco media was inoculated using a sterile loop. The growth curve was assessed as described in chapter 3 to evaluate the *M. smegmatis* expansion phases by measuring the OD_{600} at 3 to 10 hours intervals. A sample of culture was plated onto Lemco agar plate to evaluate the concentration of bacteria. The optimum time of culture was taken during the expansion phase and chosen according to the growth curve.

2.4.4 Escherichia coli culture

2.4.4.1 Making competent E. coli cells

E. coli cells were plated onto an LB agar plate and incubated at 37°C overnight. A single colony was picked and added to 200 mL of LB medium to be cultured to an OD_{600} of 0.4-0.6. Cells were then centrifuged at 1333 x g for 20 minutes at 4°C and the pellet was washed in 40 mL of ice cold TFB1 solution and centrifuged. Cells were then resuspended in 20 mL of ice cold TFB2 solution and aliquoted into pre-chilled eppendorf tubes and stored at -80°C.

2.4.4.2 Transformation of competent bacteria

Transformation of either TOP10 or Rosetta *E.coli* strains was performed by thawing 25 µL of competent cells on ice for 5 minutes. 50-100 ng of plasmid DNA was added to the bacterial aliquot and incubated for 5 minutes on ice. The cells were then heat shocked in a water bath at 42°C for 2 minutes and placed directly on ice for a 5 minute recovery period. Cells were then streaked onto a LB agar medium plate (supplemented with 50 mg/L carbenicillin) and grown overnight at 37 °C. Several colonies that grew on the plate were then picked and cultured overnight in LB medium (supplemented with 50 mg/L carbenicillin).

2.5 Protein manufacture

2.5.1 Buffers and reagents

Lysis buffer: 10 mM TRIS pH8.1, 10 mM MgCl2, 150 mM NaCl, 10% Glycerol.

Triton wash buffer: 0.5% Triton X, 50 mM TRIS pH8.1, 100 mM NaCl, 2 mM EDTA.

Re-suspension buffer: 50 mM TRIS pH8.1, 100 mM NaCl, 2 mM EDTA.

Guanidine buffer : 6 M guanidine, 50 mM TRIS pH8.1, 100 mM NaCl, 2mM EDTA.

pMHC I refold buffer: 50 mM TRIS pH8 (Fisher scientific), 2 mM EDTA pH8 (Fisher scientific) and 400 mM L-arginine (SAFC).

TCR refold buffer: 2.5 M Urea (Fisher scientific), 50 mM TRIS pH8, 2 mM EDTA pH8 and 400 mM L-arginine (SAFC).

Biomix A: 0.5 M Bicine buffer, pH8.3.

Biomix B: 100 mM ATP, 100 mM MgO(Ac)2, 500 μM Biotin.

BIAcore buffer: 10 nM HEPES pH7.4, 150 nM NaCl, 3 mM EDTA and 0.005% (v/v) Surfactant p20.

Crystal buffer: 10 mM TRIS pH 8.1 and 10 mM NaCl.

2.5.2 Protein expression vectors

MHC constructs: The sequence that encodes for the alpha chain of HLA-A*0201 and MR1 (residues 1-248: α1, α2, and α3 domains) and β2m chain were designed according to previous work performed by Jonathan Boulter (Boulter et al., 2003) and synthesised and inserted into a plasmid by Geneart. The N-terminus of the α chain of HLA-A*0201 was tagged with a biotinylation sequence (GGGLNDIFEAQKIEWH) (Altman et al., 1996, O'Callaghan C et al., 1999) allowing tetramerisation of pMHC monomer or adherence to streptavidin BIAcore chips. Proteins were expressed without the biotinylation tag for crystallisation studies.

TCR construct: D454 TCR α chain (residues 1-207) and D454 β chain (residues 1-247) DNA sequences were designed according to previous work to introduce an artificial inter-chain disulfide located on the α and β constant domain (Boulter et al., 2003).

pGMT7 vector: pGMT7 vector contains a penicillin/ carbenicillin resistance cassette and the T7 RNA polymerase promoter inducible by Isopropyl β-D-1-thiogalactopyranoside (IPTG) (Garboczi et al., 1996).

2.5.3 Cloning of DNA construct into pGMT7 vector

The MHC α chain, β2m, αTCR and βTCR chains sequences were inserted into the pGMT7 expression plasmid allowing protein expression under the control of the T7 RNA polymerase promoter, within a Rosetta DE3 *E.coli* system. Quality control of the plasmid sequence was performed by DNA sequencing by Central Biotechnology Services at Cardiff University (CBS). The steps of the cloning are described below.

2.5.3.1 Enzymatic digestion

DNA plasmids and pGMT7 vector required an enzymatic digestion with BamH1 and EcoR1 restriction endonucleases (New England Biolabs). The digestion was performed in a final volume of 20 µL with 1µg of target DNA and 1-2 µL of restriction enzyme. After 2 hours incubation at 37°C, fragments obtained were separated by agarose gel electrophoresis.

2.5.3.2 Agarose gel purification and ligation

The enzymatic digestion samples were mixed with a DNA loading buffer (Bioline). The DNA fragments were loaded and separated by electrophoresis at 100 V for 1 hour in a 1% agarose gel (Invitrogen) containing 1X SYBR safe DNA gel stain (Invitrogen) diluted with TRIS-acetate-EDTA buffer. To estimate the size of the DNA fragments obtained from the enzymatic digestion, a molecular weight marker (HypperLadder I, Bioline) was loaded on the gel. Inserts and vectors were extracted and purified from the agarose gel using the QIAquick gel extraction kit (Qiagen) according to the manufacturer's recommendations. Insert and vectors concentration were measured using a NanoDrop ND 1000 (Thermo Scientific).

Gel extracted inserts were ligated with pGMT7 vector using 1 μL of T4 DNA ligase (New England Biolabs) and 50 ng of pGMT7 vector with a molecular ratio of vector to insert of 1:1, 1:3 and 1:5 in a final volume of 10 μL of DNA ligase buffer (New England Biolabs). The mixture was incubated at room temperature for 30 minutes.

2.5.3.3 Plasmid amplification in TOP10 E.coli

Ligation products were transformed and amplified overnight into TOP10 *E.coli*. The plasmids were purified from the bacteria using the QIAquick PCR DNA extraction kit (Qiagen) according to the manufacturer's instructions.

2.5.4 Expression of inclusion bodies in Rosetta E. coli

Expression plasmids were transformed into Rosetta *E.coli* and plated onto agar plate supplemented with 50 μg/mL of carbenicillin. A starter culture was set up to verify the expression of the plasmid by picking and culturing a single colony in 30 mL of TYP media supplemented with 50 μg/mL of carbenicillin. The starter culture was grown at 37°C and shaken at 220 rpm until the suspension reached an optical density (OD_{600}) between 0.4 and 0.6. The expression of the plasmid was induced with or without IPTG at a final concentration of 0.5 mM for 3 hours. 20 μL of suspension cultures was analysed by sodium dodecyl sulfate-polyacrylamide gel electrophoresis (SDS-PAGE). The gel was stained with SimplyBlue SafeStain (invitrogen) and destained in ddH_2O.

After verifying the quality and quantity of the protein expression of the starter culture on the SDS-PAGE gel, the IPTG free starter culture was added to 1 L of TYP media supplemented with 50 μg/mL of carbenicillin and incubated at 37°C and shaken at 220 rpm to reach an OD_{600} of 0.4-0.6. The culture was induced with 0.5 M of IPTG (final concentration 0.5 mM) for 3 hours.

Cells were harvested and centrifuged at 4000 rpm for 20 minutes with a Legend RT centrifuge (Sorvall) with a Heraeus 6445 rotor. The cell pellet was re-suspended in 40 mL of lysis buffer and sonicated on ice at 50-60% power for 20 minutes using 2 second interval using a MS73 probe (Bandelin). The sonicated pellet was incubated with 200 μL of 20 mg/mL DNAase (Sigma) for over an hour and then resuspended with 100 mL of Triton wash buffer and centrifuged for 20 minutes at 10,000 rpm using an Evolution RC ultracentrifuge and a SLA-1500 rotor (Sorvall). The supernatant was discarded and the pellet was scraped and resuspended into 100 mL of triton wash buffer.

The pellet was then centrifuge again for 20 minutes at 10,000 rpm, the supernatant was discarded and the pellet was washed with 100 mL of Resuspension buffer and centrifuged 20 minutes at 10,000 rpm. The pellet was resuspended in 10 mL of guanidine buffer. The concentration of inclusion bodies was measured using a NanoDrop ND 1000 (Thermo Scientific) and were stored at -20°C. A 20 µL sample was harvested at each wash to be analysed by SDS-PAGE gel electrophoresis to assess the purity of the inclusion bodies.

2.5.5 Manufacture of soluble pMHC I and TCR monomers

2.5.5.1 Refolding of soluble pMHC I

For the refolding of inclusion bodies in one litre of refold buffer , 30 mg/L of the heavy chain HLA-A*0201 with (if used for tetramerisation) or without biotin tag and 30 mg/L of β_2m inclusion bodies were denaturated in 6 mL of a solution of 8 M guanidine buffer supplemented with 10 mM Dithiothreitol (DTT; Sigma) for 30 minutes at 37 °C. The refold was initiated by transferring first 200 µL of peptide (20 µg/mL in DMSO, Proimmune, UK) then the denaturated heavy chain and β_2m into 1L of 4 °C pMHC I refold buffer supplemented at the last minute with the 4 mM cystamine (Sigma) and 6 mM cysteamine (Sigma). The mixture was incubated overnight at 4 °C under gentle stirring. The following day, the refold buffer was transferred into a 12.4 kDa molecular weight cut-off (MWCO) dialysis tube (Sigma) and dialysed in 20 L of water supplemented with 10 mM TRIS pH8 bucket for 24 hours at 4 °C. Dialysed refold mixture was then filtered through a 0.45 µm filter membrane (Millipore) and analysed by ion exchange chromatography and gel filtration (described in section 2.5.6.1 and 2.5.6.2).

2.5.5.2 Biotinylation of pMHC I

Refolded and purified pMHC I was concentrated to a final volume of 700 µL using a 20 mL Vivaspin column with a 10 kDa cut off (Sartorious). The biotinylation process consists on the addition of 100 µL Biomix A, 100 µL Biomix B, 100 µL d-Biotin 500 µM (Avadin) and 2 µL BirA enzyme (Avadin) to the concentrated pMHC I. The mix was incubated overnight at RT. Excess of biotin was removed by centrifuging the mix using a Vivaspin column (10 kDa MWCO: Sartorious).

2.5.5.3 Refolding of soluble αβ TCR

For a 1 L TCR refold, 60 mg/mL α chain and 30 mg/mL β chain were denaturated individually at a final concentration of 10 mg/mL in guanidine buffer supplemented with 10 mM DTT for 30 minutes. The denaturated chains were added dropwise to a 4 °C TCR refold buffer supplemented at the last minute with the 4 mM cystamine (Sigma) and 6 mM cysteamine (Sigma). The refold was mixed for 3 hours at 4°C and then transferred into 12.4 kDa MWCO dialysis tubing (Sigma), and dialysed in 20 L of 10 mM TRIS pH 8.1 until refold conductivity was under 2000 μS/cm. Dialysed TCR refolds was then filtered and purified as described for the pMHC I refold protocol in section 2.5.5.1.

2.5.6 Purification of pMHC I and αβTCR monomers

2.5.6.1 Anion exchange chromatography

pMHC I and αβTCR refold products were purified initially by anion exchange chromatography followed by a gel filtration using a ÄKTA Fast Protein Liquid Chromatography (FPLC) using a Poros 50HQ column (Applied Biosystems) in conjunction with Unicorn software. The column was equilibrated with a buffer A (10 mM TRIS) at a flowrate of 20 ml/min. The refold product was loaded onto the column and fractionally eluted with a salt gradient (0-1M NaCl in 10 mM TRIS). The collected fractions were analysed by Coomassie-stained SDS-PAGE gel. The fractions containing the protein of interest were pooled and concentrated down to 500 μL in a 10 kDa MWCO Vivaspin 20 or Vivaspin 4 (Satorius) by centrifugation 20 minutes at 1200 x g. Protein concentration was determined using a NanoDrop ND1000 (Thermo Scientific).

2.5.6.2 Size exclusion chromatography

After a first purification by anion exchange, pMHC and αβTCR monomers were purified by size exclusion on a 24 mL Superdex 200 10/300 GL column (GE Healthcare) pre-equilibrated with PBS buffer (for pMHC tetramerisation) or BIAcore buffer (BIAcore analysis) or crystal buffer (for crystallisation). Elution was performed at 0.5 mL/min and fractions of 1 mL were collected to be analysed on Coomassie-stained SDS-PAGE gel. The pooled fractions of interested were concentrated down as described above.

2.5.7 Tetramerisation of pMHC I

The tetramerisation of pMHC I was carried out on ice and in the dark using R-phycoerythrin (PE) (Molecular probes) conjugated streptavidin. Streptavidin contains four binding sites for biotin therefore four biotinylated pMHC can be added to one streptavidin-PE molecule. The concentration of Streptavidin-PE was calculated to obtain an equimolar ratio of 1 streptavidin-PE for 4 biotinylated pMHC I monomers (1:4 ratio). 5 aliquots of equal volume of streptavidin-PE was added at 20 minutes intervals by gentle mixing. 5 aliquots were enough to ensure full saturation of all four biotin-binding sites of the streptavidin. The pMHC I tetramers were stored at 4 °C for a maximum of a week prior to cell staining.

2.5.8 Structural methods

2.5.8.1 Crystallisation using the sitting drop vapour diffusion technique

In order to ascertain optimum concentration buffer for target protein, variation of pH, salt concentration and precipitant were evaluated using commercial screens such as JBS basic screen (JenaBioscience), PACT premier (Molecular Dimensions) and in-house designed screen (Bulek et al., 2012). Protein was concentrated to 10 mg/mL in 10 mM TRIS, pH 8.1 and 10 mM NaCl. 0.2 µL of protein and 0.2 µL of crystallisation buffer were dispensed into each small reaction well of a 96 well Intelli-plates (Art Robbins Instruments-ARI) using the crystal Phoenix robot (ARI). 60 µL of crystallisation buffer were dispensed into each large reservoir. Intelli-plates were sealed, incubated at RT and analysed for crystal formations at 48 hours, 1 week and thereafter every 2 weeks. Selected crystals were cryoprotected with 25% ethylene-glycol and flash cooled in liquid nitrogen in Litho loops (Molecular Dimensions) to be analysed at Diamond light source, Oxford.

*2.5.8.2 HLA-A*0201-LLDAHIPQL and HLA-A*0201-MIDAHIPQV diffraction data collection and model refinement*

Diffraction data were collected at beam-line I04.1 at a fixed wavelength of 0.9163Å at Diamond light source in Oxford, with a Pilatus 2M detector. Using a rotation method, 200 frames were recorded each covering 1° of rotation. Reflection intensities were estimated with the MOSFLM package (McCoy et al., 2007) and the high resolution HLA-A*0201 structure published by my laboratory (pdb reference 4I4W) was used as a model for molecular replacement. Refinement and rebuilding of HLA-A*0201-LLDAHIPQL and HLA-A*0201-MIDAHIPQV was carried out using the modelling programme, COOT (Emsley and Cowtan, 2004) and the data scaled, reduced and analysed with the CCP4 package (Krissinel et al., 2004, Murshudov et al., 1997).

2.5.9 Surface plasmon resonance

2.5.9.1 Preparation of the gold sensor chip

D454 TCR binding assay was performed using a BIAcore 3000 (GE Healthcare). Briefly, an CM5 sensor chip (GE Healthcare) was activated by using an amine coupling solution (GE Healthcare) containing 10 mM N-(3-dimethylaminopropyl)-N^3-ethylcarbodiimide (EDC) and 400 mM M-hydroxysuccinimide (NHS). The sensor chip was coated with a solution of streptavidin (200 µg/mL in 10 mM acetate pH 4.5 (Sigma-Aldrich)). The chip was finally washed with 1 M ethanolamine hydrochloride in order to deactivate any remaining reactive groups left on the sensor chip surface.

2.5.9.2 Equilibrium-binding assay

About 1 µM of either biotinylated HLA-A*0201-LLDAHIPQL and biotinylated HLA-A*0201-MIDAHIPQV soluble molecules in BIAcore buffer were coupled to individual streptavidin coated CM5 sensor chip. The pMHCs were injected to coat the CM5 sensor chip. The equilibrium binding assay was performed by injecting 10 serial dilutions of D454 TCR over the sensor chip at 45 µl/min at 25°C. Results were analysed using BIAevaluation 3.1 and Origin 6.1 softwares. The constant of dissociation (K_D) values were calculated assuming a 1:1 molecular interaction ($A + B \leftrightarrow AB$) by plotting specific equilibrium-binding responses against protein concentrations followed by non-linear least squares fitting of the Langmuir binding equation $AB = \frac{B \times ABmax}{K_D + B}$.

CHAPTER 3. GENERATION OF T-CELL RESPONSES TO MYCOBACTERIUM SMEGMATIS

3.1 Introduction

3.1.1 T-cell responses to bacteria

A successful immune response to bacteria is characterised by the development of a tailored network of innate and adaptive immune cells that efficiently communicate with each other to eradicate or suppress bacteria in order to maintain homeostasis. Certain bacterial species have evolved to actively seek host immune cells for their survival and propagation. These bacteria have the ability to survive and persist within the body by manipulating the cellular pathways and immune responses deployed against them by the host. This evasion and manipulation is often to the detriment to the host. Certain species of *Mycobacterium* such as *M. tuberculosis* and *M. bovis,* as well as other gram positive and negative bacteria, induce the down-regulation of MHC II at the surface of an infected host cell (Barrionuevo et al., 2012, Ibana et al., 2011, Pecora et al., 2009), thereby evading optimal T-cell responses. Moreover, during *M. leprae* infection an inhibitory environment is created by the induction of regulatory T-cell subsets, thereby reducing cytotoxicity towards infected cells (Bobosha et al., 2014).

A range of T-cell subsets are deployed by the immune system during bacterial challenge. Cytotoxic and T_H cells recognise bacterial peptides presented by classical MHC I and II and provide some defence against bacterial threat, although delayed in certain infections, such as *M. tuberculosis* (Blomgran et al., 2012, Wallgren, 1948). Furthermore, bacterial-derived antigens are also recognised by innate-like T-cell subsets such as γδ T-cells, natural killer (NK) T-cells and mucosal associated invariant T-cells (MAITs). γδ T-cells play a role during bacterial challenge, especially during the early phases, both directly and indirectly by influencing the inflammatory response and other T-cell subsets (Ladel et al., 1996). Moreover, murine models have shown that γδ T-cells curb bacterial dissemination post infection (Zachariadis et al., 2006, Hiromatsu et al., 1992). CD1d-restricted NK T-cells have been shown to play a role in tailoring immune responses towards a T_H1 or a T_H2 phenotype depending on the type of bacterial antigen (Venkataswamy and Porcelli, 2010).

The newly characterised MHC class I-related protein 1 (MR1) restricted T-cell subset, MAITs, play an important role in early bacterial infection and especially in respiratory bacterial infection (Le Bourhis et al., 2010, Gold et al., 2010, Chua et al., 2012). Overall, it is thought that unconventional T-cells, present during the early stage of infection, play a role in bridging the innate and adaptive immune systems (Meierovics et al., 2013) and are therefore instrumental in host defence.

The understanding of T-cell responses to bacteria is an important and currently active area of research. A greater understanding of the T-cell subsets involved and their roles during bacterial challenge would help to develop strategies to overcome sub-optimal immunity to certain species of bacteria and the rise of drug resistant strains. In this chapter, I dissected the T-cell response raised against APC that had phagocytosed *M. smegmatis*.

3.1.2 *Mycobacterium smegmatis* as a model to study T-cell responses to bacteria

M. smegmatis is a fast growing non-pathogenic bacterium that was first isolated from human penis smegma (Brown-Elliott and Wallace, 2002). *M. smegmatis* is rapidly phagocytosed and processed by APC, with antigens being presented on MHC I and II (Bohsali et al., Harriff et al., Jondal et al., 1996). Importantly for my studies, *M. smegmatis* could be handled in the Bio-safety level 1 facilities (Singh and Reyrat, 2009) that were available in the Institute of Infection and Immunity at Cardiff University. *M. smegmatis* grows rapidly, in a host cell independent fashion, allowing easy culture and availability for experiments. Additionally, *M. smegmatis* shares close homologues to 12 virulent factors from *M. tuberculosis* (Reyrat and Kahn, 2001).

3.1.3 Aims

The purpose of the first component of my studies was to dissect the $CD3^+$ T-cell subsets generated during the boosting of PBMC with APC that had phagocytosed *M. smegmatis*. I aimed to optimise the boosting parameters to trigger a sufficient T-cell response to *M. smegmatis*, thus allowing the responding T-cells to be characterised with monoclonal antibodies, against cells surface markers, and flow cytometry. I wanted to assess the distribution of αβ and γδ TCR usage as well as their CD4 and CD8 co-receptor expression.

3.2 Results

3.2.1 Experimental Approach

Multiple parameters needed to be optimised in order to establish whether it was feasible to routinely elicit T-cell responses to *M. smegmatis in vitro* as described in **Table 3.1**. Both the multiplicity of infection (MOI) (1:10 APC:*M. smegmatis*) and PBMC to APC ratio (10:1) were based on previous literature (Connelly et al., 2007, Verma et al., 1979, Bohsali et al., 2010) and advice from Dr Matthias Eberl (Institute of Infection and Immunity, Cardiff University). Other parameters required more in depth optimisation: Firstly, *M .smegmatis* growth was assessed to define the kinetics of expansion allowing it to be used at optimal health and to achieve the desired MOI. Secondly, APCs were tested for their ability to trigger a T-cell response against *M. smegmatis*, without high background when APCs were used alone. Thirdly, I explored two assay outputs for identifying responding T-cells by flow cytometry.

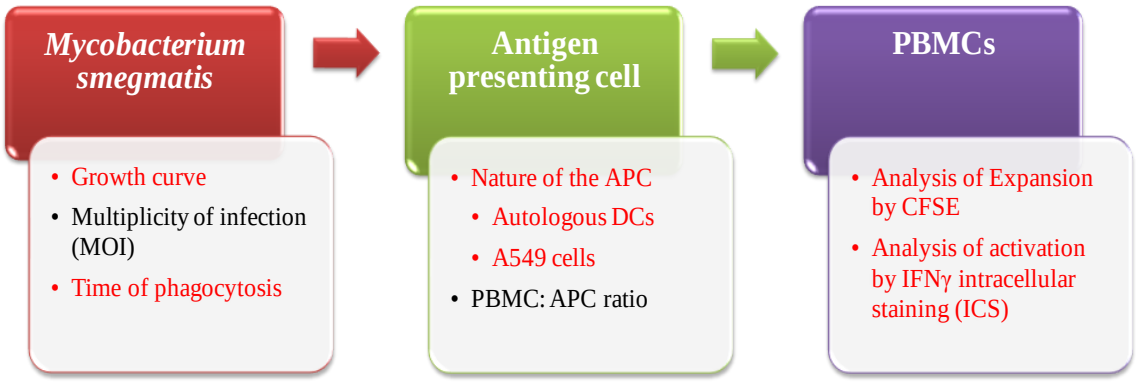

Table 3.1 The parameters optimised in order to dissect T-cell responses to *M. smegmatis.*
The parameters optimised in this study are highlighted in red and those based on current literature shown in black.

3.2.2 Monitoring growth of *M. smegmatis* in culture

The different phases of *M. smegmatis* growth were determined by measuring the optical density (OD: 600 nm) at different time points during culture over 75 hours (**Figure 3.1 A**) in Lemco media. The OD_{600} readings were accompanied by growing time-point matched samples on Lemco agar plates for 48 hours to establish the number of colony forming units (CFU) per mL of culture (**Figure 3.1 B**). This allowed the OD_{600} of the culture to be related to the number of bacteria present (**Figure 3.1 C**) allowing *M. smegmatis* to be harvested from culture at a given time-point and co-cultured with an APC to give the desired MOI. *M. smegmatis* could not be readily detected by reading the OD_{600} during the initial phase of growth (0-30 hours) (**Figure 3.1 A**). Bacterial growth could be measured during this phase by the number of CFUs formed on agar plates (**Figure 3.1 B**). Exponential growth could be measured between 30 and 55 hours by OD_{600} (**Figure 3.1 B**). After 55 hours OD_{600} plateaued and declined due to dormancy and/or death (**Figure 3.1 B**). The rapid growth phase seemed the most appropriate time to harvest *M. smegmatis* for the phagocytosis, as they were still duplicating and were likely to be in good condition. Based on these observations *M. smegmatis* was harvested between 40-50 hours with an OD of 0.25 to 1 and the actual number of *M. smegmatis* enumerated retrospectively by agar culture.

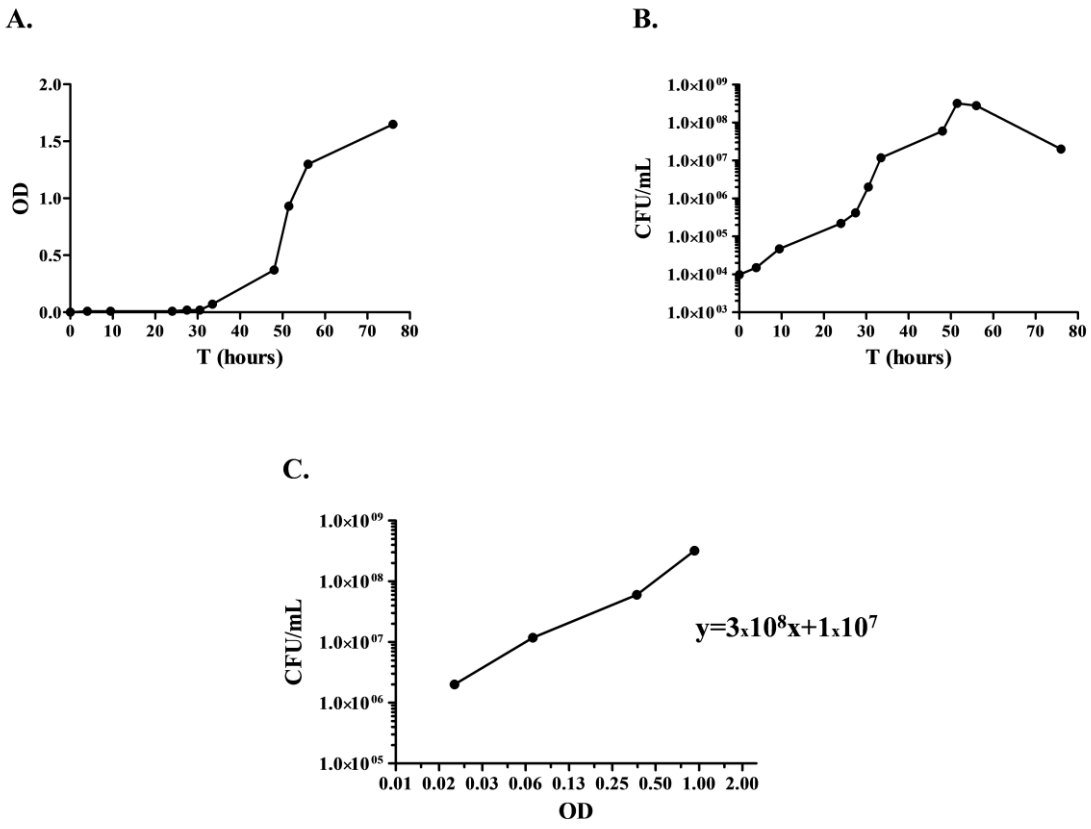

Figure 3.1 Monitoring *M. smegmatis* growth in culture by reading optical density. *M. smegmatis* was grown in 10 mL of Lemco media (Chapter 2) for 75 hours. **(A)** The optical density (OD: 600 nm) was taken at the times indicated. **(B)** A matched sample was also plated on antibiotic free Lemco agar plates to establish the number colony forming units (CFU) after 48 hours. **(C)** The CFU/mL were plotted versus OD for the time points when the *M. smegmatis* were growing most rapidly and appeared healthy. A linear regression curve and associated equation (displayed on the plot in C) were used to establish the CFU/mL from OD_{600} readings. This standardisation was performed for each *M. smegmatis* culture.

3.2.3 Using DC to present *M. smegmatis* antigens

Dendritic cells (DCs) are considered to be professional APCs (Corinti et al., 2000) and prime naive T-cells by presenting antigens on MHC I and II (Pozzi et al., 2005). DCs efficiently phagocytose *M. smegmatis* (Bohsali et al., 2010). DCs can be generated *in vitro* by the culture of blood-derived monocytes in GM-CSF and IL-4 as described in Chapter 2. T-cell responses to *M. smegmatis*-loaded APC were monitored by dilution of carboxyfluorescein succinimiydyl ester (CFSE) using flow cytometry (Quah et al., 2007). CFSE is passively taken up by cells and converted to a fluorescent molecule by cell intrinsic esterases (Wang et al., 2005). The fluorescent intensity of the CFSE is diluted as the cells divide as it shared between daughter cells (Quah et al., 2007). During a pilot experiment, autologous DCs were generated from two donors and subsequently incubated with or without (±) *M. smegmatis* and then co-cultured for 8 days with CFSE labelled PBMC from the same donors. I chose day 8 for flow cytometric analysis based on prior experience of generating antigen-specific T-cell lines, as it allows sufficient duration for responding T-cells to proliferate at least once and then be detected by CSFE dilution. At day 8, cells were labelled with a viability dye (Vivid) and anti-CD3 and were sequentially gated as shown in **Figure 3.2 A and B**, with CFSE low (responding) $CD3^+$ T-cells appearing in all cultures. Donors 1 and 2 (**Figure 3.2 C and D**) gave background T-cell responses (DCs alone) of 3.51% and 0.89%, and *M. smegmatis* specific T-cell responses (% seen with DCs with *M. smegmatis* minus the % seen with DCs alone) of 11.79% and 18.01% respectively. T-cells responding to DCs loaded with *M. smegmatis* gave a stereotypical CFSE dilution profile, with clearly defined populations of T-cells with varying CFSE fluorescence intensities. I intended to add more conditions during the pilot experiment but the DC yield at the end of the procurement process restricted my plans. Ideally, sufficient PBMC needed to be set-up at the start of the assays so the number of cells available for analysis allowed all the necessary controls to be included for robust dissection of any responding T-cells. Efforts to scale up the approach using DCs were made by taking more blood from each donor, although there were ethical limitations imposed on how much blood could be taken. I therefore examined the use of an alternative, immortalized APC.

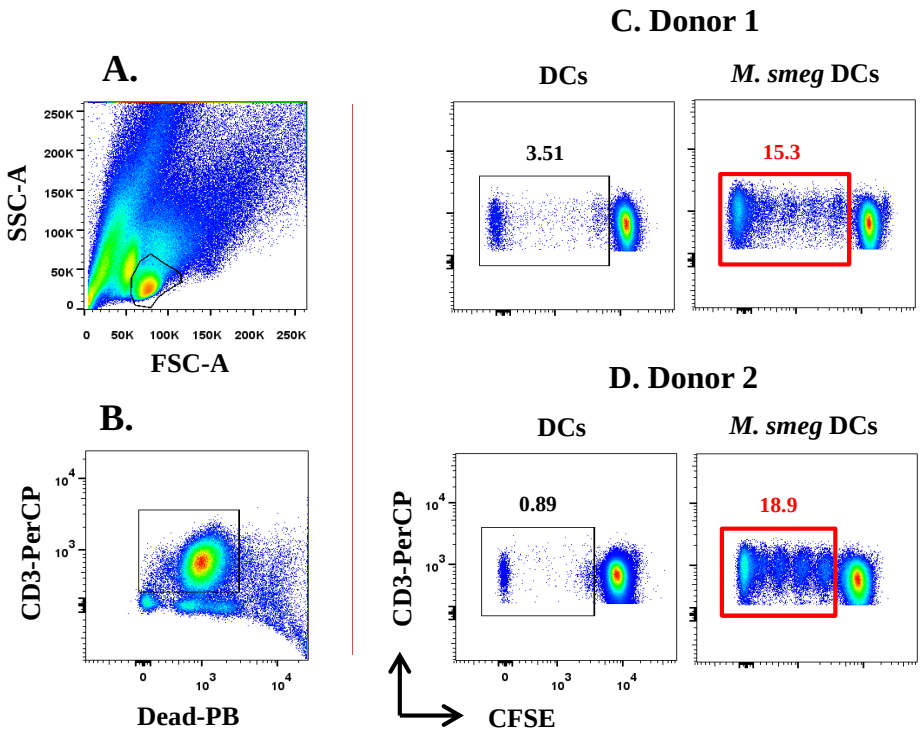

Figure 3.2 Autologous dendritic cells were capable of eliciting specific CD3$^+$ T-cell responses to *M. smegmatis*.

PBMC from two donors were labelled with carboxyfluorescein succinimiydyl ester (CFSE) and incubated for 8 days with autologous DCs that had been co-cultured ± *M. smegmatis*. Cells were also stained for viability and CD3 and sequentially gated based on forward and side scatter (**A**) followed by viable/CD3$^+$ cells (**B**) and displayed as pseudocolour dots plots with CD3 versus CFSE fluorescence (**C** and **D**). The degree of T-cell proliferation was assessed by the loss of CFSE fluorescence as shown by the gates in C and D. The percentage of cells residing in the proliferating gate is shown inset for each dot plot.

3.2.4 A lung epithelial cell line phagocytoses *M. smegmatis*

The immortalised epithelial cell line, A549, has been used in studies involving phagocytosis of bacteria (de Astorza et al., 2004, Kim et al., 2011) and made a good candidate APC. The use of A549 cells means that large amounts of uniform APC can be generated easily but also has some potential disadvantages. First, using a potentially HLA-mismatched APC for presentation to donor PBMC runs the risk of generating allo-reactive T-cell responses. Alloreactivity arises when T-cells recognise self peptides bound to non-self MHC. By definition, such complexes are not encountered in the thymus and are therefore considered as foreign (Felix and Allen, 2007, Kourilsky and Claverie, 1989). Allo-reactivity is dramatically demonstrated when HLA mismatched donated organs are rejected after transplantation (Benichou et al., 1999). Second, using HLA mismatched APC can exclude boosting of responses through classical HLA and therefore result in an underestimation of such responses. Non-HLA matched APC should still be capable of antigen presentation to unconventional T-cells. I first confirmed that A549 cells could phagocytose *M. smegmatis*, before using them for this study.

Based on a previous study (Davey et al., 2011) *M. smegmatis* phagocytosis by A549 cells was set-up to evaluate the percentage of bacterial uptake over time. A549 cells were co-cultured for 0.5, 1, 1.5 and 2 hour(s) with *M. smegmatis* constitutively expressing green fluorescent protein (GFP) (*M. smegmatis-gfp*$^{+}$). After 2 hours >17% of A549 cells stained for GFP (**Figure 3.3**). This value is likely to be an underestimate as once phagocytosed, *M. smegmatis* is degraded, thereby halting GFP gene expression. Furthermore, studies have shown that the half-life of GFP inside fibroblasts is 2.8 hours (Halter et al., 2007). However, I considered that a confirmed uptake of bacterium by ~20% of APC was acceptable for this study as this value is similar to that that has been reported using DCs (M. Eberl, personal communication).

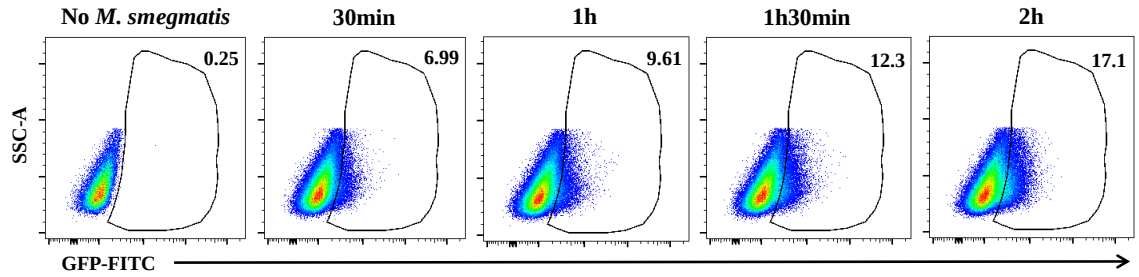

Figure 3.3 A549 cells cultured with *M. smegmatis* expressing green fluorescent protein (GFP) appeared GFP$^+$.
A549 cells were cultured ± *M. smegmatis-gfp*$^+$ at a MOI of 10:1 and incubated for 0.5, 1, 1.5 and 2 hour(s). To stop the phagocytosis, *M. smegmatis-gfp*$^+$ were washed off the A549 cells 5 times using PBS and low speed centrifugation. The samples were then analysed by flow cytometry. The gates shown were set on the sample of A549 cells that had not been cultured with *M. smegmatis-gfp*$^+$. The percentage of cells residing in the GFP$^+$ gate is shown for each dot plot. Cells were also stained with the viability dye (Vivid) and gated based on their forward and side scatter and viability.

Although it was encouraging that a proportion of A549 cells co-cultured with *M. smegmatis-gfp*$^+$ was GFP$^+$ by flow cytometry it was imperative to confirm that the fluorescence seen was due to phagocytosis and not simply due to *M. smegmatis* association with the cell surface of A549, In order to confirm that the bacterium were intracellular, I examined the 2 hour sample using confocal microscopy. A representative image is shown in **Figure 3.4**, with 2 (28.6%) of the 7 clearly visible cells showing GFP fluorescence in discreet intracellular compartments. No fluorescence was seen to be associated with the A549 cell membrane even though > 1000 individual cells were visualised. These data confirmed that A549 cells were phagocytosing *M. smegmatis*, making this cell line suitable for use as an APCs in this study.

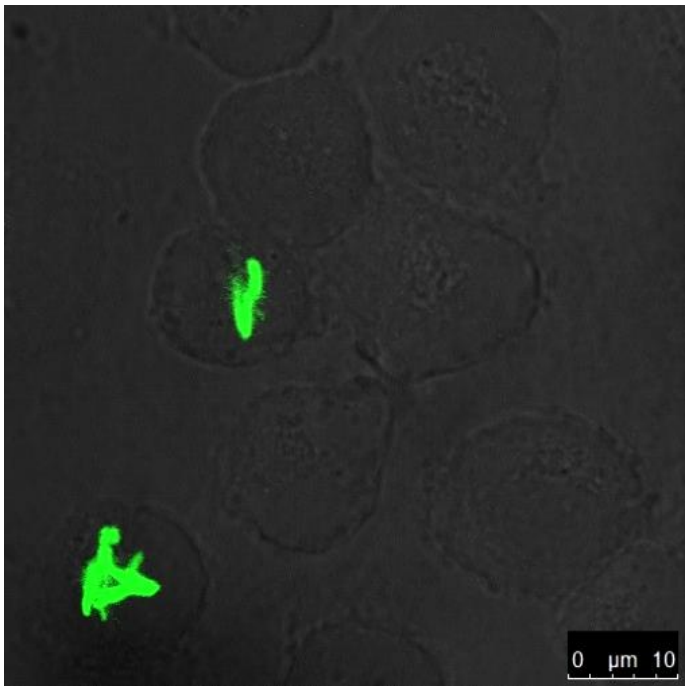

Figure 3.4 A549 cells co-cultured with *M. smegmatis* expressing green fluorescent protein (GFP) had discreet areas of GFP fluorescence when imaged by confocal microscopy.

M. smegmatis-gfp^{+} were added to A549 cells at an MOI of 10:1 and co-cultured for 2 hours. The cells were subsequently washed 5 times to remove excess bacteria and imaged by confocal fluorescence microscopy at 489 nm (emission at 518 nm). A representative image is shown (scale in bottom right hand corner) in a plane that shows the GFP fluorescence most clearly.

3.2.5 *M. smegmatis*-loaded A549 cells induce specific T-cell responses

Once the ability of A549 cells to phagocytose *M. smegmatis* was confirmed I proceeded to using these cells (± *M. smegmatis*) as targets for T-cell boosting from the PBMC of two donors. As the number of A549 cells was not limiting, T-cell boosting was analysed at 3, 8 and 13 days post-boosting to assess how responses developed over time *in vitro*. Additionally, cells were stained with antibodies for the co-receptors, CD4 and CD8. No *M. smegmatis* responding T-cells (CFSE low) were present at day 3 (**Figure 3.5 C and F**), suggesting a relatively low precursor frequency in the peripheral blood of donors or that cells were slow to respond. The responding T-cells accumulated as the assay progressed with the greatest proportion of cells being seen in the dividing gate at day 13 (**Figure 3.5 E and H**). I did not have enough cells to continue the time course beyond day 13. On day 8, the percentage of T-cells responding to *M. smegmatis*-loaded A549 cells (minus background T-cell responses to A549 cells alone) was similar to that seen when DCs were used for boosting: 8.21% and 15.6% with A549 cells (donors 3 and 4 **Figure 3.5**) and 11.8% and 18% with DCs (donors 1 and 2 **Figure 3.2**). At day 13, the donors gave specific T-cell responses of 13.4% (donor 3 **Figure 3.5 E**) and 58.6% (donor 4 **Figure 3.5 H**) of the $CD3^+$ T-cells residing in the responding, CFSE low gate. The background T-cell response (A549 cells without *M. smegmatis*) for donor 3 increased dramatically to 28.2% at day 13 (**Figure 3.5 E**), from 3.29 % at day 8, possibly due to allo-reactivity. This reduced the fold-difference between the background and *M. smegmatis*-specific T-cell responses from 3.5 at day 8 to 1.5 at day 13. In comparison, the fold-difference for donor 4 increased from 8.3 at day 8 (**Figure 3.5 G**) to 11 (**Figure 3.5 H**) at day 13.

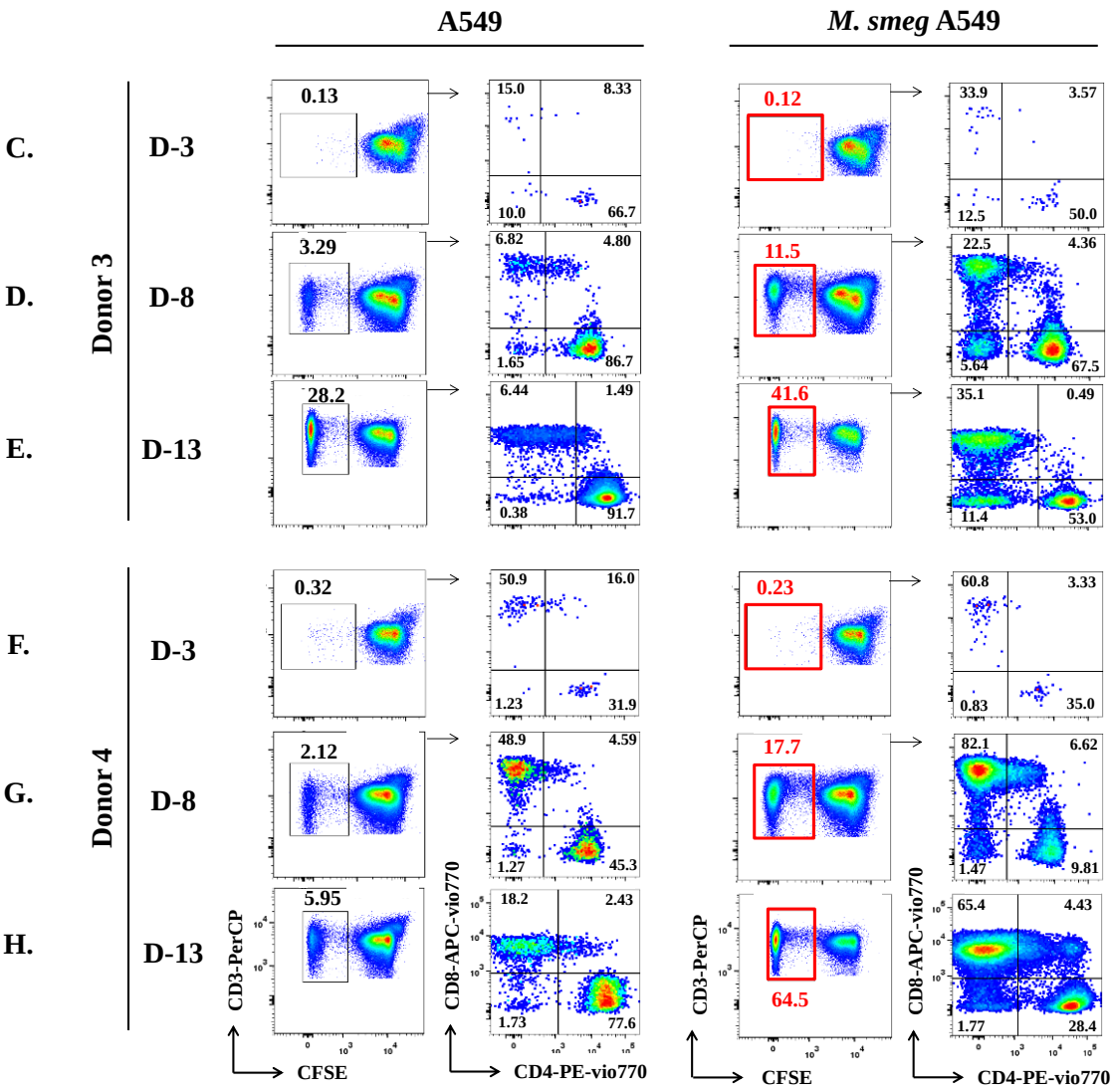

Figure 3.5 A549 cells cultured with *M. smegmatis* were capable of inducing specific T-cell responses.

PBMC from two donors were labelled with CFSE and incubated for 3 **(C** and **F)**, 8 **(D** and **G)** and 13 **(E** and **H)** days with A549 cells that had been cultured with and without *M. smegmatis*. The cells were also stained for viability, CD3, CD4 and CD8, and sequentially gated based on their forward and side scatter (**Figure 3.2 A**) followed by viable/$CD3^+$ cells (**Figure 3.2 B**) and displayed as pseudocolour dots plots with CD3 versus CFSE fluorescence. The degree of T-cell proliferation was assessed by the loss of CFSE fluorescence as shown by the black (A549 cells alone) and red (A549 cells with *M. smegmatis*) gates. The cells residing in the dividing gates (black and red) were further gated as indicated (arrows) and displayed as CD8 versus CD4 pseudocolour plots. The percentage of cells residing in the proliferating and quadrant gates are shown inset for each dot plot.

An equivalent T-cell growth was observed when exposed to *M. smegmatis*-loaded A549 cells and DCs at day 8 (**Figure 3.2 and 3.5**). However a vast majority of CFSE low cells resided in one population when stimulated with *M. smegmatis*-loaded A549 cells rather than distinct T-cell populations seen when stimulated with *M. smegmatis*-loaded DCs. In each case there was some background division of T-cells. This background could be due to many factors including prior exposure to antigen *in vivo* or response to mitogens present in the media, that were either constitutive (e.g. IL2) or produced by the target APC. Additionally, alloreactivity could be responsible when A549 cells were used due to the potential for HLA mismatching. Overall, from the pilot studies, DCs and A549 triggered *M. smegmatis*-specific T-cell expansion far above the background seen with uninfected APCs. The limitations associated with using DCs meant that the A549 cells offered a more attractive option as the APC of choice going forward.

3.2.6 Dissection of *M. smegmatis*-specific T-cell responses in multiple donors

Once boosting parameters were optimised, I extended my studies to further donors and initiated the dissection of T-cell responses to *M. smegmatis* (a summary of all the donors used for this study and the various parameters used can be found in appendix A1). I also extended my studies beyond proliferation (CFSE dilution) to include Intracellular Cytokine Staining (ICS). PBMC from six donors were set-up in the same manner as previously described but without pre-labelling the cells with CFSE, cultured for 13 days and restimulated with A549 cells ± *M. smegmatis*, for 5 hours prior to ICS. All six donors produced IFNγ-secreting cells in response to re-stimulation with *M. smegmatis* with an average response of 6.3% of $CD3^+$ cells (range of 1.8-12.9 %, **Figure 3.6**) with a greater difference between the background and *M. smegmatis* specific T cell responses when compared to the CFSE experiments (12.6 versus 3.6 fold). Across all the experiments (CFSE and ICS data), using A549 cells as the APC, all of the donors exhibited induction of *M. smegmatis*-specific T-cells above background (*p*=0.03, 2-tailed, paired T-test). Collectively, the *M. smegmatis*-specific T-cell responses ranged from 1.6% to 56.4% of $CD3^+$ cells at day 13, with an average response of 12.9%.

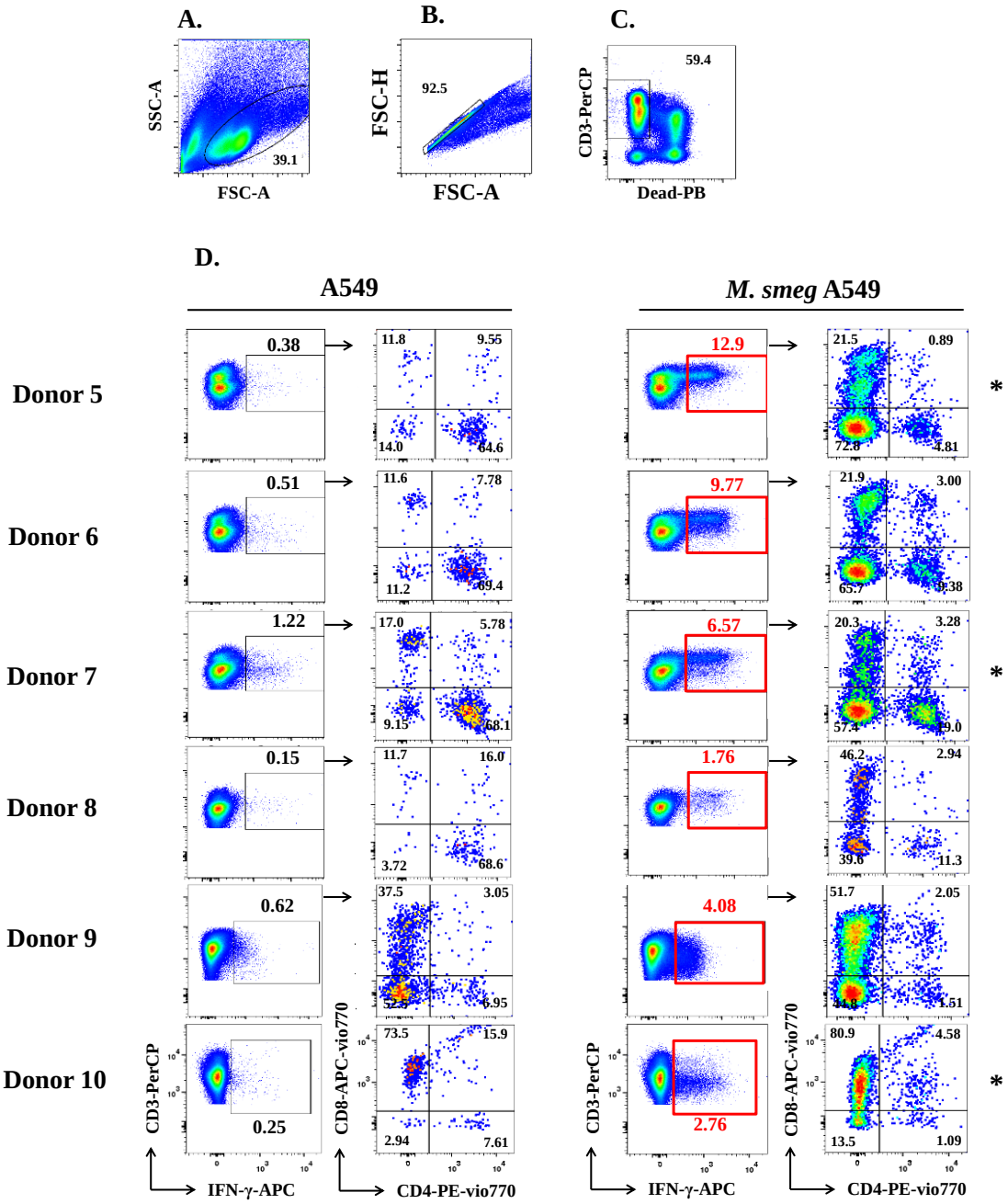

Figure 3.6 Multiple donors elicit specific T-cell responses to *M. smegmatis* and the responding cells had a skewed distribution of CD4 and CD8 expression.

PBMC from six donors were incubated for 13 days with A549 cells that had been cultured with *M. smegmatis*. Subsequently, T-cells were restimulated with A549 cells that had been cultured with and without *M. smegmatis* and stained for IFNγ (intracellular), viability, CD3, CD4 and CD8. The cells were sequentially gated based on their forward and side scatter **(A)**, for single **(B)** and viable/CD3$^+$ cells **(C)** and displayed as pseudocolour dots plots with CD3 versus IFNγ fluorescence as shown. The degree of T-cell response was assessed by the appearance of IFNγ$^+$ cells as shown by the black (A549 cells alone) and red (A549 cells with *M. smegmatis*) gates. The percentage of cells residing in the responding gate is shown inset for each dot plot. The cells residing in the responding gates were further gated as indicated (arrow) and displayed as CD8 versus CD4 pseudocolour plots with large dots. The percentage of cells residing in the quadrant gates are shown inset for each dot plot.

3.2.7 Co-receptor phenotyping of *M. smegmatis*-specific T-cells

Of the 10 donors that gave *M. smegmatis*-specific T-cell responses in previous experiments, 8 (2 with CSFE and 6 from the ICS experiments) were also analysed for CD4 and CD8 co-receptor expression (stained for viability, CD3, CD4 and CD8 and sequentially gated as described in **Figures 3.6**), All four possible subsets: $CD4^+$, $CD8^+$, $CD4^+CD8^+$ (double positive: DP) and $CD4^-CD8^-$ (double negative: DN), appeared in the cultures to varying degrees. $CD3^+$ T-cells in the responding gates (CFSE low or $IFN\gamma^+$), where compared for CD4 and CD8 expression between PBMC exposed to A549 cells ± *M. smegmatis*. In comparison to PBMC cultured with A549 cells alone, $CD4^+$ and DP T-cells (relatively low frequency for the latter) had a significantly reduced frequency than with A549 cells with *M. smegmatis* (p=0.0095 and p=0.034 respectively, **Figure 3.7**). This suggests that these $CD4^+$ and DP T-cells present with A549 cells alone may either be responding to the A549 cells or they had a survival advantage *in vitro* over the other T-cell subsets, when antigenic stimulation is absent. In contrast, the DN T-cell subset was significantly enriched when A549 cells were loaded with *M. smegmatis* compared to A549 cells alone (p=0.024 **Figure 3.7**): six of the donors (3 (**Figure 3.5**), 5, 6, 7, 8 and 10 (**Figure 3.6**)) exhibited this skew, with 4.6-30 fold (mean of 10.4) more DN T-cells residing in the responding gates when compared with A549 cells alone. There was also a significant (p=0.005) skewing towards $CD8^+$ T cells with 6 of the 8 donors (3, 4 (**Figure 3.5**), 5, 6, 8 and 9 (**Figure 3.6**)) exhibiting the shift when *M. smegmatis* was present, with an average 3-fold increase. 5 of 8 donors gave a skewing towards both $CD8^+$ and DN T-cells. 2 out of 8 donors were skewed towards just $CD8^+$ T-cells (donors 4 (**Figure 3.5**) and 9 (**Figure 3.6**)). The remaining donor (10) exhibited an expansion towards the DN population only (**Figure 3.6**).

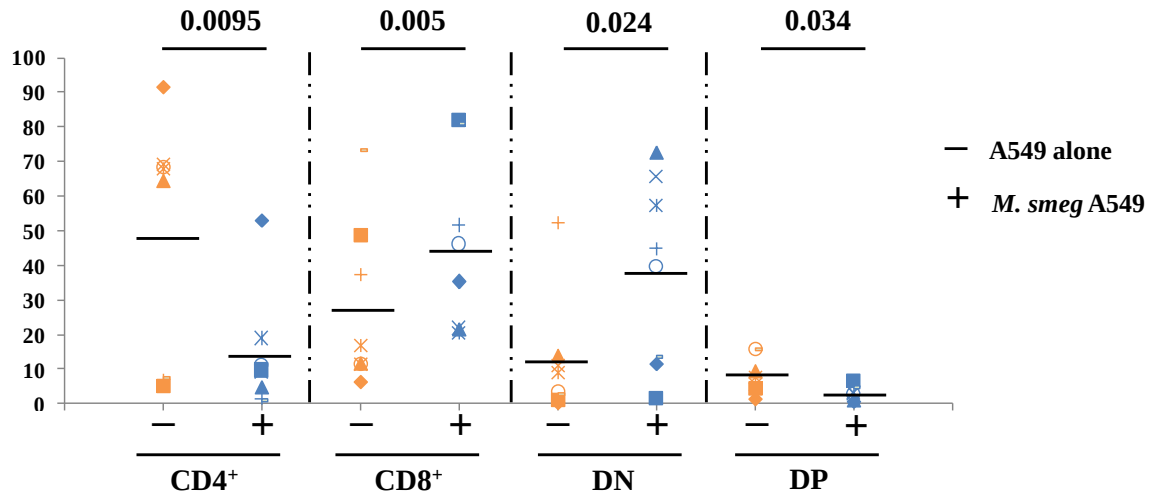

Figure 3.7 Statistically significant skewing of CD4 and CD8 expression of CD3$^+$ T-cells following culture of PBMCs with *M. smegmatis*-loaded A549 targets.
CD3$^+$ T-cells from 8 donors PBMC exposed to A549 cells ± *M. smegmatis*, as assessed by T-cell proliferation (**Figure 3.5**) or production of IFNγ (**Figure 3.6**), were analysed for CD4 and CD8 co-receptor expression. The proportion of CD3$^+$IFNγ$^+$ or CD3$^+$CFSE^{low} that were single positive for CD8$^+$ or CD4$^+$, DN: or DP were compared statistically (2-tailed, paired T-test) between A549 cells without (–) and with (+) *M. smegmatis*.

3.2.8 *M. smegmatis*-specific T-cells are enriched for γδ TCR

There were enough cells from donors 5, 7 and 10 (indicated by * in **Figure 3.6**) to further dissect the responding population in terms of αβ and γδ TCRs (**Figure 3.8**). Pan-TCR antibodies were used to stain the cells alongside antibodies for CD3, CD4 and CD8. Donors 5 and 7 had a greater proportion of $CD3^+$ $IFN\gamma^+$ $\gamma\delta TCR^+$ in the A549 cells with *M. smegmatis* cultures, compared to the A549 cells alone cultures, with 91% and 72.9% of $CD3^+IFN\gamma^+$ cells expressing γδTCR (background of 19.5% and 12.1%) respectively. For both donors 5 and 7 the $\gamma\delta TCR^+$ T-cells were predominately DN T-cells. The DN phenotype γδ T-cells is consistent with the fact that they are not HLA-restricted (Yachie et al., 1989). Despite a decrease in the proportion of $\alpha\beta TCR^+$ T-cells in the presence of *M. smegmatis* for donor 5, the distribution of CD4 and CD8 was skewed towards $CD8^+$ T-cells (56.7% with and 4.79% without *M. smegmatis*). The data for donor 10 shows responding cells were enriched for $\alpha\beta TCR^+$ T-cells, with 88.1% versus 74.4% for A549 cells with and without *M. smegmatis* respectively. Despite the relative neutrality for donor 10, there seems to be a skewing towards DN T-cells in the $\gamma\delta TCR^+$ gate (52.8% versus 12.3 % for A549 cells with and without *M. smegmatis*), and perhaps for $\alpha\beta TCR^+$ gated cells (7.5 % versus 0 % for A549 cells with and without *M. smegmatis*). T-cells could not be cleanly divided into γδ T-cells and αβ T-cells based on antibody staining. There might be several reasons for this such as the lack of separation by flow cytometry including down-regulation of TCR during ICS and steric hindrance between anti-CD3 and anti-TCR antibodies

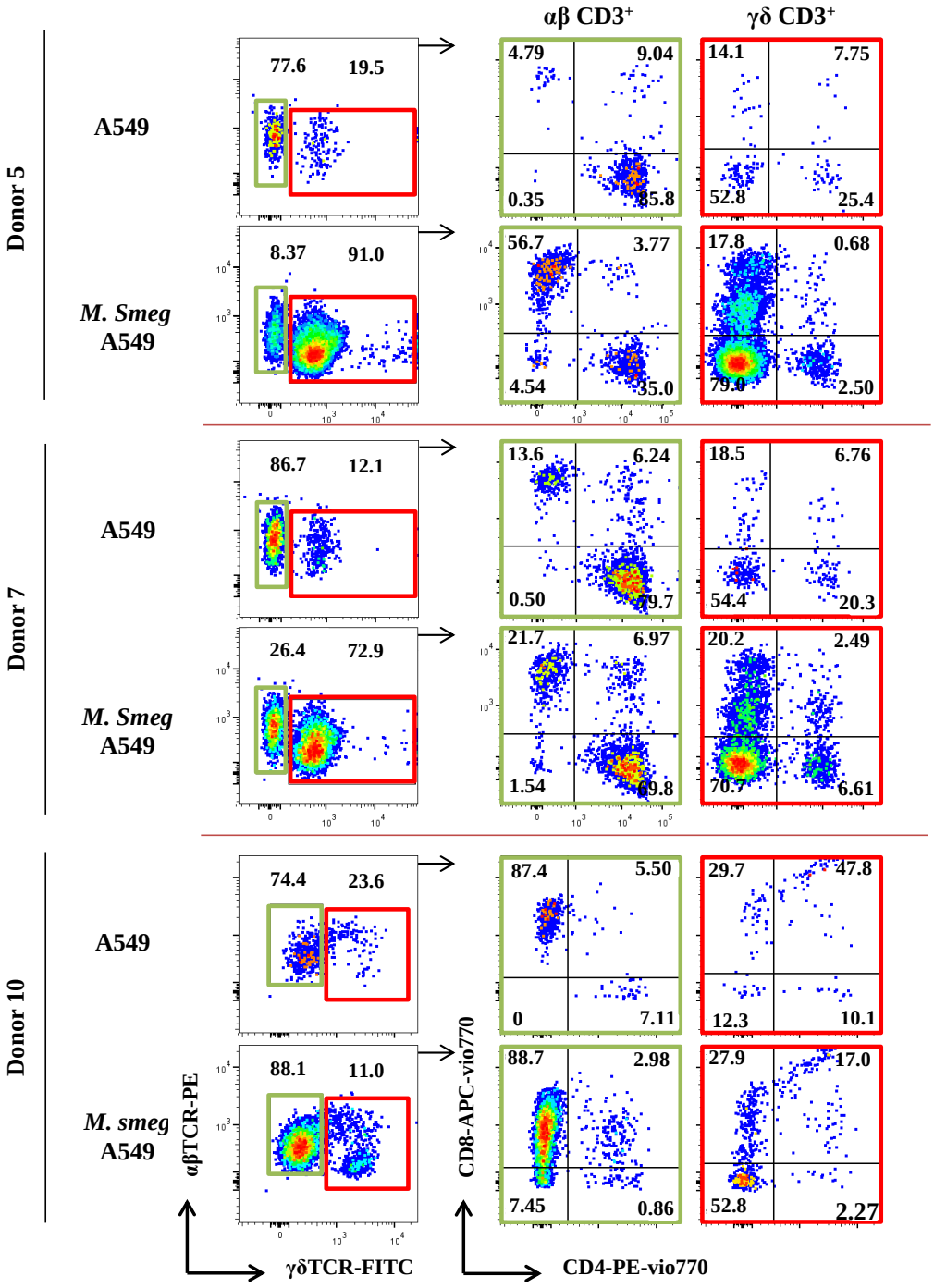

Figure 3.8 Gamma delta T-cells were enriched in two out of three donors following culture with A549 cells pre-incubated with *M. smegmatis*.

PBMC from three donors (* in **Figure 3.5**) were incubated with A549 cells that had been cultured with *M. smegmatis* for 13 days and restimulated with and without *M. smegmatis* prior to staining for IFNγ (intracellular), viability, αβTCR, γδTCR, CD3, CD4 and CD8. The cells were sequentially gated based on forward and side scatter, single, viable $CD3^+IFN\gamma^+$ cells and displayed as pseudocolour dots plots with αβTCR versus γδTCR fluorescence as shown. The cells in the green ($CD3^+\alpha\beta TCR^+$) and red ($CD3^+\gamma\delta TCR^+$) gates were further gated as indicated (arrow) and displayed as CD8 versus CD4 pseudocolour plots with large dots. The percentage of cells residing in the quadrant gates are shown inset for each dot plot.

3.2.9 Vα7.2 Jα33 TCRs are enriched in PBMCs primed with *M. smegmatis*

Mucosal associated invariant T-cells (MAITs) are characterised by usage of an invariant TCRα chain. This chain is made from Vα7.2 (Arden nomenclature) or TRAV1-2 (IMGT nomenclature), with junction (J) region 33. MAITs can be $CD8\alpha^+$ or DN (Reantragoon et al., 2013, Gapin, 2009). In order to examine whether *M. smegmatis* induced MAITs, I set up further experiments with two donors as above but stained with an antibody for the Vα7.2 TCR. PBMCs were primed with *M. smegmatis*-loaded A549 cells and cultured for 30 days prior to exposure to A549 cells ± *M. smegmatis* and ICS. Addition of Vα7.2 TCR antibody to the polychromatic phenotyping panel was highly sensitive to antibody concentration and it took me several weeks to optimise the protocol (hence the 30 day time point for this experiment). Post boosting with *M. smegmatis*, PBMCs were stained for viability and with monoclonal antibodies for αβTCR, CD4, CD8 and Vα7.2 TCR (**Figure 3.9**). Minimal background T-cell responses of 0.42% and 0.82% were seen for donor 11 and 12 respectively. In the presence of *M. smegmatis*, the proportion of $CD3^+IFN\gamma^+$ cells were the highest generated throughout this study, with 25.5% and 34.6% for donor 11 and 12 respectively (**Figure 3.9**). The increase in reactive T-cells could be due to donor differences, an increased accumulation of expanding T-cells with time (30 versus 13 days) and/or the steady demise of T-cells that did not get a survival signal, as they did not respond to antigen during the initial boosting. Both donors had a greater proportion of $CD3^+IFN\gamma^+V\alpha7.2^+$ T-cells (78.4% and 31.3% for donor 11 and 12 respectively) with *M. smegmatis*-loaded A549 cells compared to A549 cells alone (10.9% and 5.3% for donor 11 and 12 respectively) (**Figure 3.9**). The *M. smegmatis* responding $V\alpha7.2^+$ T-cells were enriched for a $CD8^+$ phenotype when compared to the A549 cells alone cultures. The discrimination of $V\alpha7.2^+$ from $V\alpha7.2^-$ was not clean, and it is possible that some Vα7.2 expressing T-cells, but temporarily low or apparently null, reside in the negative population due to TCR down regulation. Frustratingly, the pan αβTCR antibody did not perform as previously seen in **section 3.2.8**, possibly for reasons already discussed. For these reasons it is hard to interpret the data for the $CD3^+IFN\gamma^+V\alpha7.2^-$ population without improved resolution and/or by using antibodies against other cell surface markers, such as the γδTCR. The distribution of CD4 and CD8 on the $V\alpha7.2^-$ T-cells was not that dissimilar between A549 cells ± *M. smegmatis*, with only a slight skew towards $CD8^+$ and DN T-cells for donor 11 and $CD8^+$ T-cells for donor 12 with *M. smegmatis*.

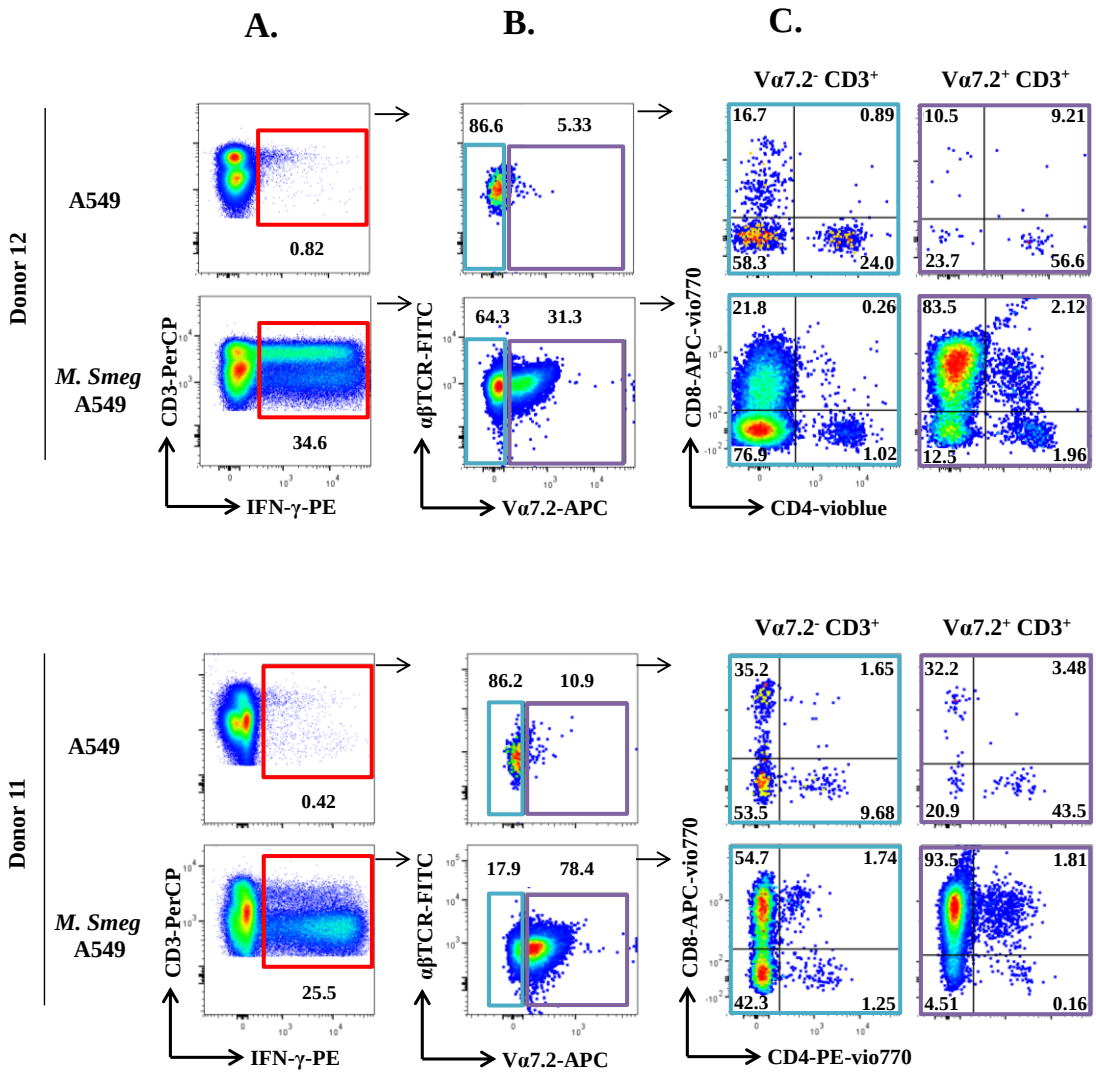

Figure 3.9 Mucosal associated invariant T-cells were enriched in *M. smegmatis* primed PBMC.

PBMC from two donors were incubated for 30 days with A549 cells that had been incubated with *M. smegmatis*. The cells were restimulated with A549 cells that had been incubated ± *M. smegmatis* and stained for IFNγ (intracellular), viability, αβTCR, CD3, CD4, CD8 and a monoclonal antibody against the variable alpha segment 7.2TCR (Vα7.2), which is associated with MAITs. The cells were sequentially gated based on forward and side scatter, single cells and displayed as pseudocolour dots plots with CD3 versus IFNγ (PE) then αβTCR versus Va7.2 (APC). The CD4 and CD8 expression was assessed on the Vα7.2 negative (blue) and positive (purple) cells as indicated by the associated gate colour, with percentages shown inset. Donor 11 was also stained with a monoclonal antibody against CD161 and the percentage of T-cells staining with CD161 shown inset (red) for the Vα7.2 negative and positive cells.

3.3 Discussion

The aim of this chapter was to dissect the T-cell populations generated during *M. smegmatis* antigen presentation by APCs. *M. smegmatis* was chosen for its ease of handling in the laboratory as well as its ability to be phagocytosed by specialised APCs such as DCs (Bohsali et al., 2010) and the lung epithelial cell line A549. T-cells are known to expand upon stimulation with cognate antigen. This expansion can be viewed by flow cytometry when cells are labelled with CFSE as this dye dilutes between daughter cells. CFSE dilution was used to observe T-cell responses to *M. smegmatis*-loaded autologous DCs and A549 cells. Both APC produced similar results but as DCs were limited in number, I continued with A549 targets.

A549 cells were used to present *M. smegmatis* antigens to two donor PBMCs stained with CFSE. T-cell expansion was analysed at 3, 8 and 13 days. On average, T-cell expansion at day 13 was higher than at 8 days (39% compared to 11.9% of CFSE low $CD3^+$ T-cells respectively). Subsequent experiments were performed after 13 days of exposure to *M. smegmatis* antigens. A high background of CFSE dilution in response to A549 cells was observed, therefore I examined another readout; IFNγ ICS. Background activation was considerably less with ICS. An IFNγ ICS was performed on 6 donor PBMCs to analyse the phenotype of *M. smegmatis*-specific T-cells. Interestingly, IFNγ $^+CD3^+$ T-cells skewed towards a CD8 and DN phenotype (**Figure 3.7**). Analysis of *M. smegmatis* responsive αβ and γδ T-cells populations for three of the 6 donors showed a significant enrichment of γδ T-cells mostly exhibiting a DN phenotype which is concordant with the literature (Brenner et al., 1987, Groh et al., 1989). The αβ and γδ T-cell populations were not clearly separated due to a very low anti-αβTCR and -γδTCR antibody staining. The low TCR antibody staining observed could be due to antibody steric competition between the anti-CD3 and -TCR antibodies that stain the same protein complex: CD3-TCR. However, in the case of the αβTCR antibody, this possibility has been tested for and ruled out by the manufacturer (Biolegend). I obtained clear separation with the anti-αβTCR and anti-CD3 antibodies used in my stainings with unstimulated PBMC. To conclude, the most likely reason for the poor separation was TCR down-regulation upon stimulation.

Two separate donor PBMCs were analysed for their distribution of Vα7.2 J33 TCR expressing population generated during *M. smegmatis* boosting of naive T-cells. A Vα7.2 J33 TCR is indicative of MAIT cells. There was a clear expansion of $IFN\gamma^{+}CD3^{+}V\alpha7.2TCR^{+}$ population stimulated by *M. smegmatis*-loaded A549 cells with both donor PBMC. These results make it likely that *M. smegmatis* induced MAITs. MAITs and their specificity are explored in more detail in Chapter 4.

The aim of this chapter was to dissect the T-cell subsets generated during exposure to *M. smegmatis* antigens. To this end I used IFNγ as a readout of T-cell activation as it is the classic T_H1 cytokine. It is possible that the choice of this cytokine skewed my results. However similar results were seen when examining T-cell proliferation by CFSE dilution and flow cytometry. I would also have liked to have simultaneously examined NK T cell populations by staining with CD56 and/or an antibody specific for the NK T Type 1 Vα24 invariant TCR chain. However, I was limited by the number of channels of the flow cytometer I had available to me. The use of other flow cytometers, such as the BD FACSAria II, allows the detection of 15 parameters simultaneously and could be used to include NK T-cell markers and isolate them from other T-cell subsets. Moreover, the development of new flow cytometers such as the Cytometer by Time of Flight (CyTOF) allows the detection of as many as 100 markers. This technology consists on using antibody labelled with heavy metals to stain single cells. Heavy metal time of flight is measured by mass spectrometry. This technology permits to combine multiple antibodies to look at T-cell polyfunctionality, memory phenotypes and specific markers and therefore improve the stringency of T-cell subsets dissection (Newell et al., 2012, Bendall et al., 2011, Ornatsky et al., 2006).

In conclusion, this study provides a preliminary insight into some of the T-cell subsets induced by *ex vivo* exposure to *M. smegmatis*-loaded cells. Due to the expression of certain analogous *M. tuberculosis* proteins, its low pathogenicity and high immunogenicity, *M. smegmatis* has become an attractive bacterium to use for the design of *M. tuberculosis* vaccines (Zhao et al., 2012, Sweeney et al., 2011). My results indicate that both conventional and unconventional "HLA-restricted" T-cells contribute to mycobacterial immunity. I next planned to examine these two types of T-cell responses in detail.

CHAPTER 4. RECOGNITION OF MYCOBACTERIA BY AN UNCONVENTIONAL T-CELL

4.1 Introduction

4.1.1 *Mycobacterium tuberculosis*-specific unconventional T-cells

The last five years has seen an increase in the number of studies examining the role of unconventional T-cells in infectious disease, particularly in *M. tuberculosis* infection. These studies include examination of the role of CD1-restricted T-cells, γδ T-cells and MAITs. Lipid-specific, CD1-restricted T-cells (described in Chapter 1) have an important role in immunity to mycobacteria. Circulating CD1-restricted T-cells from skin lesions of leprosy patients expressed a T_H1 profile (Sieling et al., 2000) and exhibited cytotoxic activity (Rosat et al., 1999). Downregulation of CD1a, CD1b and CD1c molecules at the surface of *M. tuberculosis* infected cells emphasises their likely importance in the control of *M. tuberculosis* infection (Stenger et al., 1998).

CD1d-restricted, NKT type 1 (formerly iNK) T-cells are now known to play a central role during various bacterial infections by producing a cytokine environment necessary for the recruitment of innate and adaptive cells (Kinjo et al., 2006, Nieuwenhuis et al., 2002). In TB infection, activity of iNK T-cells was shown to be characterised by the secretion of GM-CSF, a soluble factor that promotes maturation of *M. tuberculosis* infected macrophages *in vitro* leading to the inhibition of *M. tuberculosis* growth (Rothchild et al., 2014).

γδ T-cells also participate to the TB-specific immune response (Kasmar et al., 2011). The Vγ9/Vδ2 T-cell subset is known to be reactive to phospho-antigens including the (E)-4-hydroxy-3-methyl-but-2-enyl pyrophosphate (HMB-PP) produced by mycobacteria species and other bacteria (Eberl et al., 2003). Elevated numbers of Vγ9/Vδ2 T-cells have been observed in the peripheral blood and cerebrospinal fluid of TB infected patients (Kabelitz et al., 1990, Dieli et al., 1999).

While some inroads have been made in understanding unconventional T-cell biology during TB infection, much remains to be discovered. In this chapter, I will focus on an anti-microbial unconventional T-cell subset that has recently come to the forefront of T-cell biology: the Mucosal Associated Invariant T-cell (MAIT).

4.1.2 Mucosal Associated Invariant T-cells (MAITs)

4.1.2.1 MAIT cells have a specific phenotypic signature

The first evidence of MAITs existence was described by Porcelli and team in the 1990's where they observed a peripheral CD8/CD4 DN population expressing a semi-invariant TCR Vα chain (TRAV1-2/ TRAJ33 (IGMT nomenclature) or Vα7.2/Jα33 (Arden nomenclature) pairing preferentially with biased Vβ chain usage (Vβ2, Vβ11 and Vβ13) (Porcelli et al., 1993). The high conservation of the TCRα sequence combined with biased TCRβ usage indicated that MAITs recognize a very limited spectrum of antigens compared to conventional αβ T-cells. Interestingly, further TCR sequencing revealed a low degree of variation in CDR3α loop sequence that likely resulted in minor degeneracy in ligand recognition by the TCRα chain (Treiner et al., 2005). Collectively, these studies suggested that MAITs must be a functionally specialized T-cell subset.

Since 2003, the number of studies focusing on MAITs has rapidly increased and we are finally unravelling the biology of this mysterious T-cell subset. In 2003, Treiner and team found that MAITs were restricted to the non polymorphic ubiquitously expressed molecule MHC-Related Protein 1 (MR1) (Treiner, 2003). As shown in Chapter 3, MAIT cells can be $CD8^+$, $CD8^-$ and $CD8^-/CD4^-$ DN (Tilloy et al., 1999). A small frequency of $CD4^+$ MAITs was also detected in Chapter 3. MAITs express the C-lectin CD161 marker (Dusseaux et al., 2011) known to be highly expressed on T-cells that express IL-17 pro-inflammatory molecule such as the T_H17 subset (Walker et al., 2012). Moreover, MAITs possess a memory phenotype of $CD45RA^-$, $CD45RO^{hi}$, $CD95^{hi}$, $CD62L^{lo}$ (Dusseaux et al., 2011).

4.1.2.2 MAIT cell biology

MAIT cells constitute about 5-10% of T-cells in a healthy human blood. MAITs are enriched in some tissues such as liver, lung alveoli and gut epithelia where they can reach >50% of total T-cells (Dusseaux et al., 2011, Treiner et al., 2003). Like conventional T-cells, MAITs are generated in the thymus where they undergo positive and negative selection (Treiner et al., 2003, Martin et al., 2009). Germ free mice exhibit a marked depletion of peripheral MAITs suggesting that they have an important role in bacterial infections (Martin et al., 2009). *In vitro* studies have shown that MAITs can recognise gram positive and gram negative bacteria as well as fungi (Le Bourhis et al., 2010).

The role of MAITs in host defence has been demonstrated *in vivo* in mice where they are important in establishing and maintaining an inflammatory environment (Meierovics et al., 2013). Furthermore, peripheral MAITs have the ability to release granzyme A and B conferring cytotoxic activity (Le Bourhis et al., 2010, Aaltonen et al.).

4.1.2.3 MAITs in TB

MAITs are a major T-cell population in the lungs of healthy humans and are capable of recognizing *M. tuberculosis* antigen regardless of any previous exposure to the bacterium (Gold et al., 2008). MAIT frequency is low during acute TB infection but elevated during the TB latency (Gold et al., 2008) phase suggesting that MAITs are involved in the containment of *M. tuberculosis* expansion during latency.

4.1.3 MHC class I related protein-1

The gene for MHC related protein-1 (MR1) was discovered by a Japanese team in the 1990's, when they detected mRNA transcript of an MHC-related gene located on chromosome 1 outside the conventional HLA locus (Hashimoto et al., 1995). The MR1 gene sequence is highly conserved between individuals as well as between mammalian species suggesting that it has an important evolutionary role. MR1 shares strong sequence homologies with classical MHC class I molecules. MR1 is composed of a heavy chain subdivided in three α domains (α1, α2, α3). Like classical MHC I, MR1 heavy chain associates with β2m (Miley et al., 2003). The percentage of amino acid homology in the peptide-binding groove between classical MHC I and MR1 is 40-50%. Overall, MR1 is significantly more related to MHC I than other MHC related molecules such as the CD1 family of molecules suggesting that it is more likely to present a peptide than a lipid-based antigen (Hashimoto et al., 1995). MR1 is ubiquitously expressed on almost all nucleated cells and is essential for the recognition of bacteria by MAITs (Riegert et al., 1998). Interestingly, MR1 is up-regulated on pathogen infected cells which increases the activity of MAITs during active infection (Le Bourhis et al., 2013). MR1 is required for the positive selection of MAITs in the thymus (Gold and Lewinsohn, 2013). The level of MR1 expression on the cell surface is usually low compared to classical MHC I.

At the outset of my studies, I was provided with a MAIT clone raised from a patient with latent TB infection that killed *M. tuberculosis*-infected DCs via MR1. My goal was to determine the mechanism of this important molecular recognition.

4.1.4 Aims

When I started my studies with MAITs the ligand they recognised was unknown. The shape and function of the MR1 molecule suggested that it presented parts of bacteria to MAITs and there was speculation about this ligand being a peptide due to the strong homology between MR1 and conventional MHC class I molecules. The focus of this chapter was to characterise the ligand recognised by *M. tuberculosis*-specific MAITs. I was provided with a MAIT clone termed D426 B1 by Prof. David Lewinsohn at the University of Oregon. At the beginning of this work my goals were to:

- Test whether MR1 molecule presented a peptide ligand to MAITs.
- Refold MR1 monomers and produce MR1 tetramers.
- Stain D426 B1 cells with MR1 tetramer.

4.2 Results

4.2.1 Mycobacterium tuberculosis-reactive MAIT clone

Professor David Lewinsohn provided me with a MAIT cloned from the peripheral blood of a TB infected patient (patient D426). This MAIT clone was termed D426 B1. The D426 B1 TCR had been sequenced to verify expression of the invariant MAIT TCRα Vα7.2/Jα33 and D426 B1 clonality. D426 B1 expressed a Vβ 13.5 chain (Gold et al., 2010), the most common Vβ chain expressed by MAIT cells in the peripheral blood (Porcelli et al., 1993).

4.2.2 D426 B1 MAIT clone effector functions

4.2.2.1 D426 B1 clone effector functions in response to M. smegmatis

T-cell effector function is characterized by the release of specialized cytokines upon TCR interaction with an infected cell. MAITs are known to exhibit a T_H1 cytokine profile as well as a cytotoxic function to target cells infected with *Shigella flexneri* (Le Bourhis et al., 2013) or *Salmonella typhimurium* (Gras et al.). My collaborators have demonstrated that the D426 B1 MAIT clone can be activated by *M. tuberculosis* infected DCs via MR1 presentation (Gold et al., 2010).

In order to assess if the D426 B1 clone was able to exhibit MAIT-like effector functions, I examined the activity when these cells were presented with *M. smegmatis*-infected DCs from an MHC-I/II mismatched donor. As mentioned in Chapter 3, I chose to use *M. smegmatis* to present bacterial antigen to MAITs as the bacterium grows rapidly and is relatively easy to culture. It was also possible to work with *M. smegmatis* under the containment level 2 facilities I had available to me. *M. smegmatis* infected human cells are good activators of MAITs (Chapter 3, **Figure 3.7**).

I first examined D426 B1 cytotoxic activity by chromium release assay. Chromium cytotoxic assays are routinely used in my laboratory to quantify ^{51}Cr release from ^{51}Cr-loaded APCs following lysis by cytotoxic T-cells. The percentage of killing is directly deducted using the following formulas: % cytotoxicity = [(experimental release − spontaneous release) / (maximal release − spontaneous release)] × 100. Monocytes from a healthy donor PBMCs were extracted and differentiated into DCs as described in Chapter 2, and then infected with *M. smegmatis* and labelled with the radioactive chromium isotope ^{51}Cr. D426 B1 T-cells were incubated with the *M. smegmatis* infected or uninfected- ^{51}Cr-labelled DCs for 4h. Supernatants were harvested and D426 B1 cytotoxicity was analysed by measuring the ^{51}Cr released from *M. smegmatis* infected DCs (**Figure 4.1.A.)**. Expression of IFNγ and MIP-1β was simultaneously measured by ELISA (**Figure 4.1.B.**). Over the 4h experiment, more than 70% of *M. smegmatis* infected DCs were killed by D426 B1 cells. These cells did not lyse uninfected DCs (**Figure 4.1.A.)**. As expected, D426 B1 cells secreted MIP-1β (>600 pg/mL) and IFNγ (>350 pg/mL) in response to *M. smegmatis* infected DC (**Figure 4.1.B.**).

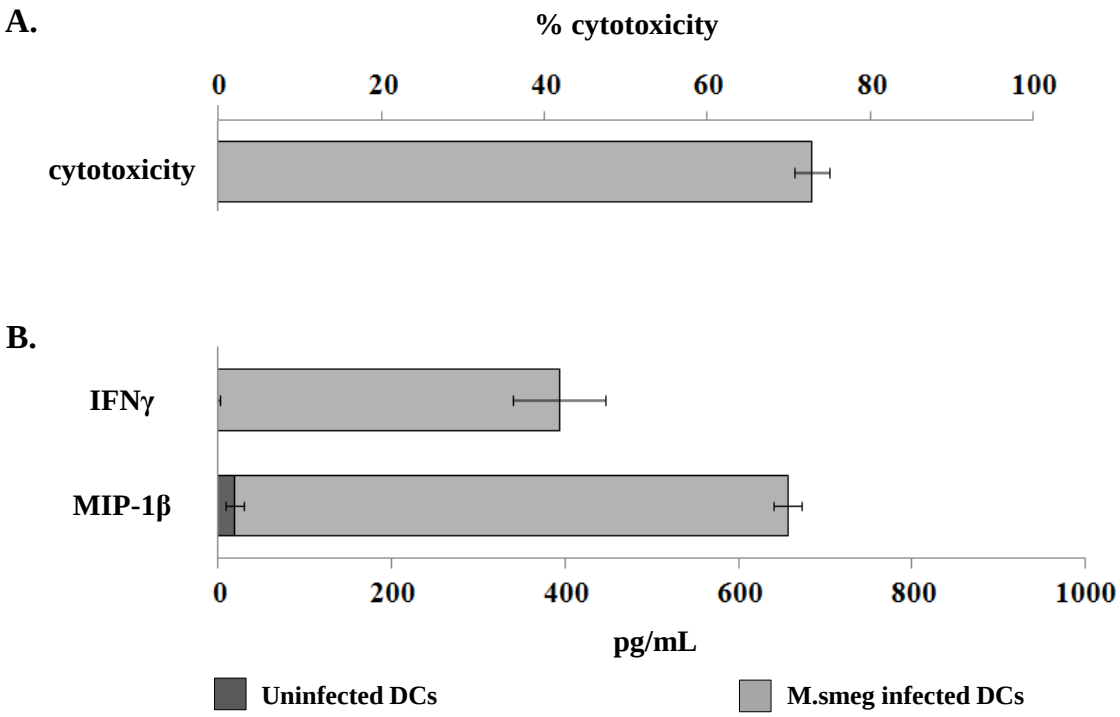

Figure 4.1. Quantification of the cytotoxic and cytokine profile of the D426 B1 clone to *Mycobacterium smegmatis* infected dendritic cells.
Heterologous dendritic cells (DC) were labelled with Cr^{51} for an hour followed by a wash in R10. DCs were left to rest for an hour then washed in R10. $2x10^3$ Cr^{51} labelled DCs were infected with *M. smegmatis* and presented to $1x10^4$ D426 B1 MAIT clone. Cells were incubated for four hours and the supernatant was harvested. (**A.**) D426 B1 cytotoxicity was analyzed by measuring the Cr^{51} release of DCs using a micro-beta counter. The percentage of cytotoxicity was calculated using the formula: % cytotoxicity = [(experimental release − spontaneous release) / (maximal release − spontaneous release)] × 100. (**B.**) Release of IFNγ and MIP-1β cytokines by D426 B1 was measured by ELISA.

Since, D426 B1 clone could kill non-HLA matched DCs infected with *M. smegmatis* and produce T_H1 cytokines, we hypothesized that this response was restricted by a non-polymorphic MHC; most likely MR1.

4.2.3 D426 B1 clone recognises short peptides

4.2.3.1 Antigen presenting cells for MAIT profiling

To avoid recognition through conventional MHCs two APCs, hMR1-HeLa cells and A549, were selected due to their mismatched HLA expression with donor D426 and ease of culture. Moreover, our collaborators have previously shown that D426 B1 clone recognises *M. tuberculosis* infected A549 cells (Gold et al., 2010). I therefore reasoned that A549 cells must efficiently present epitopes to D426 B1.

4.2.3.2 D426 B1 clone peptide sizing scan and peptide library screening

I next aimed to investigate whether MAIT cells could recognize and/or be activated by peptides. For this aim, I used different length combinatorial peptide libraries (CPLs) laid out in positional scanning format. **Figure 4.2** shows a graphical representation of a nonamer CPL.

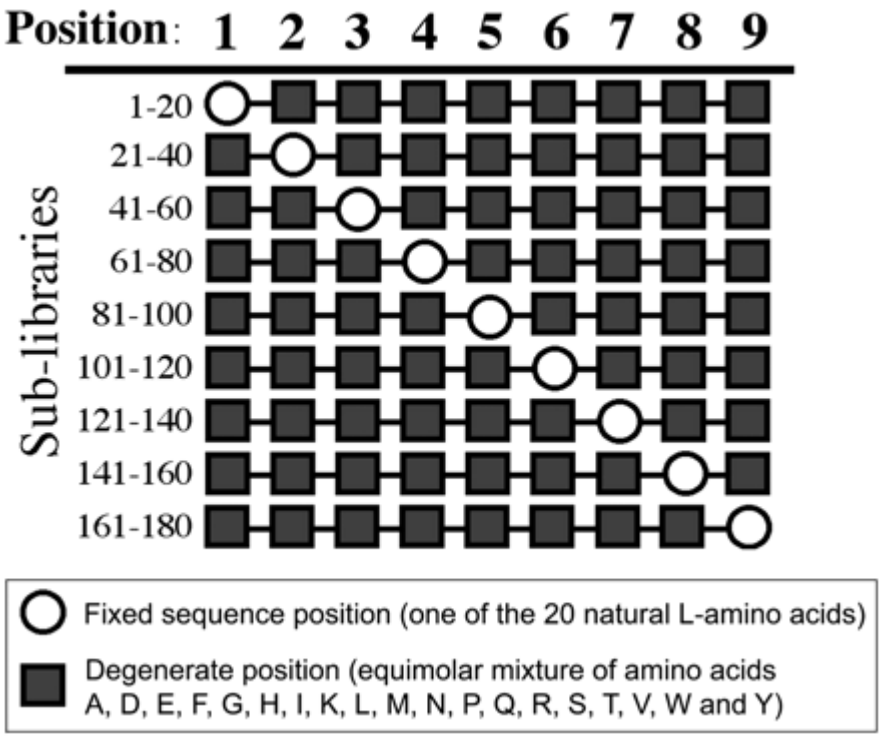

Figure 4.2. Representation of a nonamer combinatorial library (Wooldridge et al., 2010).

The nonamer CPL is divided into sub-libraries of peptide mixtures. In each peptide mixture, one of the 20 proteogenic amino acids (A, C, D, E, F, G, H, I, K, L, M, N, P, R, S, T, V, W and Y) is fixed at one position (circle) while the other are degenerate between the 19 natural amino acids (square) with the exception of the cysteine. Peptides within each mixture are present at equimolar concentration. Each sub-library corresponds to a complete scan of the peptide diversity at one position and is composed of 20 peptide mixtures each with one amino acid fixed at one position along the 9-mer peptide backbone. For example, the first mixture consists of peptides with alanine at position P1 and positions P2 to P9 are degenerate. The second mixture consists of peptide with alanine at position P2 with the other positions are degenerate. The nonamer CPL contains in total 4.9×10^{11} peptides.

Briefly, a CPL is series of sub-libraries that when combined that contain almost all possible peptides of a defined length. Each mixture is composed of peptides that have a fixed amino acid at a specific position and an equimolar mix of 19 amino acids at each other position along the peptide backbone. Cysteine is used as a "fixed' amino acid but is not included as part of the equimolar mix to limit the possibilities of oxidation. Thus the only possible peptides known to be missing from a complete library of a given length are those that contain more than one cysteine. CPL screens have been used to map a T-cell epitope (Yin et al., 2011). My laboratory has had great success using these tools (Wooldridge et al., 2012, Ekeruche-Makinde et al., 2012, Ekeruche-Makinde et al., 2013) including mapping unknown T-cell epitopes (unpublished).

D426 B1 clone was challenged with a single sub-library (position 4) of octamer (8mer), nonamer (9mer), decamer (10mer), undecamer (11mer), dodecamer (12mer) and tridecamer (13mer) CPLs in order to determine the optimum peptide length recognized by D426 B1. Unexpectedly, it has recently been shown by our group that CD8 T-cells are "preprogrammed" to recognize peptides of defined length (Ekeruche-Makinde et al., 2013). hMR1-HeLa cells were pulsed with position 4 peptide mixtures from the five CPLs and were used as targets for D426 B1 in overnight assays. Potential alloreactivity of D426 B1 with hMR1-HeLa was controlled for by incubating T-cells with hMR1-HeLa with 5% of DMSO (the solvent used to reconstitute the peptide library mixtures). The supernatants were harvested and analysed by MIP-1β ELISA. Interestingly, only the position 4 mixtures of the nonamer CPL activated D426 B1. Indeed, D426 B1 secreted >150 pg/mL of MIP-1β when stimulated with the position 4 proline of the 9mer CPL. These results suggested that D426 B1 can recognise a 9mer peptide with a proline at position 4 (**Figure 4.3**).

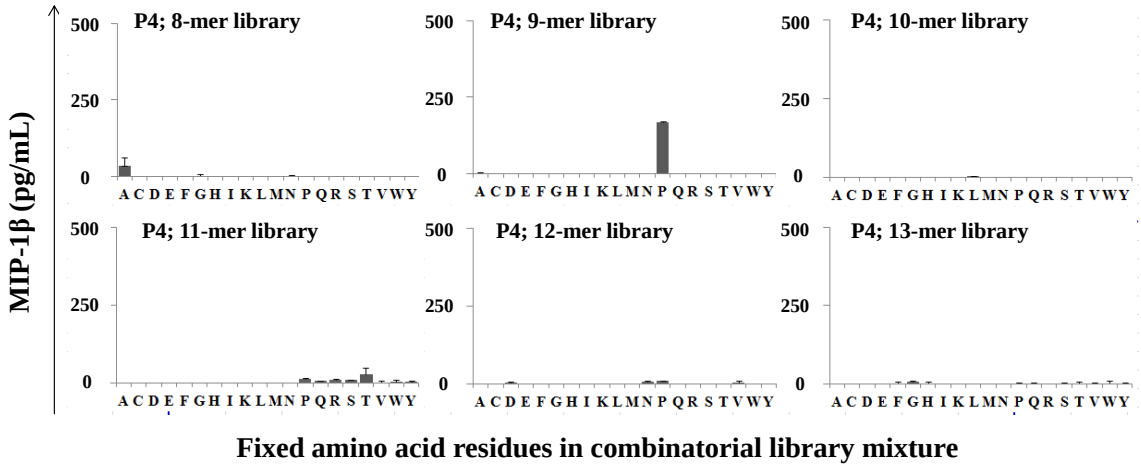

Figure 4.3. Screening of D426 B1 cells using position 4 mixtures of the 8mer, 9mer, 10mer, 11mer, 12mer and 13mer combinatorial peptide libraries (CPLs).
D426 B1 were stimulated overnight with hMR1-HeLa pulsed with position 4 peptide mixtures from six CPLs. The supernatants were harvested and responses to the CPLs were analyzed by MIP-1β ELISA. Responses are displayed as a cluster of six histogram plot representing a set of 20 mixtures having a define amino acid listed on the x-axis. Each histogram represents the position 4 along the peptide backbone of the different peptide length of CPLs.

4.2.3.3 D426 B1 nonamer peptide library screenings

D426 B1 was next challenged with hMR1-HeLa cells pulsed with the full nonamer peptide library. Individual D426 B1 responses were quantified by the release of MIP-1β by ELISA. CPL screening showed a preference for defined residues in the peptide core at positions P3, P4, P5, P6, P7 and P8. However, at the peptide termini such as P1, P2 and P9, D426 B1 did not react to any of the CPL sub-mixtures (**Figure 4.4 A.**). The overall D4261 B1 response to the nonamer CPL is summarized in **Figure 4.4 B**.

A.

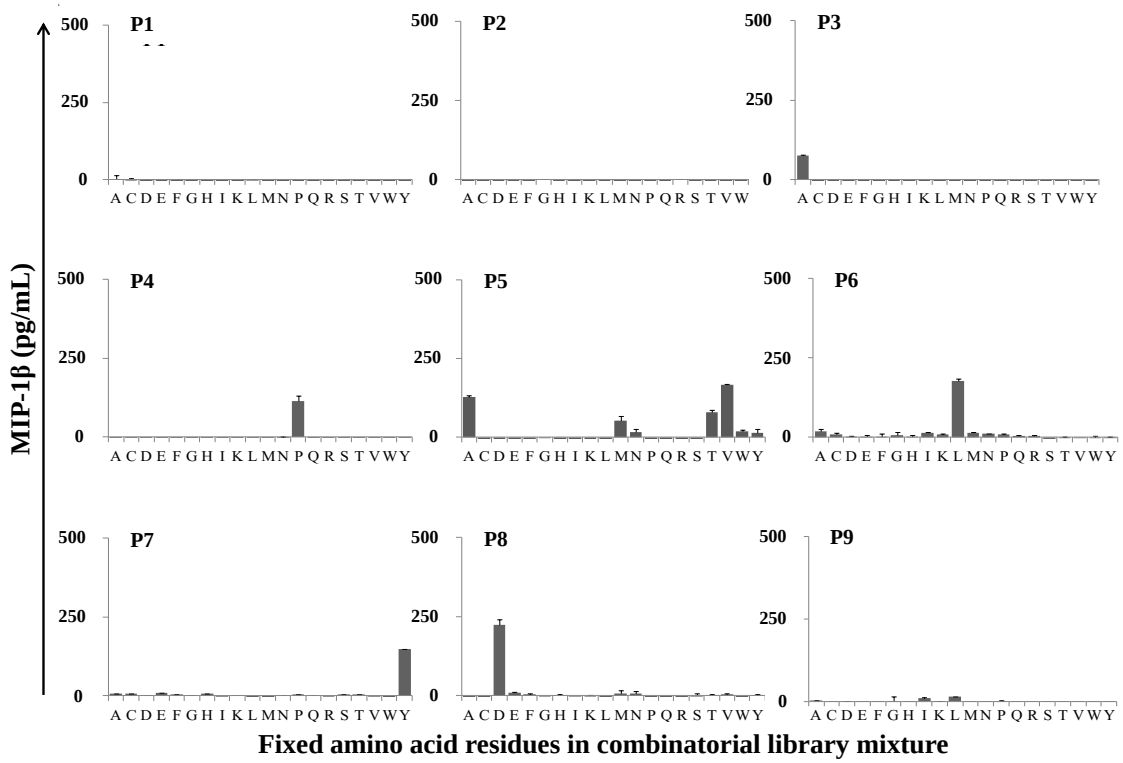

B.

1	2	3	4	5	6	7	8	9
		A	P	A V M T N W Y	L A	Y	D	

MIP-1β (pg/mL) colour code:
125-250 Red
63-125 Green
5- 63 Blue

Figure 4.4. Complete nonamer combinatorial peptide library (CPL) screen on the D426 B1 MAIT T-cell clone.

hMR1-HeLa cells were pulsed with the nonamer peptide library mixtures and presented to D426 B1. The response to the library mixtures was measured by MIP-1β ELISA. **A.** The nine histograms represent the nine amino acid positions along the peptide backbone (from N-term to C-term) numbered as P1 to P9. Each histogram represents D426 B1 MIP-1β responses to 20 set of CPL sub-mixtures with a define amino acid fixed at each position and plotted on the x axis. **B.** Shows a summary of the data in **A**. Each mixture is characterized by the single letter nomenclature of the amino acids fixed within the mixtures. The magnitude of response is characterized by the MIP-1β concentration released by D426 B1 seen in the screen and is assigned with colour codes ranging from red to blue.

The lack of any recognition of sub-mixtures at P1, P2 and P9 might suggest that the MAIT TCR does not make contacts outside of the central region of the peptide and/or that these positions are not required for MR1-binding. It is also possible that the MAIT TCR might be restricted to a small number of peptides thus the concentration of individual immunogenic peptides within the CPL sub-mixtures may be too low to trigger a measurable response at P1, P2 and P9. Nonetheless, a conserved D426 B1 immunogenic peptide sequence was retrieved from D426 B1 screening with the nonamer CPL: xx**APVLYDL.**

4.2.3.4 Design of D426 B1 peptide agonists

From the D426 B1 screening with the nonamer CPL, a core 9mer immunogenic sequence was retrieved: xx**APVLYDL**. A search with National Centre for Biotechnology Information (NCBI), revealed several epitopes from the *M. tuberculosis* proteome with similarity to the CPL suggested sequence. These epitopes and their protein origin are listed in **Table 4.1**. Interestingly, these sequences are often conserved with other bacterial species providing a potential, and exciting, explanation for how MAITs are able to recognise several different pathogens.

	Protein in *M. tuberculosis*	**Species excluding *M. tuberculosis***
DDLPVLYEL	peptide chain release factor 2	*M. avium/smegmatis/abscessus*
DHAPVLVDL	exodeoxyribonuclease III protein xthA	*M.bovis/smegmatis/cosmeticum*
FWHKVLYDL	leucyl-tRNA synthetase leuS	*Staphylococcus aureus, Lactobacillus delbrueckii, Streptococcus agalactiae, M. xenopi*
TSGPVNYDL	conserved hypothetical protein	Only *M. tuberculosis*
GLEEVLYEL	DNA-directed RNA polymerase subunit beta	*M. ulcerans/liflandii/africanum*
MRPPALYDT	conserved alanine rich protein	*M. paratuberculosis/ avium/xenopi*

Table 4.1. Blast of *M. tuberculosis* protein sequences sharing identities with xxAPVLYDL.

I also designed some predicted optimal, but non-natural, peptide agonists for D426 B1. These sequences were: IR**APVLYDL,** IR**APA**L**YDL,** IR**APVLYD**I**,** MR**APA**L**YD** ISV**PVLY**A**L**, IR**AP**A**LYD**I (bold letters indicate the optimal residues determined by CPL screen while non-bold residues are amino acids that also showed in the screen).

For custom agonist screening, hMR1-HeLa cells were pulsed with a titration of individual peptides from 10^{-4} to 10^{-14} M and presented to D426 B1. Supernatants were analysed by MIP-1β ELISA. D426 B1 reacted to all the peptides. MIP-1β was still detected when D426 B1 was stimulated with a concentration as low as ~10^{-13} M of IRAPVLYDL, IRAPALYDL, IRAPVLYDI and MRAPALYDL peptides indicating that D426 B1 is very sensitive to these particular agonists (**Figure 4.5**).

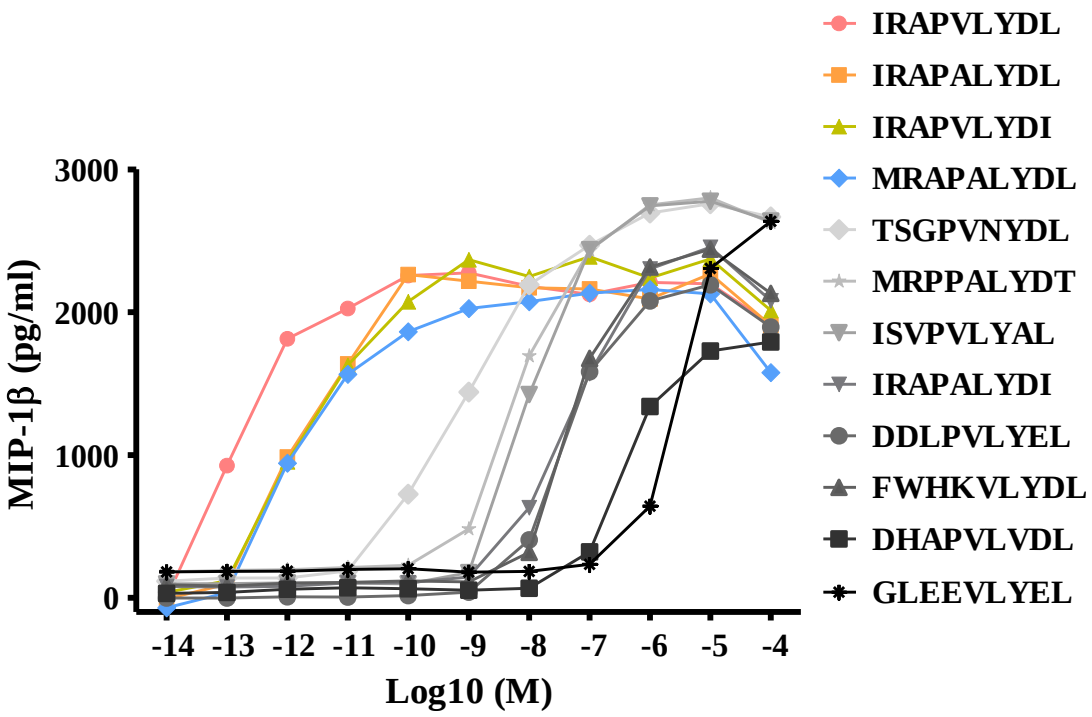

Figure 4.5. D426 B1 TCR recognition of titrated peptides ligand suggested from nonamer CPL screening.
$6x10^5$ hMR1-HeLa cells were pulsed with a titration of peptides designed predicted by the nonamer CPL screen and presented overnight to $3x10^5$ D426 B1 MAITs. Supernatant were harvested and analyzed by MIP-1β ELISA.

4.2.4 D426 B1 clone does not recognize peptide through MR1

Once I had identified potential ligands, the next step was to verify if the peptides were restricted by the MR1 molecule. To achieve this, two blocking antibodies were used. The first antibody was provided by Ted Hansen (Washington University, School of Medicine) and is a conformation dependant anti-MR1 blocking antibody (clone 26.5) (Huang et al., 2005). The second antibody was an anti-MHC I (clone W6/32) blocking antibody that targets the constant region found on the α chain of MHC I region associated to β2m molecule. W6/32 is known to bind to HLA-A, -B, -C and -E (Chouaib et al., 1988). 26.5 and W6/32 antibodies were used to block the D426 B1 response to peptide in order to verify MHC restriction.

My first attempt of blocking the D426 B1 response was performed by stimulating D426 B1 with the IRAPVLYDL peptide in the absence of APC (T-cell-to-T-cell presentation) (**Figure 4.6**). D426 B1 cells were first treated with either, the anti-MR1 clone 26.5 blocking antibody, W6/32 blocking antibody or no antibody and then stimulated with peptide overnight. Activation was measured by MIP-1β ELISA (**Figure 4.6**). The D426 B1 response was not completely blocked by either of the antibodies. However, reduced sensitivity in the presence of W6/32 was noted. Several hypotheses can be proposed to explain these results. First, blocking antibodies are not optimum tools to block T-cell activation as they cannot provide an absolute antibody saturation of all surface bound MHCs. Second, MIP-1β is arguably the most sensitive read out for T-cell activation (Laugel et al., 2007). Highly immunogenic peptides may trigger T-cell activation through low numbers of pMHC "missed" by antibody blocking.

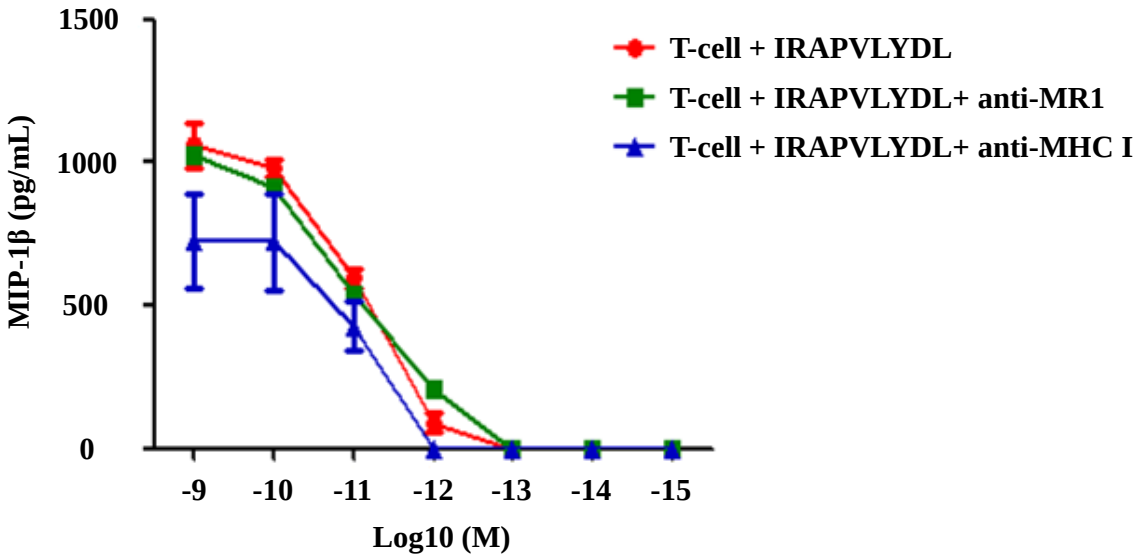

Figure 4.6. Identifying the MHC restriction of candidate ligands through antibody blocking.

$3x10^5$ D426 B1 cells were first treated with 50 μg/mL of anti-MR1 (clone 26.5) or anti-MHC I (clone W6/32) blocking antibodies and then with a titration of IRAPVLYDL peptide. The cells were incubated overnight and the T-cell response was analyzed by measuring the MIP-1β release by ELISA.

In order to limit the possibility of 'leakiness' during antibody blocking experiments I decided to utilise less potent peptide antigens. To this end, I used sub-mixtures from the nonamer CPL instead of IRAPVLYDL to stimulate D426 B1. Indeed, the CPL sub-mixtures appeared less sensitive than to IRAPVLYDL in my initial assays so these responses would be more responsive to T-cell blocking via an antibody to the restricting element. The chosen CPL sub-mixtures were those that best activated D426 B1 clone (**Figure 4.4.A.**). These CPL sub-mixtures were named after the number corresponding to the position of the fixed amino acid and the single letter amino acid code fixed at this position: position 3 alanine (3A), position 4 proline (4P), position 5 alanine (5A), position 5 valine (5V), position 6 leucine (6L), position 7 tyrosine (7Y) and position 8 aspartic acid (8D). As detailed above, D426 B1 cells were treated with both anti-MR1 (clone 26.5) and anti-MHC I (clone W6/32) blocking antibodies and 10 μM of nonamer CPL sub-mixtures. Supernatants were harvested after 24 hours incubation and responses to the peptide mixtures were analyzed by MIP-1β ELISA. In the absence of antibody, D426 B1 was activated by all CPL sub-mixtures characterized by a secretion of < 200 pg/mL MIP-1β. However, D426 B1 responses to CPL sub-mixtures were not blocked after treatment with anti-MR1 26.5 blocking antibody indicating that D426 B1 responded to the peptide in an MR1-independent manner. In contrast, the CPL sub-mixture responses were completely abrogated when using the W6/32 MHC I antibody (**Figure 4.7**). These results indicate that D426 B1 recognizes peptide presented by a classical MHC class I molecule and not by MR1.

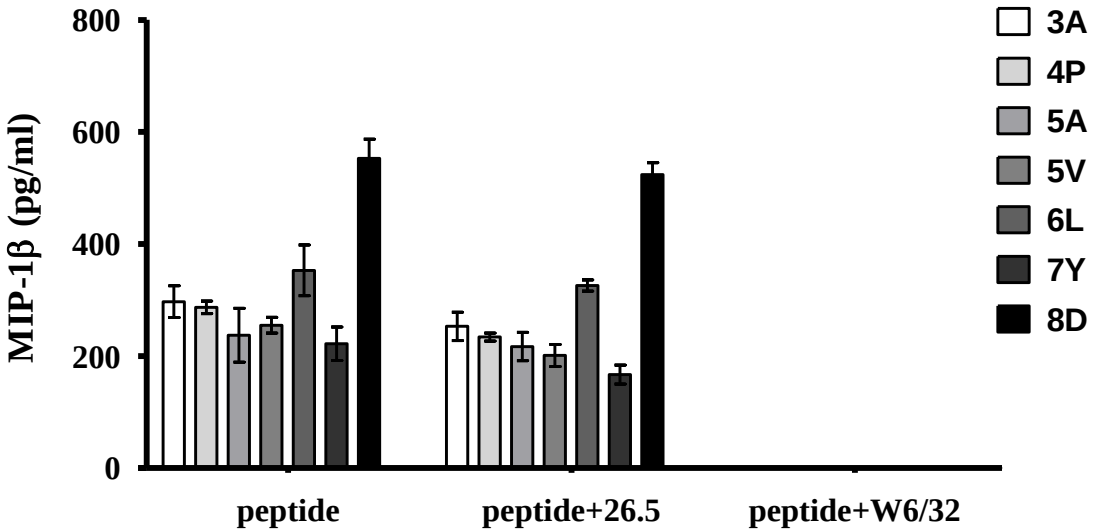

Figure 4.7. Blocking of the D426 B1 response to CPL sub-mixtures.
$3x10^5$ D426 B1 cells were treated with either and an anti-MR1 (clone 26.5), anti-MHC class I blocking (clone W6/32) antibodies or no antibody for an hour. 10 μM of seven nonamer CPL mixtures were added to D426 B1 and the cells were incubated overnight at 37°C. Supernatants were harvested and analysed by MIP-1β ELISA.

These experiments pointed towards two potential conclusions. First, I deemed it was possible that D426 B1 could have more than one specificity such that it could see one ligand in the context of MR1 *and* a peptide ligand in context of a classical HLA molecule. Second, it was also possible that the D426 B1 MAIT clone was not, as claimed, a monoclonal population. I therefore set about further characterisations of the D426 B1.

4.2.4.1 Polyfunctional profiling of the D426 B1 clone through intracellular staining with an agonist peptide

The cytokine release profile of D426 B1 was measured by intracellular staining (ICS) upon stimulation with IRAPVLYDL peptide. ICS permits discrimination of individual responder cells within a population by measuring cytokine production at the single cell level. D426 B1 MAIT clone was stimulated with or without IRAPVLYDL peptide for 4 h. The ability of all T-cells within the D426 B1 line to be triggered via the TCR was assessed using an anti-CD3 antibody. The cytokine profile of the D426 B1 line was measured by production of intracellular MIP-1β, IFNγ and TNFα by ICS. Additionally, up-regulation of CD107a, a marker of degranulation and a surrogate marker of CD8 T-cell killing, was measured (Betts et al., 2003). Analysis was carried out by polychromatic flow cytometry. As expected, unstimulated D426 B1 did not stain for cytokines. However, upon anti-CD3 antibody stimulation D426 B1 T-cells stained for numerous cytokines. Importantly, these experiments identified a distinct, minority peptide-specific population constituting only ~10% total T-cells (**Figure 4.8.B.**).

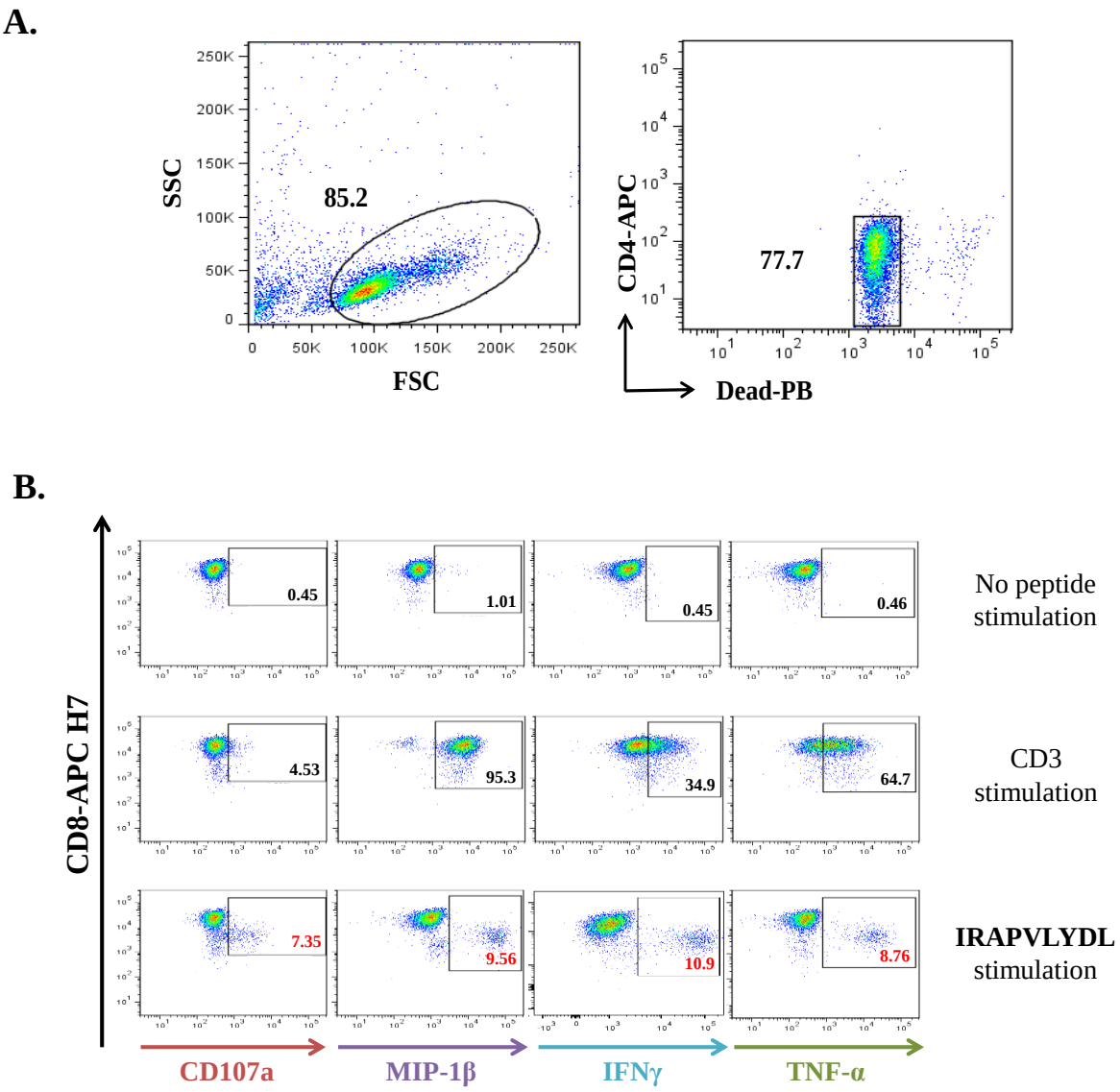

Figure 4.8. Intracellular staining of D426 B1 cell line stimulated with IRAPVLYDL peptide.

$3x10^5$ D426 B1 cells were treated with Golgi Stop and Golgi Plug and stimulated for four hours with 5% DMSO (**1st line quadrants**) 1 µg/mL of anti-CD3 antibody (**2nd line quadrants**) or 50 µM of IRAPVLYDL (**3rd line quadrants**). An ICS was performed as explain in Chapter 2 and cells were analysed by flow cytometry. (**A.**) **Gating strategy**. D426 B1 cells were first gated using the SSC vs FCS. Alive CD4 negative T-cells were then isolated. (**B.**) D426 B1 cells were stained using anti-CD107a, MIP-1β, IFNγ, and TNFα antibodies.

These results appeared to confirm the presence of a peptide-specific contaminant population within the well characterised D426 B1 MAIT clone (Gold et al., 2010) I obtained from my collaborators in Portland. In order to formally confirm this disappointing possibility, I sequenced the TCR chains present in the clone.

4.2.4.2 TCR sequencing of the D426 B1 clone

To determine the clonality of the D426 B1 clone, 5' Rapid Amplification of cDNA Ends (RACE)-based TCR sequencing was carried out to evaluate clonal purity. Two TCRα and two TCRβ chains were detected within the D426 B1 cell line. The presence of the Vα7.2/Jα33 α chain variant in D426 B1 confirmed that at least one population was a MAIT cell (**Table 4.2**). The presence of a Vα1.4/Jα45 clonotype in ~15% of the culture indicated a contaminating CD8 T-cell within the D426 B1 culture.

A. TCRα chain sequencing

TRAV (IMGT)	Vα (Arden)	CDR3α	TRAJ	Freq (%)
1-2	7.2	CAVRDSNYQLI	33	85.71
8-3	1.4	CAVGRGGADGLT	45	14.29

B. TCRβ chain sequencing

TRBV (IMGT)	Vβ (Arden)	CDR3β	TRBJ	Freq (%)
6-4	13.5	CASSDSGESGTEAF	1-1	59.14
15	24.1	CATSMMGYNEQF	2-1	40.86

Table 4.2. 5'RACE TCR sequencing of D426 B1 line (kindly performed by Dr James Mclaren, Cardiff University).
The TCR Vα and TCR Vβ chains and CDR3 loop sequence, J region and the frequency of the different populations within the D426 B1 T-cell clone.

The discovery that the MAIT clone I had been using in my studies was not a monoclonal population was a huge disappointment. In order to formally confirm that the clone was not a single, dual TCR population of cells I decided to attempt to clone out the peptide-specific population.

4.2.5 Separation of the peptide-specific clone from the D426 B1 polyclonal culture

In order to separate out the two clonotypes within the D426 B1 cell line, an IFNγ capture assay was performed (as described in Chapter 2) after 4 h stimulation with 50 μM of IRAPVLYDL peptide. The IFNγ positive and negative fractions were rested overnight in T-cell culture medium prior to a cloning step in a 96-well plate at 0.5 cell/well. Only one clone expanded well from the IFNγ negative fractions and was called D12. Two clones expanded well from the IFNγ positive fraction and were called A5 and A6 according to their position on the 96 well-plate. All clones were stimulated with 50 μM of IRAPVLYDL overnight and the response to the peptide was analysed by measuring the release of MIP-1β by ELISA. The D12 T-cell clone did not respond to IRAPVLYDL peptide. In contrast, clones A5 and A6 responded to this peptide (**Figure 4.9**).

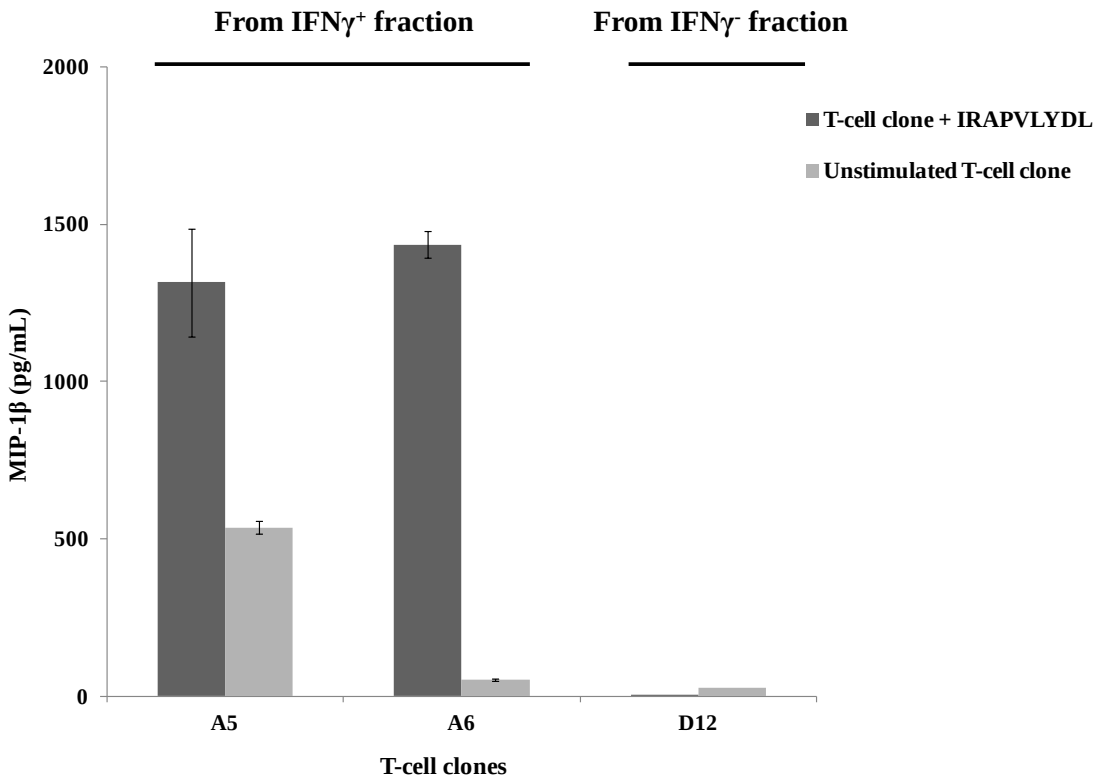

Figure 4.9. D426 B1 T-cell clones specificity for IRAPVLYDL.
A5, A6 and D12 T-cell clones extracted from the D426 B1 cell line IFNγ$^+$ fraction and IFNγ$^-$ fraction separated in response to peptide were stimulated with 50 μM of IRAPVLYDL peptide overnight. Supernatants were harvested and analyzed by MIP-1β by ELISA. Dark grey bars represent T-cell clones stimulated with peptide while light grey bars represent unstimulated T-cell clones.

Overall, the "separation" of the D426 B1 subpopulations was successful as we established peptide-specific T-cell clones (A5 and A6) and a peptide unresponsive T-cell clone (D12). Unfortunately only the A6 T-cell clone continued to expand in culture to sufficient number for further assays. For ease of description, this clone was renamed from A6 to "Morpheus". I next set about further characterising this peptide-specific T-cell clone.

4.2.5.1 The peptide-specific T-cell clone Morpheus is not a MAIT

Morpheus clone was first stained with an anti-Vα7.2 antibody to verify MAIT cell lineage using clone 3C6 (Martin et al., 2009). A Vα7.2-positive population was revealed in the D426 B1 starting culture. However, Morpheus did not stain with Vα7.2 (**Figure 4.10 A**). TCR sequencing of Morpheus showed just one α chain and one β chain as expected (**Figure 4.10 B**). These chains were identical to the additional chains seen in the starting "monoclonal" D426 B1 population.

A.

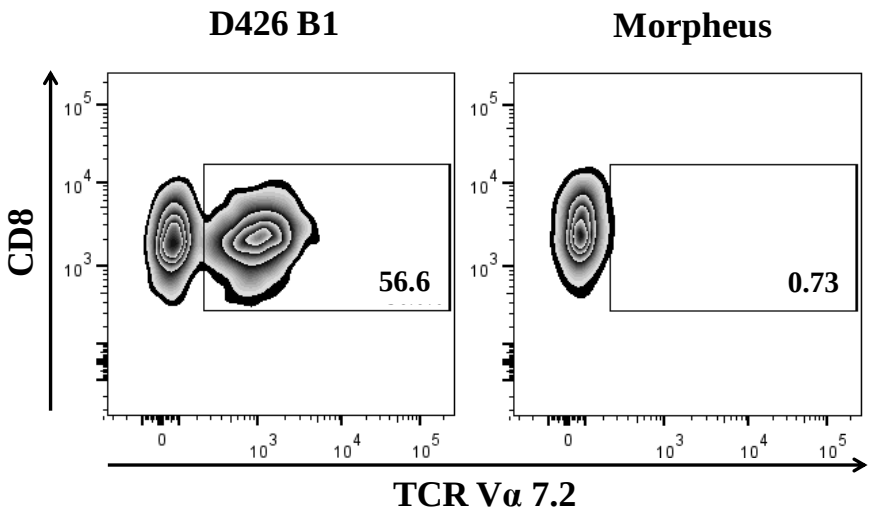

B.

TCR (Arden et al.)	CDR3	TRJ
Vα 1.4	**CAVGRGGADGLT**	**45**
Vβ 24.1	**CATSMMGYNEQF**	**2-1**

Figure 4.10. Morpheus clone is not a MAIT cell.

(**A.**) Vα7.2 staining of D426 B1 cell line and Morpheus clone. $3x10^5$ D426 B1 cells or Morpheus cells were stained with an anti-CD8 and Vα7.2 antibodies for 30 minutes on ice, washed once and analysed by flow cytometry. (**B.**) 5'RACE TCR sequencing of Morpheus clone. Morpheus clone TCR was analyzed by 5'RACE sequencing by Dr. James McLaren. The TCR Vα and TCR Vβ chains are described using Arden et al. nomenclature as well as the CDR3 loop sequence and the J region usage.

These results indicate that the D426 B1 line was a polyclonal CD8 T-cell culture. The "pure" D12 clone isolated in the IFNγ negative fraction in response to peptide is likely to be a true MAIT. Unfortunately, this clone could not be maintained in culture long enough to confirm its reactivity or determine which TCR chains it expressed. Collectively, these data indicated that MAITs do not recognize peptides ligands.

4.2.5.2 Morpheus is not activated by M. smegmatis infected A549 presenting cells

A number of techniques can be used to determine the MHC restriction of a T-cell. Blocking antibodies are often used in studies to block T-cell responses but this approach can be unreliable. Cell lines without the classic MHC alleles have been extremely useful in determining MHC-restriction. Unfortunately, at present, there is no MR1 knockout cell line available to allow formal assignment of MR1-restiction to D426 B1. However, since MR1 is ubiquitously expressed on almost all nucleated human cell lines, I hypothesized that if Morpheus was MR1-restricted, it would be activated by the HLA mismatched A549 cell line infected with *M. smegmatis*. To verify this hypothesis, A549 cells were infected with *M. smegmatis* and presented to the D426 B1 line (positive control), the NLV2-F3 T-cell clone specific for the HLA-A*0201-restricted CMV-derived epitope NLVPMVATV (negative control) and Morpheus. MIP-1β secretion was then measured by ELISA. As expected, the D426 B1 line secreted MIP-1β when presented with *M. smegmatis* infected A549 target cells. However, the NLV2-F3 and Morpheus did not respond (**Figure 4.11**). These results suggest that Morpheus is not restricted by MR1.

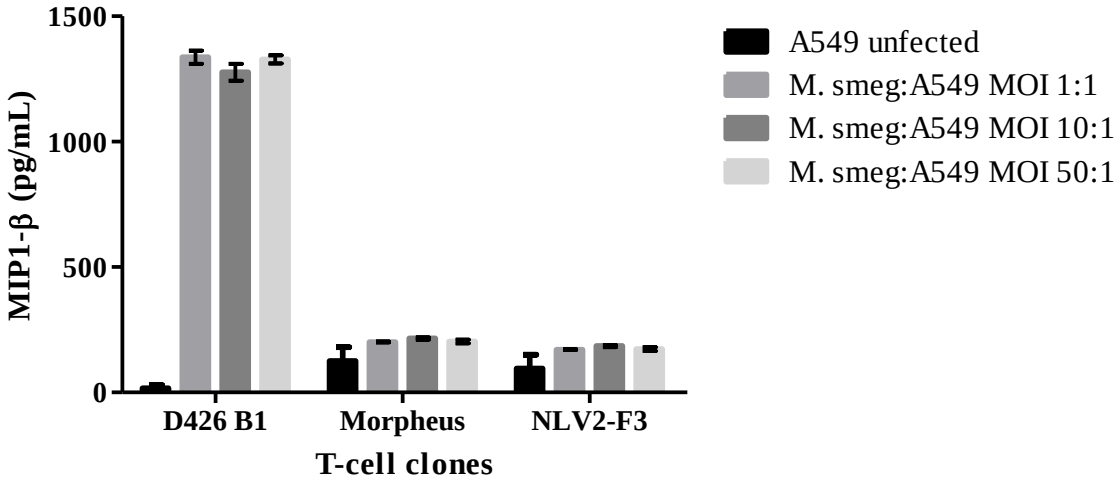

Figure 4.11. Assessing of M. smegmatis A549 cells specificity of three CD8 T-cells. $3x10^5$ D426 B1, Morpheus and CMV-specific NLV2-F3 cells were stimulated overnight with A549 cells infected or not uninfected with different M. smegmatis:A549 MOIs (1:1, 10:1 and 50:1). T-cell activation was measured in the supernatant by MIP-1β ELISA.

In parallel with my studies to find the restriction element was for Morpheus, I also continued to study the MAIT cell ligand by attempting to manufacture soluble, biotin-tagged MR1.

4.2.6 Production of soluble MR1

4.2.6.1 Production of MR1 inclusion bodies

To produce novel multimers and determine the molecular basis of MR1 antigen presentation, I undertook experiments to express and refold MR1 in recombinant form. MR1 cDNA construct was designed with the inclusion of a biotin-tag sequence at C-terminus, named MR1tag. BamH1 and EcoR1 restriction sites were added to 5' and 3' sequence terminus of MR1tag and β2m DNA constructs to allow cloning into pGMT7 vector. MR1tag and β2m DNA expression constructs were separately transfected into Rosetta *E.coli* by heat shocking the bacterial cell membrane. Bacterial colonies were individually picked and amplified in LB media. The expression efficiency of the DNA constructs was assessed by activating the lac operon using Isopropyl β-D-1-thiogalactopyranoside (IPTG) for 3 h. A sample of the bacterial culture was harvested before and after induction with IPTG. The samples were denaturated using DTT and run on a sodium dodecyl sulphate-polyacrylamide gel electrophoresis (SDS-PAGE) for analysis of MR1tag and β2m expression.

The MR1tag alpha chain is 34 kDa and 293 amino acids in length. **Figure 4.12.A** shows IPTG induced significant MR1tag alpha chain. Inclusion bodies from bacterial cultures were purified of bacterial impurities using a deoxiribonuclease (DNAase) treatment and detergent washes (protocol described in Chapter 2). Purity of MR1tag alpha chain inclusion bodies was assessed by running a sample denaturated with DTT on SDS-PAGE. The MR1tag alpha chain was produced by bacteria after IPTG compared to IPTG unstimulated bacteria. However after the last purification step, the MR1tag inclusion bodies contained a small amount of bacterial impurities (**Figure 4.12.B)**.

A. MR1 expression in Rosetta before and after IPTG induction

B. MR1 inclusion bodies after processing

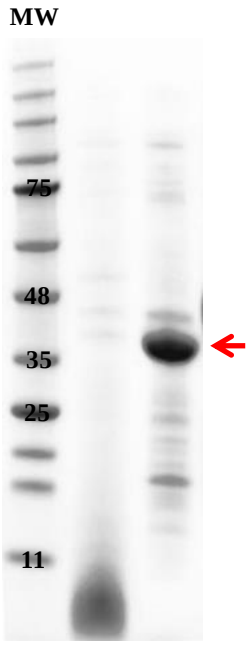

Figure 4.12. MR1 inclusion bodies (IB) production.
(**A.**) MR1 expression in *E. coli* strain Rosetta before and after IPTG induction. SDS-PAGE gel of DTT denaturated Rosetta *E.coli* extract before (left lane) and after (right lane) three hours of IPTG induction. MR1 protein is indicated by the red arrow. **(B.)** MR1 inclusion bodies after processing. After large scale IPTG induction of MR1 plasmid transformed Rosetta *E.coli*, MR1 inclusion bodies were processed and a sample was run on an SDS-PAGE gel to verify purity. Bacterial culture IPTG untreated (left lane) and sample from the last step of IB purification (right lane) were run on the gel. MR1 protein is indicated by the red arrow.

4.2.6.2 The refolding and purification of MR1

In order to produce MR1 protein in multimeric form, MR1tag alpha chain was refolded with β2m as described in Chapter 2. Briefly, MR1tag and β2m inclusion bodies were denaturated with DTT for 30 minutes at 37 °C and added to a 4 °C chilled refold buffer (50 mM Tris, 2 mM EDTA, 400 mM L-arginine and 2.5 M Urea, pH8) and agitated overnight at 4 °C. MR1 protein refold was first purified by anion exchange chromatography. The chromatogram obtained indicated a large amount of different MR1tag protein forms with different charges (**Figure 4.13 A.**). Fractions 21-42 were pooled and analysed as well as the individual fraction 11 by SDS-PAGE. Fraction 11 did not contain any MR1tag protein but only the β2m chain (11.9 kDa). The pooled 21-42 fractions contained MR1tag and β2m at ~1:1 ratio suggesting that this was correctly refolded MR1 protein. Unfortunately, the fraction contained minor contaminant proteins of different sizes mostly likely from *E.coli* (**Figure 4.13 B.**).

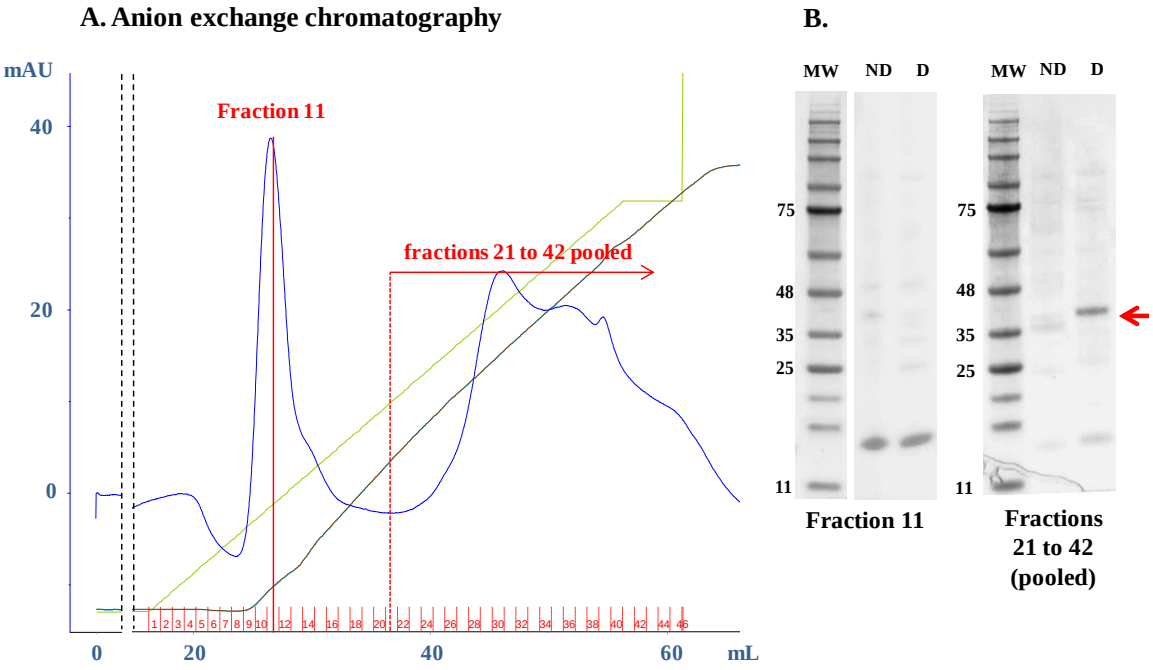

Figure 4.13. Anion exchange chromatography of MR1. (A.) Anion exchange chromatogram.
Purification of MR1tag refolded product by anion exchange chromatography. The blue, green and brown lines represent milli-absorbance units (mAU), % of eluting buffer (1M NaCl, 10mM Tris, pH 8) and % of conductivity respectively. **(B.) SDS-PAGE gel of eluted fraction 11 and pooled fractions 21-42.** Samples were denaturated with DTT (D) or not denaturated (ND) for three minutesat 95°C and run on SDS-PAGE. Purified MR1tag protein is indicated by the red arrow.

To remove these protein contaminants, size exclusion chromatography was performed. The pooled fractions were first concentrated using a Vivaspin column and run on a Superdex 200 10/300 GL column (**Figure 4.14 A**). Fractions 5-8 were pooled and analyzed by SDS-PAGE. The gel indicated the presence of the MR1tag protein in these fractions and reduced levels of contaminant proteins (**Figure 4.14 B.**).

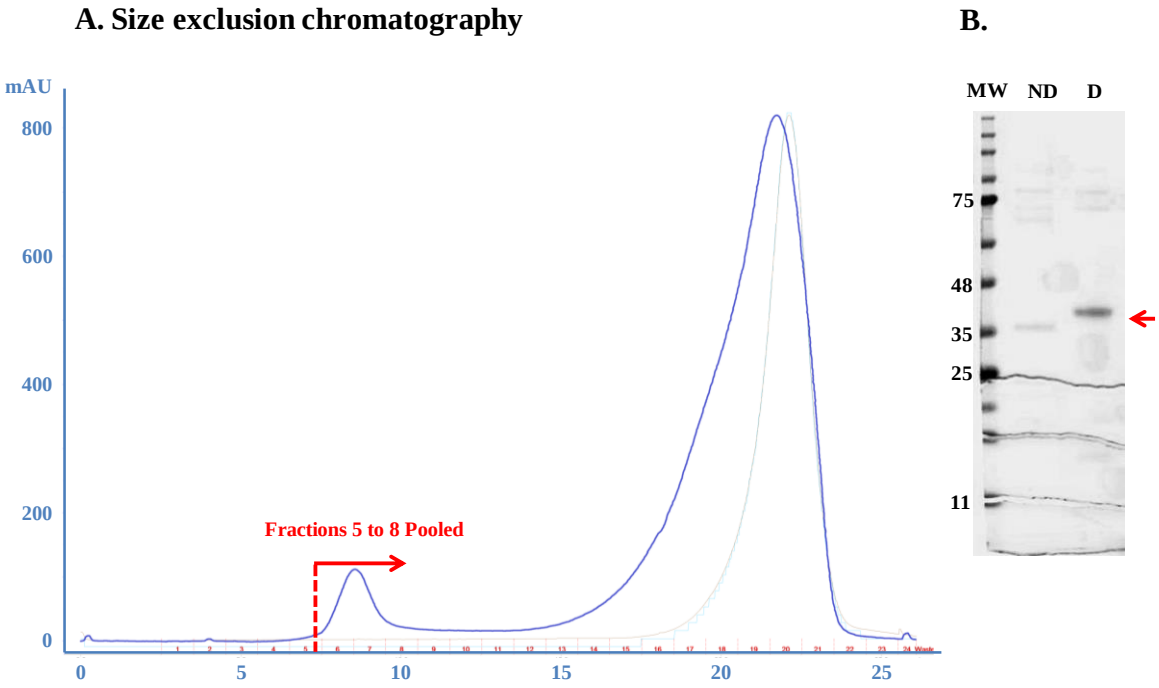

Figure 4.14. MR1 tag size exclusion chromatography.
(A.) Size exclusion chromatogram. Purification of anion exchange chromatography purified pooled fractions 21-42 containing MR1tag refolded protein. **(B.) SDS-PAGE gel of eluted pooled fractions 5-8.** Samples were denaturated with DTT (D) or not denaturated (ND) for three minutes at 95°C and run on an SDS-PAGE. Purified MR1tag protein is indicated by the red arrow.

A fully folded MR1tag protein was successfully refolded even though the concentration obtained was far from below that obtained during the refold of MHC I soluble monomers with peptide. I next planned on biotinylating the MR1 monomer so that I could build MR1 fluorescent tetramers. However, during the course of these studies my supervisor, Prof. Andrew Sewell, spoke about my results with Prof. Jamie Rossjohn from Monash University in Australia. Prof. Rossjohn said that they had already defined the MAIT ligands and that a manuscript was submitted. After this conversation I was advised to switch to other studies by my supervisory team. I therefore moved to examining conventional *M. tuberculosis*-specific T-cells (see Chapter 5). A few months later Prof. Rossjohn and team published two papers. The first study revealed the first structure of MR1 in complex with a vitamin B metabolite: the 6-formyl pterin (6-FP)

(Kjer-Nielsen et al., 2012). 6-FP does not activate MAIT cells. The second paper showed how MR1 could present other ligands from the riboflavin biosynthetic pathway and that some of these ligands acted as agonists of the MAIT TCR (Patel et al., 2013). Studies with MR1 tetramers appeared in October 2013 (Reantragoon et al., 2013). I am glad that we heard about it prior to publication as this work would have precluded publication of my own studies.

4.3 Discussion

When I started my studies, the nature of the ligand presented by MR1 to MAIT cells was unknown. There was widespread interest in this important topic but we believed that we were well placed to compete in this exciting area due to my laboratory having extensive expertise with T-cells, TCRs, refolding pMHC and CPL screens. Due to certain physiologic and sequence similarities to pMHC I and CD1, it was speculated that MR1 would present either peptide or lipid based antigens. Indeed, as mentioned earlier, MR1 shares a high sequence homology with MHC I molecules (Hashimoto et al., 1995). For example, MR1 has MHC-like folding and the MR1 α1 and α2 chains share about 40-45% homology with those from MHC I. Moreover, studies of the MR1 antigen binding groove has shown more hydrophilic residues than in CD1 grooves suggesting that presentation of peptide-based ligands would be more likely than lipid-based ligands (Hansen et al., 2007). However, in contrast to MHC I, the surface expression of MR1 is TAP and proteasome independent (Huang et al., 2008). This discovery does not refute the hypothesis that MR1 could present peptides to MAITs as there are many TAP-independent peptide epitopes described in the literature. Indeed one such group of these antigens, the so-called Cinderella epitopes (Seidel et al., 2012) appear to serve a function in counteracting escape mutations that result in deficiencies in MHC I presentation that would otherwise allow tumour escape. My studies aimed to investigate whether MAITs recognized peptide bound in the MR1 groove. For this purpose, Prof David Lewinsohn provided me a well characterised human MAIT clone (D426 B1). This clone was used extensively for MAIT characterisation in a seminal paper published in the high impact journal *PLoS Biology* (Gold et al., 2010).

The D426 B1 CD8 T-cell clone was extracted from a TB infected patient and exhibited MAIT-like phenotype markers such as Vα7.2 (Jα33) chain expression in complex with a Vβ13.5 chain, expression of IFNγ, MIP-1β and TNFα cytokines and cytotoxicity in response to *M. tuberculosis* infected DCs (Gold et al., 2010).

In order to determine whether a MAIT could recognise a peptide I decided to use combinatorial peptide libraries. A pilot screen of D426 B1 with a nonamer CPL showed that position 4 might be important. We have recently described how CD8 T-cells can exhibit a specific preference for peptides of a defined length (Ekeruche-Makinde et al., 2013). As the peptide length recognised by D426 B1 was unknown, D426 B1 was challenged with position 4 CPLs sub-mixtures from 8 to 13 amino acids in length. D426 B1 only responded to the 9mer library. Having determined the preferred peptide length I then proceeded to undertake a full nonamer CPL screen. D426 B1 reacted to specific sub-libraries at all positions except the peptide termini (P1, P2 and P9). This screen allowed the generation of a MAIT-specific peptide motif. This motif was used to screen the *M. tuberculosis* proteome for peptide sequences that might be recognised by D426 B1. In total 12 out of 12 peptides generated in this way were recognised including TSGPVNYDL, MRPPALYDT, ISVPVLYAL real sequences derived from mycobacteria. Four optimal but non-natural peptides of sequence IRAPVLYDL, IRAPALYDL, IRAPVLYDI and MRAPALYDL were recognised at very low concentration ($<10^{-13}$ M), indicating that D426 B1 was highly sensitive to these four peptides. D426 B1 was particularly sensitive to IRAPVLYDL peptide therefore I decided to use this peptide to confirm MR1-restriction by antibody blocking. Initial results gave poor blocking of D426 B1 response to IRAPVLYDL with both anti-MR1 (clone 26.5) and MHC I (clone W6/32) blocking antibodies. Antibody blocking of MHC can be very "leaky" when a good ligand and sensitive effector function are used in combination. I therefore decided to try weaker ligands in the form of individual 9mer CPL sub-mixtures. Reduction of antigen potency allowed complete blocking of D426 B1 response to peptide sub-mixtures with anti-MHC I antibody but was unaffected by anti-MR1 antibody. This worrying result suggested that either the D426 B1 clone had dual specificity for an MR1-restricted and an MHC I-restricted ligand or questioned whether D426 B1 was a monoclonal population. The clonality of D426 B1 was then examined by determining whether only a subpopulation responded to peptide using IFNγ ICS. Unfortunately, these experiments revealed that only ~10% of cells responded to peptide, suggesting that the D426 B1 clone sent by our collaborators was not monoclonal.

Confirmation of D426 B1 polyclonality was performed by D426 B1 TCR sequencing that revealed two TCRα and two TCRβ chains. However, it still remained possible that D426 B1 was a dual TCR T-cell.

Therefore I next endeavoured to sub-clone D426 B1 after exposure to IRAPVLYDL peptide in order to verify if whether D426 B1 was polyclonal or a single cell bearing two distinct TCRs. Cells were divided into responders and non-responders by IFNγ capture prior to cloning by limiting dilution. One clone grew well from the non-responding population (D12 T-cell clone) and two clones grew from the responder population (A5 and A6 T-cell clones). A5 and A6 clones responded to IRAPVLYDL peptide by MIP-1β ELISA whereas the D12 clone failed to respond. Therefore, these results suggested that D426 B1 was two clones. TCR sequencing of A6 (renamed Morpheus) showed that the clone had a non-MAIT TCRα chain. In order to determine where the contamination with Morpheus had arisen, I obtained a fresh early stock of D426 B1 clone from Portland and stained it with anti-Vα7.2 antibody. These results showed that this clone was 98% $V\alpha7.2^{+}$ leading Portland to call it a monoclonal MAIT population. In hindsight, it seems likely that the 2% of cells that did not stain with anti-Vα7.2 antibody were Morpheus. The percentage of Morpheus within D426 B1 clone was seen to expand when cultured in Cardiff in human serum while my collaborators from Portland used FBS.

In parallel to the investigations above, I was interested in refolding MR1 to manufacture MR1 tetramers. MR1 was refolded from inclusion bodies without addition of an antigen. The refold yield was not nearly as impressive as some MHC I monomers. I believe that I was able to refold some MR1 due to the presence of residual *E. coli* impurities in the inclusion bodies that might have bound in the MR1 groove allowing it to refold. However, my supervisor Prof. Andrew Sewell learned from Prof. Jamie Rossjohn at Monash University that his team already refolded MR1 with intermediates in the riboflavin biosynthetic pathway and showed that these reagents specifically stained MAITs. Therefore, my supervisor suggested that I should shift my studies to looking at conventional T-cells in *M. tuberculosis* infection as I would be unlikely to be able to publish my own MAIT studies in prominent journals. Studies from the Rossjohn and other laboratories have substantially enhanced our understanding of MAIT cells in the last 12 months. These exciting discoveries will be discussed later in Chapter 6. Regardless the disappointment of discovery that D426 B1 was not a monoclonal MAIT cell, data obtained in this chapter allowed me to conclude that the *M. tuberculosis* specific MAIT cell population in D426 B1 provided by my collaborator Prof. David Lewinsohn does not recognise an MR1-restricted peptide.

CHAPTER 5. RECOGNITION OF A POTENTIAL PAN-MYCOBACTERIUM HLA-A*0201-RESTRICTED T-CELL EPITOPE

5.1 Introduction

T-cells play a major role in clearance during acute *M. tuberculosis* infection and are largely responsible for inducing the latency phase (Urdahl et al., 2011). After *M. tuberculosis* transmission, communication between the innate and adaptive immune system is mainly driven by the presentation of MHC II epitopes to helper CD4 T-cells by *M. tuberculosis* infected macrophages (Green et al., 2013). Activation of *M. tuberculosis*-specific CD4 T-cells triggers secretion of cytokines including IFNγ release by T_H1 cells that promotes and enhances CD8 T-cell activity (Green et al., 2013) in addition to activation and maturation of macrophages and DCs. During chronic infection the above functions are performed by CD8 T-cells in addition to CD4 T-cells (Lazarevic et al., 2005). CD8 T-cells are not the major players during acute infection but play an increasingly important role as infection proceeds and are believed to be particularly important in bringing the disease to its latency phase (Lazarevic et al., 2005).

Although CD8 T-cell effector activity plays a role in *M. tuberculosis* latency, it is usually insufficient to clear the bacterium. Therefore, most *M. tuberculosis* vaccine development strategies aim to trigger a more potent CD8 T-cell response. Many studies have focused on secreted proteins by bacteria as potential vaccine candidates. *M. tuberculosis* secreted proteins such as ESAT-6 and CFP-10 are known to be very immunogenic and are the focus of clinical studies (Anhui Zhifei Longcom Biologic Pharmacy Co., Ltd. Phase I clinical human tolerability study of recombinant *Mycobacterium tuberculosis* ESAT6-CFP10. clinicaltrials.gov). Responses to these proteins have also being examined as candidate diagnostics (Weldingh and Andersen, 2008, Aagaard et al., 2006). ESAT-6 and CFP-10 trigger *M. tuberculosis* associated T-cell-mediated immunity (Majlessi et al., 2003) and induce strong immune responses when administered in prophylactic or therapeutic vaccination (van Dissel et al., 2011, Hoang et al., 2013). ESAT-6 and CFP-10 are secreted by a membrane bound secretion system called ESX-1 belonging to the Type VII secretion systems (T7SSs) family (Simeone et al., 2009).

The T7SSs family is composed of 5 systems of secretion (ESX-1, ESX-2, ESX-3, ESX-4 and ESX-5) that are responsible for the secretion of several proteins that serve a variety of functions that include roles in bacterial growth, survival inside and outside macrophages, and transmission (Pym et al., 2003, Gao et al., 2004). ESX-1 has been extensively studied; less is known about the other T7SSs and the proteins they secrete. Recently, there has been a rise of interest about the ESX-3 secretion system and associated secreted proteins. The ESX-3 system leads to the secretion of a heterodimeric complex formed by the Esx-G (or TB9.8) and Esx-H (or TB10.4) proteins. Recent studies have linked Esx-G/Esx-H heterodimer to *M. tuberculosis* virulence in macrophages as it prevents *M. tuberculosis* transport to lysosomes and prevents phagolysosome maturation thereby affecting degradation and processing of *M. tuberculosis* antigens onto MHCs (Mehra et al., 2013). The Esx-G/Esx-H complex has been shown to be highly immunogenic (Hervas-Stubbs et al., 2006, Skjot et al., 2002) and Esx-G has been shown to trigger an IFNγ response in *M. bovis* and BCG vaccinated cattle (Mustafa et al., 2006). Moreover, it has been claimed that an Esx-G-Ag85 fusion vaccine provides protective immunity in humans (Dietrich et al., 2005). The Esx-G and Esx-H sequences are conserved between Mycobacteria species indicating that these proteins must undertake important biological roles (**Figure 5.1**).

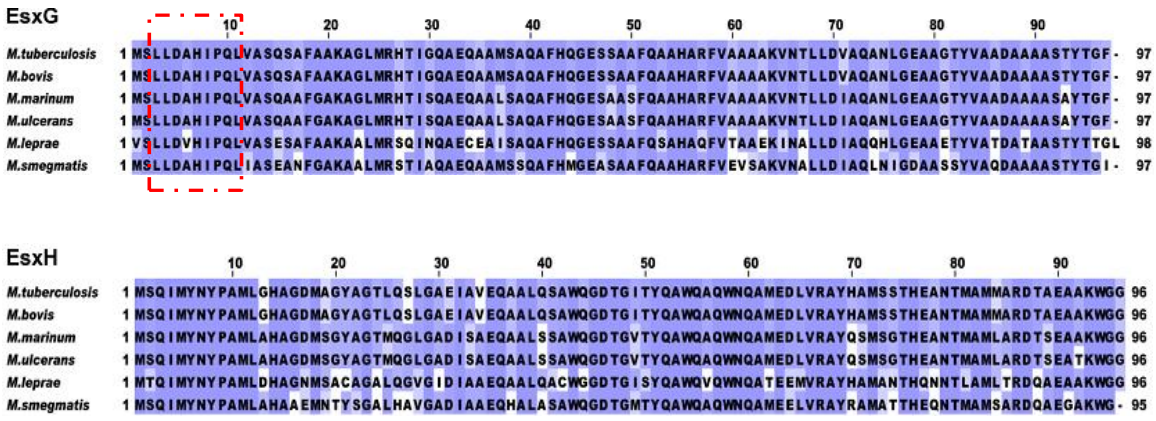

Figure 5.1 Sequences alignment of Esx-G and Esx-H in Mycobacteria species
The Esx-G and Esx-H amino acid sequence from *M. tuberculosis*, *M. bovis*, *M. marinum*, *M. ulcerans*, *M. leprae* and *M. smegmatis*. Figure reproduced from Ilghari et al., 2011.

My studies described in Chapter 4 were brought to a close by my supervisor once we realised that the Melbourne group had discovered the MAIT ligand and already refolded MR1 with agonist ligands that then stained human MAITs. As I had lost a substantial amount of time chasing my finding that MAITs can recognise peptide, I was advised to switch my studies away from unconventional T-cells towards conventional HLA-restricted T-cells against *M. tuberculosis* as my laboratory has extensive experience in characterising these cells. I was particularly interested in studying T-cells that recognise the HLA-A*0201-restricted, Esx-G-derived 9mer LLDAHIPQL peptide (residues 3-11) (shown in **Figure 5.1**). The choice of LLDAHIPQL peptide as an antigen was heavily influenced by the work of the Lewinsohn laboratory who found that HLA-A*0201-LLDAHIPQL restricted CD8 T-cell clones from latent TB infected patient could be activated by *M. tuberculosis* (H37Rv)-infected dendritic cells (Lewinsohn et al., 2007) (Immune Epitope Database and Analysis Resource. Epitope ID: 37140/ Reference ID: 1026754). The LLDAHIPQL sequence is conserved across Mycobacteria species (Ilghari et al., 2011) indicating that it might prove to be a good candidate to explore as a potential pan-Mycobacterial vaccine target. Prof. Lewinsohn provided me with an LLDAHIPQL-specific T-cell clone (D454) grown from a TB patient so I initiated studies on characterising this T-cell, the TCR and the antigen it recognises.

5.1.1 Aims

The aim of this chapter was to characterise the D454 T-cell clone and prove that it bound to HLA*0201-LLDAHIPQL. Prof. Lewinsohn was particularly interested in the prospect of manufacturing a high affinity TCR against this antigen for use in therapeutics and as a potential diagnostic. After discussions between Professor Lewinsohn and our collaborators at Immunocore Ltd, who manufacture such TCRs, it was agreed that there might be an interest in designing such a reagent provided that there was hard proof that the D454 TCR bound to HLA*0201-LLDAHIPQL. My aim was to manufacture a soluble version of the D454 TCR and characterise its binding to HLA*0201-LLDAHIPQL. I also aimed to get a structure of HLA*0201-LLDAHIPQL and the D454 TCR in complex with this epitope. This structure would be the first ever TCR-pMHC structure for a bacterially-derived antigen. The structure would also be highly informative about precisely which of the six CDR loops to target during the phage display and directed evolution process required to enhance the affinity. The specific aims of this chapter were to:

1. Manufacture HLA-A*0201-LLDAHIPQL to make pMHC multimers for T-cell staining

2. Characterise D454 recognition of HLA-A*0201-LLDAHIPQL by tetramer staining

3. Examine D454 ligand recognition by CPL screen and determine positions in the LLDAHIPQL peptide important for the recognition and the design of a strong agonist altered peptide ligand (APL) for the D454.

4. Manufacture of D454 αβTCR for use in biophysical and structural studies.

5. Produce a D454 TCR-HLA*0201-LLDAHIPQL crystal structure

5.2 Results

5.2.1 D454 is specific for HLA-A*0201-LLDAHIPQL

*5.2.1.1 Manufacture of soluble HLA-A*0201-LLDAHIPQL monomers for tetramer production*

In order to investigate D454 recognition of HLA-A*0201-LLDAHIPQL I engineered soluble pMHC monomers. Biotin-tagged and un-tagged HLA-A*0201-LLDAHIPQL monomers were generated for use in different assays. Biotin-tagged monomers allowed production of tetramers using fluorochrome-conjugated streptavidin. These pMHC tetramers were then used to stain D454 (see section 5.2.2.3). The biotin moiety also allowed binding of the pMHC to streptavidin-coated BIAcore chips for surface plasmon resonance (SPR) analysis (see section 5.2.3.2). Biotin-tags are not particularly rigid structures and can interfere with protein crystallisation. I therefore also produced un-tagged HLA-A*0201-LLDAHIPQL monomers for structural analysis (see section 5.2.3.3).

Tagged and untagged HLA-A*0201 and β2m inclusion bodies were produced in *E. coli* Rosetta after IPTG induction as described in Chapter 2. Tagged and untagged HLA-A*0201 inclusion bodies were refolded with β2m inclusion bodies together with the LLDAHIPQL peptide. Refolded pMHC products were purified by anion exchange and size exclusion chromatography. I present here only the refold purification steps performed on tagged HLA-A*0201-LLDAHIPQL as they are identical to those performed on untagged HLA-A*0201-LLDAHIPQL.

Anion exchange chromatography allows separation of proteins according to their charge under a gradient of salt (here NaCl) on a positively charged matrix (in this case a HQ-Poros column). Most proteins are negatively charged at neutral pHs. The elution of proteins from the column was measured using UV light at a wavelength of 280 nm and 1 mL eluted fractions were collected. Tagged HLA-A*0201-LLDAHIPQL was found in 6 fractions at a maximum quantity of 350 mAU (**Figure 5.2 A**). Tagged HLA-A*0201-LLDAHIPQL monomers fractions were collected and concentrated. The tag was then biotinylated overnight using the enzyme Bir-A that catalyses the transfer of biotin to the tag. After biotinylation of the tag sequence, excess biotin was removed by concentrating biotinylated pMHC monomers using a Vivaspin column. Biotinylated HLA-A*0201-

LLDAHIPQL monomers were then purified by size exclusion chromatography (**Figure 5.2 B**).

Fractions containing biotinylated HLA-A*0201-LLDAHIPQL monomers were pooled to be analysed in reduced (linearised protein) using DTT or non reduced (folded protein) conditions on an SDS-PAGE gel in order to assess the quality and purity of biotinylated HLA-A*0201-LLDAHIPQL monomers (**Figure 5.2 C**). About 2 mg of biotinylated HLA-A*0201-LLDAHIPQL monomers were produced at >95% purity after these purification steps.

Biotinylated HLA-A*0201-LLDAHIPQL was used for the purpose of tetramer staining of D454 (section 5.2.1.2) and surface plasmon resonance (section 5.2.3.2). Untagged HLA-A*0201-LLDAHIPQL monomers were crystallised for structural analysis (section 5.2.3.3).

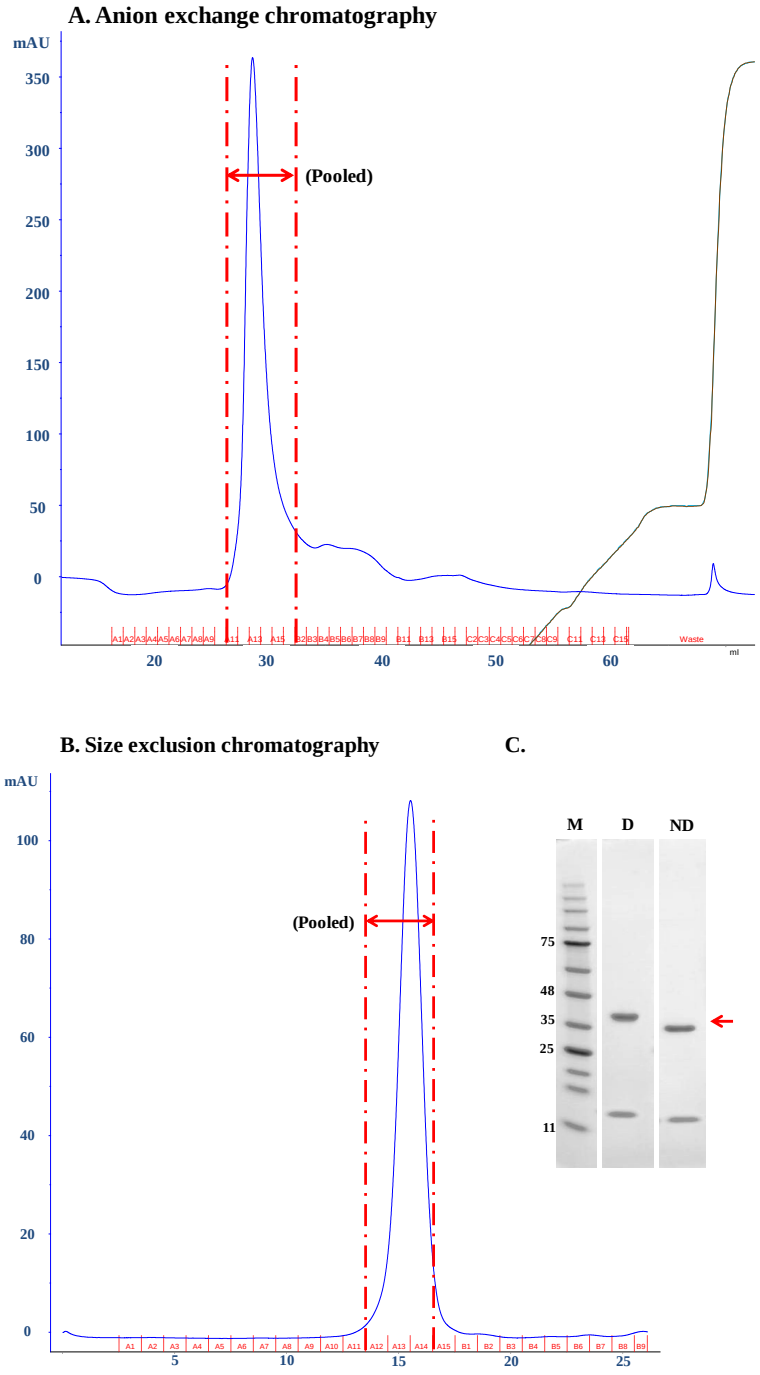

Figure 5.2 Steps of LLD/A2tag refold product purification.

A. Anion exchange chromatogram of tagged HLA-A*0201-LLDAHIPQL refold. The blue, green and brown lines represent milli-absorbance units (mAU), % of eluting buffer (1 M NaCl, 10 mM Tris, pH 8) and % of conductivity respectively. Red dotted lines correspond to the pooled fractions. **B.** Biotinylated HLA-A*0201-LLDAHIPQL size exclusion chromatogram of pooled anion exchange fractions. The blue line corresponds to milli-absorbance unit (mAU) and the dashed lines represent the pooled fractions. **C.** Analysis of pooled eluted size exclusion fractions by SDS-PAGE. Sample A12, A13 and A14 (in red) were pooled and denaturated or not denaturated with 500 mM DTT and run on an SDS-PAGE gel. Purified biotinylated HLA-A*0201-LLDAHIPQL monomers are indicated by red arrows.

*5.2.1.2 HLA-A*0201-LLDAHIPQL tetramer staining of D454*

D454 T-cell affinity was assessed by tetramer staining using HLA-A*0201-LLDAHIPQL tetramers. Due to a naturally weak TCR-pMHC interaction, multimerisation of pMHC allow the cooperative interaction with TCRs at cell surface resulting in an improvement of pMHC tetramer avidity compared to pMHC monomeric interaction. Therefore, this avidity stabilises the binding of pMHC tetramer to the cell surface thus the specific-T-cell staining intensity is enhanced and allows a better isolation of the T-cell subsets of interest (Wooldridge et al., 2009).

HLA-A*0201-LLDAHIPQL tetramers were produced by saturating streptavidin tetramer backbones coupled with Phycoerythrin (PE) with soluble biotinylated HLA-A*0201-LLDAHIPQL monomers as described in Chapter 2. A negative control staining was included using a CMV-specific epitope HLA-A*0201-NLVPMVATV. Cells were treated with 50 nM of Dasatinib prior antibody staining to prevent TCR downregulation upon pMHC tetramer interaction. Dasatinib is a protein kinase inhibitor (PKI) that targets Lck protein and prevents TCR signalling therefore downregulation of the TCR from the T-cell surface (Lissina et al., 2009). The gating strategy consisted of gating live (Vivid-PB) $CD3^+$ (anti-CD3 antibody) and $CD8^+$ (anti-CD8 antibody) T-cells (**Figure 5.3 A**). D454 did not stain with the CMV-specific control HLA-A*0201 tetramer (MFI: 192 compared to MFI: 180 for no tetramer). HLA-A*0201-LLDAHIPQL tetramer stained D454 but only weakly (MFI: 423) (**Figure 5.3 B**). This poor staining indicated that although the D454 is HLA-A*0201-LLDAHIPQL specific it probably binds to this antigen with relatively low affinity.

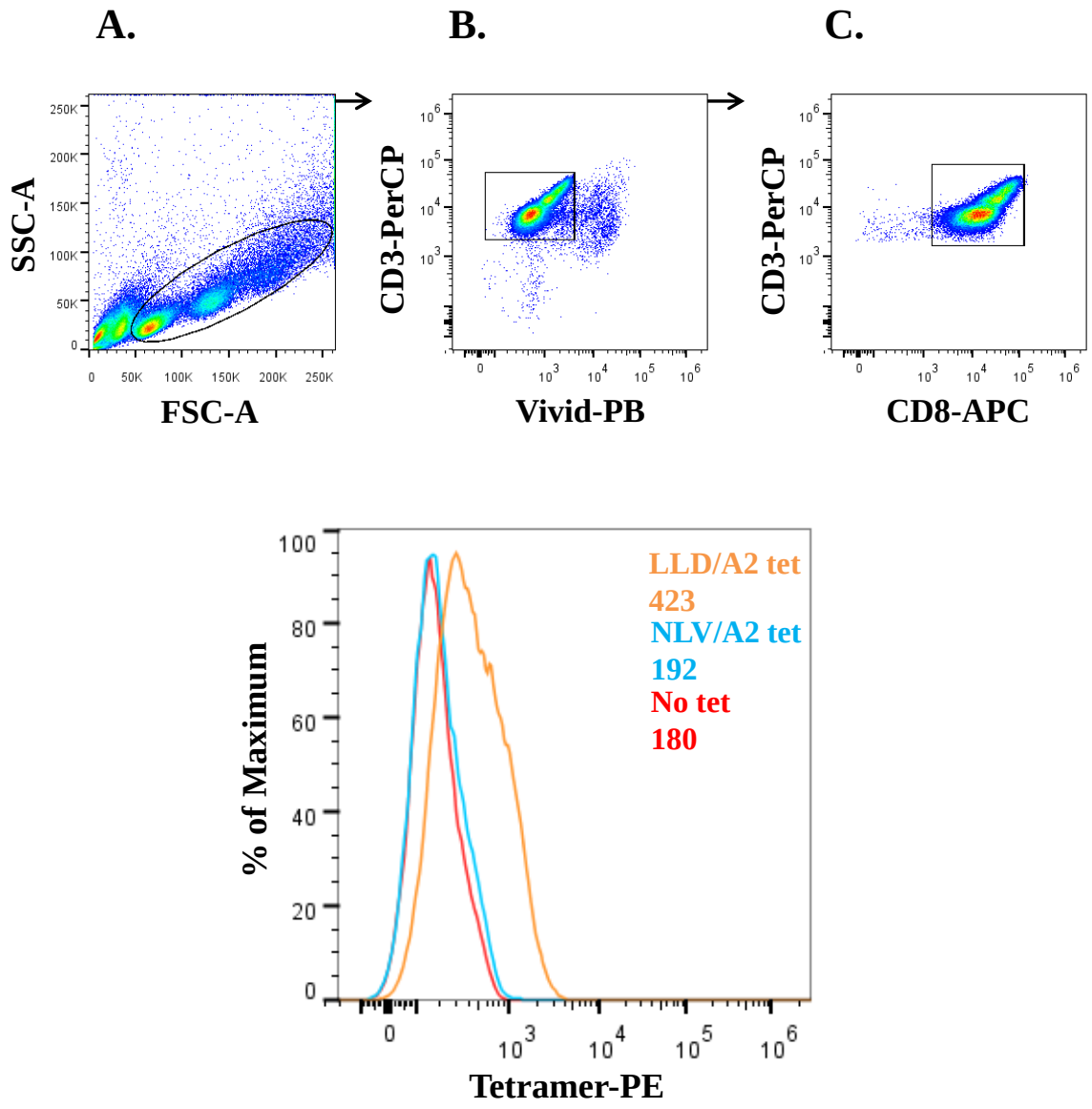

Figure 5.3 LLD/A2 poorly stained D454 T-cells.
$3x10^5$ D454 T-cells were first treated with 50 nM Dasatinib for 30 minutes followed by 0.4 µg of HLA-A*0201-LLDAHIPQL or HLA-A*0201-NLVPMVATV tetramer-PE for 30 min. Cells were then stained for the following markers: Dead cells (Vivid-PB), CD3 (anti-CD3-PerCP Cy5.5 antibody) and CD8 (anti-CD8-APC antibody) for 20 min. Cells were analysed by flow cytometry. **A.** Gating strategy consisting on staining alive (Vivid), $CD3^+$ (anti-CD3-PerCP), $CD8^+$ (anti-CD8-APC) cells. **B**. Staining of D454 T-cells with HLA-A*0201-LLDAHIPQL (orange), HLA-A*0201-NLVPMVATV (blue: negative control) tetramers-PE or no tetramer staining (red). MFI values are indicated for each condition.

D454 clone was successfully stained with HLA-A*0201-LLDAHIPQL tetramer confirming the specificity of D454 TCR for HLA-A*0201-LLDAHIPQL. However, the staining was poor suggesting that the affinity of the D454 TCR might be relatively weak. Therefore it would be useful to have a high affinity ligand for this TCR that could be used as a positive control in SPR or tetramer staining. It is also substantially easier to produce TCR-pMHC co-crystals when the TCR affinity is K_D <10 μM. As these complexes have identical solvent-exposed surfaces to the wild type TCR-pMHC protein they can then be used for crystal seeding (David Cole, unpublished observations). We have also found that using high affinity ligands and low amounts of TCR is an efficient way of determining optimal crystallisation conditions for a given TCR. In order to optimise the LLDAHIPQL peptide I undertook a 9mer CPL screen using D454.

5.2.2 Characterisation of D454 ligand recognition by CPL

As described above, the aim of this section was to attempt to build an improved peptide agonist for D454 using the data generated from a CPL screen.

5.2.2.1 Design of agonists predicted by CPL screen

Combinatorial peptide libraries (CPLs) offer an insight into the optimal peptide sequences recognised by a TCR and are very useful for the design of high affinity, potent agonist peptides. D454 T-cells were challenged with a nonamer CPL and T-cell responses to CPL mixtures correlated with the secretion of MIP-1β were quantified by ELISA. As MIP-1β is already preformed in T-cells, it is secreted rapidly and in large quantity upon TCR activation (Wagner et al., 1998). This feature makes MIP-1β a sensitive readout of CD8 T-cell activation. Measurement of MIP-1β by ELISA allows quantification of T-cell activation by each CPL sub-library.

The magnitude of MIP-1β secreted, and thus D454 T-cell response to the nonamer CPL, was overall low compared to that is observed in our laboratory with other viral or bacterial specific CD8 T-cell clones (Ekeruche-Makinde et al., 2013). Indeed, the MIP-1β concentration secreted did not exceed 500 pg/mL (**Figure 5.4**). Moreover, D454 T-cells were reactive to few nonamer CPL mixtures indicating that the TCR had a preference for relatively few specific amino acids at each position along the peptide backbone. These two observations indicated that D454 TCR was probably not particularly cross-reactive.

The core amino acids localised between positions P2 to P7 were mainly restricted to LLD cognate amino acids: X**LDAHIP**XX. However, at position P4 and P6 D454 also recognised glycine and valine as well as alanine and isoleucine respectively: XXX**A(G)**X**I(V)**XXX. The D454 recognition motif appeared to be more flexible at the N- and C-terminus of the peptide (P1, P8 and P9). These data predicted that substitution of wild type amino acids at these positions might produce a peptide that was a more potent agonist of the D454 T-cell clone than the cognate *M. tuberculosis*-derived sequence. (**Figure 5.4**).

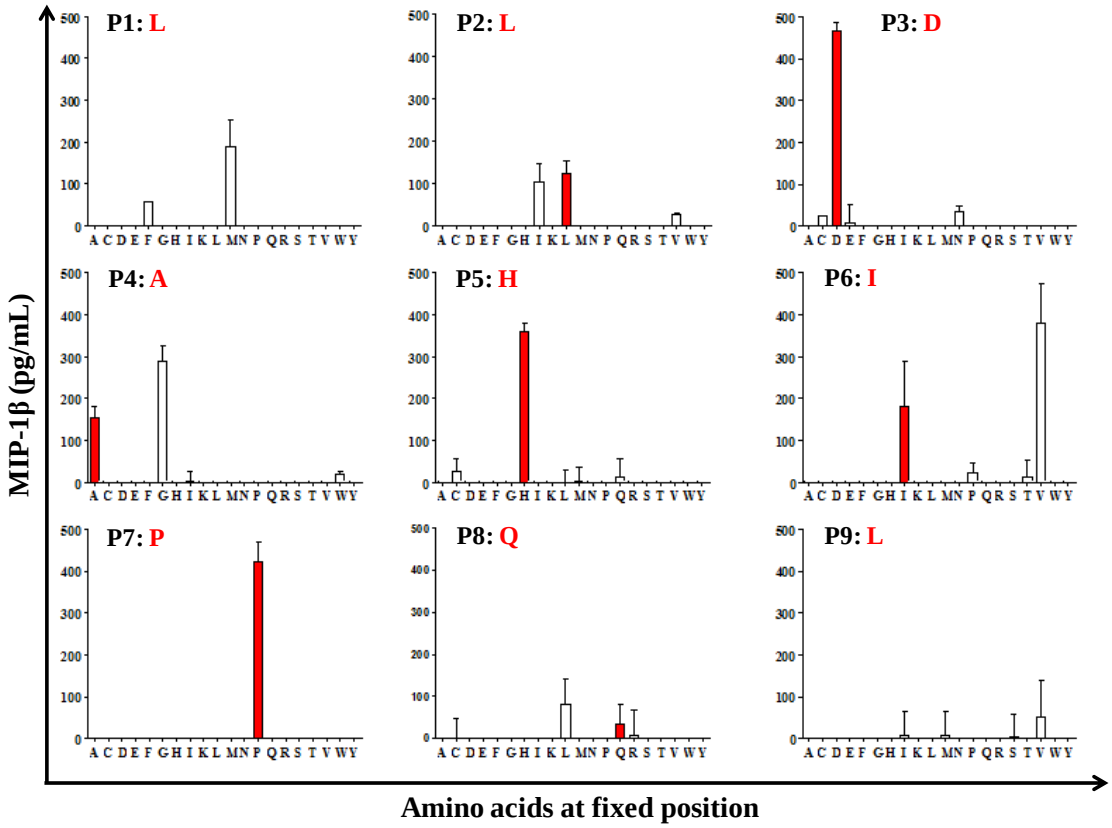

Figure 5.4 CPL screening histogram of D454.
$6x10^4$ C1R A2 cells were pulsed with 180 mixtures from the nonamer CPLs and were used to stimulate overnight $3x10^4$ D454 CD8 T-cells. D454 T-cell responses to library mixtures were quantified by measuring the release of MIP-1β by ELISA. Responses are displayed as a cluster of 9 histograms P1-P9 representing the positions of the fixed amino acids along the peptides. For each position (P), a set of 20 mixtures having the defined fixed amino acids is represented on the *x*-axis. The red bars represent the mixtures with the fixed amino acids corresponding to the D454 cognate peptide (LLDAHIPQL).

D454 amino acid preferences along the nonamer peptide backbone observed are summarised in **Figure 5.5** and were based on data obtained on **Figure 5.4**.

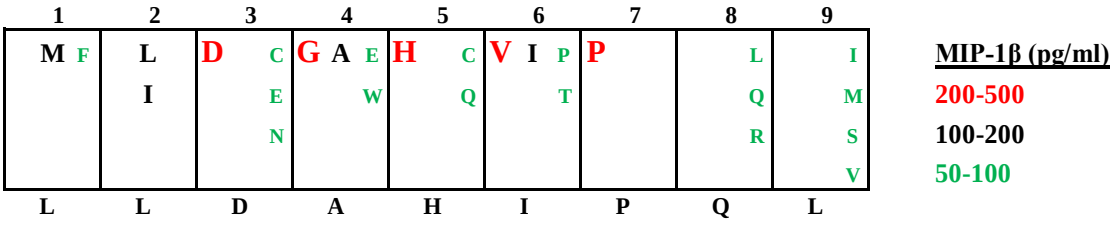

Figure 5.5 Summary of the nonamer CPL screen of the D454 T-cell line.
D454 reactivity to the mixtures is represented by the single letter amino acid code nomenclature for the fixed amino acid within the mixture at each position along the nonamer peptide backbone. The magnitude of D454 T-cell response is represented by a colour code where red is the highest and green the lowest responses.

5.2.2.2 Identification of D454 potent agonists from CPL data

A set of 30 agonist peptides were selected for testing based on the CPL data above **Table 5.1**. D454 T-cell sensitivity for these agonist peptides was tested with MIP-1β as readout.

LLDAHIPQL	LLDAHIPQL
MLD**G**H**V**PQ**V**	**F**LD**G**HIPQL
FLD**G**HVP**LV**	**F**LDAH**V**PQL
MIDAHIPQ**V**	**F**LDAHIP**L**L
FLDAHIPQ**L**	**M**LDAHIP**LV**
MLDAHIPQL	**M**LDAHIPQL
L**I**DAHIPQL	**MI**DAHIPQL
LLD**G**HIPQL	**F**LDAHIP**LV**
LLDAH**V**PQL	**F**LDAHIPQ**V**
LLDAHIP**L**L	**FI**DAHIPQ**V**
LLDAHIPQ**V**	**MI**D**G**H**V**P**LV**
LLD**G**H**V**PQL	**FI**D**G**H**V**PQL
LLD**G**HIPQ**V**	**MI**D**G**H**V**PQL
LLD**G**H**V**PQ**V**	**F**L**IG**H**V**P**LV**
FIDAHIPQL	**FI**D**G**H**V**P**LV**
	MLDAHIPQ**V**

Table 5.1 Peptide sequences designed from D454 nonamer CPL screen.
Residues in bold correspond to those in the cognate LLDAHIPQL. Cognate peptide is indicates in red at the top of each column.

D454 cells were challenged with C1R-A2 pulsed with a titration of individual peptides listed above (**Table 5.1**). T-cell sensitivity to an antigen was defined by the half maximum effective concentration EC50. It represents the peptide concentration with which half of the maximum T-cell response is inhibited. EC50 allows an easy comparison of the potency of different peptides. D454 T-cell MIP-1β release was still detectable by ELISA at LLDAHIPQL concentration of $>10^{-10}$ M (100 pM) (**Figure 5.6**). EC50 of LLDAHIPQL peptide was calculated at $1.1x10^{-9}$ M. Most of the peptides tested were more potent agonists of D454 T-cells than the *M. tuberculosis*-derived sequence. However, substitution of glutamine at position 8 by leucine impact dramatically on the D454 sensitivity (LLDAHIP**L**L: EC50 7.3×10^{-9} M). D454 was most sensitive to the MIDAHIPQV peptide of those tested (EC50 = 1.7×10^{-11}) making this sequence >100 more potent than the *M. tuberculosis*-derived LLDAHIPQL peptide.

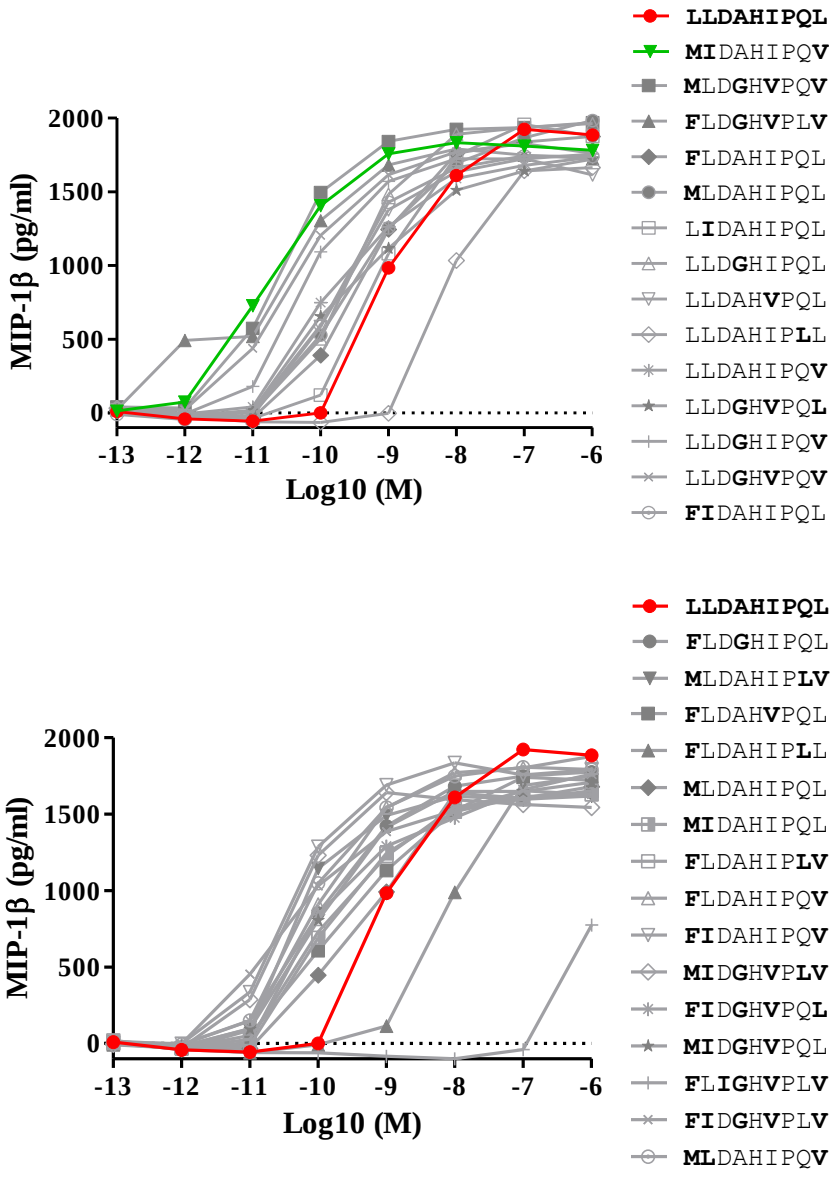

Figure 5.6 D454 cells sensitivity to 30 agonist peptides.
6 x 10^5 C1R A2 were pulsed with a titration of individual peptides and presented to 3 x 10^5 D454 T-cells. Cells were incubated overnight and D454 cells response to the peptides was quantify by MIP-1β ELISA. The red line corresponds to D454 activation profile to LLDAHIPQL peptide titration. The green lines correspond to D454 activation profile to the most potent MIDAHIPQV agonist titration.

*5.2.2.3 D454 TCR affinity for HLA-A*0201-MIDAHIPQV*

In order to compare the affinity of D454 for HLA-A*0201-LLDAHIPQL and HLA-A*0201-MIDAHIPQV, biotinylated HLA-A*0201-MIDAHIPQV monomers were produced using the same protocol used in section 5.2.1.1 and were purified by anion exchange and size exclusion chromatographies. HLA-A*0201-MIDAHIPQV tetramers were produced.

The affinity of D454 for the cognate LLDAHIPQL and optimal MIDAHIPQV peptides, in complex with HLA-A*0201, were evaluated using tetramer staining and analysed by flow cytometry using HLA-A*0201-NLVPMVATV as a negative control. The gating strategy consisted of gating live (Vivid) CD3+ (anti-CD3 antibody) and CD8+ (anti-CD8 antibody) T-cells and identical to **Figure 5.3 A, B and C**. As expected, HLA-A*0201-LLDAHIPQL tetramer stained weakly D454, as only 21% of T-cell clones were stained by tetramer. However, more than 96% of D454 were stained with optimal agonist HLA-A*0201-MIDAHIPQV tetramer. These data confirmed that D454 have a higher affinity for HLA-A*0201-MIDAHIPQV than for HLA-A*0201-LLDAHIPQL.

A HLA-A*0201-MIDAHIPQV tetramer negative population was revealed by the staining representing about 4% of D454 T-cells (**Figure 5.7**). This population was not detected during the RACE TCR sequencing performed in section 5.2.3.1.a. (**Table 5.2)**. Attempts to remove the tetramer negative CD8 population were unsuccessful. These data seem to suggest that, like the D426 B1 clone I had received from Portland, the D454 T-cell clone also contained a contaminant CD8 T-cell. Fortunately, on this occasion the polyclonal nature of D454 did not cause me any major issues.

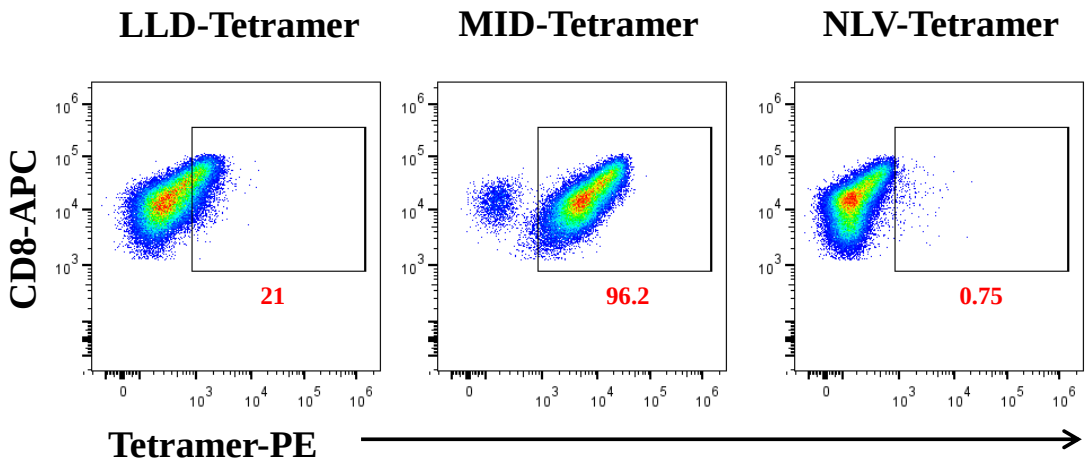

Figure 5.7. Staining of D454 T-cell line with LLD-, MID- and NLV-HLA-A*0201 tetramers.

3 x 10^5 D454 T-cells were first treated with 50 nM Dasatinib for 30 minutes followed by staining with 0.4 µg of HLA-A*0201-LLDAHIPQL/MIDAHIPQV/NLVPMVATV tetramer-PE for 30 minutes. Cells were then stained for the following markers: Dead cells (Vivid-PB), CD3 (anti-CD3-PerCP Cy5.5 antibody) and CD8 (anti-CD8-APC antibody) for 20 minutes. Cells were analysed by flow cytometry. **A.** Gating strategy. Cells of interest were live, $CD3^+$, $CD8^+$ and were identified by antibody staining using a dead cells marker (Vivid-PB), an anti-CD3-PerCP Cy5.5 antibody and an anti-CD8-APC antibody. **B.** D454 T-cells were treated with a 50 nM Dasatinib (protein kinase inhibitor PKI) followed by 0.4 µg of HLA-A*0201-LLDAHIPQL/MIDAHIPQV/NLVPMVATV tetramer-PE.

5.2.3 Characterisation of D454 TCR affinity for HLA-A*0201-LLDAHIPQL and HLA-A*0201-MIDAHIPQV

5.2.3.1 Manufacture of soluble D454 TCR

5.2.3.1.a RACE TCR sequencing of D454 TCR T-cell clone

D454 α and β TCR cDNA sequences chains were amplified by 5' RACE technology and sequenced by Cardiff University Central Biotechnology Centre (**Table 5.2)**.

A. D454 TCRα chain sequencing

TRAV	Vα (Arden et.al.)	CDR3α	TRAJ	Freq (%)
12-1	2.1	CVVNVLYSGAGSYQLT	28	100.00

B. D454 TCRβ chain sequencing

TRBV	Vβ (Arden et.al.)	CDR3β	TRBJ	Freq (%)
14	16.1	CASSQALGAGNTEAF	1-1	100

Table 5.2. RACE TCR sequencing of D454 TCR.

5.2.3.1.b Production of soluble D454 TCR monomers

Production of soluble D454 TCR chains were undertaken in order to produce soluble D454 TCR for SPR and structural analyses. The design protocol of α and β TCR DNA sequences of D454 TCR was identical to the one used for the design of HLA-A*0201-LLDAHIPQL (see section 5.2.1.3.a.). The α and β TCR IB expression was quality controlled by running a sample of bacteria culture denaturated with DTT on SDS-PAGE. The α and β TCR chain molecular weights were 22.7 kDa and 27.7 kDa respectively and were detectable in the bacteria culture after IPTG treatment (**Figure 5.8**). IBs for all chains contained impurities, probably bacterial proteins, identifiable on the gel as protein smears as well as individual bands of different molecular sizes (**Figure 5.8**).

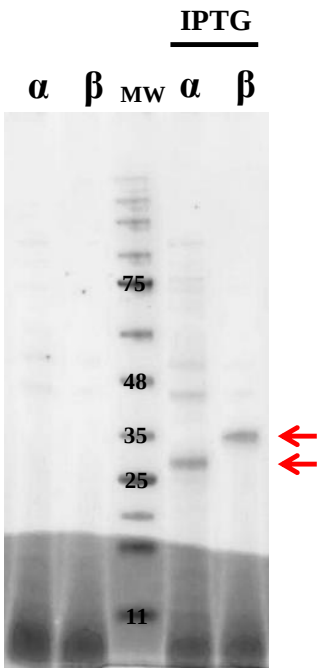

Figure 5.8. Quality control of D454 α and β TCR chains expression by *E. coli* Rosetta assessed by SDS-PAGE gel.
E. coli Rosetta transformed with either αTCR-pGMT7 and βTCR-pGMT7 plasmids were induced (right lanes) or not (left lanes) with IPTG for 3 hours. Bacterial culture samples were treated with DTT and denaturated at 95 °C before being run on an SDS-PAGE. The red arrows are pointing out the TCR chain products.

Production of soluble TCR from inclusion bodies is performed routinely by my laboratory and consists on re-suspending IBs in guanidine buffer (6M guanidine, 50 mM TRIS, 2 mM EDTA, 100 mM NaCl) and individually treating the α and β TCR IBs with 10 mM DTT for 30 minutes and refolding both chains for 4 hours at 4 °C in a cold refold buffer (Chapter 2) to produce a fully folded αβ TCR heterodimer. During αβ TCR refolding, aggregation of unfolded α and β chains can occur. In order to remove aggregates, different steps of purification were required. First, αβ TCR refolds were purified by anion exchange chromatography and eluted according to charge using a NaCl gradient. Anion exchange chromatography purified αβ TCR pooled fractions were then purified by size exclusion chromatography to improve the purity of αβ TCR (**Figure 5.9 A**). Quality of αβ TCR monomers was assessed by running denaturated (DTT treatment) or non-denaturated fractions by SDS-PAGE.

A sample of each of eight D454 αβ TCR eluted fractions were SDS-PAGE as described above. Under denaturating conditions, all fractions contained both α and β TCR chains running at ~25 kDa and ~30 kDa respectively. Under non-denaturing conditions, α and β TCR chains ran as a single band of ~50.4 kDa (**Figure 5.9 B**). Aggregates varied in

size and appeared as a smear on the gel in each fraction. Fraction 2 to 7 contained fully folded D454 αβ TCR heterodimers. However, fractions 4 and 5 were purest; I therefore pooled these two fractions (**Figure 5.9 B**).

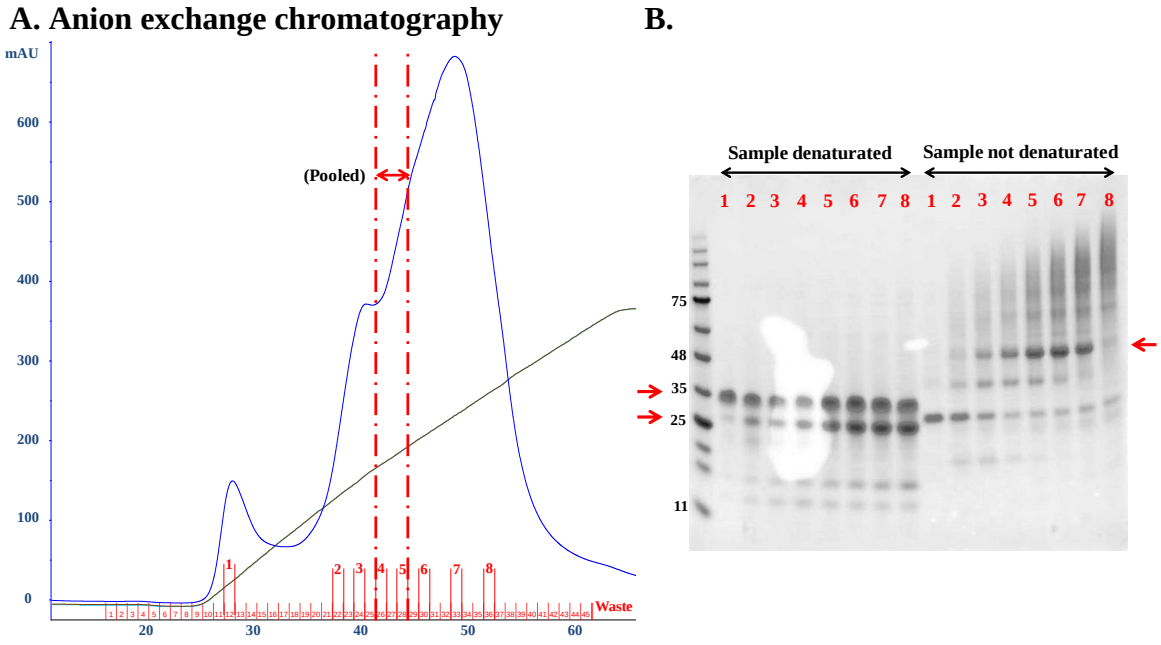

Figure 5.9. Purification of D454 TCR refold product by anion exchange chromatography.
A. Anion exchange chromatogram of D454 TCR refold. The blue, green and brown lines represent milli-absorbance units (mAU), % of eluting buffer (1M NaCl, 10mM Tris, pH 8) and % of conductivity respectively. Red dotted lines correspond to the pooled fractions. **B.** Analysis of 8 eluted fractions (in red) by SDS-PAGE. Sample 1, 2, 3, 4, 5, 6, 7 and 8 (in red) were denaturated or not denaturated with 500 mM DTT and run on SDS-PAGE. Purified D454 proteins are indicated by red arrows.

In order to improve the purity of D454 αβ TCR heterodimers after anion exchange the pooled fractions 4 and 5 were further purified by size exclusion chromatography (**Figure 5.10 A**) and analysed by SDS-PAGE. Non-denaturated fractions 5 to 7 contained folded D454 αβ TCR heterodimers and the lowest concentration of aggregates therefore fractions these three fractions were pooled (**Figure 5.10 B**).

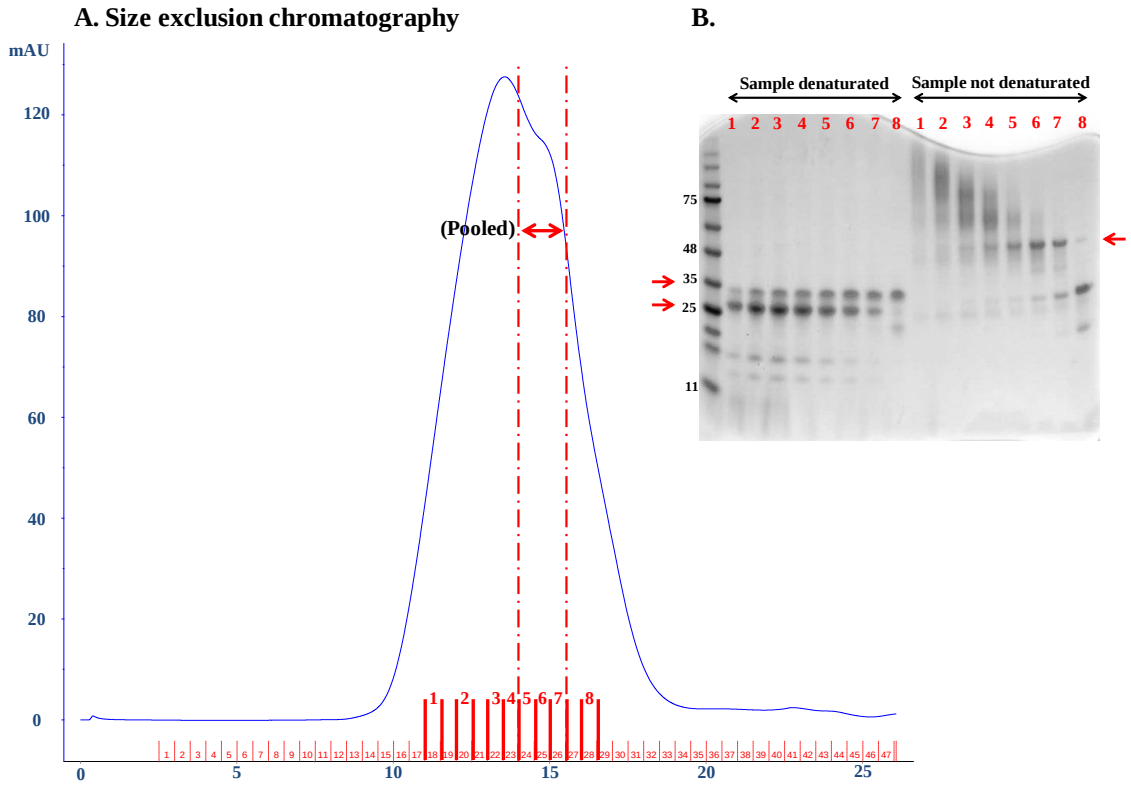

Figure 5.10. First purification of D454 TCR by size exclusion chromatography.
A. D454 TCR size exclusion chromatogram of pooled anion exchange fractions. The blue line corresponds to milli-absorbance unit (mAU) and the dashed lines represent the pooled fractions. **B.** Analysis of the D454 TCR size exclusion fractions by SDS-PAGE. Sample 1, 2, 3, 4, 5, 6, 7 and 8 (in red) were denaturated or not denaturated with 500mM DTT and run on a SDS-PAGE gel. Purified D454 proteins are indicated by red arrows.

To improve purity, size exclusion chromatography was repeated with the pooled fractions (**Figure 5.11 A**). The concentration of aggregates was greatly reduced after this third chromatographic separation. Fractions 3, 4 and 5 were pooled (**Figure 5.11 B**).

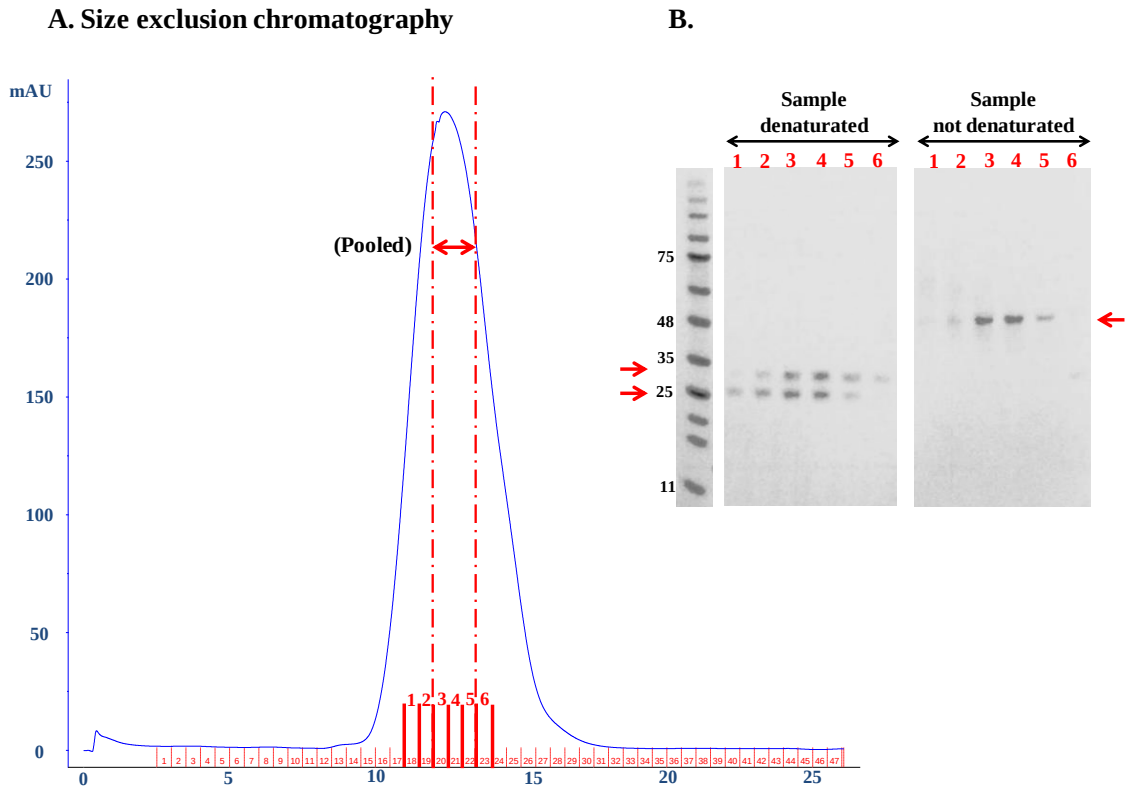

Figure 5.11. Second purification of D454 TCR by size exclusion chromatography. A. D454 TCR size exclusion chromatogram of pooled anion exchange fractions. The blue line corresponds to milli-absorbance unit (mAU) and the dashed lines represent the pooled fractions. **B.** Analysis of the D454 TCR size exclusion fractions by SDS-PAGE. Sample 1, 2, 3, 4, 5 and 6, (in red) were denaturated or not denaturated with 500 mM DTT and run on a SDS-PAGE gel. Purified D454 TCR and TCRα and TCRβ are indicated by red arrows.

D454 αβ TCR heterodimer concentration was low, therefore several refolding and purification steps of D454 αβ TCR were necessary to produce sufficient protein for biophysics and crystallisation. After these laborious, cumulative steps of purification, the purity of D454 αβ TCR heterodimer was estimated to only be ~80%; far lower than for other TCRs we have refolded.

*5.2.3.2 Biophysical analysis of the D454 TCR interaction with HLA-A*0201-LLDAHIPQL and HLA-A*0201-MIDAHIPQV*

The D454 TCR produced in section 5.2.3.1 was only ~80% pure and therefore not ideal for SPR where an accurate TCR concentration is required. Moreover, it is possible that the impurities present might inhibit TCR binding to MHC.

Nevertheless, I was able to use the protein I had produced to directly compare the binding of HLA-A*0201-LLDAHIPQL and HLA-A*0201-MIDAHIPQV; providing an accurate comparative affinity for the two ligands. The modification of only three amino acids at position P1 and anchor position P2 and P9 improve greatly the affinity of D454 for cognate peptide. Indeed, D454 affinity was 8-fold increased for the altered peptide HLA-A*0201-MIDAHIPQV (**Figure 5.12**).

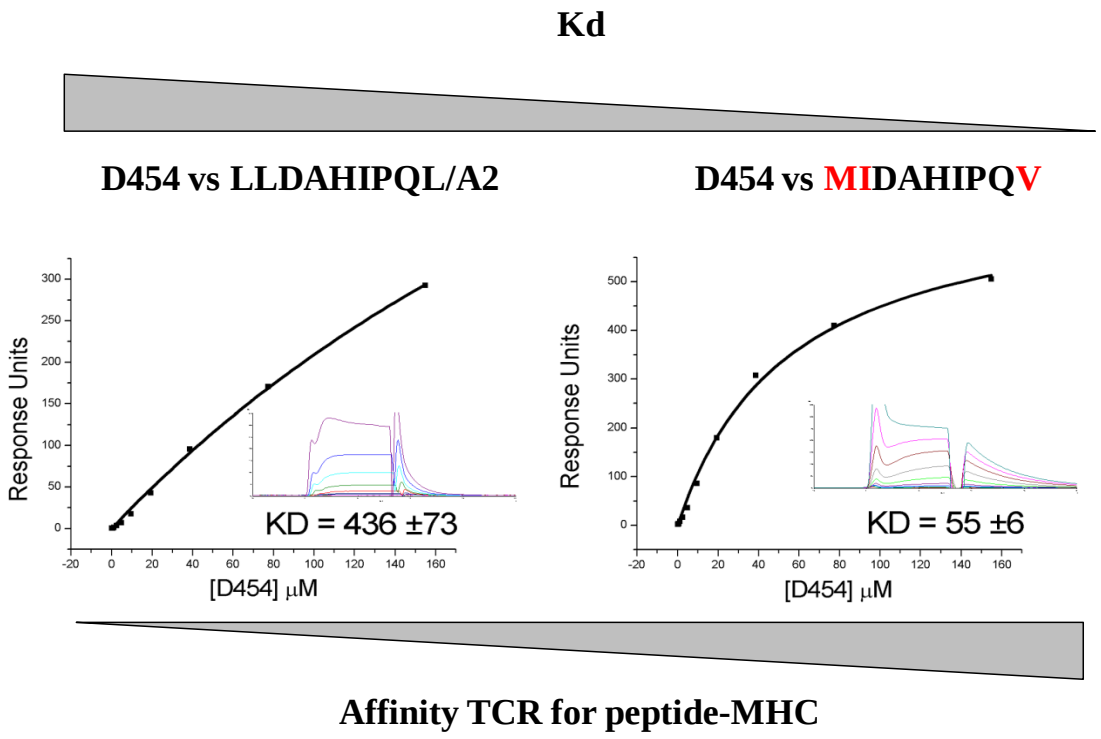

Figure 5.12. Estimation of the D454 binding affinity to HLA-A*0201-LLDAHIPQL and HLA-A*0201-MIDAHIPQV.
Ten serial dilution of D454 TCR were used to analyse binding to HLA-A*0201-LLDAHIPQL or HLA-A*0201-MIDAHIPQV monomers. The constant of dissociation (K_D) was evaluated by plotting the concentration of D454 TCR on the x-axis and the responses obtained unit obtained for each concentration. The equilibrium binding constant (K_D) values were calculated assuming a 1:1 interaction ($A + B \leftrightarrow AB$) by plotting specific equilibrium-binding responses against protein concentrations followed by non-linear least squares fitting of the Langmuir binding equation $AB = \frac{B \times ABmax}{K_D + B}$.

Even though an accurate value of the D454 TCR affinity for HLA-A*0201-LLDAHIPQL and HLA-A*0201-MIDAHIPQV monomers could not be measured, these data confirm that the D454 TCR binds better to the potent agonist HLA-A*0201-MIDAHIPQV than to the wild-type HLA-A*0201-LLDAHIPQL ligand.

*5.2.3.3 Structural studies of HLA-A*0201 in complex with LLDAHIPQL and MIDAHIPQL*

D454 TCR, HLA-A*0201-LLDAHIPQL and HLA-A*0201-MIDAHIPQV purified soluble monomers obtained in section 5.2.1.1 were used to generate protein crystals using the sitting drop vapour diffusion technique in multiple crystallisation screens. Multiple attempts to produce D454 TCR-antigen co-crystals failed. However, I was able to generate crystals of HLA-A*0201-LLDAHIPQL and HLA-A*0201-MIDAHIPQV in 20% PEG 3350 and 200 mM Ammonium Nitrate. Electron diffraction patterns were collected for these two pMHC at Diamond Light Source synchrotron, Didcot, UK. Data extracted from the diffraction patterns were compared to a known HLA-A*0201 model using the technique of molecular replacement. Molecular replacement was successful in space $P12_11$ for both HLA-A*0201-LLDAHIPQL and HLA-A*0201-MIDAHIPQV meaning that structures solved were consistent with the presence of one molecule per asymmetric unit. The resolution of the HLA-A*0201-LLDAHIPQL and HLA-A*0201-MIDAHIPQV structures were very high at 1.72 Å and 1.63 Å respectively. The molecular visualisation software, PyMol, was used to directly visualise and superimpose the conformations HLA-A*0201-LLDAHIPQL and HLA-A*0201-MIDAHIPQV. The data set and refinement statistics for the LLD HLA-A*0201-LLDAHIPQL and HLA-A*0201-MIDAHIPQV structures are shown in **Table 5.3**.

LLD/A2	
Data set statistics	
Space group	P 12_11
Unit cell parameters (Å,°)	a=56.33, b=79.51, c=56.61
Radiation source	DIAMOND I04.1
Resolution (Å)	**47.72-1.72**
Unique reflections	47853
Completeness (%)	99.9
Multiplicity	3.8
I/Sigma (I)	14.2
Rmerge	0.08
Refinement statistics	
No reflections used	47853
Rfactor (%)	17.6
Rfree (%)	21.3
Bond lengths (Å)	0.019
Bond angles (°)	1.97
Mean B value ($Å^2$)	23.714
Outliers Ramachandran plot (%)	0
Overall ESU based on maximum likelihood (Å)	0.057

MID/A2	
Data set statistics	
Space group	P 1 21 1
Unit cell parameters (Å,°)	a=56.56, b=79.46, c=56.77
Radiation source	DIAMOND I04.1
Resolution (Å)	**50.44-1.63**
Unique reflections	53372
Completeness (%)	99.87
Multiplicity	3.7
I/Sigma (I)	10.1
Rmerge (%)	0.133
Refinement statistics	
No reflections used	53372
Rfactor (%)	16.5
Rfree (%)	18.9
Bond lengths (Å)	0.019
Bond angles (°)	2.156
Mean B value ($Å^2$)	19.689
Outliers Ramachandran plot (%)	0
Overall ESU based on maximum likelihood (Å)	0.059

Table 5.3. Data collection and refinement statistics of LLD/A2 and MID/A2 complex structures.

Superposition of the LLDAHIPQL and MIDAHIPQV peptides inside the HLA-A*0201 groove allowed comparison of how these two peptides are presented to T-cells (**Figure 5.13 A**). Residues at positions P1 (leucine: Leu1 or methionine: Met1), P5 (histidine: His5) and P8 (glutamine: Glu8) were sticking up outside of the groove toward the solvent. These residues are likely to make important contacts with the TCR. The bulging residue histidine at position P5 is expected to play a major role in the TCR docking. However, positions P2 (Leu2 or isoleucine: Ile2), P6 (Ile6) and P9 (Leu9 or valine: Val9) were sticking down inside the HLA-A*0201 groove, therefore were more likely to stabilise peptide binding to HLA-A*0201 (**Figure 5.13 B**). Indeed, studies have shown that residues at P2 and P9 are the primary MHC anchors for HLA-A*0201 in nonamer peptides (Falk et al., 1991).

A.

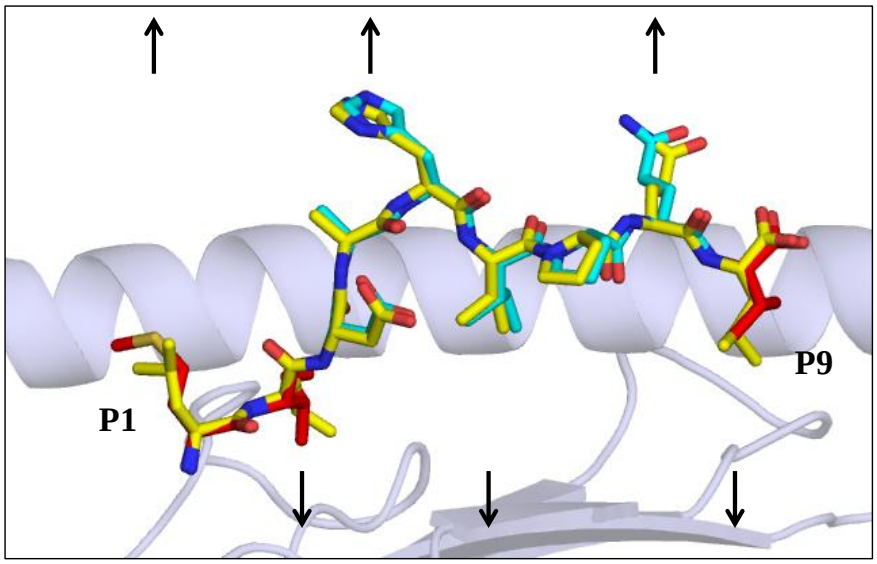

B.

Figure 5.13. Comparison of the conformation of LLDAHIPQL and MIDAHIPQV peptides inside the A2 groove.

(**A.**) Superposition of LLDAHIPQL and MIDAHIPQV inside the HLA-A*0201 groove. Only one HLA-A*0201 groove α helix is represented here in light transparent blue. LLDAHIPQL is represented in yellow while MIDAHIPQL is represented in blue. Substituted residues on MIDAHIPQL peptide are represented in red. Arrows are representing amino acids that are sticking outside or inside the HLA-A*0201 groove. (**B.**) Amino acid sequence of LLDAHIPQL and MIDAHIPQV peptides and the residues along the nonamer peptide backbone that are sticking outside and inside the HLA-A*0201 groove.

Close inspection of the peptide structures allowed me to understand how the amino acid substitutions in the LLDAHIPQL peptide might impact on D454 TCR binding. At position P1, the substitution of leucine (Leu1) with a methionine (Met1) did not stabilise the residue inside the HLA-A*0201 groove. Indeed, the number of contacts was higher between Leu1 and HLA-A*0201 groove residues than for Met1 (33 and 30 contacts respectively) (**Table 5.4**). However, Met1 is a longer residue than Leu1, therefore Met1 extended further up away from the HLA-A*0201 groove allowing the possibility of more contact with D454 TCR than Leu1 (**Figure 5.14 left quadrant**). The long residue Ile2 in the MIDAHIPQV peptide made two more Van der Walls interactions with the HLA-A*0201 groove than LLDAHIPQL Leu2 residue making in total 34 contacts with the HLA-A*0201 residues compared to 31 for Leu2 (**Figure 5.14 middle quadrant**). As mentioned earlier, modification of anchor residues can improve the docking of the peptide inside the HLA-A*0201 groove. Therefore Ile2 might marginally improve MIDAHIPQV interaction with HLA-A*0201 groove. At position P9, MIDAHIPQV Val9 residue made a similar number of contacts with the HLA-A*0201 groove than the LLDAHIPQL Leu9 residue, even though the valine residue is shorter than the leucine. Interestingly, substitution of the Leu9 for Val9 has a knock on effect on neighbour glutamine residue at position P8 (Glu8). Indeed, Val9 seems to "push" Glu8 away from the HLA-A*0201 groove toward the solvent and might increase the number of contacts with the TCR (**Figure 5.14 right quadrant**).

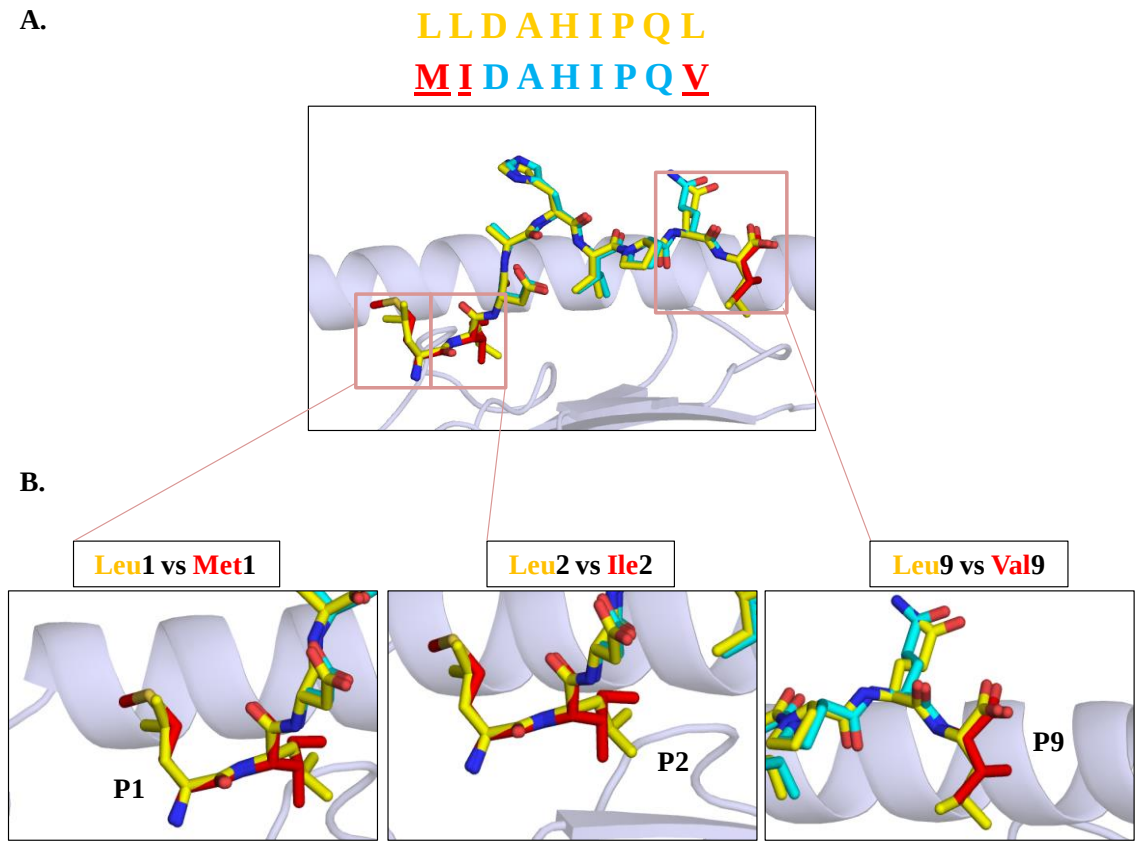

Figure 5.14. Comparison of LLDAHIPQL and MIDAHIPQV residues at position P1, P2 and P9.
(**A.**) Superposition of LLDAHIPQL and MIDAHIPQV inside the HLA-A*0201 groove. (**B.**) Close up of LLDAHIPQL and MIDAHIPQV peptide residues at position P1 (Leu1 vs Met1 left quadrant), P2 (Leu2 vs Ile2 middle quadrant) and P9 (Leu9 vs Val9 right quadrant).

	LLDAHIPQL with A2			MIDAHIPQV with A2		
	Leu1 : A2	Leu2 : A2	Leu9 : A2	Met1 : A2	Ile2 : A2	Val9 : A2
Total contacts	33	31	29	30	34	30
VdW contacts	30	29	25	27	32	26
H-bonds	3	2	4	3	2	4

Table 5.4. Number of contact between LLDAHIPQL or MIDAHIPQV peptides and A2 groove residues at position P1, P2 and P9.
This table presents the number of total contacts, Van der Walls (VdW) interactions and hydrogen bonds (H-bonds) between LLDAHIPQL peptide residues Leu1, Leu2 and Leu9 with A2 groove residues, as well as between MIDAHIPQV peptide residues Met1, Ile2 and Val9 with HLA-A*0201 groove residues. The full table of contacts between both peptides and HLA-A*0201 are presented in appendix A2 and A3.

5.3 Discussion

In this chapter I aimed to characterise the recognition of the immunogenic EsxG derived LLDAHIPQL peptide by an HLA-A*0201-restricted CD8 T-cell clone (D454). The specificity of D454 for HLA-A*0201-LLDAHIPQL was confirmed by tetramer staining. However, HLA-A*0201-LLDAHIPQL tetramer stained D454 weakly indicating a low affinity of D454 TCR for HLA-A*0201-LLDAHIPQL. In order to investigate into the mechanism involved in HLA-A*0201-LLDAHIPQL recognition by D454 TCR, I decided to determine the peptide residues important for this recognition. To this end, I undertook a nonamer CPL screen of D454. CPLs have been widely used to get an insight into T-cell peptide repertoire preferences (Wooldridge et al., 2012), to optimise antigen and improve T-cell recognition of cognate peptide (Cole et al., 2010) or even to map natural ligand for T-cell clones (Yin et al., 2011). 30 peptides were designed based on the CPL screen were tested. Most proved to be optimal agonists. The MIDAHIPQV sequence performed best and was 100-fold more potent than the LLDAHIPQL cognate peptide in activating D454. Substitution of leucine at position P1 and P2 for hydrophobic amino acids (phenylalanine, methionine or isoleucine) or at position P9 (valine) improved peptide potency. All the best three agonist peptides possessed a valine at position P9 indicating that this residue is optimum for the T-cell recognition. Structural analysis of the interaction between LLDAHIPQL or MIDAHIPQV peptides with HLA-A*0201 gave an insight into the impact of the amino acid substitution at position P1, P2 and P9 and provided a possible mechanism for the improved recognition of HLA-A*0201-MIDAHIPQV compared with HLA-A*0201-LLDAHIPQL. Amino acid substitution at position P1, P2 and P9 had a minor structural effect on peptide anchorage to the HLA-A*0201 groove. The number of contacts between MIDAHIPQV with HLA-A*0201 groove residues was slightly higher than with LLDAHIPQL peptide. The Met1 side chain of the MIDAHIPQV peptide extends further outside the HLA-A*0201 groove than Leu1 in the LLDAHIPQL peptide providing an opportunity for enhanced contacts with the D454 TCR. Substitution of Leu9 for Val9 pushed the solvent exposed Glu8 residue further away from the HLA-A*0201 groove (and towards a cognate TCR). These changes probably explain the enhanced potency of MIDAHIPQV. Unfortunately, I was unable to co-crystallise the D454 TCR with either antigen despite multiple attempts.

An estimation of D454 TCR affinity characterised by the constant of dissociation (K_D) showed that D454 TCR had a ~8-fold higher affinity for HLA-A*0201-MIDAHIPQV than HLA-A*0201-LLDAHIPQL. These data were supported by tetramer staining of D454 T-cell where staining was greater with HLA-A*0201-MIDAHIPQV than with HLA-A*0201-LLDAHIPQL.

Generation of potent, optimal agonist peptides by amino acid substitution of immunogenic cognate antigen such as MIDAHIPQV peptide could lead to the development of new diagnostic tools as well as new vaccine approaches. Several teams have already developed tetramers as a diagnostic tool for the detection of T-cell-associated immune responses against diseases. Tetramers developed were used to target T-cells involved in bacterial or various infections (Gratama and Cornelissen, 2003), in autoimmune diseases (Brottveit et al., 2011) and in cancers and were shown to provide information regarding the nature of the T-cells involved, as well as their frequencies and location. However, due to the low affinity of certain antigens, notably self antigen (Wooldridge et al., 2009, Aleksic et al., 2012, Cole et al., 2007), the challenge is to increase the sensitivity of tetramer detection. The use of HLA-A*0201-MIDAHIPQV tetramers could improve the threshold of detection of *M. tuberculosis*/LLDAHIPQL specific T-cell responses in HLA-A*0201 patients. Indeed, I could detect an HLA-A*0201-MIDAHIPQV tetramer negative population in D454 T-cell population that could not be detected by HLA-A*0201-LLDAHIPQL tetramer. Therefore, using HLA-A*0201-MIDAHIPQV tetramer would allow accurate measurement of D454 specific T-cells in patient samples that could not be detected by HLA-A*0201-LLDAHIPQL tetramer.

In summary, in this chapter, I successfully characterised the recognition of an immunogenic *M. tuberculosis* epitope by a CD8 T-cell by identifying the key peptide residues necessary for TCR recognition and design superior agonist by using CPL technology. Moreover, I succeeded in crystallising and solving the first ever molecular structure of a real *M. tuberculosis* epitope in complex with an MHC class I epitope.

CHAPTER 6. DISCUSSION AND FUTURE WORK

6.1 Discussion

Understanding immune responses to bacterial infection, and notably to life-threatening diseases such as TB, is of major importance to the development of diagnostic tools and effective vaccines. T-cells orchestrate the immune system and sit at the heart of approaches aimed at combating *M. tuberculosis* infection. In this thesis, I provided an insight into the T-cell network involved during exposure to Mycobacterial antigens and showed that it involved both conventional, peptide-recognising, MHC-restricted T-cells and unconventional T-cells that recognise other MHC-like platforms. Understanding the respective roles and importance of these T-cell subsets will be pivotal to approaches for diagnosing and treating bacterial infection.

In the chapter 3, I dissected T-cell responses to *M. smegmatis* phagocytosed by A549 cells. I used *M. smegmatis* as it grows well in culture and could be used in the facilities that were available to me. *M. smegmatis* cannot multiply in the host intracellular environment so is not infectious. However, this bacterium can still be phagocytosed and degraded by specialised phagocytic antigen presenting cells (DCs) or macrophage-type cell lines such as A549 cells which then present bacterial antigens to T-cells (Davey et al., 2011). My studies identified certain actors involved in the immune response to mycobacterium. After exposure to *M. smegmatis*, the frequency of responding CD3 T-cells was donor dependant and varied between 2 and 10 % of all T-cells. The majority of *M. smegmatis*-specific $CD3^+$ cells were CD8 T-cells although there were also expanded populations of DN T-cells. The *M. smegmatis*-specific DN T-cell population consisted mainly of γδ T-cells. γδ T-cells play a major role during early bacterial infection and are thought to provide a bridge between the innate response and the classical adaptive immunity undertaken by B-cells and αβ T-cells (Ladel et al., 1996). Strikingly, the majority of the responding CD8 T-cell population were MAITs characterised by the Vα7.2 J33 markers. These results emphasise the potential importance of MAITs in bacterial infections (Le Bourhis et al., 2010, Gold et al., 2010, Chua et al., 2012).

This study provided a preliminary insight into T-cell responses induced by exposure to *M. smegmatis* phagocytosed by an APC *in vitro*. It would have been interesting to further dissect these responses by varying parameters such as antigen load and duration

of exposure as well as examining different effector read-outs. My experiments used IFNγ secretion as a read-out of T-cell activation.

The use of this classic T_H1 cytokine obviously biased my results towards these IFNγ producer cells. It remains possible that other effective cells also responded but did not make IFNγ. In order to have a wider representation of *M. smegmatis* responding T-cells, I could have included examination of other effector markers such as CD107a, CD69, RANTES, TNFα and IL-2. T-cells are not restricted to the expression of only one cytokine. Certain T-cell populations can exhibit heterogeneity in their effector functions and it is becoming apparent that the range of functions that are elicited by a single T-cell is of vital importance to the effectiveness of an immune response. Indeed, it has been demonstrated that immunity to some pathogens correlates with the ability of individual responding cells to multitask by simultaneously responding with multiple effector functions. For example, 'polyfunctional' CD4 and CD8 T-cells are known to be associated with the control of HIV replication *in vivo* (Wherry et al., 2003, Harari et al., 2004, Almeida et al., 2007). Other studies have aimed to examine T-cell polyfunctionality in bacterial infections such as TB. Recombinant TB antigen-based human vaccines stimulate individual T-cells to secrete IFNγ, IL-2 and TNFα (Beveridge et al., 2007, Scriba et al., 2010). BCG vaccination of infants is also known to trigger the expansion of polyfunctional T-cells (Soares et al., 2008). These studies provide evidence that polyfunctional T-cells might be associated with protection in chronic TB. Curiously, polyfunctional T-cells are highly represented during T-cell responses to active TB but are less frequent during TB latency (Caccamo et al., 2010). Therefore it has been suggested that polyfunctional T-cells could act as a biomarker of active TB (Caccamo et al., 2010).

The high frequency of MAITs induced in my experiments with *M. smegmatis* made me especially keen to examine what these cells were recognising. When I started my studies, little was known about MAITs, their role in bacterial infection or the nature of the bacterial antigen they recognised. Knowledge of MAITs was limited by the availability of reagents for identifying these cells in *ex vivo* samples. I knew that several laboratories were trying to define the ligand presented to MAITs by MR1. The nature of the MR1 binding groove and its similarity to classical MHC I molecules suggested that it might present a peptide.

As my laboratory has extensive expertise with CPLs, I set out to establish whether a MAIT could recognise a peptide using these tools. If MAITs recognised a peptide, I was particularly excited by the prospect of using peptide-MR1 tetramers for tracking of MAITs in patient samples.

I was provided with a well-characterised CD8 MAIT clone (D426 B1) by my collaborator, Prof David Lewinsohn. My studies in Chapter 4 showed that D426 B1 could recognise peptides. These data were then used to show that this MAIT clone could recognise *M. tuberculosis*-derived peptides. Unfortunately, subsequent analyses revealed that this D426 B1 response was not restricted by MR1 and was attributed to a non-MAIT contaminant population in D426 B1 sample leading me to conclude that MAITs do not recognise peptide through MR1.

I set out to continue my hunt for the MAIT ligand by attempting to refold soluble MR1. During these studies my supervisor heard that the Melbourne group had already discovered a ligand for MAITs and successfully manufactured MR1 tetramers. I was advised to discontinue my studies. The studies of McCluskey, Rossjohn and colleagues finally started to hit the press late in 2012 and revealed some fascinating insights into MAIT biology. The first study showed the structure of the MR1 molecule in complex with a folic acid (Vitamin B9) metabolite, 6-formyl pterin (6-FP) (Kjer-Nielsen et al., 2012). Although, 6-FP fits inside MR1 groove, it is not a MAIT agonist. Subsequent studies have demonstrated that other metabolites from the riboflavin (Vitamin B2) pathway activate MAITs when presented by MR1 (Patel et al., 2013). This presentation of a bacterial metabolite by MR1 was highly unexpected and revealed that T-cells could recognise more than just foreign peptides or lipids.

The overall conformation of MR1 is very similar to classic MHC I molecules. However, the antigen cavity in MR1 groove is smaller and mainly hydrophobic allowing it to accommodate ring-based metabolites. The MAIT TCR interacts mainly with the MR1 groove and makes very limited contacts with the antigen (Patel et al., 2013, Lopez-Sagaseta et al., 2013). **Figure 6.1** shows a MAIT TCR in complex with MR1-6-FP and MR1 loaded with the MAIT agonist: 7-hydroxy-6-methyl-8-D-ribityllumazine (Ri-6-Me-7-OH). These figures were generated using coordinates published by Prof. Jamie Rossjohn and colleagues in 2013 (Patel et al., 2013). Antigen recognition by the MAIT TCR involved mainly the Vα7.2 Jα33-encoded CDR3α loop which is diagonally positioned above MR1-antigen and acts as an antigen sensor. Interestingly, all MAIT

agonists described to date share a ribityl group that is recognised by MAIT TCR tyrosine residue at position 95 on the CDR3α loop (Y95α) (Patel et al., 2013).

The ribityl group acts as a bridge that facilitates the interaction with the CDR3α loop.

Indeed the distance between the Y95α and the terminal hydroxide of the ribityl group of the Ri-6-Me-7-OH (2.83 Å) is favourable for TCR binding to MR1-antigen (**Figure 6.1 B**). The absence of the ribityl group in the 6-FP increases the distance to Y95α (4.93 Å) and explains why this interaction is too weak to activate MAITs (**Figure 6.1 A**).

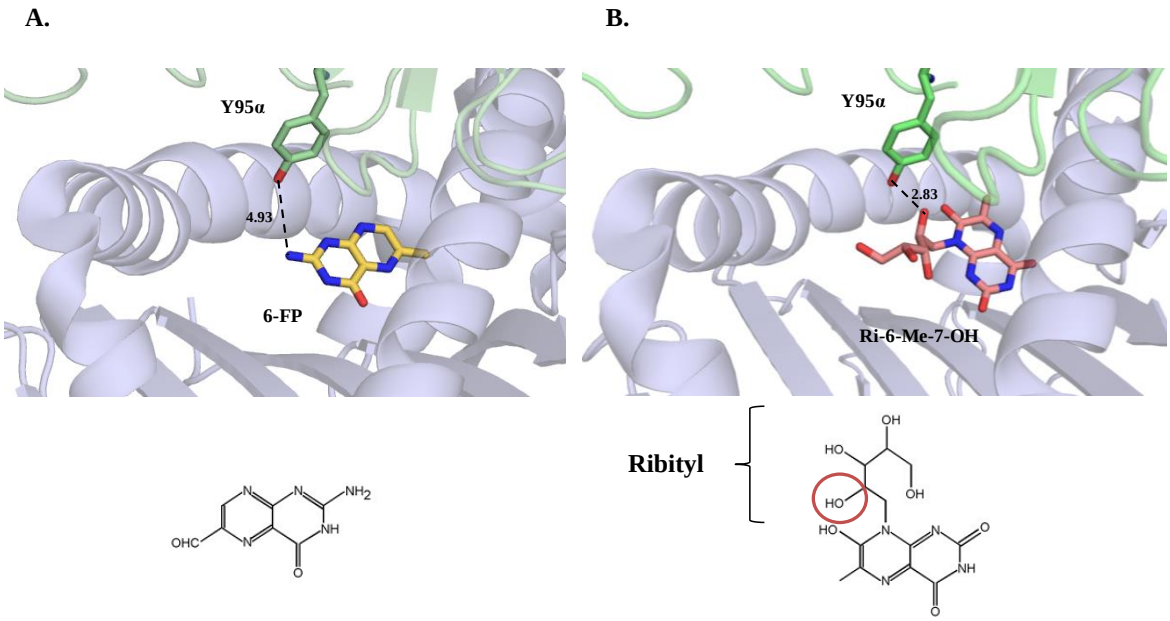

Figure 6.1 MAIT TCR recognition of MR1-vitamin antigens.
Interaction between the MAIT TCR CDR3α Tyr95α and (**A.**) the nitrogen hydride group of the 6-forym pterin (6-FP) and (**B.**) the terminal hydroxyl from the ribityl group (circled in red) of the 7-hydroxy-6-methyl-8-D-ribityllumazine (Ri-6-Me-7-OH) loaded in MR1 groove. Crystal structure of MAIT TCR in complex with MR1-6-FP and MR1-Ri-6-Me-7-OH are respectively 4L4T and 4L4V respectively and were both published by Prof. Jamie Rossjohn and team (Patel et al., 2013). Chemical structures of 6-FP and Ri-6-Me-7-OH were taken from (Gapin, 2014).

In hindsight, it is striking that the ability of MAITs to respond to different micro-organisms corresponds to whether they possess a riboflavin-biosynthesis pathway (Le Bourhis et al., 2010, Gold et al., 2010, Kjer-Nielsen et al., 2012). However, much further work will be needed to truly dissect what MAITs recognise as riboflavin

metabolites are expressed by some commensal bacteria so could easily diffuse through epithelial layers to eventually activate MAITs leading to unwanted inflammation.

The discovery of MR1 ligand has considerably improved the characterisation of MAIT-mediated immunity. The generation of multimeric MR1-antigen has improved the detection of MAITs *ex vivo*. The combination of non-specific phenotype markers (CD3, CD161 and Vα7.2) with MR1-antigen tetramer strengthens the stringency of MAIT detection (Reantragoon et al., 2013). Interestingly, 5-15 % of MR1-antigen-specific MAITs were shown to express Vα7.2 Jα12 and Vα7.2 Jα20 TCR chains (Reantragoon et al., 2013). These results raised questions regarding the rigidity of the MAIT nomenclature. New data shows that the MAITs induced by *Listeria*, *Salmonella* and *M. smegmatis* express different TCRs (Gold et al., 2014). These data are highly suggestive of the fact that cells infected with these pathogens present subtly different antigens to MAITs. The important molecular details of this recognition remain to be discovered but may be key to how MAITs discriminate between commensal and pathogenic bacteria.

Due to the above discoveries I was advised to switch my studies to examining conventional T-cell responses to Mycobacteria. I was particularly interested in T-cell responses to the HLA*0201-restricted epitope LLDAPHIPQL. This sequence originates from the immunogenic *M. tuberculosis* EsxG protein which triggers a strong CD8 T-cell response (Hervas-Stubbs et al., 2006, Skjot et al., 2002). Furthermore, LLDAPHIPQL is conserved between different Mycobacterial species, thereby opening up the potential that responses to this epitope might be broadly protective and offer pan-Mycobacterial immunity.

My collaborators in Portland provided me with a T-cell clone, D454, that recognised HLA*0201-LLDAPHIPQL that had been isolated from the blood of a patient with chronic TB. This T-cell is activated by *M. tuberculosis* infected DCs (Lewinsohn et al., 2007). I isolated the TCR from this clone and showed that it had a relatively low affinity for HLA-A*0201-LLDAHIPQL, by tetramer staining and SPR. Dissection of the recognition profile of D454 by CPL revealed that this clone preferred a nonamer peptide suggesting that better peptide agonists could be designed. I explored this avenue as such a ligand might have helped detection of HLA-A*0201-LLDAPHIPQL-specific T-cells. I also hoped that such a ligand would aid my attempts to structurally study the D454

TCR. 30 peptides were designed and tested as agonists of the D454 T-cell. The sequence MIDAHIPQV proved to be the best of those tested and was >100 fold more potent than the wild type LLDAPHIPQL sequence in an antigen titration experiment. The threshold of detection of D454 population by tetramer staining was greatly enhanced by using reagents folded with HLA-A*0201-MIDAHIPQV.

Moreover, an HLA-A*0201-MIDAHIPQV negative contaminant population was detected using this reagent suggesting that D454, like D426 B1, was not a monoclonal population. I aimed at understanding the molecular mechanisms involved in D454 TCR interaction with HLA-A*0201-LLDAHIPQL. To this end, I attempts to crystallise soluble D454 TCR in complex with HLA-A*0201-LLDAHIPQL and HLA-A*0201-MIDAHIPQV. Unfortunately, my attempts to generate a co-crystal structure were unsuccessful. However, I successfully solved both HLA-A*0201-LLDAHIPQL and HLA-A*0201-MIDAHIPQV structures. The former represents the first crystal structure of HLA-A*0201 presenting a bacterial antigen ever analysed. Combination of structural analysis of HLA-A*0201-LLDAHIPQL and HLA-A*0201-MIDAHIPQV as well as data generated from the nonamer CPL screen revealed the key peptide residues involved in D454 recognition of pMHC. Counter intuitively, two of the three positions that are altered in the MIDAHIPQV sequence are primary anchor positions where the amino acid side chain is thought to be buried within the MHC groove rather than facing the TCR. Indeed, the leucine to valine change at position 9 gave the biggest enhancement in peptide potency. Structures of HLA-A*0201-LLDAHIPQL and HLA-A*0201-MIDAHIPQV show that the change in primary anchors had knock-on effects on neighbouring residues thereby altering the topography of the peptide-HLA landscape. My group have recently demonstrated that changes in peptide anchor positions can have marked effects on TCR engagement (Cole et al., 2010). These results have recently been backed up by structural analyses (David Cole unpublished).

6.2 Future work

During the course of my PhD, I have learned many lessons. The most valuable is to verify the quality and specificity of reagents provided by collaborators even when they have been used in high profile publications. Neither the D426 B1 MAIT cell clone or the D454 HLA-A*0201-LLDAHIPQL-specific T-cell clone were actually monoclonal. While this lack of clonality with the conventional T-cell did not affect my work, the contamination of the D426 B1 MAIT with a regular CD8 T-cell cost me dearly as it

resulted in me exploring the possibility that MAITs recognise peptide ligands presented by MR1. If I had my time over again I would certainly confirm the clonality of T-cell clones prior to investing major effort into them.

My work could proceed to many future directions and I will explore some of these possibilities below.

6.2.1 Comparative studies using other Mycobacteria and bacterial species

One way of expanding my studies would be to look at the T-cell responses generated by other bacterial species. I used *M. smegmatis* due to the ease of culture and compatibility with the containment facilities that were available to me. Ideally, I would have also liked to work with pathogenic Mycobacteria such as *M. tuberculosis* and *M. leprae*. Due to the similarities between these organisms it is not unlikely that there might be crossover in the T-cell responses they induce. Any such pan-mycobacterial T-cells might make very good candidates to look to induce during vaccination. One candidate T-cell type that could potentially recognise a wide range of bacterial species is MAITs.

A very recent study demonstrated that the MAITs raised against different microorganisms displayed subtly different TCRs (Gold et al., 2014). This difference suggests that these microorganisms present a different array of MR1-associated antigens. Given this evidence, it would be very interesting to isolate MR1 from cells infected with different microorganisms using MR1-specific antibody and then elute MR1-bound antigens prior to identification by mass spectrometry. Identification of specific MR1-associated antigens from different bacteria could prove to be especially important for inducing the right kind of MAITs to combat a specific infection. A similar approach that aimed to elute lipid moieties associated with CD1a, CD1b, CD1c and CD1d when cells are infected with different bacteria would also be highly informative.

6.2.2 Clonotypic analyses of bacterially-induced T-cells

During my studies I showed that it was possible to isolate *M. smegmatis*-specific T-cells. The modern development in nucleic acid sequencing methods allows now the sequencing of all TCR chains available in a sample. The sequence analysis of all the TCR α and β chains in the *M. smegmatis*-specific T-cells induced from multiple individuals would be highly illuminating. These analyses would reveal any invariant or ‘public’ TCR chains that occurred within these populations.

6.2.2.1 Invariant TCR chains

Two invariant TCR α chains have already been identified and correspond to those used by NKT type 1 and MAITs. As there are invariant TCR chains associated with recognition of MR1- and CD1d-associated antigens it is not unreasonable to hypothesise that similar chains exist that are involved in recognition of other non-classical MHC molecules such as CD1a, CD1b, CD1c and HLA-E. It is possible that clonotypic analyses would reveal further unconventional T-cell subsets that have invariant or semi-invariant TCR α or β chains. Therefore, it would be very interesting to study any such T-cell subsets and to establish the roles they play in bacterial infection. Deep clonotypic analyses of TCR chains of T-cells that target bacteria would be expected to identify such chains. Once identified, these unconventional T-cells could be enriched with TCR variable domain-specific antibody prior to cloning attempts.

6.2.2.2 Public TCRs

A full clonotypic analysis of the TCR chains used by *M. smegmatis*-specific T-cells from multiple individuals would also reveal any public TCR chains. Public TCRs are residue identical TCRs that are used to fight specific infections in all individuals with a given HLA type (Lim et al., 2000, Annels et al., 2000, Yu et al., 2007). Such TCRs are routinely found in all systems where they have been looked for. Public TCRs make ideal candidates for targeted vaccination (Davenport et al., 2007, Miles et al., 2006, Venturi et al., 2008). I could have continued my research by identifying public TCRs that target HLA-A*0201-LLDAHIPQL and designed an optimal peptide agonist for it using CPL screening technology. My experiments and those by other members of my laboratory show that it is often possible to produce peptides that are 100-fold more potent than the natural peptide. These super peptides could be used to vaccinate individuals with the corresponding HLA and would be significantly better at inducing such responses.

						Cell markers observed		
Donor	**APC used**	**MOI priming *M. smeg*:APC**	**MOI assay *M. smeg*:APC**	**Analysis date after priming**	**T-cell responses measured by:**	**1st level**	**2nd level**	**3rd level**
Donor 1	Autologous DCs	10:1	x	D-8	CFSE staining	CFSE, CD3	x	x
Donor 2	Autologous DCs	10:1	x	D-8	CFSE staining	CFSE, CD3	x	x
Donor 3	A549	10:1	x	D-3, 8 and 13	CFSE staining	CFSE, CD3	CD8, CD4	x
Donor 4	A549	10:1	x	D-3, 8 and 13	CFSE staining	CFSE, CD3	CD8, CD4	x
Donor 5	A549	10:1	10:1	D-13	IFNγ ICS	IFNγ, CD3	αβTCR, γδ TCR	CD8, CD4
Donor 6	A549	10:1	10:1	D-13	IFNγ ICS	IFNγ, CD3	CD8, CD4	x
Donor 7	A549	10:1	10:1	D-13	IFNγ ICS	IFNγ, CD3	αβTCR, γδ TCR	CD8, CD4
Donor 8	A549	10:1	10:1	D-13	IFNγ ICS	IFNγ, CD3	CD8, CD4	x
Donor 9	A549	10:1	10:1	D-13	IFNγ ICS	IFNγ, CD3	CD8, CD4	x
Donor 10	A549	10:1	10:1	D-13	IFNγ ICS	IFNγ, CD3	αβTCR, γδ TCR	CD8, CD4
Donor 11	A549	10:1	10:1	D-13	IFNγ ICS	IFNγ, CD3	αβTCR, Vα7.2 TCR	CD8, CD4
Donor 12	A549	10:1	10:1	D-13	IFNγ ICS	IFNγ, CD3	αβTCR, Vα7.2TCR	CD8, CD4

Appendix A1. Summary of all the donors used for Chapter 3 study and the various parameters.

```
/1/A/   5(MET). / CE [ C]:  /1/C/   1(LEU). / N  [ N]:   3.86
/1/A/   7(TYR). / CZ [ C]:  /1/C/   1(LEU). / N  [ N]:   3.99
/1/A/   7(TYR). / OH [ O]:  /1/C/   1(LEU). / N  [ N]:   2.87
/1/A/   5(MET). / SD [ S]:  /1/C/   1(LEU). / N  [ N]:   3.78
/1/A/ 171(TYR). / CZ [ C]:  /1/C/   1(LEU). / N  [ N]:   3.54
/1/A/ 171(TYR). / OH [ O]:  /1/C/   1(LEU). / N  [ N]:   2.68
/1/A/ 171(TYR). / CE2[ C]:  /1/C/   1(LEU). / N  [ N]:   3.47
/1/A/   7(TYR). / OH [ O]:  /1/C/   1(LEU). / CA [ C]:   3.32
/1/A/  63(GLU). / OE1[ O]:  /1/C/   1(LEU). / CA [ C]:   3.62
/1/A/ 171(TYR). / OH [ O]:  /1/C/   1(LEU). / CA [ C]:   3.48
/1/A/ 167(TRP). / CG [ C]:  /1/C/   1(LEU). / CB [ C]:   3.66
/1/A/ 167(TRP). / CD2[ C]:  /1/C/   1(LEU). / CB [ C]:   3.76
/1/A/ 171(TYR). / OH [ O]:  /1/C/   1(LEU). / CB [ C]:   3.96
/1/A/  66(LYS). / NZ [ N]:  /1/C/   1(LEU). / CG [ C]:   3.48
/1/A/  63(GLU). / OE2[ O]:  /1/C/   1(LEU). / CG [ C]:   3.72
/1/A/  66(LYS). / NZ [ N]:  /1/C/   1(LEU). / CD1[ C]:   3.94
/1/A/  59(TYR). / CE2[ C]:  /1/C/   1(LEU). / CD1[ C]:   3.76
/1/A/  63(GLU). / CD [ C]:  /1/C/   1(LEU). / CD1[ C]:   3.82
/1/A/  63(GLU). / OE2[ O]:  /1/C/   1(LEU). / CD1[ C]:   3.32
/1/A/ 163(THR). / CG2[ C]:  /1/C/   1(LEU). / CD2[ C]:   3.79
/1/A/ 167(TRP). / CD1[ C]:  /1/C/   1(LEU). / CD2[ C]:   3.93
/1/A/ 167(TRP). / NE1[ N]:  /1/C/   1(LEU). / CD2[ C]:   3.61
/1/A/ 167(TRP). / CE2[ C]:  /1/C/   1(LEU). / CD2[ C]:   3.82
/1/A/  66(LYS). / NZ [ N]:  /1/C/   1(LEU). / CD2[ C]:   3.89
/1/A/ 159(TYR). / OH [ O]:  /1/C/   1(LEU). / C  [ C]:   3.86
/1/A/   7(TYR). / CZ [ C]:  /1/C/   1(LEU). / C  [ C]:   3.88
/1/A/   7(TYR). / OH [ O]:  /1/C/   1(LEU). / C  [ C]:   3.28
/1/A/   7(TYR). / CE2[ C]:  /1/C/   1(LEU). / C  [ C]:   3.81
/1/A/  63(GLU). / OE1[ O]:  /1/C/   1(LEU). / C  [ C]:   3.69
/1/A/ 159(TYR). / CE1[ C]:  /1/C/   1(LEU). / O  [ O]:   3.49
/1/A/ 159(TYR). / CZ [ C]:  /1/C/   1(LEU). / O  [ O]:   3.47
/1/A/ 159(TYR). / OH [ O]:  /1/C/   1(LEU). / O  [ O]:   2.66
/1/A/   7(TYR). / CE2[ C]:  /1/C/   1(LEU). / O  [ O]:   3.64
/1/A/  66(LYS). / NZ [ N]:  /1/C/   2(LEU). / N  [ N]:   3.79
/1/A/   7(TYR). / CZ [ C]:  /1/C/   2(LEU). / N  [ N]:   3.87
/1/A/  63(GLU). / CD [ C]:  /1/C/   2(LEU). / N  [ N]:   3.73
/1/A/  63(GLU). / OE1[ O]:  /1/C/   2(LEU). / N  [ N]:   2.85
/1/A/  99(TYR). / OH [ O]:  /1/C/   2(LEU). / CA [ C]:   3.73
/1/A/  63(GLU). / OE1[ O]:  /1/C/   2(LEU). / CA [ C]:   3.81
/1/A/  99(TYR). / OH [ O]:  /1/C/   2(LEU). / CB [ C]:   3.74
/1/A/  66(LYS). / NZ [ N]:  /1/C/   2(LEU). / CB [ C]:   3.97
/1/A/  63(GLU). / OE1[ O]:  /1/C/   2(LEU). / CB [ C]:   3.58
                            /1/C/   2(LEU). / CG [ C]:   3.42
/1/A/  67(VAL). / CA [ C]:  /1/C/   2(LEU). / CD1[ C]:   3.93
/1/A/  63(GLU). / O  [ O]:  /1/C/   2(LEU). / CD1[ C]:   3.64
/1/A/  66(LYS). / CB [ C]:  /1/C/   2(LEU). / CD1[ C]:   3.87
/1/A/  67(VAL). / N  [ N]:  /1/C/   2(LEU). / CD1[ C]:   3.69
/1/A/  63(GLU). / OE1[ O]:  /1/C/   2(LEU). / CD1[ C]:   3.75
/1/A/  45(MET). / CE [ C]:  /1/C/   2(LEU). / CD1[ C]:   3.60
/1/A/  67(VAL). / CB [ C]:  /1/C/   2(LEU). / CD1[ C]:   3.75
/1/A/  99(TYR). / OH [ O]:  /1/C/   2(LEU). / CD2[ C]:   3.35
/1/A/   9(PHE). / CZ [ C]:  /1/C/   2(LEU). / CD2[ C]:   3.68
/1/A/   9(PHE). / CE2[ C]:  /1/C/   2(LEU). / CD2[ C]:   3.98
/1/A/   7(TYR). / CG [ C]:  /1/C/   2(LEU). / CD2[ C]:   3.87
/1/A/   7(TYR). / CD1[ C]:  /1/C/   2(LEU). / CD2[ C]:   3.61
/1/A/   7(TYR). / CE1[ C]:  /1/C/   2(LEU). / CD2[ C]:   3.70
/1/A/  99(TYR). / OH [ O]:  /1/C/   2(LEU). / C  [ C]:   3.85
/1/A/ 159(TYR). / CE1[ C]:  /1/C/   2(LEU). / C  [ C]:   3.78
/1/A/ 159(TYR). / OH [ O]:  /1/C/   2(LEU). / C  [ C]:   3.97
/1/A/  66(LYS). / NZ [ N]:  /1/C/   2(LEU). / C  [ C]:   3.67
/1/A/ 159(TYR). / CE1[ C]:  /1/C/   2(LEU). / O  [ O]:   3.88
/1/A/  66(LYS). / CD [ C]:  /1/C/   2(LEU). / O  [ O]:   3.98
/1/A/  66(LYS). / CE [ C]:  /1/C/   2(LEU). / O  [ O]:   3.88
/1/A/  66(LYS). / NZ [ N]:  /1/C/   2(LEU). / O  [ O]:   2.83
                            /1/C/   9(LEU). / N  [ N]:   3.94
/1/A/  77(ASP). / CG [ C]:  /1/C/   9(LEU). / N  [ N]:   3.63
/1/A/  77(ASP). / OD1[ O]:  /1/C/   9(LEU). / N  [ N]:   2.90
/1/A/ 143(THR). / CG2[ C]:  /1/C/   9(LEU). / CA [ C]:   3.95
/1/A/ 147(TRP). / CZ2[ C]:  /1/C/   9(LEU). / CA [ C]:   3.94
/1/A/  77(ASP). / OD1[ O]:  /1/C/   9(LEU). / CA [ C]:   3.79
/1/A/ 143(THR). / OG1[ O]:  /1/C/   9(LEU). / CB [ C]:   3.97
/1/A/  77(ASP). / CG [ C]:  /1/C/   9(LEU). / CB [ C]:   3.92
/1/A/  77(ASP). / OD1[ O]:  /1/C/   9(LEU). / CB [ C]:   3.67
/1/A/  77(ASP). / CG [ C]:  /1/C/   9(LEU). / CG [ C]:   3.50
/1/A/  77(ASP). / OD1[ O]:  /1/C/   9(LEU). / CG [ C]:   3.71
/1/A/ 116(TYR). / CZ [ C]:  /1/C/   9(LEU). / CG [ C]:   3.88
/1/A/  77(ASP). / OD2[ O]:  /1/C/   9(LEU). / CG [ C]:   3.76
/1/A/  81(LEU). / CD2[ C]:  /1/C/   9(LEU). / CD1[ C]:   3.33
/1/A/  77(ASP). / CB [ C]:  /1/C/   9(LEU). / CD1[ C]:   3.82
/1/A/  77(ASP). / CG [ C]:  /1/C/   9(LEU). / CD1[ C]:   3.90
/1/A/ 116(TYR). / CE1[ C]:  /1/C/   9(LEU). / CD1[ C]:   3.18
/1/A/ 116(TYR). / CZ [ C]:  /1/C/   9(LEU). / CD1[ C]:   3.33
/1/A/ 116(TYR). / OH [ O]:  /1/C/   9(LEU). / CD1[ C]:   3.58
/1/A/ 147(TRP). / CH2[ C]:  /1/C/   9(LEU). / CD2[ C]:   3.61
/1/A/ 147(TRP). / CZ2[ C]:  /1/C/   9(LEU). / CD2[ C]:   3.63
/1/A/ 143(THR). / OG1[ O]:  /1/C/   9(LEU). / C  [ C]:   3.87
/1/A/ 146(LYS). / NZ [ N]:  /1/C/   9(LEU). / C  [ C]:   3.26
                            /1/C/   9(LEU). / O  [ O]:   2.83
/1/A/  80(THR). / CG2[ C]:  /1/C/   9(LEU). / O  [ O]:   3.90
/1/A/ 143(THR). / CB [ C]:  /1/C/   9(LEU). / OXT[ O]:   3.69
/1/A/ 143(THR). / OG1[ O]:  /1/C/   9(LEU). / OXT[ O]:   2.82
/1/A/ 143(THR). / CG2[ C]:  /1/C/   9(LEU). / OXT[ O]:   3.61
/1/A/ 146(LYS). / NZ [ N]:  /1/C/   9(LEU). / OXT[ O]:   2.92
```

Appendix A2. Total contacts between LLDAHIPQL peptide and HLA-A*0201 molecule.

```
/1/A/   5(MET). / CE [ C]:  /1/C/   1(MET). / N  [ N]:   3.90
/1/A/ 167(TRP). / CB [ C]:  /1/C/   1(MET). / N  [ N]:   3.85
/1/A/   7(TYR). / OH [ O]:  /1/C/   1(MET). / N  [ N]:   2.93
/1/A/   5(MET). / SD [ S]:  /1/C/   1(MET). / N  [ N]:   3.91
/1/A/ 171(TYR). / CZ [ C]:  /1/C/   1(MET). / N  [ N]:   3.42
/1/A/ 171(TYR). / OH [ O]:  /1/C/   1(MET). / N  [ N]:   2.57
/1/A/ 171(TYR). / CE2[ C]:  /1/C/   1(MET). / N  [ N]:   3.38
/1/A/   7(TYR). / OH [ O]:  /1/C/   1(MET). / CA [ C]:   3.32
/1/A/  63(GLU). / OE1[ O]:  /1/C/   1(MET). / CA [ C]:   3.45
/1/A/ 171(TYR). / OH [ O]:  /1/C/   1(MET). / CA [ C]:   3.39
/1/A/ 167(TRP). / CG [ C]:  /1/C/   1(MET). / CB [ C]:   3.78
/1/A/ 167(TRP). / CD2[ C]:  /1/C/   1(MET). / CB [ C]:   3.89
/1/A/ 171(TYR). / OH [ O]:  /1/C/   1(MET). / CB [ C]:   3.82
/1/A/  66(LYS). / NZ [ N]:  /1/C/   1(MET). / CG [ C]:   3.23
/1/A/  63(GLU). / OE2[ O]:  /1/C/   1(MET). / CG [ C]:   3.45
/1/A/  66(LYS). / NZ [ N]:  /1/C/   1(MET). / SD [ S]:   3.73
/1/A/ 167(TRP). / NE1[ N]:  /1/C/   1(MET). / SD [ S]:   3.98
/1/A/ 167(TRP). / CE2[ C]:  /1/C/   1(MET). / CE [ C]:   3.66
/1/A/ 167(TRP). / CZ2[ C]:  /1/C/   1(MET). / CE [ C]:   3.54
/1/A/  63(GLU). / OE2[ O]:  /1/C/   1(MET). / CE [ C]:   3.93
/1/A/ 167(TRP). / CH2[ C]:  /1/C/   1(MET). / CE [ C]:   3.76
/1/A/ 159(TYR). / OH [ O]:  /1/C/   1(MET). / C  [ C]:   3.83
/1/A/   7(TYR). / CZ [ C]:  /1/C/   1(MET). / C  [ C]:   3.86
/1/A/   7(TYR). / OH [ O]:  /1/C/   1(MET). / C  [ C]:   3.37
/1/A/   7(TYR). / CE2[ C]:  /1/C/   1(MET). / C  [ C]:   3.83
/1/A/  63(GLU). / OE1[ O]:  /1/C/   1(MET). / C  [ C]:   3.66
/1/A/ 159(TYR). / CE1[ C]:  /1/C/   1(MET). / O  [ O]:   3.50
/1/A/ 159(TYR). / CZ [ C]:  /1/C/   1(MET). / O  [ O]:   3.50
/1/A/ 159(TYR). / OH [ O]:  /1/C/   1(MET). / O  [ O]:   2.71
/1/A/   7(TYR). / CE2[ C]:  /1/C/   1(MET). / O  [ O]:   3.71
/1/A/   7(TYR). / CZ [ C]:  /1/C/   2(ILE). / N  [ N]:   3.85
/1/A/  63(GLU). / CD [ C]:  /1/C/   2(ILE). / N  [ N]:   3.84
/1/A/  63(GLU). / OE1[ O]:  /1/C/   2(ILE). / N  [ N]:   2.90
/1/A/  99(TYR). / OH [ O]:  /1/C/   2(ILE). / CA [ C]:   3.78
/1/A/ 159(TYR). / OH [ O]:  /1/C/   2(ILE). / CA [ C]:   3.86
/1/A/  63(GLU). / OE1[ O]:  /1/C/   2(ILE). / CA [ C]:   3.93
/1/A/  99(TYR). / OH [ O]:  /1/C/   2(ILE). / CB [ C]:   3.40
/1/A/  63(GLU). / OE1[ O]:  /1/C/   2(ILE). / CB [ C]:   3.93
/1/A/  66(LYS). / CB [ C]:  /1/C/   2(ILE). / CG1[ C]:   3.82
/1/A/  66(LYS). / CE [ C]:  /1/C/   2(ILE). / CG1[ C]:   3.79
/1/A/  63(GLU). / OE1[ O]:  /1/C/   2(ILE). / CG1[ C]:   3.40
/1/A/  70(HIS). / NE2[ N]:  /1/C/   2(ILE). / CD1[ C]:   3.81
/1/A/  67(VAL). / CA [ C]:  /1/C/   2(ILE). / CD1[ C]:   3.74
/1/A/  67(VAL). / CB [ C]:  /1/C/   2(ILE). / CD1[ C]:   3.76
/1/A/  63(GLU). / O  [ O]:  /1/C/   2(ILE). / CD1[ C]:   3.81
/1/A/  66(LYS). / CB [ C]:  /1/C/   2(ILE). / CD1[ C]:   3.48
/1/A/  66(LYS). / C  [ C]:  /1/C/   2(ILE). / CD1[ C]:   3.76
/1/A/  67(VAL). / N  [ N]:  /1/C/   2(ILE). / CD1[ C]:   3.53
/1/A/   7(TYR). / CG [ C]:  /1/C/   2(ILE). / CG2[ C]:   3.75
/1/A/   7(TYR). / CD1[ C]:  /1/C/   2(ILE). / CG2[ C]:   3.36
/1/A/   7(TYR). / CE1[ C]:  /1/C/   2(ILE). / CG2[ C]:   3.14
/1/A/   7(TYR). / CZ [ C]:  /1/C/   2(ILE). / CG2[ C]:   3.36
/1/A/   7(TYR). / OH [ O]:  /1/C/   2(ILE). / CG2[ C]:   3.93
/1/A/   7(TYR). / CE2[ C]:  /1/C/   2(ILE). / CG2[ C]:   3.72
/1/A/   7(TYR). / CD2[ C]:  /1/C/   2(ILE). / CG2[ C]:   3.88
/1/A/  63(GLU). / OE1[ O]:  /1/C/   2(ILE). / CG2[ C]:   3.90
/1/A/  99(TYR). / OH [ O]:  /1/C/   2(ILE). / C  [ C]:   3.84
/1/A/  66(LYS). / NZ [ N]:  /1/C/   2(ILE). / C  [ C]:   3.84
/1/A/ 159(TYR). / CE1[ C]:  /1/C/   2(ILE). / C  [ C]:   3.79
/1/A/ 159(TYR). / OH [ O]:  /1/C/   2(ILE). / C  [ C]:   3.98
/1/A/  66(LYS). / CD [ C]:  /1/C/   2(ILE). / O  [ O]:   3.81
/1/A/  66(LYS). / NZ [ N]:  /1/C/   2(ILE). / O  [ O]:   2.86
/1/A/ 159(TYR). / CE1[ C]:  /1/C/   2(ILE). / O  [ O]:   3.97
/1/A/  66(LYS). / CE [ C]:  /1/C/   2(ILE). / O  [ O]:   3.71
/1/A/  77(ASP). / CG [ C]:  /1/C/   9(VAL). / N  [ N]:   3.79
/1/A/  77(ASP). / OD1[ O]:  /1/C/   9(VAL). / N  [ N]:   2.96
/1/A/ 143(THR). / OG1[ O]:  /1/C/   9(VAL). / CA [ C]:   3.89
/1/A/ 143(THR). / CG2[ C]:  /1/C/   9(VAL). / CA [ C]:   3.80
/1/A/ 147(TRP). / CZ2[ C]:  /1/C/   9(VAL). / CA [ C]:   3.93
/1/A/ 143(THR). / OG1[ O]:  /1/C/   9(VAL). / CB [ C]:   3.64
/1/A/ 143(THR). / CG2[ C]:  /1/C/   9(VAL). / CB [ C]:   3.99
/1/A/ 147(TRP). / CZ2[ C]:  /1/C/   9(VAL). / CG1[ C]:   3.95
/1/A/ 116(TYR). / CE1[ C]:  /1/C/   9(VAL). / CG1[ C]:   3.89
/1/A/ 116(TYR). / CZ [ C]:  /1/C/   9(VAL). / CG1[ C]:   3.76
/1/A/  77(ASP). / OD2[ O]:  /1/C/   9(VAL). / CG1[ C]:   3.96
/1/A/  81(LEU). / CD1[ C]:  /1/C/   9(VAL). / CG2[ C]:   3.82
/1/A/  77(ASP). / CB [ C]:  /1/C/   9(VAL). / CG2[ C]:   3.93
/1/A/  77(ASP). / CG [ C]:  /1/C/   9(VAL). / CG2[ C]:   3.83
/1/A/  77(ASP). / OD1[ O]:  /1/C/   9(VAL). / CG2[ C]:   3.66
/1/A/  84(TYR). / OH [ O]:  /1/C/   9(VAL). / C  [ C]:   3.71
/1/A/ 143(THR). / OG1[ O]:  /1/C/   9(VAL). / C  [ C]:   3.66
/1/A/ 146(LYS). / CE [ C]:  /1/C/   9(VAL). / C  [ C]:   3.75
/1/A/ 146(LYS). / NZ [ N]:  /1/C/   9(VAL). / C  [ C]:   3.62
/1/A/ 146(LYS). / CE [ C]:  /1/C/   9(VAL). / O  [ O]:   3.55
/1/A/ 146(LYS). / NZ [ N]:  /1/C/   9(VAL). / O  [ O]:   2.93
/1/A/  80(THR). / CG2[ C]:  /1/C/   9(VAL). / O  [ O]:   3.65
/1/A/  84(TYR). / CZ [ C]:  /1/C/   9(VAL). / OXT[ O]:   3.65
/1/A/  84(TYR). / OH [ O]:  /1/C/   9(VAL). / OXT[ O]:   2.84
/1/A/  84(TYR). / CE2[ C]:  /1/C/   9(VAL). / OXT[ O]:   3.60
/1/A/ 143(THR). / CA [ C]:  /1/C/   9(VAL). / OXT[ O]:   3.78
/1/A/ 143(THR). / CB [ C]:  /1/C/   9(VAL). / OXT[ O]:   3.49
/1/A/ 143(THR). / OG1[ O]:  /1/C/   9(VAL). / OXT[ O]:   2.70
/1/A/ 146(LYS). / CE [ C]:  /1/C/   9(VAL). / OXT[ O]:   3.52
/1/A/ 143(THR). / CG2[ C]:  /1/C/   9(VAL). / OXT[ O]:   3.66
```

Appendix A3. Total contacts between MIDAHIPQV peptide and HLA-A*0201 molecule.

REFERENCES

Fifteen year follow up of trial of BCG vaccines in south India for tuberculosis prevention. 1999. *Indian J Med Res,* 137**,** 14 p following p571.

AAGAARD, C., GOVAERTS, M., MEIKLE, V., VALLECILLO, A. J., GUTIERREZ-PABELLO, J. A., SUAREZ-GUEMES, F., MCNAIR, J., CATALDI, A., ESPITIA, C., ANDERSEN, P. & POLLOCK, J. M. 2006. Optimizing antigen cocktails for detection of Mycobacterium bovis in herds with different prevalences of bovine tuberculosis: ESAT6-CFP10 mixture shows optimal sensitivity and specificity. *J Clin Microbiol,* 44**,** 4326-35.

AALTONEN, T., ABAZOV, V. M., ABBOTT, B., ABOLINS, M., ACHARYA, B. S., ADAMS, M., ADAMS, T., ADELMAN, J., AGUILO, E., ALEXEEV, G. D., ALKHAZOV, G., ALTON, A., ALVAREZ GONZALEZ, B., ALVERSON, G., ALVES, G. A., AMERIO, S., AMIDEI, D., ANASTASSOV, A., ANCU, L. S., ANNOVI, A., ANTOS, J., AOKI, M., APOLLINARI, G., APPEL, J., APRESYAN, A., ARISAWA, T., ARNOUD, Y., AROV, M., ARTIKOV, A., ASAADI, J., ASHMANSKAS, W., ASKEW, A., ASMAN, B., ATRAMENTOV, O., ATTAL, A., AURISANO, A., AVILA, C., AZFAR, F., BACKUSMAYES, J., BADAUD, F., BADGETT, W., BAGBY, L., BALDIN, B., BANDURIN, D. V., BANERJEE, S., BARBARO-GALTIERI, A., BARBERIS, E., BARFUSS, A. F., BARINGER, P., BARNES, V. E., BARNETT, B. A., BARRETO, J., BARRIA, P., BARTLETT, J. F., BARTOS, P., BASSLER, U., BAUER, D., BAUER, G., BEALE, S., BEAN, A., BEAUCHEMIN, P. H., BEDESCHI, F., BEECHER, D., BEGALLI, M., BEGEL, M., BEHARI, S., BELANGER-CHAMPAGNE, C., BELLANTONI, L., BELLETTINI, G., BELLINGER, J., BENITEZ, J. A., BENJAMIN, D., BERETVAS, A., BERI, S. B., BERNARDI, G., BERNHARD, R., BERTRAM, I., BESANCON, M., BEUSELINCK, R., BEZZUBOV, V. A., BHAT, P. C., BHATNAGAR, V., BHATTI, A., BINKLEY, M., BISELLO, D., BIZJAK, I., BLAIR, R. E., BLAZEY, G., BLESSING, S., BLOCKER, C., BLOOM, K., BLUMENFELD, B., BOCCI, A., BODEK, A., BOEHNLEIN, A., BOISVERT, V., BOLINE, D., BOLTON, T. A., BOOS, E. E., BORISSOV, G., et al. Combination of Tevatron searches for the standard model Higgs boson in the W+W- decay mode. *Phys Rev Lett,* 104**,** 061802.

ADAMS, S., ROBBINS, F. M., CHEN, D., WAGAGE, D., HOLBECK, S. L., MORSE, H. C., 3RD, STRONCEK, D. & MARINCOLA, F. M. 2005. HLA class I and II genotype of the NCI-60 cell lines. *J Transl Med,* 3**,** 11.

ALBERT, M. L., SAUTER, B. & BHARDWAJ, N. 1998. Dendritic cells acquire antigen from apoptotic cells and induce class I-restricted CTLs. *Nature,* 392**,** 86-9.

ALEKSIC, M., LIDDY, N., MOLLOY, P. E., PUMPHREY, N., VUIDEPOT, A., CHANG, K. M. & JAKOBSEN, B. K. 2012. Different affinity windows for virus and cancer-specific T-cell receptors: implications for therapeutic strategies. *Eur J Immunol,* 42**,** 3174-9.

ALMEIDA, J. R., PRICE, D. A., PAPAGNO, L., ARKOUB, Z. A., SAUCE, D., BORNSTEIN, E., ASHER, T. E., SAMRI, A., SCHNURIGER, A.,

THEODOROU, I., COSTAGLIOLA, D., ROUZIOUX, C., AGUT, H., MARCELIN, A. G., DOUEK, D., AUTRAN, B. & APPAY, V. 2007. Superior control of HIV-1 replication by CD8+ T cells is reflected by their avidity, polyfunctionality, and clonal turnover. *J Exp Med,* 204**,** 2473-85.

ALTMAN, J. D., MOSS, P. A., GOULDER, P. J., BAROUCH, D. H., MCHEYZER-WILLIAMS, M. G., BELL, J. I., MCMICHAEL, A. J. & DAVIS, M. M. 1996. Phenotypic analysis of antigen-specific T lymphocytes. *Science,* 274**,** 94-6.

ANDERSEN, P. & DOHERTY, T. M. 2005. The success and failure of BCG - implications for a novel tuberculosis vaccine. *Nat Rev Microbiol,* 3**,** 656-62.

ANNELS, N. E., CALLAN, M. F., TAN, L. & RICKINSON, A. B. 2000. Changing patterns of dominant TCR usage with maturation of an EBV-specific cytotoxic T cell response. *J Immunol,* 165**,** 4831-41.

ARBELAEZ, M. P., NELSON, K. E. & MUNOZ, A. 2000. BCG vaccine effectiveness in preventing tuberculosis and its interaction with human immunodeficiency virus infection. *Int J Epidemiol,* 29**,** 1085-91.

ARSTILA, T. P., CASROUGE, A., BARON, V., EVEN, J., KANELLOPOULOS, J. & KOURILSKY, P. 1999. A direct estimate of the human alphabeta T cell receptor diversity. *Science,* 286**,** 958-61.

BAFICA, A., SCANGA, C. A., FENG, C. G., LEIFER, C., CHEEVER, A. & SHER, A. 2005. TLR9 regulates Th1 responses and cooperates with TLR2 in mediating optimal resistance to Mycobacterium tuberculosis. *J Exp Med,* 202**,** 1715-24.

BAKKE, O. & DOBBERSTEIN, B. 1990. MHC class II-associated invariant chain contains a sorting signal for endosomal compartments. *Cell,* 63**,** 707-16.

BANAIEE, N., KINCAID, E. Z., BUCHWALD, U., JACOBS, W. R., JR. & ERNST, J. D. 2006. Potent inhibition of macrophage responses to IFN-gamma by live virulent Mycobacterium tuberculosis is independent of mature mycobacterial lipoproteins but dependent on TLR2. *J Immunol,* 176**,** 3019-27.

BARRIONUEVO, P., DELPINO, M. V., POZNER, R. G., VELASQUEZ, L. N., CASSATARO, J. & GIAMBARTOLOMEI, G. H. 2012. Brucella abortus induces intracellular retention of MHC-I molecules in human macrophages down-modulating cytotoxic CD8(+) T cell responses. *Cell Microbiol*.

BENDALL, S. C., SIMONDS, E. F., QIU, P., AMIR EL, A. D., KRUTZIK, P. O., FINCK, R., BRUGGNER, R. V., MELAMED, R., TREJO, A., ORNATSKY, O. I., BALDERAS, R. S., PLEVRITIS, S. K., SACHS, K., PE'ER, D., TANNER, S. D. & NOLAN, G. P. 2011. Single-cell mass cytometry of differential immune and drug responses across a human hematopoietic continuum. *Science,* 332**,** 687-96.

BENDELAC, A., LANTZ, O., QUIMBY, M. E., YEWDELL, J. W., BENNINK, J. R. & BRUTKIEWICZ, R. R. 1995. CD1 recognition by mouse NK1+ T lymphocytes. *Science,* 268**,** 863-5.

BENDELAC, A., SAVAGE, P. B. & TEYTON, L. 2007. The biology of NKT cells. *Annu Rev Immunol,* 25**,** 297-336.

BENICHOU, G., VALUJSKIKH, A. & HEEGER, P. S. 1999. Contributions of direct and indirect T cell alloreactivity during allograft rejection in mice. *J Immunol,* 162**,** 352-8.

BERZOFSKY, J. A. & TERABE, M. 2008. NKT cells in tumor immunity: opposing subsets define a new immunoregulatory axis. *J Immunol,* 180**,** 3627-35.

BETTS, M. R., BRENCHLEY, J. M., PRICE, D. A., DE ROSA, S. C., DOUEK, D. C., ROEDERER, M. & KOUP, R. A. 2003. Sensitive and viable identification of antigen-specific CD8+ T cells by a flow cytometric assay for degranulation. *J Immunol Methods,* 281**,** 65-78.

BEVERIDGE, N. E., PRICE, D. A., CASAZZA, J. P., PATHAN, A. A., SANDER, C. R., ASHER, T. E., AMBROZAK, D. R., PRECOPIO, M. L., SCHEINBERG, P., ALDER, N. C., ROEDERER, M., KOUP, R. A., DOUEK, D. C., HILL, A. V. & MCSHANE, H. 2007. Immunisation with BCG and recombinant MVA85A induces long-lasting, polyfunctional Mycobacterium tuberculosis-specific CD4+ memory T lymphocyte populations. *Eur J Immunol,* 37**,** 3089-100.

BJORKMAN, P. J., SAPER, M. A., SAMRAOUI, B., BENNETT, W. S., STROMINGER, J. L. & WILEY, D. C. 1987. Structure of the human class I histocompatibility antigen, HLA-A2. *Nature,* 329**,** 506-12.

BLOM, B. & SPITS, H. 2006. Development of human lymphoid cells. *Annu Rev Immunol,* 24**,** 287-320.

BLOMGRAN, R., DESVIGNES, L., BRIKEN, V. & ERNST, J. D. 2012. Mycobacterium tuberculosis inhibits neutrophil apoptosis, leading to delayed activation of naive CD4 T cells. *Cell Host Microbe,* 11**,** 81-90.

BLOMGRAN, R. & ERNST, J. D. 2011. Lung neutrophils facilitate activation of naive antigen-specific CD4+ T cells during Mycobacterium tuberculosis infection. *J Immunol,* 186**,** 7110-9.

BOBOSHA, K., WILSON, L., VAN MEIJGAARDEN, K. E., BEKELE, Y., ZEWDIE, M., VAN DER PLOEG-VAN SCHIP, J. J., ABEBE, M., HUSSEIN, J., KHADGE, S., NEUPANE, K. D., HAGGE, D. A., JORDANOVA, E. S., ASEFFA, A., OTTENHOFF, T. H. & GELUK, A. 2014. T-cell regulation in lepromatous leprosy. *PLoS Negl Trop Dis,* 8**,** e2773.

BOHSALI, A., ABDALLA, H., VELMURUGAN, K. & BRIKEN, V. The non-pathogenic mycobacteria M. smegmatis and M. fortuitum induce rapid host cell apoptosis via a caspase-3 and TNF dependent pathway. *BMC Microbiol,* 10**,** 237.

BOHSALI, A., ABDALLA, H., VELMURUGAN, K. & BRIKEN, V. 2010. The non-pathogenic mycobacteria M. smegmatis and M. fortuitum induce rapid host cell

apoptosis via a caspase-3 and TNF dependent pathway. *BMC Microbiol,* 10**,** 237.

BORG, N. A., WUN, K. S., KJER-NIELSEN, L., WILCE, M. C., PELLICCI, D. G., KOH, R., BESRA, G. S., BHARADWAJ, M., GODFREY, D. I., MCCLUSKEY, J. & ROSSJOHN, J. 2007. CD1d-lipid-antigen recognition by the semi-invariant NKT T-cell receptor. *Nature,* 448**,** 44-9.

BOULTER, J. M., GLICK, M., TODOROV, P. T., BASTON, E., SAMI, M., RIZKALLAH, P. & JAKOBSEN, B. K. 2003. Stable, soluble T-cell receptor molecules for crystallization and therapeutics. *Protein Eng,* 16**,** 707-11.

BRANDT, L., FEINO CUNHA, J., WEINREICH OLSEN, A., CHILIMA, B., HIRSCH, P., APPELBERG, R. & ANDERSEN, P. 2002. Failure of the Mycobacterium bovis BCG vaccine: some species of environmental mycobacteria block multiplication of BCG and induction of protective immunity to tuberculosis. *Infect Immun,* 70**,** 672-8.

BRENNER, M. B., MCLEAN, J., SCHEFT, H., RIBERDY, J., ANG, S. L., SEIDMAN, J. G., DEVLIN, P. & KRANGEL, M. S. 1987. Two forms of the T-cell receptor gamma protein found on peripheral blood cytotoxic T lymphocytes. *Nature,* 325**,** 689-94.

BRITTON, W. J. & LOCKWOOD, D. N. 2004. Leprosy. *Lancet,* 363**,** 1209-19.

BROTTVEIT, M., RAKI, M., BERGSENG, E., FALLANG, L. E., SIMONSEN, B., LOVIK, A., LARSEN, S., LOBERG, E. M., JAHNSEN, F. L., SOLLID, L. M. & LUNDIN, K. E. 2011. Assessing possible celiac disease by an HLA-DQ2-gliadin Tetramer Test. *Am J Gastroenterol,* 106**,** 1318-24.

BROWN-ELLIOTT, B. A. & WALLACE, R. J., JR. 2002. Clinical and taxonomic status of pathogenic nonpigmented or late-pigmenting rapidly growing mycobacteria. *Clin Microbiol Rev,* 15**,** 716-46.

BROWN, J. H., JARDETZKY, T. S., GORGA, J. C., STERN, L. J., URBAN, R. G., STROMINGER, J. L. & WILEY, D. C. 1993. Three-dimensional structure of the human class II histocompatibility antigen HLA-DR1. *Nature,* 364**,** 33-9.

BULEK, A. M., MADURA, F., FULLER, A., HOLLAND, C. J., SCHAUENBURG, A. J., SEWELL, A. K., RIZKALLAH, P. J. & COLE, D. K. 2012. TCR/pMHC Optimized Protein crystallization Screen. *J Immunol Methods,* 382**,** 203-10.

CACCAMO, N., GUGGINO, G., JOOSTEN, S. A., GELSOMINO, G., DI CARLO, P., TITONE, L., GALATI, D., BOCCHINO, M., MATARESE, A., SALERNO, A., SANDUZZI, A., FRANKEN, W. P., OTTENHOFF, T. H. & DIELI, F. 2010. Multifunctional CD4(+) T cells correlate with active Mycobacterium tuberculosis infection. *Eur J Immunol,* 40**,** 2211-20.

CALMETTE, A. 1931. Preventive Vaccination Against Tuberculosis with BCG. *Proc R Soc Med,* 24**,** 1481-90.

CHAN, J., XING, Y., MAGLIOZZO, R. S. & BLOOM, B. R. 1992. Killing of virulent Mycobacterium tuberculosis by reactive nitrogen intermediates produced by activated murine macrophages. *J Exp Med,* 175**,** 1111-22.

CHOUAIB, S., BENSUSSAN, A., TERMIJTELEN, A. M., ANDREEFF, M., MARCHIOL-FOURNIGAULT, C., FRADELIZI, D. & DUPONT, B. 1988. Allogeneic T cell activation triggering by MHC class I antigens. *J Immunol,* 141**,** 423-9.

CHUA, W. J., TRUSCOTT, S. M., EICKHOFF, C. S., BLAZEVIC, A., HOFT, D. F. & HANSEN, T. H. 2012. Polyclonal mucosa-associated invariant T cells have unique innate functions in bacterial infection. *Infect Immun,* 80**,** 3256-67.

COHN, Z. A. 1963. The fate of bacteria within phagocytic cells. I. The degradation of isotopically labeled bacteria by polymorphonuclear leucocytes and macrophages. *J Exp Med,* 117**,** 27-42.

COLDITZ, G. A., BERKEY, C. S., MOSTELLER, F., BREWER, T. F., WILSON, M. E., BURDICK, E. & FINEBERG, H. V. 1995. The efficacy of bacillus Calmette-Guerin vaccination of newborns and infants in the prevention of tuberculosis: meta-analyses of the published literature. *Pediatrics,* 96**,** 29-35.

COLDITZ, G. A., BREWER, T. F., BERKEY, C. S., WILSON, M. E., BURDICK, E., FINEBERG, H. V. & MOSTELLER, F. 1994. Efficacy of BCG vaccine in the prevention of tuberculosis. Meta-analysis of the published literature. *JAMA,* 271**,** 698-702.

COLE, D. K., EDWARDS, E. S., WYNN, K. K., CLEMENT, M., MILES, J. J., LADELL, K., EKERUCHE, J., GOSTICK, E., ADAMS, K. J., SKOWERA, A., PEAKMAN, M., WOOLDRIDGE, L., PRICE, D. A. & SEWELL, A. K. 2010. Modification of MHC anchor residues generates heteroclitic peptides that alter TCR binding and T cell recognition. *J Immunol,* 185**,** 2600-10.

COLE, D. K., LAUGEL, B., CLEMENT, M., PRICE, D. A., WOOLDRIDGE, L. & SEWELL, A. K. 2012. The molecular determinants of CD8 co-receptor function. *Immunology,* 137**,** 139-48.

COLE, D. K., PUMPHREY, N. J., BOULTER, J. M., SAMI, M., BELL, J. I., GOSTICK, E., PRICE, D. A., GAO, G. F., SEWELL, A. K. & JAKOBSEN, B. K. 2007. Human TCR-binding affinity is governed by MHC class restriction. *J Immunol,* 178**,** 5727-34.

CONNELLY, M. A., MOULTON, R. A., SMITH, A. K., LINDSEY, D. R., SINHA, M., WETSEL, R. A. & JAGANNATH, C. 2007. Mycobacteria-primed macrophages and dendritic cells induce an up-regulation of complement C5a anaphylatoxin receptor (CD88) in CD3+ murine T cells. *J Leukoc Biol,* 81**,** 212-20.

COOPER, A. M., MAYER-BARBER, K. D. & SHER, A. 2011. Role of innate cytokines in mycobacterial infection. *Mucosal Immunol,* 4**,** 252-60.

CORINTI, S., MEDAGLINI, D., PREZZI, C., CAVANI, A., POZZI, G. & GIROLOMONI, G. 2000. Human dendritic cells are superior to B cells at presenting a major histocompatibility complex class II-restricted heterologous antigen expressed on recombinant Streptococcus gordonii. *Infect Immun,* 68**,** 1879-83.

COSMA, C. L., SHERMAN, D. R. & RAMAKRISHNAN, L. 2003. The secret lives of the pathogenic mycobacteria. *Annu Rev Microbiol,* 57**,** 641-76.

CRESSWELL, P. 2000. Intracellular surveillance: controlling the assembly of MHC class I-peptide complexes. *Traffic,* 1**,** 301-5.

DAVENPORT, M. P., PRICE, D. A. & MCMICHAEL, A. J. 2007. The T cell repertoire in infection and vaccination: implications for control of persistent viruses. *Curr Opin Immunol,* 19**,** 294-300.

DAVEY, M. S., LIN, C. Y., ROBERTS, G. W., HEUSTON, S., BROWN, A. C., CHESS, J. A., TOLEMAN, M. A., GAHAN, C. G., HILL, C., PARISH, T., WILLIAMS, J. D., DAVIES, S. J., JOHNSON, D. W., TOPLEY, N., MOSER, B. & EBERL, M. 2011. Human neutrophil clearance of bacterial pathogens triggers anti-microbial gammadelta T cell responses in early infection. *PLoS Pathog,* 7**,** e1002040.

DAVID, V., HOCHSTENBACH, F., RAJAGOPALAN, S. & BRENNER, M. B. 1993. Interaction with newly synthesized and retained proteins in the endoplasmic reticulum suggests a chaperone function for human integral membrane protein IP90 (calnexin). *J Biol Chem,* 268**,** 9585-92.

DAVIS, J. M. & RAMAKRISHNAN, L. 2009. The role of the granuloma in expansion and dissemination of early tuberculous infection. *Cell,* 136**,** 37-49.

DE ASTORZA, B., CORTES, G., CRESPI, C., SAUS, C., ROJO, J. M. & ALBERTI, S. 2004. C3 promotes clearance of Klebsiella pneumoniae by A549 epithelial cells. *Infect Immun,* 72**,** 1767-74.

DE LALLA, C., LEPORE, M., PICCOLO, F. M., RINALDI, A., SCELFO, A., GARAVAGLIA, C., MORI, L., DE LIBERO, G., DELLABONA, P. & CASORATI, G. 2011. High-frequency and adaptive-like dynamics of human CD1 self-reactive T cells. *Eur J Immunol,* 41**,** 602-10.

DEGEN, E. & WILLIAMS, D. B. 1991. Participation of a novel 88-kD protein in the biogenesis of murine class I histocompatibility molecules. *J Cell Biol,* 112**,** 1099-115.

DIELI, F., SIRECI, G., DI SANO, C., CHAMPAGNE, E., FOURNIE, J. J. & SALERNO, J. I. 1999. Predominance of Vgamma9/Vdelta2 T lymphocytes in the cerebrospinal fluid of children with tuberculous meningitis: reversal after chemotherapy. *Mol Med,* 5**,** 301-12.

DIETRICH, J., AAGAARD, C., LEAH, R., OLSEN, A. W., STRYHN, A., DOHERTY, T. M. & ANDERSEN, P. 2005. Exchanging ESAT6 with TB10.4 in an Ag85B fusion molecule-based tuberculosis subunit vaccine: efficient

protection and ESAT6-based sensitive monitoring of vaccine efficacy. *J Immunol,* 174**,** 6332-9.

DIEUDE, M., STRIEGL, H., TYZNIK, A. J., WANG, J., BEHAR, S. M., PICCIRILLO, C. A., LEVINE, J. S., ZAJONC, D. M. & RAUCH, J. 2011. Cardiolipin binds to CD1d and stimulates CD1d-restricted gammadelta T cells in the normal murine repertoire. *J Immunol,* 186**,** 4771-81.

DUSSEAUX, M., MARTIN, E., SERRIARI, N., PEGUILLET, I., PREMEL, V., LOUIS, D., MILDER, M., LE BOURHIS, L., SOUDAIS, C., TREINER, E. & LANTZ, O. 2011. Human MAIT cells are xenobiotic-resistant, tissue-targeted, CD161hi IL-17-secreting T cells. *Blood,* 117**,** 1250-9.

EBERL, M., HINTZ, M., REICHENBERG, A., KOLLAS, A. K., WIESNER, J. & JOMAA, H. 2003. Microbial isoprenoid biosynthesis and human gammadelta T cell activation. *FEBS Lett,* 544**,** 4-10.

EGEN, J. G., ROTHFUCHS, A. G., FENG, C. G., HORWITZ, M. A., SHER, A. & GERMAIN, R. N. 2011. Intravital imaging reveals limited antigen presentation and T cell effector function in mycobacterial granulomas. *Immunity,* 34**,** 807-19.

EKERUCHE-MAKINDE, J., CLEMENT, M., COLE, D. K., EDWARDS, E. S., LADELL, K., MILES, J. J., MATTHEWS, K. K., FULLER, A., LLOYD, K. A., MADURA, F., DOLTON, G. M., PENTIER, J., LISSINA, A., GOSTICK, E., BAXTER, T. K., BAKER, B. M., RIZKALLAH, P. J., PRICE, D. A., WOOLDRIDGE, L. & SEWELL, A. K. 2012. T-cell receptor-optimized peptide skewing of the T-cell repertoire can enhance antigen targeting. *J Biol Chem,* 287**,** 37269-81.

EKERUCHE-MAKINDE, J., MILES, J. J., VAN DEN BERG, H. A., SKOWERA, A., COLE, D. K., DOLTON, G., SCHAUENBURG, A. J., TAN, M. P., PENTIER, J. M., LLEWELLYN-LACEY, S., MILES, K. M., BULEK, A. M., CLEMENT, M., WILLIAMS, T., TRIMBY, A., BAILEY, M., RIZKALLAH, P., ROSSJOHN, J., PEAKMAN, M., PRICE, D. A., BURROWS, S. R., SEWELL, A. K. & WOOLDRIDGE, L. 2013. Peptide length determines the outcome of TCR/peptide-MHCI engagement. *Blood,* 121**,** 1112-23.

EMSLEY, P. & COWTAN, K. 2004. Coot: model-building tools for molecular graphics. *Acta Crystallogr D Biol Crystallogr,* 60**,** 2126-32.

FALK, K., ROTZSCHKE, O., STEVANOVIC, S., JUNG, G. & RAMMENSEE, H. G. 1991. Allele-specific motifs revealed by sequencing of self-peptides eluted from MHC molecules. *Nature,* 351**,** 290-6.

FEHLING, H. J., KROTKOVA, A., SAINT-RUF, C. & VON BOEHMER, H. 1995. Crucial role of the pre-T-cell receptor alpha gene in development of alpha beta but not gamma delta T cells. *Nature,* 375**,** 795-8.

FELIX, N. J. & ALLEN, P. M. 2007. Specificity of T-cell alloreactivity. *Nat Rev Immunol,* 7**,** 942-53.

GAO, L. Y., GUO, S., MCLAUGHLIN, B., MORISAKI, H., ENGEL, J. N. & BROWN, E. J. 2004. A mycobacterial virulence gene cluster extending RD1 is required for cytolysis, bacterial spreading and ESAT-6 secretion. *Mol Microbiol,* 53**,** 1677-93.

GAPIN, L. 2009. Where do MAIT cells fit in the family of unconventional T cells? *PLoS Biol,* 7**,** e70.

GAPIN, L. 2014. Check MAIT. *J Immunol,* 192**,** 4475-80.

GARBOCZI, D. N., GHOSH, P., UTZ, U., FAN, Q. R., BIDDISON, W. E. & WILEY, D. C. 1996. Structure of the complex between human T-cell receptor, viral peptide and HLA-A2. *Nature,* 384**,** 134-41.

GODFREY, D. I., HAMMOND, K. J., POULTON, L. D., SMYTH, M. J. & BAXTER, A. G. 2000. NKT cells: facts, functions and fallacies. *Immunol Today,* 21**,** 573-83.

GODFREY, D. I., PELLICCI, D. G., PATEL, O., KJER-NIELSEN, L., MCCLUSKEY, J. & ROSSJOHN, J. 2010a. Antigen recognition by CD1d-restricted NKT T cell receptors. *Semin Immunol,* 22**,** 61-7.

GODFREY, D. I., STANKOVIC, S. & BAXTER, A. G. 2010b. Raising the NKT cell family. *Nat Immunol,* 11**,** 197-206.

GOLD, M. C., CERRI, S., SMYK-PEARSON, S., CANSLER, M. E., VOGT, T. M., DELEPINE, J., WINATA, E., SWARBRICK, G. M., CHUA, W. J., YU, Y. Y., LANTZ, O., COOK, M. S., NULL, M. D., JACOBY, D. B., HARRIFF, M. J., LEWINSOHN, D. A., HANSEN, T. H. & LEWINSOHN, D. M. 2010. Human mucosal associated invariant T cells detect bacterially infected cells. *PLoS Biol,* 8**,** e1000407.

GOLD, M. C., EHLINGER, H. D., COOK, M. S., SMYK-PEARSON, S. K., WILLE, P. T., UNGERLEIDER, R. M., LEWINSOHN, D. A. & LEWINSOHN, D. M. 2008. Human innate Mycobacterium tuberculosis-reactive alphabetaTCR+ thymocytes. *PLoS Pathog,* 4**,** e39.

GOLD, M. C., EID, T., SMYK-PEARSON, S., EBERLING, Y., SWARBRICK, G. M., LANGLEY, S. M., STREETER, P. R., LEWINSOHN, D. A. & LEWINSOHN, D. M. 2013. Human thymic MR1-restricted MAIT cells are innate pathogen-reactive effectors that adapt following thymic egress. *Mucosal Immunol,* 6**,** 35-44.

GOLD, M. C. & LEWINSOHN, D. M. 2013. Co-dependents: MR1-restricted MAIT cells and their antimicrobial function. *Nat Rev Microbiol,* 11**,** 14-9.

GOLD, M. C., MCLAREN, J. E., REISTETTER, J. A., SMYK-PEARSON, S., LADELL, K., SWARBRICK, G. M., YU, Y. Y., HANSEN, T. H., LUND, O., NIELSEN, M., GERRITSEN, B., KESMIR, C., MILES, J. J., LEWINSOHN, D. A., PRICE, D. A. & LEWINSOHN, D. M. 2014. MR1-restricted MAIT cells display ligand discrimination and pathogen selectivity through distinct T cell receptor usage. *J Exp Med,* 211**,** 1601-10.

GOLDEN, M. P. & VIKRAM, H. R. 2005. Extrapulmonary tuberculosis: an overview. *Am Fam Physician,* 72**,** 1761-8.

GOODRIDGE, J. P., LEE, N., BURIAN, A., PYO, C. W., TYKODI, S. S., WARREN, E. H., YEE, C., RIDDELL, S. R. & GERAGHTY, D. E. 2013. HLA-F and MHC-I open conformers cooperate in a MHC-I antigen cross-presentation pathway. *J Immunol,* 191**,** 1567-77.

GRANGE, J. M. & YATES, M. D. 1986. Infections caused by opportunist mycobacteria: a review. *J R Soc Med,* 79**,** 226-9.

GRAS, S., WILMANN, P. G., CHEN, Z., HALIM, H., LIU, Y. C., KJER-NIELSEN, L., PURCELL, A. W., BURROWS, S. R., MCCLUSKEY, J. & ROSSJOHN, J. A structural basis for varied alphabeta TCR usage against an immunodominant EBV antigen restricted to a HLA-B8 molecule. *J Immunol,* 188**,** 311-21.

GRATAMA, J. W. & CORNELISSEN, J. J. 2003. Diagnostic potential of tetramer-based monitoring of cytomegalovirus-specific CD8+ T lymphocytes in allogeneic stem cell transplantation. *Clin Immunol,* 106**,** 29-35.

GREEN, A. M., DIFAZIO, R. & FLYNN, J. L. 2013. IFN-gamma from CD4 T cells is essential for host survival and enhances CD8 T cell function during Mycobacterium tuberculosis infection. *J Immunol,* 190**,** 270-7.

GROH, V., PORCELLI, S., FABBI, M., LANIER, L. L., PICKER, L. J., ANDERSON, T., WARNKE, R. A., BHAN, A. K., STROMINGER, J. L. & BRENNER, M. B. 1989. Human lymphocytes bearing T cell receptor gamma/delta are phenotypically diverse and evenly distributed throughout the lymphoid system. *J Exp Med,* 169**,** 1277-94.

HALTER, M., TONA, A., BHADRIRAJU, K., PLANT, A. L. & ELLIOTT, J. T. 2007. Automated live cell imaging of green fluorescent protein degradation in individual fibroblasts. *Cytometry A,* 71**,** 827-34.

HANSEN, T. H., HUANG, S., ARNOLD, P. L. & FREMONT, D. H. 2007. Patterns of nonclassical MHC antigen presentation. *Nat Immunol,* 8**,** 563-8.

HARARI, A., PETITPIERRE, S., VALLELIAN, F. & PANTALEO, G. 2004. Skewed representation of functionally distinct populations of virus-specific CD4 T cells in HIV-1-infected subjects with progressive disease: changes after antiretroviral therapy. *Blood,* 103**,** 966-72.

HARLY, C., GUILLAUME, Y., NEDELLEC, S., PEIGNE, C. M., MONKKONEN, H., MONKKONEN, J., LI, J., KUBALL, J., ADAMS, E. J., NETZER, S., DECHANET-MERVILLE, J., LEGER, A., HERRMANN, T., BREATHNACH, R., OLIVE, D., BONNEVILLE, M. & SCOTET, E. 2012. Key implication of CD277/butyrophilin-3 (BTN3A) in cellular stress sensing by a major human gammadelta T-cell subset. *Blood,* 120**,** 2269-79.

HARRIFF, M. J., BURGDORF, S., KURTS, C., WIERTZ, E. J., LEWINSOHN, D. A. & LEWINSOHN, D. M. TAP mediates import of Mycobacterium tuberculosis-

derived peptides into phagosomes and facilitates loading onto HLA-I. *PLoS One,* 8**,** e79571.

HART, P. D., ARMSTRONG, J. A., BROWN, C. A. & DRAPER, P. 1972. Ultrastructural study of the behavior of macrophages toward parasitic mycobacteria. *Infect Immun,* 5**,** 803-7.

HASHIMOTO, K., HIRAI, M. & KUROSAWA, Y. 1995. A gene outside the human MHC related to classical HLA class I genes. *Science,* 269**,** 693-5.

HAYDAY, A. & VANTOUROUT, P. 2013. A long-playing CD about the gammadelta TCR repertoire. *Immunity,* 39**,** 994-6.

HERVAS-STUBBS, S., MAJLESSI, L., SIMSOVA, M., MOROVA, J., ROJAS, M. J., NOUZE, C., BRODIN, P., SEBO, P. & LECLERC, C. 2006. High frequency of CD4+ T cells specific for the TB10.4 protein correlates with protection against Mycobacterium tuberculosis infection. *Infect Immun,* 74**,** 3396-407.

HIROMATSU, K., YOSHIKAI, Y., MATSUZAKI, G., OHGA, S., MURAMORI, K., MATSUMOTO, K., BLUESTONE, J. A. & NOMOTO, K. 1992. A protective role of gamma/delta T cells in primary infection with Listeria monocytogenes in mice. *J Exp Med,* 175**,** 49-56.

HOANG, T., AAGAARD, C., DIETRICH, J., CASSIDY, J. P., DOLGANOV, G., SCHOOLNIK, G. K., LUNDBERG, C. V., AGGER, E. M. & ANDERSEN, P. 2013. ESAT-6 (EsxA) and TB10.4 (EsxH) based vaccines for pre- and post-exposure tuberculosis vaccination. *PLoS One,* 8**,** e80579.

HOLLER, P. D. & KRANZ, D. M. 2003. Quantitative analysis of the contribution of TCR/pepMHC affinity and CD8 to T cell activation. *Immunity,* 18**,** 255-64.

HOPE, J. C., THOM, M. L., MCAULAY, M., MEAD, E., VORDERMEIER, H. M., CLIFFORD, D., HEWINSON, R. G. & VILLARREAL-RAMOS, B. 2011. Identification of surrogates and correlates of protection in protective immunity against Mycobacterium bovis infection induced in neonatal calves by vaccination with M. bovis BCG Pasteur and M. bovis BCG Danish. *Clin Vaccine Immunol,* 18**,** 373-9.

HUANG, S., GILFILLAN, S., CELLA, M., MILEY, M. J., LANTZ, O., LYBARGER, L., FREMONT, D. H. & HANSEN, T. H. 2005. Evidence for MR1 antigen presentation to mucosal-associated invariant T cells. *J Biol Chem,* 280**,** 21183-93.

HUANG, S., GILFILLAN, S., KIM, S., THOMPSON, B., WANG, X., SANT, A. J., FREMONT, D. H., LANTZ, O. & HANSEN, T. H. 2008. MR1 uses an endocytic pathway to activate mucosal-associated invariant T cells. *J Exp Med,* 205**,** 1201-11.

IBANA, J. A., SCHUST, D. J., SUGIMOTO, J., NAGAMATSU, T., GREENE, S. J. & QUAYLE, A. J. 2011. Chlamydia trachomatis immune evasion via downregulation of MHC class I surface expression involves direct and indirect mechanisms. *Infect Dis Obstet Gynecol,* 2011**,** 420905.

ILGHARI, D., LIGHTBODY, K. L., VEVERKA, V., WATERS, L. C., MUSKETT, F. W., RENSHAW, P. S. & CARR, M. D. 2011. Solution structure of the Mycobacterium tuberculosis EsxG.EsxH complex: functional implications and comparisons with other M. tuberculosis Esx family complexes. *J Biol Chem,* 286**,** 29993-30002.

JAHNG, A., MARICIC, I., AGUILERA, C., CARDELL, S., HALDER, R. C. & KUMAR, V. 2004. Prevention of autoimmunity by targeting a distinct, noninvariant CD1d-reactive T cell population reactive to sulfatide. *J Exp Med,* 199**,** 947-57.

JANEWAY, C. A., JR. & MEDZHITOV, R. 2002. Innate immune recognition. *Annu Rev Immunol,* 20**,** 197-216.

JONDAL, M., SCHIRMBECK, R. & REIMANN, J. 1996. MHC class I-restricted CTL responses to exogenous antigens. *Immunity,* 5**,** 295-302.

KABELITZ, D., BENDER, A., SCHONDELMAIER, S., SCHOEL, B. & KAUFMANN, S. H. 1990. A large fraction of human peripheral blood gamma/delta + T cells is activated by Mycobacterium tuberculosis but not by its 65-kD heat shock protein. *J Exp Med,* 171**,** 667-79.

KALYAN, S. & KABELITZ, D. 2013. Defining the nature of human gammadelta T cells: a biographical sketch of the highly empathetic. *Cell Mol Immunol,* 10**,** 21-9.

KANG, D. D., LIN, Y., MORENO, J. R., RANDALL, T. D. & KHADER, S. A. Profiling early lung immune responses in the mouse model of tuberculosis. *PLoS One,* 6**,** e16161.

KARA, E. E., COMERFORD, I., FENIX, K. A., BASTOW, C. R., GREGOR, C. E., MCKENZIE, D. R. & MCCOLL, S. R. 2014. Tailored immune responses: novel effector helper T cell subsets in protective immunity. *PLoS Pathog,* 10**,** e1003905.

KASMAR, A. G., VAN RHIJN, I., CHENG, T. Y., TURNER, M., SESHADRI, C., SCHIEFNER, A., KALATHUR, R. C., ANNAND, J. W., DE JONG, A., SHIRES, J., LEON, L., BRENNER, M., WILSON, I. A., ALTMAN, J. D. & MOODY, D. B. 2011. CD1b tetramers bind alphabeta T cell receptors to identify a mycobacterial glycolipid-reactive T cell repertoire in humans. *J Exp Med,* 208**,** 1741-7.

KIM, S. Y., SOHN, H., CHOI, G. E., CHO, S. N., OH, T., KIM, H. J., WHANG, J., KIM, J. S., BYUN, E. H., KIM, W. S., MIN, K. N., KIM, J. M. & SHIN, S. J. 2011. Conversion of Mycobacterium smegmatis to a pathogenic phenotype via passage of epithelial cells during macrophage infection. *Med Microbiol Immunol,* 200**,** 177-91.

KINJO, T., NAKAMATSU, M., NAKASONE, C., YAMAMOTO, N., KINJO, Y., MIYAGI, K., UEZU, K., NAKAMURA, K., HIGA, F., TATEYAMA, M., TAKEDA, K., NAKAYAMA, T., TANIGUCHI, M., KAKU, M., FUJITA, J. & KAWAKAMI, K. 2006. NKT cells play a limited role in the neutrophilic

inflammatory responses and host defense to pulmonary infection with Pseudomonas aeruginosa. *Microbes Infect,* 8**,** 2679-85.

KIRCHHEIMER, W. F. & STORRS, E. E. 1971. Attempts to establish the armadillo (Dasypus novemcinctus Linn.) as a model for the study of leprosy. I. Report of lepromatoid leprosy in an experimentally infected armadillo. *Int J Lepr Other Mycobact Dis,* 39**,** 693-702.

KJER-NIELSEN, L., PATEL, O., CORBETT, A. J., LE NOURS, J., MEEHAN, B., LIU, L., BHATI, M., CHEN, Z., KOSTENKO, L., REANTRAGOON, R., WILLIAMSON, N. A., PURCELL, A. W., DUDEK, N. L., MCCONVILLE, M. J., O'HAIR, R. A., KHAIRALLAH, G. N., GODFREY, D. I., FAIRLIE, D. P., ROSSJOHN, J. & MCCLUSKEY, J. 2012. MR1 presents microbial vitamin B metabolites to MAIT cells. *Nature,* 491**,** 717-23.

KONIG, R., SHEN, X. & GERMAIN, R. N. 1995. Involvement of both major histocompatibility complex class II alpha and beta chains in CD4 function indicates a role for ordered oligomerization in T cell activation. *J Exp Med,* 182**,** 779-87.

KONIG, R., SHEN, X., MAROTO, R. & DENNING, T. L. 2002. The role of CD4 in regulating homeostasis of T helper cells. *Immunol Res,* 25**,** 115-30.

KOURILSKY, P. & CLAVERIE, J. M. 1989. MHC restriction, alloreactivity, and thymic education: a common link? *Cell,* 56**,** 327-9.

KRISSINEL, E. B., WINN, M. D., BALLARD, C. C., ASHTON, A. W., PATEL, P., POTTERTON, E. A., MCNICHOLAS, S. J., COWTAN, K. D. & EMSLEY, P. 2004. The new CCP4 Coordinate Library as a toolkit for the design of coordinate-related applications in protein crystallography. *Acta Crystallogr D Biol Crystallogr,* 60**,** 2250-5.

KWAN, C. K. & ERNST, J. D. 2011. HIV and tuberculosis: a deadly human syndemic. *Clin Microbiol Rev,* 24**,** 351-76.

LADEL, C. H., BLUM, C. & KAUFMANN, S. H. 1996. Control of natural killer cell-mediated innate resistance against the intracellular pathogen Listeria monocytogenes by gamma/delta T lymphocytes. *Infect Immun,* 64**,** 1744-9.

LAUGEL, B., PRICE, D. A., MILICIC, A. & SEWELL, A. K. 2007. CD8 exerts differential effects on the deployment of cytotoxic T lymphocyte effector functions. *Eur J Immunol,* 37**,** 905-13.

LAUVAU, G., KAKIMI, K., NIEDERMANN, G., OSTANKOVITCH, M., YOTNDA, P., FIRAT, H., CHISARI, F. V. & VAN ENDERT, P. M. 1999. Human transporters associated with antigen processing (TAPs) select epitope precursor peptides for processing in the endoplasmic reticulum and presentation to T cells. *J Exp Med,* 190**,** 1227-40.

LAYRE, E., COLLMANN, A., BASTIAN, M., MARIOTTI, S., CZAPLICKI, J., PRANDI, J., MORI, L., STENGER, S., DE LIBERO, G., PUZO, G. &

GILLERON, M. 2009. Mycolic acids constitute a scaffold for mycobacterial lipid antigens stimulating CD1-restricted T cells. *Chem Biol,* 16**,** 82-92.

LAZAREVIC, V., NOLT, D. & FLYNN, J. L. 2005. Long-term control of Mycobacterium tuberculosis infection is mediated by dynamic immune responses. *J Immunol,* 175**,** 1107-17.

LE BOURHIS, L., DUSSEAUX, M., BOHINEUST, A., BESSOLES, S., MARTIN, E., PREMEL, V., CORE, M., SLEURS, D., SERRIARI, N. E., TREINER, E., HIVROZ, C., SANSONETTI, P., GOUGEON, M. L., SOUDAIS, C. & LANTZ, O. 2013. MAIT cells detect and efficiently lyse bacterially-infected epithelial cells. *PLoS Pathog,* 9**,** e1003681.

LE BOURHIS, L., MARTIN, E., PEGUILLET, I., GUIHOT, A., FROUX, N., CORE, M., LEVY, E., DUSSEAUX, M., MEYSSONNIER, V., PREMEL, V., NGO, C., RITEAU, B., DUBAN, L., ROBERT, D., HUANG, S., ROTTMAN, M., SOUDAIS, C. & LANTZ, O. 2010. Antimicrobial activity of mucosal-associated invariant T cells. *Nat Immunol,* 11**,** 701-8.

LEWINSOHN, D. A., WINATA, E., SWARBRICK, G. M., TANNER, K. E., COOK, M. S., NULL, M. D., CANSLER, M. E., SETTE, A., SIDNEY, J. & LEWINSOHN, D. M. 2007. Immunodominant tuberculosis CD8 antigens preferentially restricted by HLA-B. *PLoS Pathog,* 3**,** 1240-9.

LIANG, S. C., TAN, X. Y., LUXENBERG, D. P., KARIM, R., DUNUSSI-JOANNOPOULOS, K., COLLINS, M. & FOUSER, L. A. 2006. Interleukin (IL)-22 and IL-17 are coexpressed by Th17 cells and cooperatively enhance expression of antimicrobial peptides. *J Exp Med,* 203**,** 2271-9.

LIM, A., TRAUTMANN, L., PEYRAT, M. A., COUEDEL, C., DAVODEAU, F., ROMAGNE, F., KOURILSKY, P. & BONNEVILLE, M. 2000. Frequent contribution of T cell clonotypes with public TCR features to the chronic response against a dominant EBV-derived epitope: application to direct detection of their molecular imprint on the human peripheral T cell repertoire. *J Immunol,* 165**,** 2001-11.

LISSINA, A., LADELL, K., SKOWERA, A., CLEMENT, M., EDWARDS, E., SEGGEWISS, R., VAN DEN BERG, H. A., GOSTICK, E., GALLAGHER, K., JONES, E., MELENHORST, J. J., GODKIN, A. J., PEAKMAN, M., PRICE, D. A., SEWELL, A. K. & WOOLDRIDGE, L. 2009. Protein kinase inhibitors substantially improve the physical detection of T-cells with peptide-MHC tetramers. *J Immunol Methods,* 340**,** 11-24.

LOPEZ-SAGASETA, J., DULBERGER, C. L., MCFEDRIES, A., CUSHMAN, M., SAGHATELIAN, A. & ADAMS, E. J. 2013. MAIT recognition of a stimulatory bacterial antigen bound to MR1. *J Immunol,* 191**,** 5268-77.

MACMICKING, J. D., TAYLOR, G. A. & MCKINNEY, J. D. 2003. Immune control of tuberculosis by IFN-gamma-inducible LRG-47. *Science,* 302**,** 654-9.

MAJLESSI, L., ROJAS, M. J., BRODIN, P. & LECLERC, C. 2003. CD8+-T-cell responses of Mycobacterium-infected mice to a newly identified major

histocompatibility complex class I-restricted epitope shared by proteins of the ESAT-6 family. *Infect Immun,* 71**,** 7173-7.

MARTIN, E., TREINER, E., DUBAN, L., GUERRI, L., LAUDE, H., TOLY, C., PREMEL, V., DEVYS, A., MOURA, I. C., TILLOY, F., CHERIF, S., VERA, G., LATOUR, S., SOUDAIS, C. & LANTZ, O. 2009. Stepwise development of MAIT cells in mouse and human. *PLoS Biol,* 7**,** e54.

MARTINEAU, A. R., WILKINSON, K. A., NEWTON, S. M., FLOTO, R. A., NORMAN, A. W., SKOLIMOWSKA, K., DAVIDSON, R. N., SORENSEN, O. E., KAMPMANN, B., GRIFFITHS, C. J. & WILKINSON, R. J. 2007. IFN-gamma- and TNF-independent vitamin D-inducible human suppression of mycobacteria: the role of cathelicidin LL-37. *J Immunol,* 178**,** 7190-8.

MCCOY, A. J., GROSSE-KUNSTLEVE, R. W., ADAMS, P. D., WINN, M. D., STORONI, L. C. & READ, R. J. 2007. Phaser crystallographic software. *J Appl Crystallogr,* 40**,** 658-674.

MEHRA, A., ZAHRA, A., THOMPSON, V., SIRISAENGTAKSIN, N., WELLS, A., PORTO, M., KOSTER, S., PENBERTHY, K., KUBOTA, Y., DRICOT, A., ROGAN, D., VIDAL, M., HILL, D. E., BEAN, A. J. & PHILIPS, J. A. 2013. Mycobacterium tuberculosis type VII secreted effector EsxH targets host ESCRT to impair trafficking. *PLoS Pathog,* 9**,** e1003734.

MEIEROVICS, A., YANKELEVICH, W. J. & COWLEY, S. C. 2013. MAIT cells are critical for optimal mucosal immune responses during in vivo pulmonary bacterial infection. *Proc Natl Acad Sci U S A,* 110**,** E3119-28.

MERLE, C. S., CUNHA, S. S. & RODRIGUES, L. C. 2010. BCG vaccination and leprosy protection: review of current evidence and status of BCG in leprosy control. *Expert Rev Vaccines,* 9**,** 209-22.

MILES, J. J., SILINS, S. L. & BURROWS, S. R. 2006. Engineered T cell receptors and their potential in molecular medicine. *Curr Med Chem,* 13**,** 2725-36.

MILEY, M. J., TRUSCOTT, S. M., YU, Y. Y., GILFILLAN, S., FREMONT, D. H., HANSEN, T. H. & LYBARGER, L. 2003. Biochemical features of the MHC-related protein 1 consistent with an immunological function. *J Immunol,* 170**,** 6090-8.

MURSHUDOV, G. N., VAGIN, A. A. & DODSON, E. J. 1997. Refinement of macromolecular structures by the maximum-likelihood method. *Acta Crystallogr D Biol Crystallogr,* 53**,** 240-55.

MUSTAFA, A. S., SKEIKY, Y. A., AL-ATTIYAH, R., ALDERSON, M. R., HEWINSON, R. G. & VORDERMEIER, H. M. 2006. Immunogenicity of Mycobacterium tuberculosis antigens in Mycobacterium bovis BCG-vaccinated and M. bovis-infected cattle. *Infect Immun,* 74**,** 4566-72.

NADKARNI, S., MAURI, C. & EHRENSTEIN, M. R. 2007. Anti-TNF-alpha therapy induces a distinct regulatory T cell population in patients with rheumatoid arthritis via TGF-beta. *J Exp Med,* 204**,** 33-9.

NEWELL, E. W., SIGAL, N., BENDALL, S. C., NOLAN, G. P. & DAVIS, M. M. 2012. Cytometry by time-of-flight shows combinatorial cytokine expression and virus-specific cell niches within a continuum of CD8+ T cell phenotypes. *Immunity,* 36**,** 142-52.

NIEUWENHUIS, E. E., MATSUMOTO, T., EXLEY, M., SCHLEIPMAN, R. A., GLICKMAN, J., BAILEY, D. T., CORAZZA, N., COLGAN, S. P., ONDERDONK, A. B. & BLUMBERG, R. S. 2002. CD1d-dependent macrophage-mediated clearance of Pseudomonas aeruginosa from lung. *Nat Med,* 8**,** 588-93.

NOSS, E. H., PAI, R. K., SELLATI, T. J., RADOLF, J. D., BELISLE, J., GOLENBOCK, D. T., BOOM, W. H. & HARDING, C. V. 2001. Toll-like receptor 2-dependent inhibition of macrophage class II MHC expression and antigen processing by 19-kDa lipoprotein of Mycobacterium tuberculosis. *J Immunol,* 167**,** 910-8.

O'CALLAGHAN C, A., BYFORD, M. F., WYER, J. R., WILLCOX, B. E., JAKOBSEN, B. K., MCMICHAEL, A. J. & BELL, J. I. 1999. BirA enzyme: production and application in the study of membrane receptor-ligand interactions by site-specific biotinylation. *Anal Biochem,* 266**,** 9-15.

OKOYE, I. S. & WILSON, M. S. 2011. CD4+ T helper 2 cells--microbial triggers, differentiation requirements and effector functions. *Immunology,* 134**,** 368-77.

ORNATSKY, O., BARANOV, V. I., BANDURA, D. R., TANNER, S. D. & DICK, J. 2006. Multiple cellular antigen detection by ICP-MS. *J Immunol Methods,* 308**,** 68-76.

PADOVAN, E., CASORATI, G., DELLABONA, P., MEYER, S., BROCKHAUS, M. & LANZAVECCHIA, A. 1993. Expression of two T cell receptor alpha chains: dual receptor T cells. *Science,* 262**,** 422-4.

PALMER, C. E. & LONG, M. W. 1966. Effects of infection with atypical mycobacteria on BCG vaccination and tuberculosis. *Am Rev Respir Dis,* 94**,** 553-68.

PATEL, O., KJER-NIELSEN, L., LE NOURS, J., ECKLE, S. B., BIRKINSHAW, R., BEDDOE, T., CORBETT, A. J., LIU, L., MILES, J. J., MEEHAN, B., REANTRAGOON, R., SANDOVAL-ROMERO, M. L., SULLIVAN, L. C., BROOKS, A. G., CHEN, Z., FAIRLIE, D. P., MCCLUSKEY, J. & ROSSJOHN, J. 2013. Recognition of vitamin B metabolites by mucosal-associated invariant T cells. *Nat Commun,* 4**,** 2142.

PECORA, N. D., FULTON, S. A., REBA, S. M., DRAGE, M. G., SIMMONS, D. P., URANKAR-NAGY, N. J., BOOM, W. H. & HARDING, C. V. 2009. Mycobacterium bovis BCG decreases MHC-II expression in vivo on murine lung macrophages and dendritic cells during aerosol infection. *Cell Immunol,* 254**,** 94-104.

PETO, H. M., PRATT, R. H., HARRINGTON, T. A., LOBUE, P. A. & ARMSTRONG, L. R. 2009. Epidemiology of extrapulmonary tuberculosis in the United States, 1993-2006. *Clin Infect Dis,* 49**,** 1350-7.

PETRIE, H. T., LIVAK, F., SCHATZ, D. G., STRASSER, A., CRISPE, I. N. & SHORTMAN, K. 1993. Multiple rearrangements in T cell receptor alpha chain genes maximize the production of useful thymocytes. *J Exp Med,* 178**,** 615-22.

PORCELLI, S., YOCKEY, C. E., BRENNER, M. B. & BALK, S. P. 1993. Analysis of T cell antigen receptor (TCR) expression by human peripheral blood CD4-8- alpha/beta T cells demonstrates preferential use of several V beta genes and an invariant TCR alpha chain. *J Exp Med,* 178**,** 1-16.

POULSEN, A. 1950. Some clinical features of tuberculosis. 1. Incubation period. *Acta Tuberc Scand,* 24**,** 311-46.

POZZI, L. A., MACIASZEK, J. W. & ROCK, K. L. 2005. Both dendritic cells and macrophages can stimulate naive CD8 T cells in vivo to proliferate, develop effector function, and differentiate into memory cells. *J Immunol,* 175**,** 2071-81.

PURBHOO, M. A., BOULTER, J. M., PRICE, D. A., VUIDEPOT, A. L., HOURIGAN, C. S., DUNBAR, P. R., OLSON, K., DAWSON, S. J., PHILLIPS, R. E., JAKOBSEN, B. K., BELL, J. I. & SEWELL, A. K. 2001. The human CD8 coreceptor effects cytotoxic T cell activation and antigen sensitivity primarily by mediating complete phosphorylation of the T cell receptor zeta chain. *J Biol Chem,* 276**,** 32786-92.

PYM, A. S., BRODIN, P., MAJLESSI, L., BROSCH, R., DEMANGEL, C., WILLIAMS, A., GRIFFITHS, K. E., MARCHAL, G., LECLERC, C. & COLE, S. T. 2003. Recombinant BCG exporting ESAT-6 confers enhanced protection against tuberculosis. *Nat Med,* 9**,** 533-9.

QU, C., NGUYEN, V. A., MERAD, M. & RANDOLPH, G. J. 2009. MHC class I/peptide transfer between dendritic cells overcomes poor cross-presentation by monocyte-derived APCs that engulf dying cells. *J Immunol,* 182**,** 3650-9.

QUAH, B. J., WARREN, H. S. & PARISH, C. R. 2007. Monitoring lymphocyte proliferation in vitro and in vivo with the intracellular fluorescent dye carboxyfluorescein diacetate succinimidyl ester. *Nat Protoc,* 2**,** 2049-56.

REANTRAGOON, R., CORBETT, A. J., SAKALA, I. G., GHERARDIN, N. A., FURNESS, J. B., CHEN, Z., ECKLE, S. B., ULDRICH, A. P., BIRKINSHAW, R. W., PATEL, O., KOSTENKO, L., MEEHAN, B., KEDZIERSKA, K., LIU, L., FAIRLIE, D. P., HANSEN, T. H., GODFREY, D. I., ROSSJOHN, J., MCCLUSKEY, J. & KJER-NIELSEN, L. 2013. Antigen-loaded MR1 tetramers define T cell receptor heterogeneity in mucosal-associated invariant T cells. *J Exp Med,* 210**,** 2305-20.

REYRAT, J. M. & KAHN, D. 2001. Mycobacterium smegmatis: an absurd model for tuberculosis? *Trends Microbiol,* 9**,** 472-4.

RIEGERT, P., WANNER, V. & BAHRAM, S. 1998. Genomics, isoforms, expression, and phylogeny of the MHC class I-related MR1 gene. *J Immunol,* 161**,** 4066-77.

RIVETT, A. J., PALMER, A. & KNECHT, E. 1992. Electron microscopic localization of the multicatalytic proteinase complex in rat liver and in cultured cells. *J Histochem Cytochem,* 40**,** 1165-72.

ROCHE, P. A. & CRESSWELL, P. 1991. Proteolysis of the class II-associated invariant chain generates a peptide binding site in intracellular HLA-DR molecules. *Proc Natl Acad Sci U S A,* 88**,** 3150-4.

RODRIGUES, L. C. & SMITH, P. G. 1990. Tuberculosis in developing countries and methods for its control. *Trans R Soc Trop Med Hyg,* 84**,** 739-44.

ROSAT, J. P., GRANT, E. P., BECKMAN, E. M., DASCHER, C. C., SIELING, P. A., FREDERIQUE, D., MODLIN, R. L., PORCELLI, S. A., FURLONG, S. T. & BRENNER, M. B. 1999. CD1-restricted microbial lipid antigen-specific recognition found in the CD8+ alpha beta T cell pool. *J Immunol,* 162**,** 366-71.

ROTHCHILD, A. C., JAYARAMAN, P., NUNES-ALVES, C. & BEHAR, S. M. 2014. iNKT cell production of GM-CSF controls Mycobacterium tuberculosis. *PLoS Pathog,* 10**,** e1003805.

ROWEN, L., KOOP, B. F. & HOOD, L. 1996. The complete 685-kilobase DNA sequence of the human beta T cell receptor locus. *Science,* 272**,** 1755-62.

RUDOLPH, M. G., STANFIELD, R. L. & WILSON, I. A. 2006. How TCRs bind MHCs, peptides, and coreceptors. *Annu Rev Immunol,* 24**,** 419-66.

SCHLESINGER, L. S., HULL, S. R. & KAUFMAN, T. M. 1994. Binding of the terminal mannosyl units of lipoarabinomannan from a virulent strain of Mycobacterium tuberculosis to human macrophages. *J Immunol,* 152**,** 4070-9.

SCHWARTZMAN, K. 2002. Latent tuberculosis infection: old problem, new priorities. *CMAJ,* 166**,** 759-61.

SCRIBA, T. J., TAMERIS, M., MANSOOR, N., SMIT, E., VAN DER MERWE, L., ISAACS, F., KEYSER, A., MOYO, S., BRITTAIN, N., LAWRIE, A., GELDERBLOEM, S., VELDSMAN, A., HATHERILL, M., HAWKRIDGE, A., HILL, A. V., HUSSEY, G. D., MAHOMED, H., MCSHANE, H. & HANEKOM, W. A. 2010. Modified vaccinia Ankara-expressing Ag85A, a novel tuberculosis vaccine, is safe in adolescents and children, and induces polyfunctional CD4+ T cells. *Eur J Immunol,* 40**,** 279-90.

SEIDEL, U. J., OLIVEIRA, C. C., LAMPEN, M. H. & HALL, T. 2012. A novel category of antigens enabling CTL immunity to tumor escape variants: Cinderella antigens. *Cancer Immunol Immunother,* 61**,** 119-25.

SEWELL, A. K. 2012. Why must T cells be cross-reactive? *Nat Rev Immunol,* 12**,** 669-77.

SHAFIANI, S., TUCKER-HEARD, G., KARIYONE, A., TAKATSU, K. & URDAHL, K. B. 2010. Pathogen-specific regulatory T cells delay the arrival of effector T cells in the lung during early tuberculosis. *J Exp Med,* 207**,** 1409-20.

SHEPARD, C. C. 1960. The Experimental Disease That Follows the Injection of Human Leprosy Bacilli into Foot-Pads of Mice. *J Exp Med,* 112**,** 445-54.

SHORTMAN, K., VREMEC, D. & EGERTON, M. 1991. The kinetics of T cell antigen receptor expression by subgroups of CD4+8+ thymocytes: delineation of CD4+8+3(2+) thymocytes as post-selection intermediates leading to mature T cells. *J Exp Med,* 173**,** 323-32.

SIELING, P. A., OCHOA, M. T., JULLIEN, D., LESLIE, D. S., SABET, S., ROSAT, J. P., BURDICK, A. E., REA, T. H., BRENNER, M. B., PORCELLI, S. A. & MODLIN, R. L. 2000. Evidence for human CD4+ T cells in the CD1-restricted repertoire: derivation of mycobacteria-reactive T cells from leprosy lesions. *J Immunol,* 164**,** 4790-6.

SIMEONE, R., BOTTAI, D. & BROSCH, R. 2009. ESX/type VII secretion systems and their role in host-pathogen interaction. *Curr Opin Microbiol,* 12**,** 4-10.

SINGH, A. K. & REYRAT, J. M. 2009. Laboratory maintenance of Mycobacterium smegmatis. *Curr Protoc Microbiol,* Chapter 10**,** Unit10C 1.

SKJOT, R. L., BROCK, I., AREND, S. M., MUNK, M. E., THEISEN, M., OTTENHOFF, T. H. & ANDERSEN, P. 2002. Epitope mapping of the immunodominant antigen TB10.4 and the two homologous proteins TB10.3 and TB12.9, which constitute a subfamily of the esat-6 gene family. *Infect Immun,* 70**,** 5446-53.

SOARES, A. P., SCRIBA, T. J., JOSEPH, S., HARBACHEUSKI, R., MURRAY, R. A., GELDERBLOEM, S. J., HAWKRIDGE, A., HUSSEY, G. D., MAECKER, H., KAPLAN, G. & HANEKOM, W. A. 2008. Bacillus Calmette-Guerin vaccination of human newborns induces T cells with complex cytokine and phenotypic profiles. *J Immunol,* 180**,** 3569-77.

SPITS, H. 2002. Development of alphabeta T cells in the human thymus. *Nat Rev Immunol,* 2**,** 760-72.

STEBBINS, C. C., LOSS, G. E., JR., ELIAS, C. G., CHERVONSKY, A. & SANT, A. J. 1995. The requirement for DM in class II-restricted antigen presentation and SDS-stable dimer formation is allele and species dependent. *J Exp Med,* 181**,** 223-34.

STENGER, S., NIAZI, K. R. & MODLIN, R. L. 1998. Down-regulation of CD1 on antigen-presenting cells by infection with Mycobacterium tuberculosis. *J Immunol,* 161**,** 3582-8.

SWAIN, S. L., MCKINSTRY, K. K. & STRUTT, T. M. 2012. Expanding roles for CD4(+) T cells in immunity to viruses. *Nat Rev Immunol,* 12**,** 136-48.

SWEENEY, K. A., DAO, D. N., GOLDBERG, M. F., HSU, T., VENKATASWAMY, M. M., HENAO-TAMAYO, M., ORDWAY, D., SELLERS, R. S., JAIN, P., CHEN, B., CHEN, M., KIM, J., LUKOSE, R., CHAN, J., ORME, I. M., PORCELLI, S. A. & JACOBS, W. R., JR. 2011. A recombinant Mycobacterium

smegmatis induces potent bactericidal immunity against Mycobacterium tuberculosis. *Nat Med,* 17**,** 1261-8.

TILLOY, F., TREINER, E., PARK, S. H., GARCIA, C., LEMONNIER, F., DE LA SALLE, H., BENDELAC, A., BONNEVILLE, M. & LANTZ, O. 1999. An invariant T cell receptor alpha chain defines a novel TAP-independent major histocompatibility complex class Ib-restricted alpha/beta T cell subpopulation in mammals. *J Exp Med,* 189**,** 1907-21.

TREINER, E. 2003. [MAIT lymphocytes, regulators of intestinal immunity?]. *Presse Med,* 32**,** 1636-7.

TREINER, E., DUBAN, L., BAHRAM, S., RADOSAVLJEVIC, M., WANNER, V., TILLOY, F., AFFATICATI, P., GILFILLAN, S. & LANTZ, O. 2003. Selection of evolutionarily conserved mucosal-associated invariant T cells by MR1. *Nature,* 422**,** 164-9.

TREINER, E., DUBAN, L., MOURA, I. C., HANSEN, T., GILFILLAN, S. & LANTZ, O. 2005. Mucosal-associated invariant T (MAIT) cells: an evolutionarily conserved T cell subset. *Microbes Infect,* 7**,** 552-9.

ULDRICH, A. P., LE NOURS, J., PELLICCI, D. G., GHERARDIN, N. A., MCPHERSON, K. G., LIM, R. T., PATEL, O., BEDDOE, T., GRAS, S., ROSSJOHN, J. & GODFREY, D. I. 2013. CD1d-lipid antigen recognition by the gammadelta TCR. *Nat Immunol,* 14**,** 1137-45.

URDAHL, K. B., SHAFIANI, S. & ERNST, J. D. 2011. Initiation and regulation of T-cell responses in tuberculosis. *Mucosal Immunol,* 4**,** 288-93.

VAN DISSEL, J. T., SOONAWALA, D., JOOSTEN, S. A., PRINS, C., AREND, S. M., BANG, P., TINGSKOV, P. N., LINGNAU, K., NOUTA, J., HOFF, S. T., ROSENKRANDS, I., KROMANN, I., OTTENHOFF, T. H., DOHERTY, T. M. & ANDERSEN, P. 2011. Ag85B-ESAT-6 adjuvanted with IC31(R) promotes strong and long-lived Mycobacterium tuberculosis specific T cell responses in volunteers with previous BCG vaccination or tuberculosis infection. *Vaccine,* 29**,** 2100-9.

VENKATASWAMY, M. M. & PORCELLI, S. A. 2010. Lipid and glycolipid antigens of CD1d-restricted natural killer T cells. *Semin Immunol,* 22**,** 68-78.

VENTURI, V., PRICE, D. A., DOUEK, D. C. & DAVENPORT, M. P. 2008. The molecular basis for public T-cell responses? *Nat Rev Immunol,* 8**,** 231-8.

VERMA, D. S., SPITZER, G., ZANDER, A. R., FISHER, R., MCCREDIE, K. B. & DICKE, K. A. 1979. T lymphocyte and monocyte-macrophage interaction in colony-stimulating activity elaboration in man. *Blood,* 54**,** 1376-83.

WAGNER, L., YANG, O. O., GARCIA-ZEPEDA, E. A., GE, Y., KALAMS, S. A., WALKER, B. D., PASTERNACK, M. S. & LUSTER, A. D. 1998. Beta-chemokines are released from HIV-1-specific cytolytic T-cell granules complexed to proteoglycans. *Nature,* 391**,** 908-11.

WALKER, L. J., KANG, Y. H., SMITH, M. O., THARMALINGHAM, H., RAMAMURTHY, N., FLEMING, V. M., SAHGAL, N., LESLIE, A., OO, Y., GEREMIA, A., SCRIBA, T. J., HANEKOM, W. A., LAUER, G. M., LANTZ, O., ADAMS, D. H., POWRIE, F., BARNES, E. & KLENERMAN, P. 2012. Human MAIT and CD8alphaalpha cells develop from a pool of type-17 precommitted CD8+ T cells. *Blood,* 119**,** 422-33.

WALLGREN, A. 1948. The time-table of tuberculosis. *Tubercle,* 29**,** 245-51.

WAN, Y. Y. 2010. Multi-tasking of helper T cells. *Immunology,* 130**,** 166-71.

WANG, X. Q., DUAN, X. M., LIU, L. H., FANG, Y. Q. & TAN, Y. 2005. Carboxyfluorescein diacetate succinimidyl ester fluorescent dye for cell labeling. *Acta Biochim Biophys Sin (Shanghai),* 37**,** 379-85.

WEDLOCK, D. N., DENIS, M., VORDERMEIER, H. M., HEWINSON, R. G. & BUDDLE, B. M. 2007. Vaccination of cattle with Danish and Pasteur strains of Mycobacterium bovis BCG induce different levels of IFNgamma post-vaccination, but induce similar levels of protection against bovine tuberculosis. *Vet Immunol Immunopathol,* 118**,** 50-8.

WELDINGH, K. & ANDERSEN, P. 2008. ESAT-6/CFP10 skin test predicts disease in M. tuberculosis-infected guinea pigs. *PLoS One,* 3**,** e1978.

WHERRY, E. J., TEICHGRABER, V., BECKER, T. C., MASOPUST, D., KAECH, S. M., ANTIA, R., VON ANDRIAN, U. H. & AHMED, R. 2003. Lineage relationship and protective immunity of memory CD8 T cell subsets. *Nat Immunol,* 4**,** 225-34.

WILLCOX, B. E., WILLCOX, C. R., DOVER, L. G. & BESRA, G. 2007. Structures and functions of microbial lipid antigens presented by CD1. *Curr Top Microbiol Immunol,* 314**,** 73-110.

WILLCOX, C. R., PITARD, V., NETZER, S., COUZI, L., SALIM, M., SILBERZAHN, T., MOREAU, J. F., HAYDAY, A. C., WILLCOX, B. E. & DECHANET-MERVILLE, J. 2012. Cytomegalovirus and tumor stress surveillance by binding of a human gammadelta T cell antigen receptor to endothelial protein C receptor. *Nat Immunol,* 13**,** 872-9.

WITTE, E., WITTE, K., WARSZAWSKA, K., SABAT, R. & WOLK, K. 2010. Interleukin-22: a cytokine produced by T, NK and NKT cell subsets, with importance in the innate immune defense and tissue protection. *Cytokine Growth Factor Rev,* 21**,** 365-79.

WOLF, A. J., LINAS, B., TREVEJO-NUNEZ, G. J., KINCAID, E., TAMURA, T., TAKATSU, K. & ERNST, J. D. 2007. Mycobacterium tuberculosis infects dendritic cells with high frequency and impairs their function in vivo. *J Immunol,* 179**,** 2509-19.

WOLF, P. R. & PLOEGH, H. L. 1995. How MHC class II molecules acquire peptide cargo: biosynthesis and trafficking through the endocytic pathway. *Annu Rev Cell Dev Biol,* 11**,** 267-306.

WOOLDRIDGE, L., EKERUCHE-MAKINDE, J., VAN DEN BERG, H. A., SKOWERA, A., MILES, J. J., TAN, M. P., DOLTON, G., CLEMENT, M., LLEWELLYN-LACEY, S., PRICE, D. A., PEAKMAN, M. & SEWELL, A. K. 2012. A single autoimmune T cell receptor recognizes more than a million different peptides. *J Biol Chem,* 287**,** 1168-77.

WOOLDRIDGE, L., LAUGEL, B., EKERUCHE, J., CLEMENT, M., VAN DEN BERG, H. A., PRICE, D. A. & SEWELL, A. K. 2010. CD8 controls T cell cross-reactivity. *J Immunol,* 185**,** 4625-32.

WOOLDRIDGE, L., LISSINA, A., COLE, D. K., VAN DEN BERG, H. A., PRICE, D. A. & SEWELL, A. K. 2009. Tricks with tetramers: how to get the most from multimeric peptide-MHC. *Immunology,* 126**,** 147-64.

WOOLDRIDGE, L., VAN DEN BERG, H. A., GLICK, M., GOSTICK, E., LAUGEL, B., HUTCHINSON, S. L., MILICIC, A., BRENCHLEY, J. M., DOUEK, D. C., PRICE, D. A. & SEWELL, A. K. 2005. Interaction between the CD8 coreceptor and major histocompatibility complex class I stabilizes T cell receptor-antigen complexes at the cell surface. *J Biol Chem,* 280**,** 27491-501.

YACHIE, A., UENO, Y., TAKANO, N., MIYAWAKI, T. & TANIGUCHI, N. 1989. Developmental changes of double-negative (CD3+ 4-8-) T cells in human peripheral blood. *Clin Exp Immunol,* 76**,** 258-61.

YIN, L., HUSEBY, E., SCOTT-BROWNE, J., RUBTSOVA, K., PINILLA, C., CRAWFORD, F., MARRACK, P., DAI, S. & KAPPLER, J. W. 2011. A single T cell receptor bound to major histocompatibility complex class I and class II glycoproteins reveals switchable TCR conformers. *Immunity,* 35**,** 23-33.

YU, J. J. & GAFFEN, S. L. 2008. Interleukin-17: a novel inflammatory cytokine that bridges innate and adaptive immunity. *Front Biosci,* 13**,** 170-7.

YU, X. G., LICHTERFELD, M., CHETTY, S., WILLIAMS, K. L., MUI, S. K., MIURA, T., FRAHM, N., FEENEY, M. E., TANG, Y., PEREYRA, F., LABUTE, M. X., PFAFFEROTT, K., LESLIE, A., CRAWFORD, H., ALLGAIER, R., HILDEBRAND, W., KASLOW, R., BRANDER, C., ALLEN, T. M., ROSENBERG, E. S., KIEPIELA, P., VAJPAYEE, M., GOEPFERT, P. A., ALTFELD, M., GOULDER, P. J. & WALKER, B. D. 2007. Mutually exclusive T-cell receptor induction and differential susceptibility to human immunodeficiency virus type 1 mutational escape associated with a two-amino-acid difference between HLA class I subtypes. *J Virol,* 81**,** 1619-31.

ZACHARIADIS, O., CASSIDY, J. P., BRADY, J. & MAHON, B. P. 2006. gammadelta T cells regulate the early inflammatory response to bordetella pertussis infection in the murine respiratory tract. *Infect Immun,* 74**,** 1837-45.

ZHAO, S., ZHAO, Y., MAO, F., ZHANG, C., BAI, B., ZHANG, H., SHI, C. & XU, Z. 2012. Protective and therapeutic efficacy of Mycobacterium smegmatis expressing HBHA-hIL12 fusion protein against Mycobacterium tuberculosis in mice. *PLoS One,* 7**,** e31908.

ZODPEY, S. P., SHRIKHANDE, S. N., SALODKAR, A. D., MALDHURE, B. R. & KULKARNI, S. W. 1998. Effectiveness of bacillus Calmette-Guerin (BCG) vaccination in the prevention of leprosy; a case-finding control study in Nagpur, India. *Int J Lepr Other Mycobact Dis,* 66**,** 309-15.